

**The Roles of Surface Ultrastructures in the Predatory
Life Cycle of *Bdellovibrio bacteriovorus*.**

by
Katy Evans B.Sc (Hons)
University of Nottingham

Thesis submitted to
The University of Nottingham for the
Degree of Doctor of Philosophy

March 2007

**MEDICAL LIBRARY
QUEENS MEDICAL CENTRE**

**PAGINATED
BLANK PAGES
ARE SCANNED AS
FOUND IN
ORIGINAL
THESIS**

**NO
INFORMATION
MISSING**

The work presented in this thesis is my own, unless otherwise stated. No part of this thesis has previously been submitted for examination leading to the award of a degree. This copy has been supplied on the understanding that it is copyright material and that no quotation from this thesis may be published without proper acknowledgement.

Katy Evans 2007

100529/689T

ACKNOWLEDGEMENTS

Firstly, I would like to thank my supervisor, Professor Liz Sockett for everything she has done for me and has enabled me to do both scientifically and personally. This work would not have been done without her... I would also like to thank Professor Chi Aizawa for hosting me in Japan twice and teaching me much about Japan, not just electron microscopy. Thanks also go to Roy Choudhuri for immense assistance with bioinformatics.

A huge thank you to everyone in C15 – Carey, Rich, Karen, Rob, Laura, Mike, Davy, Mark, John..... you all drive me mad but I love you for it! Special mention to Matt, Emma, Sunny D, Thorsten, Ed, Stephane, Dicky, Akhmed, Maria, Ash, Phyllis and to all the others in the department who have made me laugh so much over the last few years (I can't name everyone, that would be a thesis in itself!)

Outside of work, special mention must go to Kayte for being the closest thing to a big sister I have. Thanks go also to Jen, Tracy, Lisa, Chloe, Greg, little Dave, Double D, and all the other staff from Via and the Rose and Crown for reminding me there are other things than science!

To the girls from Liverpool, thanks for putting up with me and Natasha living in Nottingham for so long; cheers for the willingness to come down and see us even if eight of you do clutter my flat for weekends at a time!

My family have been so supportive during the course of my whole education, which would have been impossible without their love and willingness to listen to me rant, so thank you Mum and Dad for being there (big hugs to Nan, Grandad and the rest of the Evans and Wright clans).

Finally, a special mention to Jonny, I couldn't have got through the write up without you (or the nutritious meals you made me eat rather than living on cheese on toast).
Thank you, babes.

This thesis is dedicated to the memory of Charles Henry Wright.

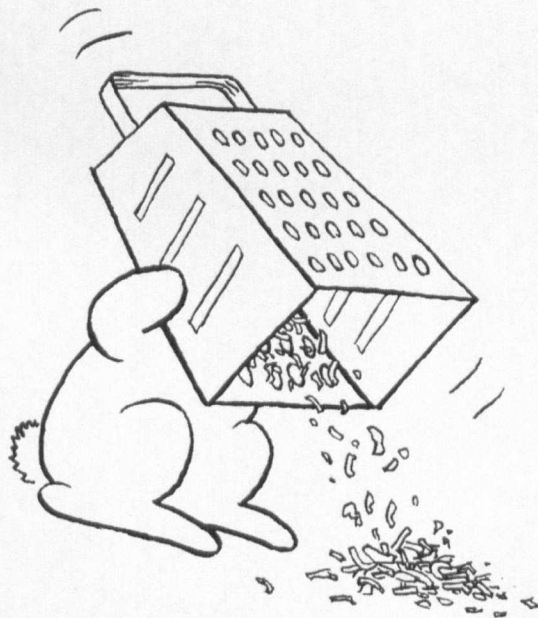
Work funded by the BBSRC

“ ‘Anyway, I suppose the rot set in when I tried to see if it was possible to breed a more inflammable cow...’

‘...Another good idea that didn’t work. I just thought, you know, that if you could find the bit in, say, an oak tree which says “be inflammable” and glue it into the bit of the cow which says “be soggy” it’d save a lot of trouble. Unfortunately, that produced a sort of bush that made distressing noises and squirted milk, but the *principle* was sound...’ ”

The God of Evolution’s views on genetic engineering, from Terry Pratchett’s “The Last Continent”

© Andy Riley, “The Bunny Suicides: part II”



ABBREVIATIONS

°C	degrees centigrade
µg	micrograms
µl	microlitre
µm	micrometre
µM	micromolar
α	alpha
β	beta
δ	delta
γ	gamma
%	percent
#	number
Amp	ampicillin
AmpR	ampicillin resistant
ATP	adenosine triphosphate
bp	base pair
BSA	bovine serum albumin
DNA	deoxyribonucleic acid
dNTPs	deoxyribonucleic triphosphates
EDTA	ethylenediaminetetra-acetic acid disodium salt
<i>x g</i>	9.81 squared metres per second (when referring to centrifugation)
g	grams
GFP	green fluorescent protein
kb	kilobase
kD	kilo Daltons
Kn	kanamycin
KnR	kanamycin resistant
L	litre
nm	nanometre
nM	nanomolar
M	molar
Mb	megabase (DNA)
mg	milligrams
min	minutes
ml	millilitre
ml ⁻¹	per millilitre
ng	nanograms
OD	optical density
PCR	polymerase chain reaction
PTA	phosphotungstic acid
PVDF	polyvinylidene difluoride
rcf	relative centrifugal force
rpm	revolutions per minute
RNA	ribonucleic acid
RTPCR	reverse transcriptase polymerase chain reaction
SDS	sodium dodecyl sulphate
SDS-PAGE	sodium dodecyl sulphate polyacrylamide gel electrophoresis
TBE	tris-borate ethylenediaminetetra-acetic acid

TEMED	N,N,N',N'-tetramethylethylenediamine
TEM	transmission electron microscopy
URA	uranyl acetate
UV	ultraviolet light
V	volts

TABLE OF FIGURES

CHAPTER 1

- 1.1 Phylogenetic tree of *Bdellovibrio* and related species
- 1.2 *B. bacteriovorus* 109J predatory life cycle
- 1.3 Comparative morphologies of *B. bacteriovorus* HD100 and 109J
- 1.4 Transmission electron micrograph of *B. bacteriovorus* HD100 invading an *E. coli* prey cell
- 1.5 Electron micrograph of *B. bacteriovorus* 109J inside a bdelloplast formed on *E. coli* DFB225.
- 1.6 *B. bacteriovorus* 109J cells septating inside a bdelloplast (*E. coli* S17-1)
- 1.7 Host-Independent (HI) cells of *B. bacteriovorus* 109J
- 1.8 Graphical representation of the HD100 genome coloured by GC content

CHAPTER 3

- 3.1 General structure of the Gram-negative flagellar complex
- 3.2 Structural representation of *Salmonella* FliC and multiple alignment of flagellin sequences from different bacteria
- 3.3 Transmission electron micrograph of *H. pylori*J99 wild type cell.
- 3.4 Transmission electron micrograph of *B. bacteriovorus* HD100, showing the characteristic single, polar, sheathed flagellum with a dampened waveform
- 3.5 Thomashow and Rittenberg's waveform analysis of 109J
- 3.6 Genomic distribution of flagellar genes in HD100
- 3.7 Genomic arrangement of *fliC* genes in HD100
- 3.8 Multiple protein alignment of HD100 FliC3 with *E. coli* (Ec) and *Salmonella enterica* serovar Typhimurium flagellins
- 3.9 Multiple alignment of *B. bacteriovorus* HD100 FliC proteins
- 3.10 TEM of *B. bacteriovorus* 109J stained with PTA and URA
- 3.11 *B. bacteriovorus* 109J attaching to an *E. coli*
- 3.12 109J bdelloplast
- 3.13 uranyl acetate stained HD100 bdelloplast
- 3.14 HD100 bdelloplast showing filament development
- 3.15 HD100 bdelloplast showing late stage filament development
- 3.16 high magnification electron micrograph showing close contacts between the *Bdellovibrio* and *E. coli* cytoplasmic membrane within a bdelloplast
- 3.17 *B. bacteriovorus* 109J late-stage bdelloplast
- 3.18 *B. bacteriovorus* 109J bdelloplast showing septating progeny in a late stage bdelloplast
- 3.19 Cartoon of *B. bacteriovorus fliC* genes and the restriction sites used to interrupt them with a kanamycin cassette
- 3.20 Alignment of the six 109J FliC proteins
- 3.21 *B. bacteriovorus* 109J *fliC::Kn* mutants (TEM)
- 3.22 Multiple protein alignment of all 109J and HD100 flagellins
- 3.23 TEM of selected cognate *B. bacteriovorus* HD100 *fliC* mutant strains
- 3.24 TEM images of 109*fliC3::Kn* HI and HIK3 and sheared flagella from these strains

- 3.25 Isolated Hook-Basal Body structures from 109*fliC3::Kn* HI and wild-type *B. bacteriovorus* 109J
- 3.26 Semi-quantitative RT-PCR of flagellin genes in 109*fliC3::Kn* HI and HIK3
- 3.27 12.5% SDS-PAGE gel showing the protein profile of sheared flagella/sheath from 109*fliC3::Kn* HI and HIK3 and distribution of flagellin peptides as determined by mass spectroscopy
- 3.28 Fluorescence assay for the predatory capability of 109*flic3::Kn* HI
- 3.29 SDS-PAGE of 109J *fliC* mutant sheared flagella
- 3.30 Multiple protein alignment of major flagellins in sheathed flagellate bacteria
- 3.31 Demonstration of the leaky prey cytoplasm in bdelloplasts

CHAPTER 4

- 4.1 Schematic drawing of the structure of GFP from *Aequorea victoria*, illustrating the 11-strand β barrel and the internal α helix that forms the chromophore
- 4.2 Strain HD100 attaching to S17-1 *E. coli*
- 4.3 Map of pMMB206
- 4.4 Top panel, GFPpMMB206 containing 109J bdelloplast, bottom, plasmid-less 109J bdelloplast
- 4.5 Map of pLOFKmgfp
- 4.6 Phenotypes of selected HD and 109 GFP+ strains (5 pages)
- 4.7 Southern blot showing selected 109JGFP strain genomic DNA digested with *EcoRI*, probed with the mini Tn10*gfpKnR* cut *Bam*HI from pLOFKmgfp
- 4.8 Western blots of GFP strain attack phase *Bdellovibrio* whole cell protein probed with anti mouse anti-GFP antibody
- 4.9 Southern blot showing selected HD100GFP strain genomic DNA digested with *EcoRI*, probed with the KnR cassette cut *Hinc*II form pUC4K
- 4.10 Agarose electrophoresis gel (0.8%) of restriction digests of potential mini Tn10*gfpKnR* containing clones
- 4.11 Theoretical restriction maps of HDGFP clones constructed from the restriction digests shown in Figure 4.10
- 4.12 Alignment of clipped sequence data (labelled HDGFP1) with the cognate sequences from the *B. bacteriovorus* HD100 genome and the mini Tn10*gfpKnR*
- 4.13 The structure of *E. coli* K12 outer membrane LPS layer and the structure of *E. coli* K12 outer membrane LPS layer
- 4.14 Alignment of the reverse complement of the DNA sequence obtained from the HDGFP14.5 construct using the universal pUC19 forward primer
- 4.15 FM4-64 labelled *B. bacteriovorus* and *E. coli* strains

CHAPTER 5

- 5.1 Transmission electron micrographs showing prey invasion
- 5.2 Extension and retraction of pili in *Pseudomonas aeruginosa*
- 5.3 Cartoon representing the general structure of the Gram-negative bacterial Type IV pilus as found in *Neisseria* and *Pseudomonas*
- 5.4 Transmission electron micrograph of wild type *M. xanthus* showing polar pilus fibres

- 5.5 Comparison of the operon structure of *pil* genes in *Myxococcus* and *B. bacteriovorus*
- 5.6 Transmission electron micrograph of *B. bacteriovorus* 109J showing anterior fibres
- 5.7 Figures taken from Burnham *et al* showing the proposed holdfast structure and anterior fibres found on *B. bacteriovorus*
- 5.8 Cartoon representing my proposed structure of the *B. bacteriovorus* HD100 Type IV pilus
- 5.9 Transmission electron micrographs of attack phase *B. bacteriovorus* freshly liberated from prey cells.
- 5.10 High resolution EM of wild type HD100 *B. bacteriovorus* showing polar ring structures
- 5.11 Alignment of *B. bacteriovorus* best PilQ homologue with the *Myxococcus xanthus* PilQ
- 5.12 Alignment of *M. xanthus* PilT with *B. bacteriovorus* PilT1
- 5.13 Alignment of *M. xanthus* PilT with *B. bacteriovorus* PilT2
- 5.14 Alignment of *B. bacteriovorus* HD100 PilA with other characterised Type IVa pilins and with Type IVb pilins
- 5.15 The structures of *N. gonorrhoeae* GC pilin and *P. aeruginosa* PAK pilin
- 5.16 Fragment produced in HD100 using pilAF and pilAR cloning primers
- 5.17 Agarose gel showing attempts to PCR the 2.37kb fragment obtained in HD100 from 109J
- 5.18 Regions most conserved at the protein level between PilAs and PilGs from different species and primer binding positions
- 5.19 Agarose gel of promising PCRs to amplify 109J *pilA* using potential conserved primers from HD100 sequences
- 5.20 Plasmid map of the HD100 *pilAG* fragment cloned into pUC19
- 5.21 Agarose gel showing digests of the putative 109J *pilAG* clone
- 5.22 Southern blot to find bands in 109J genomic DNA cut with different restriction enzymes that cross-hybridised to the HD100 *pilA* probe
- 5.23 “Dot-blot” of potential 109J *pilA* – containing clones, probed with the HD100 *pilA* gene
- 5.24 Summary of the cloning strategy used to inserttionally inactivate *pilA* in the Hd100 genome
- 5.25 PCR screens of HI and HD lines of *pil::KnR* exconjugants to find double recombinants
- 5.26 Southern Blots confirming the HI*pilA::KnR* mutants
- 5.27 TEM characterisation of merodiploid and mutant HI*pilA::Kn* strains
- 5.28 HI*pilA::Kn* mutant strains and HI*pilA/pilA::Kn* strains were grown on lawns of *E. coli* S17-1 pZMR100 (KnR) soft agar overlays
- 5.29 Morphology and predatory phenotypes of mutant and merodiploid *pilA* strains
- 5.30 Alignment of HD100 PilA with *M. xanthus* PilA
- 5.31 Western blot of whole cell proteins using the *Myxococcus xanthus* anti-PilA antibody
- 5.32 Cy5 labelling experiments using HD100
- 5.33 Stars on the life cycle of predatory *B. bacteriovorus* give a visual representation of the stages at which cultures were sampled and RNA prepared to enable transcript profiling at different stages of *Bdellovibrio* growth
- 5.34 Semi-quantitative reverse-transcription PCR of *pil* genes on RNA from *B. bacteriovorus* predatory cultures

LIST OF TABLES

Table 2.1	Bacterial strains used in this study
Table 2.2	Plasmids used in this work
Table 2.3	Primer sequences used in this study
Table 2.4	Antibiotic concentrations typically used
Table 2.5	Specific conditions for electron microscopy
Table 3.1	key to Figure 3.1
Table 3.2	Predicted molecular weights of <i>B. bacteriovorus</i> flagellin proteins
Table 4.1	Details of exconjugant numbers picked from plates, survival rate in initial lysates and percentage of GFP+ cells from those survivors
Table 4.2	Scoring of fluorescence of 109GFP strains
Table 4.3:	Scoring of fluorescence of HDGFP strains
Table 5.1	Key to figure 5.3
Table 5.2	Genes shown to be required for tfp biogenesis in <i>M. xanthus</i> and their homologues from <i>B. bacteriovorus</i>
Table 5.3	Genes required for Flp pilus formation
Table 5.4	Summary of the characteristics of Type IVa vs IVb pilin proteins
Table 5.5	Primer combinations used in both HD100 and 109J to try and amplify the <i>pilAG</i> genes

TABLE OF CONTENTS

CHAPTER 1 – INTRODUCTION

1.1:	What are <i>Bdellovibrio</i>?	1
1.2:	<i>Bdellovibrio bacteriovorus</i> strains HD100 and 109J prey range and natural environments	2
1.3:	The predatory life cycle of <i>B. bacteriovorus</i>	4
	1.3.1: The predatory life cycle – attack phase <i>B. bacteriovorus</i>	4
	1.3.2: The predatory life cycle – attachment and entry	6
	1.3.3: The predatory life cycle – establishment and growth	7
	1.3.4: The predatory life cycle – septation and lysis of the prey cell	9
1.4:	The phenomenon and applications of Host Independence in <i>Bdellovibrio</i>	10
1.5:	The <i>B. bacteriovorus</i> HD100 genome	14
1.6:	Working with <i>B. bacteriovorus</i> in the lab – experimental barriers	16
1.7:	Possible applications of <i>Bdellovibrio</i> in medicine	18
1.8:	Aims of this study	19

CHAPTER 2: MATERIALS AND METHODS

2.1:	Strains, plasmids and primers used in this work	20
2.2:	Bacterial growth conditions	24
	2.2.1: <i>Escherichia coli</i>	24
	2.2.2: <i>Bdellovibrio bacteriovorus</i> prey-dependent (HD) strains	24
	2.2.2.1: Host Independent isolation and growth of <i>Bdellovibrio bacteriovorus</i>	25
	2.2.3: <i>Myxococcus xanthus</i>	25
2.3:	DNA manipulation techniques	26
	2.3.1: Small scale isolation of plasmid DNA	26
	2.3.2: Large scale isolation of plasmid DNA	27

2.3.3: Isolation of bacterial genomic DNA	27
2.3.4: Agarose gel electrophoresis	27
2.3.5: Restriction digest of DNA	28
2.3.6: Isolation of DNA fragments from agarose gels	28
2.3.7: Dephosphorylation of vector DNA	29
2.3.8: Modification of DNA ends	29
2.3.9: Ligation of restriction fragments	29
2.3.9.1: Shotgun cloning of genomic fragments	29
2.3.10: Competence and transformation of <i>E. coli</i> with plasmid DNA	30
2.3.11: Conjugation of plasmid DNA into <i>B. bacteriovorus</i>	31
2.4: DNA sequencing	32
2.5: Amplification of DNA for cloning and mutant verification and RNA for use in expression studies	32
2.5.1: Polymerase Chain Reaction (PCR)	32
2.5.2: Purification of PCR products	33
2.5.3: Reverse transcriptase PCR (RTPCR) analysis of gene expression	34
2.5.3.1: Isolation of RNA from <i>Bdellovibrio</i>	34
2.5.3.2 Reverse transcriptase PCR (RTPCR)	34
2.6: Southern Blot hybridisations	35
2.6.1: Transfer and immobilisation of DNA onto nitrocellulose membranes	35
2.6.2: Synthesis of biotinylated probes	35
2.6.3: Hybridisation	36
2.6.4: Chemiluminescent detection	36
2.7: Protein analysis techniques	36
2.7.1: Sodium dodecyl sulphate polyacrylamide gel electrophoresis (SDS-PAGE)	36
2.7.2: Lowry protein concentration assay	37
2.7.3: Western blot analyses	38
2.7.4: Isolation of flagella, flagella sheath and flagella hook basal bodies (HBB) from <i>B. bacteriovorus</i>	38

2.7.4.1: Flagellar shearing of flagellin mutants for isolated filaments and sheath preparations	38
2.7.4.2: Isolation of Intact Flagella with Hook Basal Bodies (HBB)	39
2.7.5: Quantitative time of flight mass spectroscopy (QTOF-MS/MS) analysis of <i>B. bacteriovorus</i> isolated flagella/flagellar sheath	40
2.8: Microscopy techniques	40
2.8.1: Phase Contrast microscopy	40
2.8.2: Electron microscopy	41
2.8.3: Fluorescence microscopy	41
2.9: Fluorescence techniques	41
2.9.1: Cy5 labelling of <i>B. bacteriovorus</i>	41
2.9.2: FM-464 labelling of bacteria	42
2.9.3: Fluorescent assay for predatory capability of mutant strains of <i>Bdellovibrio</i>	42
2.10: Bioinformatic analysis of DNA and proteins	43
2.10.1: BLAST analyses	43
2.10.2: Multiple alignments	43
2.10.3: Plasmids maps and primer design for cloning and RT-PCR primers	44
2.10.4: Mass spectroscopic data analysis	44
2.10.5: Computation of protein theoretical pI/mwt	45
2.10.6: Image creation	45

Chapter 3: Flagella and their role in *B. bacteriovorus* predation

3.1: Flagella and bacterial motility – an overview	46
3.1.1: The flagellar filament	50
3.1.1.1: Multiple copies of the flagellin gene, <i>fliC</i> , exist in some bacterial species	52
3.1.2: Sheathed flagella	53
3.1.3: Flagella and the mammalian immune system	55

3.1.4: The <i>Bdellovibrio bacteriovorus</i> flagellum and motility	56
3.1.5: Genome analysis reveals that <i>B. bacteriovorus</i> HD100 has 6 flagellin genes	58
3.2: Collaborative studies of the <i>B. bacteriovorus</i> 109J flagellins	62
3.2.1: Electron microscopy – optimisation and development of imaging techniques for <i>B. bacteriovorus</i>	62
3.2.1.1: TEM observations of <i>B. bacteriovorus</i> bdelloplasts of various stages – flagella are not always shed immediately on prey penetration	65
3.2.2: Collaborative inactivation of the <i>fliC</i> genes of 109J	71
3.2.2.1: Inactivation of <i>fliC1,2,4</i> and <i>6</i> causes no gross morphological filament changes in strain 109J as examined by TEM	73
3.2.2.2: Inactivation of the cognate <i>fliC</i> genes in HD100 gave the same phenotypes by TEM as in <i>B. bacteriovorus</i> 109J	75
3.2.2.3: Inactivation of 109J <i>fliC5</i> produced truncated flagellar filaments and reduced predatory efficiency	79
3.2.3: Inactivation of 109J <i>fliC3</i> produced a strain capable only of prey-independent growth with sheath but no intact filament	79
3.2.3.1: Characterisation of the <i>fliC3</i> mutant sheath-like structure – are other flagellins retained?	81
3.2.3.2: Characterisation of the <i>fliC3</i> mutant sheath – Q-TOF MS/MS analysis of the dominant flagellin bands in 109 <i>fliC3::Kn</i> HI and HIK3	85
3.3: Is the FliC3 mutant still predatory even though it is non-motile?	86
3.4: Comparison of the sheared flagellar protein profiles of all the 109J flagellin mutant strains	88
3.5: Discussion	89
3.5.1: The entire <i>B. bacteriovorus</i> flagellum is not shed immediately upon prey entry	89
3.5.2: The role of flagellar-mediated motility in the predatory lifestyle of <i>B. bacteriovorus</i> – flagellar motility is necessary for successful predatory behaviour in liquid media but is not absolutely required for	

predation	89
3.5.3: The <i>B. bacteriovorus</i> flagellar sheath – an enduring mystery	90
3.5.4: Does the disparate distribution of <i>B. bacteriovorus</i> flagellin proteins when examined by SDS-PAGE indicate possible post-translational modification?	92
3.5.5. Possible models for the arrangement of different flagellins in the <i>B. bacteriovorus</i> 109J flagellum	92
3.5.6: Other observations of <i>B. bacteriovorus</i> biology as a result of this study	94

Chapter 4: The use of fluorescence techniques to understand *B. bacteriovorus* predation

4.1: GFP and its application in bacteria	96
4.1.1: GFP: Limitations and its prior reported uses in <i>B. bacteriovorus</i>	98
4.1.1.2: Previous use of GFP in <i>B. bacteriovorus</i>	99
4.1.2: pLOFKmgfp: construction and applications in bacteria	101
4.1.2.1: Could pLOFKmgfp be used in <i>B. bacteriovorus</i> to deliver promoterless GFP reporter genes?	103
4.2: Construction of <i>B. bacteriovorus</i> Transposon mutants	104
4.2.1: Phenotypes of selected GFP expressing <i>B. bacteriovorus</i> strains	113
4.2.1.1: Southern and Western blots of selected HD100 and 109J GFP-expressing strains show the transcriptional fusions of the <i>gfp</i> gene	114
4.2.2 Shotgun cloning and sequencing of HD100 GFP strains	115
4.2.2.1: HDGFP1 mini Tn10 <i>gfpKnR</i> insertion site	118
4.2.2.2: The mini Tn10 <i>gfpKnR</i> in HDGFP1 interrupts the gene encoding an heptosyl transferase family protein	119
4.2.2.3: HDGFP14 transposon insertion site	121

4.2.2.4: HDGFP13 transposon insertion site	122
4.3: Other fluorescence work in <i>B. bacteriovorus</i>	123
4.3.1: FM4-64 membrane staining	123
4.3.2: FM4-64 staining of <i>B. bacteriovorus</i> strains and <i>E. coli</i>	123
4.3.3: Predation of FM4-64 labelled <i>B. bacteriovorus</i> on unlabelled <i>E. coli</i>	124
4.3.4: Predation of FM4-64 labelled <i>E. coli</i> by <i>B. bacteriovorus</i>	128
4.4: Conclusions from fluorescence work in <i>B. bacteriovorus</i>	130
4.4.1: GFP transposon mutagenesis	130
4.4.2: Conclusions from FM4-64 work	131
4.4.2.1: Conclusions from FM4-64 work – implications for <i>B. bacteriovorus</i> predation	131
4.4.2.2: Conclusions from FM4-64 work – further evidence for the unusual nature of the <i>B. bacteriovorus</i> membrane	132
<u>Chapter 5: The role of Type IV pili in <i>B. bacteriovorus</i> predation</u>	135
5.1: What are Type IV pili?	136
5.1.1 General structure of the Gram-negative bacterial Type IV pilus	139
5.1.1.1: Roles of the Type IV pilus proteins in pilus formation: knowledge from other species	140
5.1.2: The genetics of Type IV pilus biogenesis	141
5.1.2.1: <i>Myxococcus xanthus</i> as a model for studying <i>B. bacteriovorus</i> Type IV pili	141
5.1.2.2: <i>M. xanthus</i> Type IV pili and mutant phenotypes	142
5.1.2.3: Conservation of Type IV pilus genes between <i>Myxococcus</i> and <i>B. bacteriovorus</i>	143
5.1.3: Previous <i>B. bacteriovorus</i> work on pilus-like fibres and hypotheses for holdfast structures	147

5.2:	Hypothesis and my evidence for <i>B. bacteriovorus</i> expressing and using Type IV pili for prey entry	149
5.3:	Electron microscopic analysis of <i>Bdellovibrio bacteriovorus</i> to ascertain the presence of pilus-like fibres on the cell surface	151
	5.3.1: Observation of pilus-like fibres on the non-flagellar pole of <i>B. bacteriovorus</i> HD100 and 109J	152
	5.3.2: Observation of ring-like structures on the anterior pole of HD100	153
	5.3.3: Are the fibres Type IV pili or Flp pili? The HD100 genome encodes an incomplete set of genes requires for Flp pilus formation	154
	5.3.4: Bioinformatic analysis to identify prospective Type IV pilus genes: multiple <i>pilQ</i> homologues are found in the HD100 genome	157
	5.3.5: Bioinformatic analysis to identify prospective Type IV pilus genes: multiple <i>pilT</i> homologues are found in the HD100 genome	159
	5.3.6: PilA and its biogenesis, structure and function	161
	5.3.6.1: PilA from other species – the crystal structures and sequence characteristics of Type IVa pilins shared by <i>Bdellovibrio</i> PilA	161
	5.3.6.1.1: How do Type IV pili bind to their target?	164
	5.3.6.2: The role of PilD in PilA maturation	165
	5.3.6.3: PilA in 109J – pilus-like fibres are seen on the pole of the <i>B. bacteriovorus</i> cell	165
	5.3.6.3.1: Attempts using PCR to clone 109J <i>pilA</i>	166
	5.3.6.3.1.1: Attempts using PCR to clone 109J <i>pilA</i> – primers designed to conserved regions of <i>pilA</i> and <i>pilG</i>	167
	5.3.6.3.1.2: Sequencing of putative HD100 and 109J <i>pilAG</i> sequences	171
	5.3.6.3.2: Southern blots of 109J genomic DNA using the HD100 <i>pilA</i> sequence as a probe	172

5.3.6.3.3: Shotgun cloning of the 109J to find <i>pilA</i> and the resulting sequences	174
5.4: HD100 <i>pilA</i> inactivation – the rationale	175
5.4.1: The strategy for <i>pilA</i> inactivation	176
5.4.1.1: Scheme showing the screening protocol for <i>B. bacteriovorus</i> mutant strains	178
5.4.2: Characterisation of the resulting mutant strains	179
5.4.2.1: No pilus fibres were seen on HI <i>pilA:KnR</i> strains under the electron microscope.	182
5.4.2.2: No predatory capability was seen in the <i>pilA::Kn</i> HD100 HI strains: growth on <i>E. coli</i> overlays and use of the fluorescent prey assay	184
5.4.2.3: Attempts to use immunology to study the PilA protein: <i>B. bacteriovorus</i> PilA does not cross react with the Myxococcal anti-PilA antibody	187
5.4.2.4: Attempts to visualise pili on the surface of <i>B. bacteriovorus</i> HD100 cells using Cy5	190
5.5: Reverse Transcriptase PCR of <i>pilA</i> and other associated <i>pil</i> genes across the HD100 life cycle	193
5.5.1: <i>pilA</i> expression	195
5.5.2: <i>pilQ</i> , Bd0867, expression	195
5.5.2: <i>pilT1</i> , Bd1510, expression	195
5.5.3: <i>pilT2</i> , Bd3852, expression	196
5.5.4: <i>pilD</i> expression	196
5.5.5: <i>tadA</i> , Bd0111 expression	197
5.5.6: <i>hit</i> , Bd0108 expression	197
5.5.7: <i>pilG</i> expression	198
5.6: Discussion	198

<u>Chapter 6: Final discussion</u>	200
6.1: Summary of research findings: the role of surface structures in the predatory lifestyle of <i>Bdellovibrio bacteriovorus</i> and implications of techniques developed	200
6.2: Further questions from this work and directions for future research	203
REFERENCES	207
APPENDIX 1	
APPENDIX 2 and 3 on accompanying CD	

ABSTRACT

Bdellovibrio bacteriovorus is a ubiquitous Gram-negative δ -proteobacterium that is predatory on other Gram negative bacteria. Its prey includes many pathogenic bacteria, including *E. coli*, *Salmonella*, *Proteus* and *Pseudomonas* species; as such, there is much interest in the study of *Bdellovibrio* with a view to its potential use as an alternative antimicrobial therapy.

Key to any future research into medical applications of this bacterium is an understanding of its predatory life cycle. Attack phase *Bdellovibrio* uses rapid flagellar motility through liquid environments to find its prey; upon collision with a suitable prey cell, it forms a strong attachment to the cell and generates a pore in the prey outer membrane. The predator then squeezes through this pore, loses its flagellum and establishes itself in the prey periplasm; the entry pore is then resealed, the prey rapidly killed with its peptidoglycan being modified to produce a rounded, osmotically stable structure termed the bdelloplast. Once safely within the bdelloplast, the *Bdellovibrio* secretes an arsenal of lytic enzymes into the prey cytoplasm which allow transport of the constituent monomers of DNA, RNA, protein et cetera from the prey back into the growing *Bdellovibrio*. The predator elongates as a spiral shaped filament within the periplasm of the prey and once the contents of the cytoplasm are exhausted, the filament septates into progeny *Bdellovibrio* which then re-synthesise flagella and lyse the remains of the prey cell to become free swimming attack phase predators.

In this thesis, the role of flagellar motility in the predatory lifestyle of *Bdellovibrio* was studied through individual insertional inactivation of each of the 6 genes found in the *B. bacteriovorus* HD100 genome that encode the flagellar filament protein, FliC. Only one was found to be essential for filament formation yet, contrary to previous hypotheses, this non-motile mutant was still found to be predatory when applied to immobilised prey in a novel fluorescence assay. Thus, the role of Type IV pili in predation was investigated through both microscopic, mutational and transcriptional means. Abolition of the Type IV pilus fibre forming protein, PilA, resulted in a mutant that had no pilus fibres and was incapable of predation using the same assay as in the non-motile FliC mutant strain.

Throughout this work, experimental challenges have necessitated the continuing development of electron microscopic techniques for whole cell, flagella, pili and bdelloplast imaging and development of fluorescence methods for use in *Bdellovibrio*, such as novel use of GFP-encoding transposon mutagenesis and chemical dye-based assays.

Work presented here has demonstrated that pili, not flagella, are the bacterial nano-machines required for prey entry and that GFP is a viable tool for future study of this fascinating and potentially therapeutic predator.

Chapter 1: Introduction

In my introduction, I illustrate what is known of predatory *Bdellovibrio bacteriovorus* with electron micrographic images that are results of my thesis work to avoid repetition in results chapters.

1.1: What are *Bdellovibrio*?

Bdellovibrio are Gram-negative δ -proteobacteria and are unusual with respect to their predatory life cycle. *Bdellovibrio* species are predatory on other Gram-negative bacteria, using them as a nutrient source for growth and division. Simply, the uni-flagellate predator attaches to, enters and consumes prey cells from within, resulting in multiplication of the *Bdellovibrio* and killing of the prey cell. *Bdellovibrio* are obligate predators and only grow and divide within the periplasm of their prey, being non-replicative outside this environment. The species at the focus my Ph.D work, *Bdellovibrio bacteriovorus*, has a sequenced genome from strain HD100 (Rendulic *et al.*, 2004) and has been physiologically studied since its discovery from soil samples in the early 1960s (Stolp and Starr, 1963). The publication of the genome sequence sparked a resurgence of interest in the *Bdellovibrio* field, which had slowed in previous years due to a lack of available genetic and molecular techniques. In combination with the genome sequence, the development of a novel method for gene interruption (Cotter and Thomashow, 1992a; Lambert *et al.*, 2003) means that this organism is once again at the forefront of scientific investigation, due to its potential medical applications and because of the fascinating biology of the predatory life cycle.

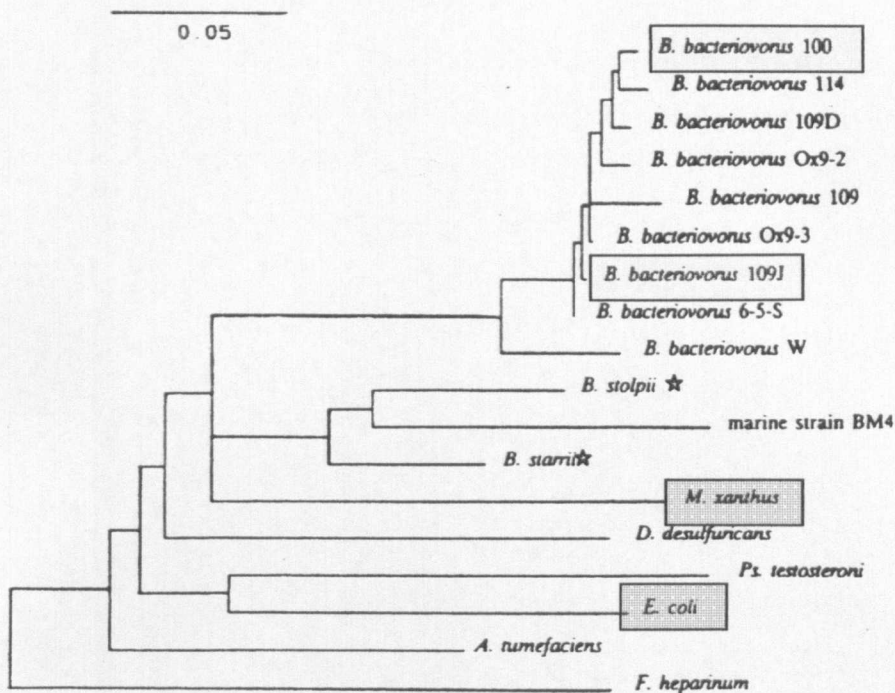


Figure 1.1: Phylogenetic tree from (Donze *et al.*, 1991) showing 12 *Bdellovibrio* strains in relation to other bacteria. “Fractional difference in 16S ribosomal RNA nucleotide sequence is given by the top scale bar; the difference between two strains is determined by summing all horizontal lines connecting the strains. Vertical distance has no significance”. Highlighted in yellow are the two main *B. bacteriovorus* strains used in this study, HD100 and 109J. Highlighted in blue are *M. xanthus*, a related δ proteobacterium also used in this work and *E. coli*, the most common prey strain used for growth of predatory *B. bacteriovorus*. *B* = *Bdellovibrio* (aside from the starred strains that have since been re-classified as related marine *Bacteriovorax* strains, (Baer *et al.*, 2000)), *D.* = *Desulfovibrio*, *M* = *Myxococcus* (both other δ proteobacteria), *Ps* = *Pseudomonas*, *E* = *Escherichia*, *A* = *Agrobacterium*, *F* = *Flavobacterium*.

1.2: *Bdellovibrio bacteriovorus* strains HD100 and 109J prey range and natural environments

B. bacteriovorus strains have an extensive prey range that includes virtually all Gram-negative bacteria (one exception for HD100 and 109J being α -proteobacteria such as *Rhodobacter sphaeroides*; L. Sockett, unpublished observation), from soil bacteria to pathogenic species (Fratamico and Whiting, 1995; Jurkevitch *et al.*, 2000) and are also most likely found associated with biofilms in nature, as biofilms themselves are susceptible to *Bdellovibrio* predation (Kadouri and O’Toole, 2005;

Williams *et al.*, 1995). This limitation to Gram-negative species is due to the need for *Bdellovibrio* to utilise the periplasm of the prey cell as an “incubator” for its growth and division; Gram-positive bacteria do not have a periplasm due to the differences in cell wall structure. This requirement also means that *Bdellovibrio* cannot use eukaryotic cells for their predatory life cycle, which will be discussed further in Section 1.7.

The diversity of bacterial species that can be preyed upon by *Bdellovibrio* also gives some indication as to their ubiquitous presence throughout a wide variety of natural environments. *Bdellovibrio* and related species have been isolated from both terrestrial and aquatic environments (Jurkevitch *et al.*, 2000; Varon and Shilo, 1980) and also from mammalian intestines, indicating that they may be an integral part of mammalian gut flora (Schwudke *et al.*, 2001). Predator-prey relationships have long been known to be an integral part of ecological relationships in controlling population levels so a single species does not become dominant in any particular environment. This also seems to be true for predatory bacteria; early work by Varon and more recent work in the Jurkevitch lab showed that there is always a very small population of prey species (*Erwinia caratovora*, *Photobacterium leiognathi* and *E. coli* in these experiments) that are seemingly resistant to *Bdellovibrio* predation, leading to classical predator-prey dynamics as the resurgent prey population is once again susceptible to predation. This led to the proposal of the development of a “plastic resistance” phenotype, rather than a stable genetic change in the prey (Shemesh and Jurkevitch, 2004; Varon, 1979). It is interesting to see predator-prey dynamics more usually obvious in the context of higher eukaryotes at the level of microscopic populations.

1.3: The predatory life cycle of *B. bacteriovorus*

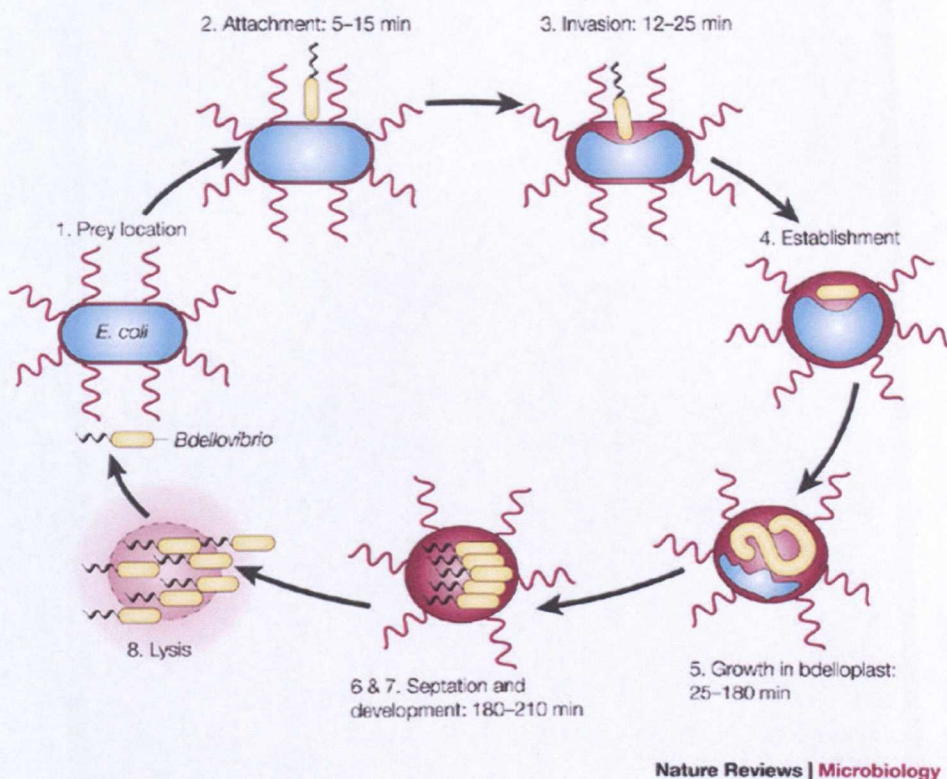


Figure 1.2: The *B. bacteriovorus* 109J predatory life cycle. Free swimming, attack phase *Bdellovibrio* locate, attach to and invade a suitable prey cell. Once the predator is established in the periplasm, the flagellum has been shed, the hole in the outer membrane used for entry re-sealed, an osmotically stable structure called the bdelloplast is formed. Within the bdelloplast, the prey cell cytoplasmic contents are broken down, transported into the growing *Bdellovibrio* filament. When the prey cell is exhausted, the filament septates, the progeny grow flagella and lyse the remnants of the prey to release more attack phase predators. The whole process takes on average 3–4 hours for 109J. Taken from (Sockett and Lambert, 2004) with kind permission.

1.3.1: The predatory life cycle – attack phase *B. bacterio vorus*

Attack phase, free swimming *B. bacteriovorus* are typically curved rods with a single, polar, sheathed flagellum and are competent to invade prey cells. Strain HD100 has this curved morphology, whilst strain 109J is almost straight, but both share the characteristic dampened waveform flagellum (See Figure 1.3 following page).

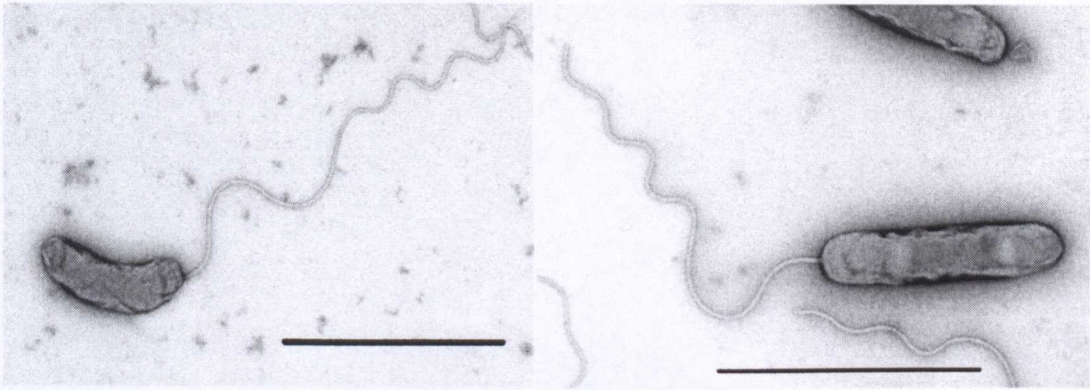


Figure 1.3: Comparative morphologies of attack phase *B. bacteriovorus* HD100 (left) and 109J (right). HD100 is more curved rather than the more classically rod-shaped 109J, but both share the characteristic single, polar, sheathed flagellum with a dampened waveform. Transmission electron micrographs, both stained using 1% uranyl acetate, bars = 2 μ m. (This thesis work)

Attack phase cells are small, typically 1/5 the size of an average *E. coli*, with HD100 cells being around 0.35 μ m x 1.1 μ m and 109J, slightly larger, 0.5 μ m x 1.5 μ m. Attack phase cells are non-replicative, so must seek prey within which to grow and divide. This occurs through a combination of flagellar-mediated motility at high speeds, with HD100 having been observed to swim at speeds of up to 160 μ m sec⁻¹ (Lambert *et al.*, 2006), apparent chemotaxis towards areas of prey-density (though the exact role played by chemotaxis remains controversial within the field) (Lambert *et al.*, 2003; Straley and Conti, 1977) and random collision. Through these collisions, *Bdellovibrio* forms reversible attachments to unsuitable prey, such as Gram-positive bacteria and abiotic surfaces, and temporarily reversible attachments to Gram-negative prey; these lead to the predator forming irreversible attachment to suitable prey species. The receptor sites required for attachment are obscure, but early work by Varon and Shilo suggests that there may be a role for the lipopolysaccharide (LPS) core sugars in prey recognition (Varon and Shilo, 1969). Certainly the resistance of certain α -proteobacteria to *Bdellovibrio* predation may be as a result of their unusual lipopolysaccharide (LPS) biochemistry: in *Rhodobacter sphaeroides*, the Lipid A component of the LPS blocks CD14-mediated activation of both human and murine immune cells, unlike LPS from other species such as *E. coli*, which is a potent immune stimulant (Kutuzova *et al.*, 2001)

1.3.2: The predatory life cycle – attachment and entry

Before invasion is achieved, *B. bacteriovorus* generates a small pore at the polar attachment site in the outer membrane of the prey cell, through which it squeezes into the periplasm of the prey (see Fig. 1.4).



Figure 1.4: Transmission electron micrograph of *B. bacteriovorus* HD100 invading an *E. coli* prey cell. The pore that is generated by the predator in the prey cell membrane is clearly smaller than the bacterium itself, so it must squeeze through – note the smaller size of the invading predator compared to the flagellar pole - to establish itself in the periplasm of the prey. Stained with 1% uranyl acetate, bar = 0.2 μ m. (This thesis work)

The enzymatic activities involved in the generation of the entry pore have only so far been profiled through enzymic work in the 1960s, and include solubilisation of some of the prey LPS amino sugars, excision of some peptidoglycan sugars and an associated burst of glycanase activity that ceases once prey penetration is completed (Thomashow and Rittenberg, 1978b, 1978c). Prey-attachment of *B. bacteriovorus* via the non-flagellar pole means that the “hydrolytic cocktail” of enzymes required for entry are likely to be applied in a localised manner that apparently prevents damage to the predator itself and limits damage to the prey. This pore is ultimately re-sealed once *B. bacteriovorus* has established itself in the periplasm.

The mechanism by which the predator squeezes through the pore it has generated in the outer membrane has been controversial for some years, with different hypotheses being put forward. These include active “drilling” through the use of flagellar motility (Burnham *et al.*, 1968) and the use of Type IV pili to enter prey (Rendulic *et al.*, 2004) which only became fully apparent once the genome had been analysed. As these hypotheses formed the basis of much of my thesis work, they will be given in-depth consideration in the relevant sections (see Chapter 3 and Chapter 5, respectively).

1.3.3: The predatory life cycle – establishment and growth

Modification/partial solubilisation of the prey peptidoglycan associated with entry (Thomashow and Rittenberg, 1978b) also results in the “rounding up” of the prey cell into an osmotically stable structure, termed the bdelloplast, within which the predator has a secure intracellular niche within which to consume the prey and grow. As an example of this “molecular security” and osmotic stability of the bdelloplast environment, I have observed bdelloplasts containing progeny *Bdellovibrio* that are motile in solutions of pH 9 where all attack phase cells are non-motile, their flagellar motors paralysed by the alkaline pH of the solution.

Prey entry and establishment in the periplasm is also associated with the, presumably regulated, loss of the *B. bacteriovorus* flagellar filament (Thomashow and Rittenberg, 1979), which will again be discussed in greater detail in Chapter 3.

Within the stable bdelloplast structure (the prey cell is rapidly killed, usually within 10-20 minutes of prey penetration), *B. bacteriovorus* is free to start degrading prey macromolecules contained within the prey cytoplasm in a controlled manner, including sugars, DNA, RNA and proteins, and transport them into the predator, which uses these for its own growth as a filament within the periplasm. The kinetics and biochemical characterisation of *B. bacteriovorus* intra-periplasmic growth are summarised in Rittenberg’s excellent review from 1982 (Rittenberg, 1982).

The exact mechanism(s) by which the predator transports its own lytic enzymes and the resultant prey molecular products are unknown. *B. bacteriovorus* has to transport charged, organic molecules across not only its own inner and outer membranes, but potentially also the inner membrane of the prey. The genome encodes a plethora of transporter proteins, but lacks Type III and IV transport systems, that could perform this function; which proteins are actually utilised is, as yet, unknown (Rendulic *et al.*, 2004). Electron microscopic observation of bdelloplasts does show that the predator's outer membrane is in extremely close contact with the cytoplasmic membrane of the prey (see Figure 1.5 below). This presents the possibility of the use of membrane vesicles that are used for secretion of degradative enzymes, such as peptidoglycan hydrolases, to damage other bacteria. In Gram-negative bacteria, the membrane vesicles fuse with the outer membrane of another cell, releasing their contents, such as enzymes, into the periplasm (for a review, see (Beveridge, 1999)). This system could provide a mechanism for secretion of hydrolytic enzymes into the prey cytoplasm from the predator; however this is pure speculation as there is no prior evidence for *Bdellovibrio* species producing membrane vesicles within the attachment/establishment phase of predation; any experiment or microscopic visualisation of this possibility would be extremely difficult. One technique which is showing tremendous promise in imaging whole bacteria in three dimensions is 3D electron tomography (reviewed in (Subramaniam, 2005)). Study of *Bdellovibrio* using this technique (currently underway in the Subramaniam lab at NIH, Bethesda) may well offer more information on these processes.

As the *B. bacteriovorus* filament growth continues, DNA replication precedes protein synthesis; the former is also completed before the latter (Gray and Ruby, 1989). The “counting” mechanism employed by the predator, to ensure that each progeny cell has a complete chromosomal copy, is a mystery (see Section 1.5 for more discussion of this).

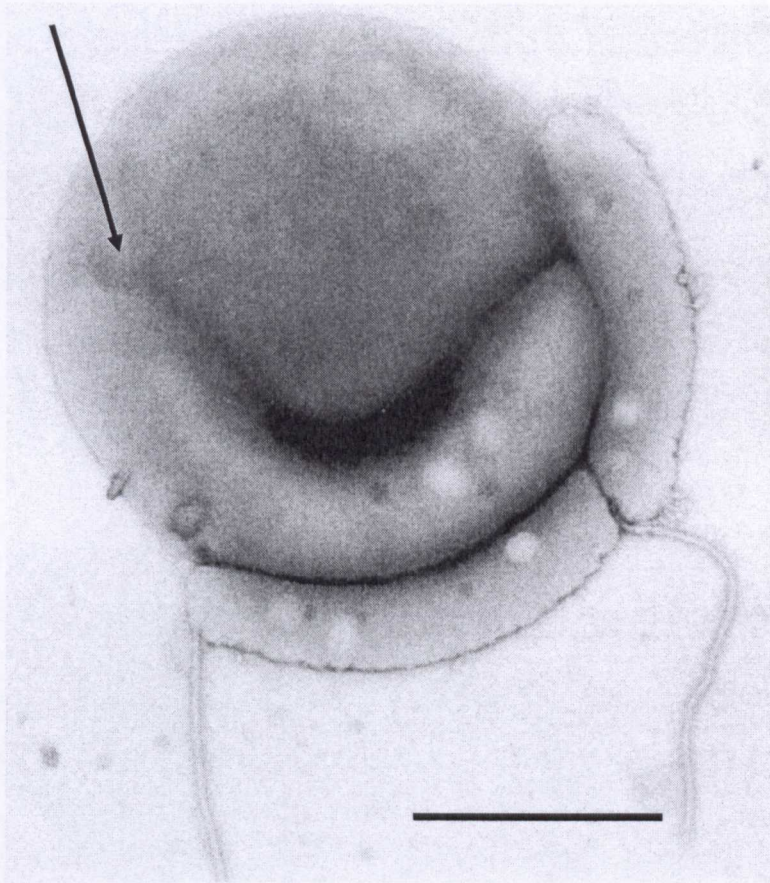


Figure 1.5: Electron micrograph of *B. bacteriovorus* 109J inside a bdelloplast formed on *E. coli* DFB225. Note the close contact (indicated by the arrow) between the membranes of the predator and prey. This figure also shows a typical bdelloplast rounded structure. NB, there are two free *Bdellovibrio* attached spuriously to the outside of the bdelloplast, probably as an artefact of removal of the bacterial culture from the EM grid. Stained with 1% phosphotungstic acid pH7, bar = 1 μm . (This thesis work)

1.3.4: The predatory life cycle – septation and lysis of the prey cell

Once the prey cell contents are exhausted, the *B. bacteriovorus* filament starts to septate and divide into progeny cells (see Fig. 1.6 below). Again, the regulatory signal(s) that start cell division is unknown. An interesting feature of *Bdellovibrio* biology is that unlike other bacteria, it does not seem to utilise classical binary fission for division, as uneven numbers of progeny are often seen when observed under the microscope. The number of progeny produced seems to depend on the initial size of

the prey, and therefore the amount of nutrients available; for example, larger cells of *Proteus mirabilis* prey produce on average more progeny *Bdellovibrio* than smaller prey such as *Salmonella enterica* serovar Typhimurium (my unpublished observation through microscopic observation).

Once the *B. bacteriovorus* filament has septated, the progeny cells synthesise flagella and are motile within the bdelloplast (see video DSCN1202 on accompanying CD, this thesis work) before a final burst of lytic activity to release the fresh attack phase *B. bacteriovorus* into the surrounding medium to seek fresh prey.

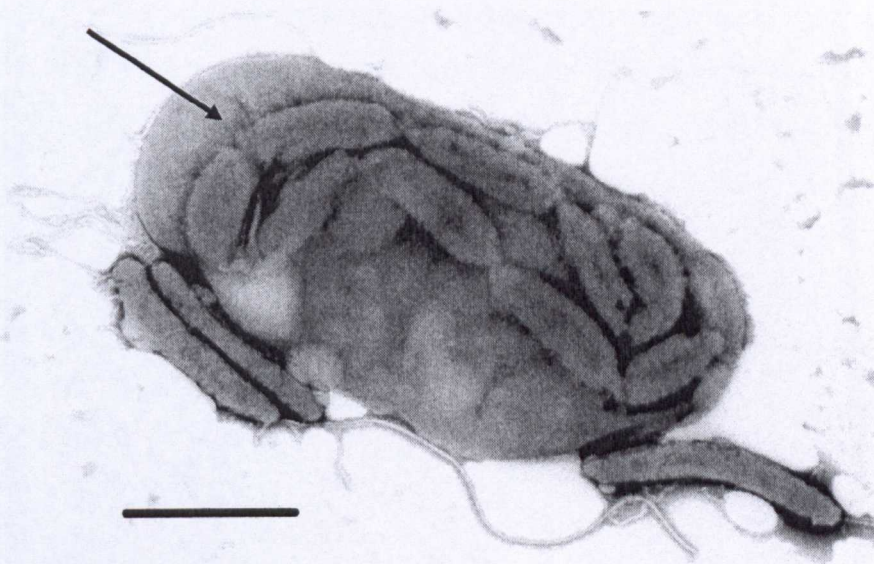


Figure 1.6: *B. bacteriovorus* 109J cells septating inside a bdelloplast (*E. coli* S17-1). There are 9, possibly 10, progeny 109J within the prey – a large number due to S17-1 being more pleiomorphic and generally larger than other *E. coli* lab strains. The arrow indicates an incomplete septa. NB, also note the 3 other spurious attack phase *Bdellovibrio* outside of the bdelloplast. Transmission electron micrograph, stained 1% phosphotungstic acid pH7, bar = 1 μ m. (This thesis work)

1.4: The phenomenon and applications of Host Independence in *B. bacteriovorus*

For *B. bacteriovorus* there is also an alternative available to the predatory life cycle described above. *B. bacteriovorus* can grow slowly axenically in the absence of prey if grown in rich media, such as PY used in this work (see Appendix 1 for media compositions). Host-Independent (HI) strains can be isolated from predatory cultures

by concentration of the predators by centrifugation and plating on rich media agar with no prey. Incubation at 29°C for a week or more results in the appearance of small, individual bacterial colonies which range from almost colourless to bright yellow (due to increased carotenoid levels (Barel and Jurkevitch, 2001)) in pigmentation.

HI *B. bacteriovorus* arise from these isolations at a frequency of 10^{-7} to 10^{-8} (Stolp and Starr, 1963); it is thought that the initial acquisition of the ability to grow axenically results from a single gene mutation. Work by Cotter and Thomashow identified a genetic locus, termed *hit* (host interaction), which was mutated in three separate HI mutant strains; however, recombination of the wild-type copy of *hit* failed to fully restore the predatory capability of these strains, indicating that there are potentially other loci involved in the development of fully axenic *B. bacteriovorus* (Cotter and Thomashow, 1992b). This hypothesis was borne out by work in the Jurkevitch lab which showed that in a larger sample of HI strains, not all had nucleotide sequence changes in the *hit* locus (Barel and Jurkevitch, 2001). It was proposed by Horowitz and colleagues in 1974 that the most logical initial mutation to cause this phenotype would be in a regulatory gene controlling growth initiation (Horowitz *et al.*, 1974). I would agree with this hypothesis, as, for example, a mutation in a regulatory gene that restricts *B. bacteriovorus* growth and division to only those periods of prey habitation would then allow growth and division without the need for establishment of the bdelloplast “incubator”, so long as the nutrients required were supplied. Further mutations in cell division regulators/genes would potentially give HI cells their ability to grow to many times the length of prey-dependent *B. bacteriovorus* as is commonly seen in many different HI strains. There are systems in other bacteria that mediate inversions of DNA segments to alter the orientation of promoters/regulatory regions, such as the *Hin/Fis* site specific recombination system that controls flagellar variation in *Salmonella enterica* serovar Typhimurium (reviewed in (Henderson *et al.*, 1999)). Mutation or activation of invertases or site-specific recombination mediators may also have a role in the generation of HI cells.

HI *B. bacteriovorus* differ from their HD (prey-dependent) parents in several ways. Perhaps the most striking is the difference in morphology. Figure 1.7 below

illustrates just some of the possible morphological phenotypes displayed by these strains. Morphologies of cells from singles colonies isolated at the same time from the same HD culture can differ; morphologies commonly seen range from spiral shapes, star shapes where several cells stem from the same point, extremely long, straight cells (up to 30 μm length, personal observation) to cells that are long but “kinked”.

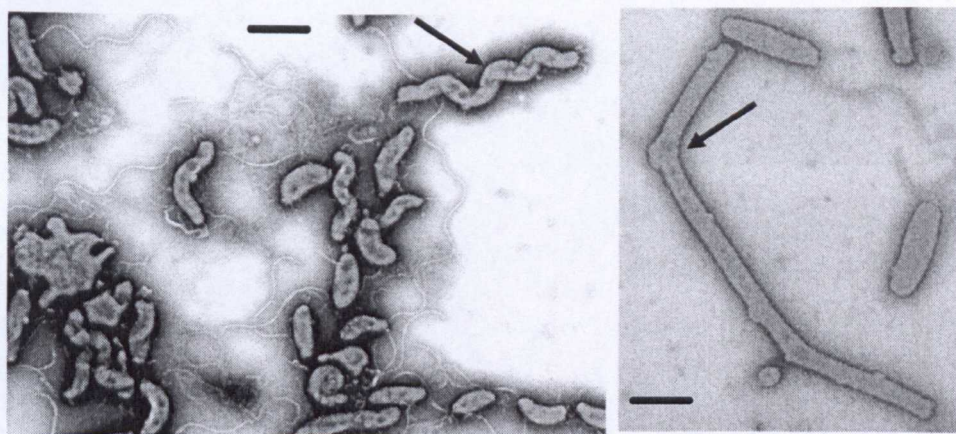


Figure 1.7: Host-Independent (HI) cells of *B. bacteriovorus* 109J. Left panel, strain HIK3, derived from parental 109JK (a Kanamycin-resistant 109J), showing the diverse morphologies exhibited even within the same culture grown without prey from an individual colony. Right panel, strain HS42, a 109J derivative. Arrow indicates the branch point where the cell has apparently failed to divide successfully, resulting in elongation of the cell. Note that HI cells are still flagellate. Transmission electron micrographs, both stained with 1% phosphotungstic acid pH7, bars = 0.2 μm . (This thesis work)

Like their parental HD *B. bacteriovorus*, HI cells are also flagellate, but have been observed to have more than one flagellar filament, unlike the HD strains which have a single, polar flagellum. On the cells with multiple flagella, the basal bodies anchoring the filaments into the cell are usually seen where the cell “kinks”; this appears to me to be where the cell has attempted division but it has not been completed successfully, resulting in an abortive cell pole. Problems with aberrant cell division would possibly support the hypothesis that a mutation associated with the development of the HI phenotype would be a regulator involved in control and timing of cell division.

Unlike their parental HD strains, HI cells can be facultatively predatory, especially when freshly isolated. Continued culturing of HIs without prey results in the loss of this weak predatory capability, again pointing to rapid accumulation (and selection for) mutations in the genome over time.

The growth cycle of HI strains has never been fully delineated as each strain seems to behave differently. Microscopic observation of the cultures over time shows that they mimic the intra-periplasmic growth of HD strains, forming filamentous cells that divide with varying degrees of success, as shown by the appearance of some long cells, and some smaller cells that seem to resemble wild-type *B. bacteriovorus* in their morphology. However, the extent to which the cells physiologically mimic the intra-cellular bdelloplast phase of their prey-dependent parental strains is currently unknown. HI also, particularly when freshly inoculated into rich media as a pure culture, go through a growth phase where all the cells are rounded up, reminiscent of bdelloplasts, a phenomenon that has yet to be explained (personal observation).

Host-Independence is a useful laboratory tool. HI growth can be used to rescue engineered mutations that would otherwise be lethal to prey-dependent *B. bacteriovorus*, for example, those that interfere with predation. This will be explored further later on in Chapters 3 and 5 as this tool has been employed in those sections of my work.

1.5: The *B. bacteriovorus* HD100 genome

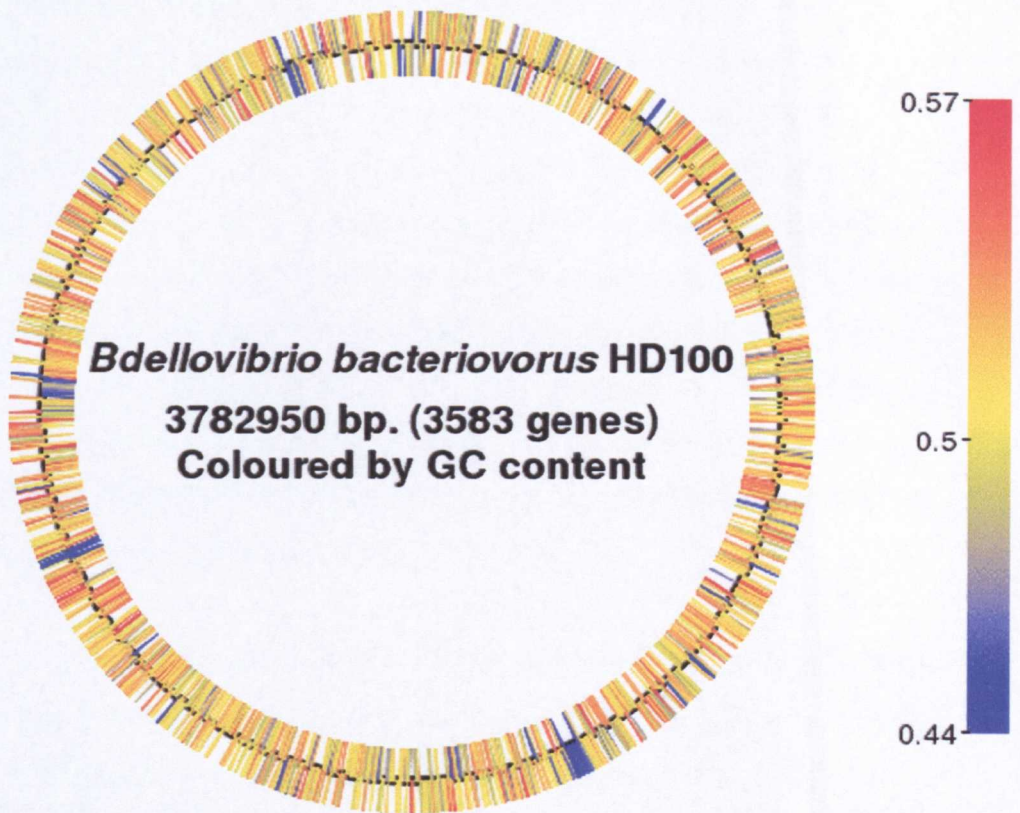


Figure 1.8: Graphical representation of the HD100 genome coloured by GC content. Genes coloured red have a GC content value greater than 0.57, those coloured yellow have a GC content value of less than 0.44. The scale bar shows the colour of genes with intermediate GC content values (within 2 standard deviations of the mean).

For such a tiny predator, *Bdellovibrio bacteriovorus* HD100 has a surprisingly large genome at 3.8Mb (Rendulic *et al.*, 2004). The enormous amount of DNA synthesis required for *Bdellovibrio* replication is demonstrated by the fact that from an average *E. coli* with a genome size of 4Mb, 4-5 progeny *Bdellovibrio* are derived, with a total genomic DNA content of 15.2 – 19Mb (Figure 1.6 earlier demonstrates that odd numbers of progeny can be obtained from a large *E. coli*, requiring immense amounts of DNA synthesis; a total of 34.2Mb of *Bdellovibrio* DNA). Again, the regulatory signal that terminates DNA synthesis when the prey precursors are exhausted is unknown.

The sequencing of the HD100 genome has opened up many interesting targets for research. *B. bacteriovorus* 109J is better characterised physiologically, but HD100 is

the type strain (DSM50701) originally isolated in 1963 (Stolp and Starr, 1963). Work in our laboratory, in collaboration with the Schuster group showed that the genome encodes 3584 predicted proteins, of which only 55% can be assigned predicted function through homology searches. At least some of the remaining 45% of predicted proteins presumably have some function in the predatory processes which, by their nature, are not found in other bacterial species. The genome sequencing of *Bacteriovorax marinus* strain SJ (a representative of the marine *Bdellovibrio* clade) at the Sanger Centre and *B. bacteriovorus* strain W, which is capable of forming a resting, encysted stage within the bdelloplast (Tudor and Conti, 1977) should shed some light on which protein products are essential for *Bdellovibrio* predation (see Chapter 5 for a consideration of possible conservation of certain pilus genes between *B. bacteriovorus* and *Bacteriovorax*).

Within the rest of the genome, HD100 has a full gene complements for both flagellar and Type IV pilus systems (see Chapters 3 and 5 respectively); the genome encodes transporters for multi-drug resistance, organic solvent resistance, amino acids, phosphates and nitrates; a large complement of hydrolytic enzymes, including over 150 proteases and peptidases, 10 glycanases, 20 deoxyribonucleases, 9 ribonucleases and 15 different lipases, which together make up one of the largest numbers of degradative enzymes seen in sequenced bacterial genomes; however, the genome lacks genes encoding Type III and IV secretion systems (Rendulic *et al.*, 2004). The large number of different proteases and peptidases alone, presumably for use with different Gram-negative prey species, provide promising targets for isolation and characterisation for future therapeutic use.

Through the course of sequencing the HD100 genome, no plasmids were found in this strain. This is not surprising considering the nature of *B. bacteriovorus* growth and division; growing as a coencytic filament that divides by septation rather than using classical binary fission may cause problems with successful plasmid segregation. This idea is supported by considering the inability of our lab, and other groups, to find a plasmid that replicates stably (Cotter and Thomashow, 1992a) (RES lab, unpublished observations; John Tudor, personal communication to RES; in conflict with the observations of (Flannagan *et al.*, 2004) who reported that pMMB206 can be stably replicated in *Bdellovibrio*; see Section 4.1.12. for further

discussion of this). The absence of native plasmids dictates the methodologies by which gene manipulation can be performed.

1.6: Working with *B. bacteriovorus* in the lab – experimental barriers

At the start of this work, only one instance of gene interruption created in *B. bacteriovorus* was reported (Lambert *et al.*, 2003) and little or no work on the use of fluorescence as a tool to probe the lifestyle of this fascinating predatory bacterium. Genetic tools were, and still are, limiting: there has been no plasmid (reproducibly) found to stably replicate in this organism, meaning there is no possibility as yet of in-trans expression or complementation – standard techniques in other systems. The non-standard metabolic requirements of *B. bacteriovorus* also mean that a “suicide” based approach to forcing gene replacements, such as the *mobsacB* sucrose suicide system (Schafer *et al.*, 1994), have not been used as yet.

B. bacteriovorus is resistant to many common antibiotics, or easily develops spontaneous resistance. For example, *B. bacteriovorus* is naturally resistant to high concentrations of ampicillin, ruling out selective gene inactivation using many other β -lactam antibiotics (Mark Martin, personal communication, RES lab observation). Spontaneous resistance mutants can be generated easily when the bacteria are grown with chloramphenicol, rifampicin and tetracycline (this work, data not shown, observational experiments) again ruling out these antibiotics as good selective makers for gene interruptions. This leaves kanamycin sulphate (standard concentration $50\mu\text{g ml}^{-1}$) as the only effective antibiotic marker for gene interruption as. Until another antibiotic resistance marker is found, only single gene disruptions will be possible in *B. bacteriovorus*.

Together, these considerations show that any kind of engineered gene interruption takes much time and effort in screening for the desired mutation. For the same reasons, point mutagenesis, which does not involve introduction of selective markers, is also as yet not feasible.

The predatory nature of *B. bacteriovorus* also complicates matters further. The addition of prey cells such as *E. coli* necessitate additional controls (with appropriate

antibiotic resistance as necessary) in any experiment and cause delays or difficulties in obtaining pure cultures of the predator for further analysis. As *B. bacteriovorus* prey dependent cells can only be grown as plaques on plates with soft agar overlays of the prey species, replica plating is extremely difficult and has as yet not been reproducibly applied, once again complicating any standard genetic screen. More pressingly, the most obvious and interesting mutants are those that reveal the predatory nature of *B. bacteriovorus*. Mutations or gene interruptions that cause a weakly predatory or predation-deficient strain are naturally not easily cultivated as prey-dependent. Therefore, Host-Independence (HI) must be employed. As explained in Section 1.4, HI *B. bacteriovorus* can be grown axenically on rich media and do not require the presence of prey cells for growth and division, providing a rescue for mutant strains that are not able to be cultured as prey-dependent. It does, however, bring its own complications. Due to the nature of the HI phenotype, the cells are themselves mutants, containing a mutation somewhere in the genome (see Section 1.4) which allows them to grow in the absence of prey. Therefore, rescuing mutants using the HI state is creating a double mutant. However, this is offset by the ability to further characterise a strain that would otherwise not be obtained through prey-dependence. In part, this problem is partially alleviated through the independent derivation of several mutant HI lines with a specific engineered gene interruption to ensure the same overall phenotype is observed.

A further complication of working with *B. bacteriovorus* is the physical size of the cells. As Joshua Lederberg called them, “nature’s fleas” are extremely small, with HD100 being on average $0.35\mu\text{m} \times 1\mu\text{m}$, causing problems for microscopists. The major drawback is using fluorescence in these bacteria. For example, Chapter 4 discusses my work in this area; the main challenge has been visualising fluorescently labelled *B. bacteriovorus*. Electron microscopy is the only reliable method for examining the physiology and other characteristics of the bacterium; in this work I have developed and furthered previous whole cell staining techniques, as against the more damaging fixation and sectioning techniques employed in earlier studies (for example, (Burnham *et al.*, 1968)), to explore different aspects of *B. bacteriovorus* biology, particularly in bdelloplast imaging. Unfortunately, electron microscopy cannot by the nature of the technique, reveal fluorescence.

1.7: Possible applications of *Bdellovibrio* in medicine

A major interest in studying *Bdellovibrio* is for its possible therapeutic applications. As mentioned in Section 1.5, the HD100 genome encodes a huge number of different proteases and peptidases that should be effective against a large number of Gram-negative pathogens (Rendulic *et al.*, 2004) that form part of the *B. bacteriovorus* prey range. The other potential application for this predatory bacterium is its potential to be a “living antibiotic”. As discussed in Section 1.2, *B. bacteriovorus* will eliminate virtually all potential prey through its natural growth and division. In theory, it may be useful in topical applications such as treating *Pseudomonas* infections of burn wounds; *Bdellovibrio* could potentially be applied in liquid form or in some sort of dressing and in combination with a low dose antibiotic (for example, ampicillin, to which *B. bacteriovorus* are naturally resistant) would eliminate the infection. Research in this area is essential due to the emergence of more and more multi-drug resistant pathogenic Gram-negative bacteria, especially those involved in mucosal infections that would be accessible to *Bdellovibrio*, such as *Pseudomonas aeruginosa*, *Stenotrophomonas maltophilia*, *Burkholderia cepacia*, *Acinetobacter baumannii* and *Klebsiella pneumoniae* (reviewed in (Falagas and Bliziotis, 2007; Waters and Ratjen, 2006))

There are some promising signs for *Bdellovibrio* therapy. Schwudke and colleagues showed that *B. bacteriovorus* HD100 has an unusual Lipopolysaccharide (LPS) Lipid A (embedded in the outer membrane of Gram-negative bacteria) that are completely missing negatively charged residues in contrast to the phosphate groups that give Lipid A an overall negative charge in other bacteria (Schwudke *et al.*, 2003). Further tests showed a reduced endotoxic activity of this novel structure, as measured by the level of cytokine induction from human macrophages (Schwudke *et al.*, 2003) compared to other bacterial LPS; *B. bacteriovorus* LPS was less of an immune stimulant than its potential pathogenic prey.

Early work in the late 1970s by Lenz and Hespell showed that *B. bacteriovorus* could not replicate when micurgically injected into rabbit ovarian tissue and other mammalian cells, most probably due to differences in cell structure between eukaryotes and Gram-negative bacteria (Lenz and Hespell, 1978). This is

encouraging for using *Bdellovibrio* as a therapeutic agent in humans. Work in our lab, in collaboration with Dr Richard Pleass (Institute of Genetics, Nottingham), has shown promising initial results for *B. bacteriovorus* predation in serum and low IgG recognition of *B. bacteriovorus* HD100 from individuals not routinely exposed to the bacterium (Aslam, Pleass, Lambert, Evans and Sockett, manuscript in preparation).

However, much more needs to be discovered about this unusual bacterium before serious clinical studies can begin. Knowing the most basic details of precisely how this predator survives and replicates, and more about its biochemistry, are essential before any medical applications are taken into consideration.

1.8: Aims of this study

The main aims of this work were to:

- elucidate the role of *B. bacteriovorus* cell surface appendages, namely flagella and pili, in the initial stages of the predatory life cycle;
- to search for any differentially regulated genes between prey-dependent and – independent *B. bacteriovorus* using GFP tagging through the creation of transposon mutants and the use of fluorescence techniques to study this unique bacterium.

More detail and introduction to each specific area is given at the beginning of the appropriate chapter.

CHAPTER 2: MATERIALS AND METHODS

2.1: Strains, plasmids and primers used in this work

All bacterial strains and plasmids are described below in Tables 1 and 2 respectively.

Species/Strain	Description	Reference
<i>Escherichia coli</i>		
<i>E. coli</i> S17-1 (standard prey bacterium)	<i>thi, pro, hsdR, hsdM^r, recA</i> ; integrated plasmid RP4-Tc::Mu-Kn::Tn7	(Simon <i>et al.</i> , 1983)
<i>E. coli</i> S17-1:pZMR100 (standard prey for KnR <i>Bdellovibrio</i>)	<i>E. coli</i> S17-1 containing pZMR100, λ defective vector, Kn ^r	(Simon <i>et al.</i> , 1983) (Rogers <i>et al.</i> , 1986)
<i>E. coli</i> S17-1: pKJE102 (used for <i>pilA</i> gene interruption in <i>Bdellovibrio</i>)	pSET151 suicide plasmid containing <i>pilA::KnR BamHI</i> and <i>XbaI</i> , fragment in conjugation donor strain S17-1	This study
<i>E. coli</i> DFB225	<i>fliG</i> null RP437 derivative	(Lloyd <i>et al.</i> , 1996)
<i>E. coli</i> DFB225 pZMR100	DFB225 containing pZMR100, λ defective vector, Kn ^r	This study, (Rogers <i>et al.</i> , 1986)
<i>E. coli</i> SM10 (conjugative strain used for pLOFKmgfp Tn10 construct into <i>Bdellovibrio</i>)	λ <i>pir thi thr leu tonA lacY supE recA::RP4-2-Tc::Mu Km</i>	(Miller and Mekalanos, 1988)
<i>E. coli</i> DH5 α (standard cloning strain)	F' <i>endA1 hsdR17 (r_k m_k⁻) supE44 thi-1 recA1 gyrA (Nal^r) relA1 Δ(lacIZYA-argF) U169 deoR (ϕ80dlacΔ(lacZ)M15)</i>	(Hanahan, 1983)
<i>Bdellovibrio bacteriovorus</i>		
<i>Bdellovibrio bacteriovorus</i> 109J	Wild-type strain 109J	(Rittenberg, 1972)
<i>Bdellovibrio bacteriovorus</i> 109JK	KnR derivative of 109J	(Lambert, 2002)
<i>Bdellovibrio bacteriovorus</i> HD100	Wild-type strain HD100, genome sequenced	(Stolp and Starr, 1963) (Rendulic <i>et al.</i> , 2004)
<i>Bdellovibrio bacteriovorus</i> HI <i>pilA/pilA::Kn</i> , strains 2.1, 3.1, 4.2, 4, 5 and 6	Merodiploid HI derivatives of HD100 with wild type and KnR interrupted <i>pilA pilA/pilA::aphII</i>	This study
<i>Bdellovibrio bacteriovorus</i> HI <i>pilA::Kn</i> strains 1.3, 6.1, 6.3	Prey-independent HD100 derivatives with KnR interrupted <i>pilA pilA::aphII</i>	This study
<i>Bdellovibrio bacteriovorus</i> 109J <i>fliC1::Kn</i>	Prey-dependent 109J <i>fliC1::aphII</i>	(Lambert <i>et al.</i> , 2006)

<i>Bdellovibrio bacteriovorus</i> 109J <i>fliC2::Kn</i>	Prey-dependent 109J <i>fliC2::aphII</i>	(Lambert <i>et al.</i> , 2006)
<i>Bdellovibrio bacteriovorus</i> 109J HI <i>fliC3::Kn</i>	Prey-independent derivative of 109J <i>fliC3::aphII</i>	(Lambert <i>et al.</i> , 2006)
<i>Bdellovibrio bacteriovorus</i> 109J <i>fliC4::Kn</i>	Prey-dependent 109J <i>fliC4::aphII</i>	(Lambert <i>et al.</i> , 2006)
<i>Bdellovibrio bacteriovorus</i> 109J <i>fliC5::Kn</i>	Prey-dependent 109J <i>fliC5::aphII</i>	(Lambert <i>et al.</i> , 2006)
<i>Bdellovibrio bacteriovorus</i> 109J <i>fliC6::Kn</i>	Prey-dependent 109J <i>fliC6::aphII</i>	(Lambert <i>et al.</i> , 2006)
<i>Bdellovibrio bacteriovorus</i> HD100 <i>fliC1::Kn</i>	Prey-dependent HD100 <i>fliC1::aphII</i>	This Study
<i>Bdellovibrio bacteriovorus</i> HD100 HI <i>fliC3::Kn</i>	Prey-independent HD100 <i>fliC3::aphII</i> derivative	This Study
<i>Bdellovibrio bacteriovorus</i> HD100 <i>fliC4::Kn</i>	Prey-dependent HD100 <i>fliC4::aphII</i>	This Study
<i>Bdellovibrio bacteriovorus</i> HD100 <i>fliC5::Kn</i>	Prey-dependent HD100 <i>fliC5::aphII</i>	This Study
<i>Bdellovibrio bacteriovorus</i> HD100 <i>fliC6::Kn</i>	Prey-dependent HD100 <i>fliC6::aphII</i>	This Study
<i>Bdellovibrio bacteriovorus</i> HDGFP strains (see section 4.2)	GFP+ KnR HD100 resulting from integration of GFP/KnR mini <i>Tn10</i> transposon from pLOFKmgfp. For details of strains, see Chapter 4	This study
<i>Bdellovibrio bacteriovorus</i> HDpLOF strains	GFP negative KnR HD100 resulting from integration of GFP/KnR mini <i>Tn10</i> transposon from pLOFKmgfp. For details of strains, see Chapter 4	This study
<i>Bdellovibrio bacteriovorus</i> 109JGFP strains	GFP+ KnR 109J resulting from integration of GFP/KnR mini <i>Tn10</i> transposon from pLOFKmgfp. For details of strains, see Chapter 4	This study
<i>Bdellovibrio bacteriovorus</i> 109JpLOF strains	GFP negative KnR 109J resulting from integration of GFP/KnR mini <i>Tn10</i> transposon from pLOFKmgfp. For details of strains, see Chapter 4	This study
<i>Myxococcus xanthus</i> <i>Myxococcus xanthus</i> DK1622	Wild Type genome sequenced strain	(Kaiser, 1979) TIGR

Table 2.1 Bacterial strains used in this study.

Plasmid	Description	Reference
pUC19	Cloning vector, ampicillin resistant (<i>bla</i>)	(Yanisch-Perron <i>et al.</i> , 1985)
pUC4K	pUC vector carrying kanamycin resistance cassette (<i>aphII</i>)	(Vieira and Messing, 1982)
pSET151	AmpR, ThioR, <i>oriT</i> , <i>lacZ^α</i> , suicide vector used for conjugal transfer of gene interruption constructs into <i>Bdellovibrio</i>	(Bierman <i>et al.</i> , 1992)
pLOFKmgfp	<i>oriR6K mob1 RP4</i> AmpR <i>lacIq</i> mini-Tn10 with promoterless <i>gfp</i> cloned upstream of <i>KnR</i> . Used for conjugation and transposition of <i>gfp</i> into the <i>Bdellovibrio</i> genome	(Stretton <i>et al.</i> , 1998)
pKJE100	pUC19 containing the 1.95kb <i>Bam</i> HI and <i>Xba</i> I digestion product of <i>pilA</i> and its flanking regions produced by PCR using <i>pilAF</i> and <i>pilAR</i> primers	This Study
pKJE101	pKJE100 with <i>Hinc</i> II-cut <i>KnR</i> cassette from pUCK4K blunt-ligated into the unique <i>Xcm</i> I site 204bp into the coding sequence of <i>pilA</i> .	This Study
pKJE102	<i>Bam</i> HI and <i>Xba</i> I fragment of <i>KnR</i> interrupted <i>pilA</i> and flanking regions from pKJE101 ligated using the same enzymes into pSET151 for conjugation into <i>Bdellovibrio</i>	This Study
pSB3000	<i>B. subtilis rpsJ</i> promoter fused to YFP (Clontech) followed by <i>rrnblt2</i> in pDest R4-R3, <i>bla</i> in backbone encoding AmpR	Gift from P. J. Hill, University of Nottingham
HDGFP1.7	<i>Eco</i> RI genomic fragment of HDGFP1 containing the mini Tn10 <i>gfpKnR</i> transposon cloned into pUC19	This study
HDGFP13.2	<i>Eco</i> RI genomic fragment of HDGFP13 containing the mini Tn10 <i>gfpKnR</i> transposon cloned into pUC19	This study
HDGFP14.5	<i>Eco</i> RI genomic fragment of HDGFP14 containing the mini Tn10 <i>gfpKnR</i> transposon cloned into pUC19	This study
pCL5511	<i>KnR</i> cassette interrupted 109J <i>fliC1</i> in suicide vector pSET151 for <i>fliC1</i> interruption in 109J and HD100	(Lambert <i>et al.</i> , 2006)
pCL5011	<i>KnR</i> cassette interrupted 109J <i>fliC2</i> in suicide vector pSET151 for <i>fliC2</i> interruption in 109J and HD100	(Lambert <i>et al.</i> , 2006)
pCL5211	<i>KnR</i> cassette interrupted 109J <i>fliC3</i> in suicide vector pSET151 for <i>fliC3</i> interruption in 109J and HD100	(Lambert <i>et al.</i> , 2006)
pCL5311	<i>KnR</i> cassette interrupted 109J <i>fliC4</i> in suicide vector pSET151 for <i>fliC4</i> interruption in 109J and HD100	(Lambert <i>et al.</i> , 2006)
pCL5411	<i>KnR</i> cassette interrupted 109J <i>fliC5</i> in suicide vector pSET151 for <i>fliC5</i> interruption in 109J and HD100	(Lambert <i>et al.</i> , 2006)
pCL5111	<i>KnR</i> cassette interrupted 109J <i>fliC6</i> in suicide vector pSET151 for <i>fliC6</i> interruption in 109J and HD100	(Lambert <i>et al.</i> , 2006)

Table 2.2 Plasmids used in this study. Please note, pLOFKmgfp carries a kanamycin resistance gene; notation is different to standard used in this thesis due to its creation by other laboratories.

Cloning Primers	5'-3' sequence
pilAF	5'CGGAATTCCAGGCGAGGGTGAACTCAGG
pilAR	5'CGGAATTCCTTGAGTCAAGCGACCGGTGC
pilAcon1_1	5'CGGGATCCCCTCGCTTGTAGAGTTGATGG
pilGcon1_2	5'CGGGATCCCCTCGCTGATCCAGAGAATAT
pilAup1_4	5'CGGGATCCCCTCGATCCAGACAGGACCTTGAT
pil11 (3' end of <i>pilG</i>)	5'TAGGGTGAAGGACTTGTGTC
M13/pUC19 universal -21 forward	5'TGTA AACGACGGCCAGT
M13/pUC19 reverse -29	5'CAGGAAACAGCTATGACC

Internal RTPCR Primers	5'-3' sequence
pilA3F_RT	5' GAAAGCTCGTCAGTCCGAAG
pilA3R_RT	5' CACCCGCTAGCACAGTACAA
pilQ1F	5' TCGTCAGGTGACTCAGAACG
pilQ1R	5' GAACACCCACTTCACCGTCT
(for <i>pilT1</i>) pilT17F	5' TCTGTGACCAATGCTCTTCG
pilT17R	5' CAAAGTCAGAATGCCGGAGT
(for <i>pilT2</i>) pilT26F	5' GAACTGGATTCGCCTACA
pilT26R	5' ACCACGATCACAAATCGATCA
pilD7F_RT	5' GCTGTTTGCGCTTTCTTACC
pilD7R_RT	5' ACGTGCAGACAACAAGTCCA
(for hit Bd0108) hit2F_RT	5' TCCTTCCATCTTGCTGACC
hit2R_RT	5' AGGCCTCATTAGGGTCTTCG
pilG8F_RT	5' GCGTTGTTGATGGTGTGTC
pilG8R_RT	5' CATCGGAGGAGGAGCTATCA
tadA1F_RT	5'CGGTATCACCCGTGAAAAGT
tadA1R_RT	5' ACGTTCAGACCGTTTTCCAC
fliC1F	5'GCATCTATCGCAGCACAACG
fliC1R	5'CCGTCGAGTCGGCATCAAATTCAA
fliC2F	5' GAACGTATCCGCTATCAACG
fliC2R	5'TAGTGCAGAGTTTGGCATCG
fliC3F	5'ATGCTCAGAGAGTTCTCTGG
fliC3R	5'AATGACTTGTTCAAGAGTCC
fliC4F	5'TCGGTACCAATGTGGCAGCG
fliC4R	5'ATTGTTGTGACTGGTTCGCC
fliC5F	5'GCTCAACGTAACCTGGTCGG
fliC5R	5'GCTCAACGTAACCTGGTCGG
fliC6F	5'TCAGCTTTAACGCCAACTGG
fliC6R	5'TCAGCTTTAACGCCAACTGG

Table 2.3 previous page: Primers used in this study; for the majority of sequencing, M13/pUC19 universal primers were used. Alternatively, internal RTPCR primers given in the table as indicated were used for RTPCR or mutant screening.

Primers used throughout this study were supplied by MWG-Biotech (except for pilAF and pilAR which were supplied by Invitrogen and treated in the same manner) and were diluted to 100pml/ μ l stock solutions with sterile distilled water and stored at -20°C. All primer sequences used in this study are listed in Table 2.3 above.

2.2: Bacterial growth conditions

All bacterial growth media sterilised by autoclaving. Antibiotic concentrations used are as stated in table 2.4. All chemicals purchased from Sigma unless otherwise stated.

2.2.1: Escherichia coli

E. coli strains were routinely cultured on YT (5g/L sodium chloride, 5g/L peptone, 8g/L tryptone, adjust to pH 7.5 using 2M NaOH. For YT agar add 10g/L agar) plates streaked to single colonies; these were then inoculated in YT broth of appropriate volume with the necessary antibiotics and grown at 37°C, 200rpm shaking overnight. *E. coli* were either grown as prey strains for *B. bacteriovorus* or for use in DNA cloning. Storage of plates was at 4°C for up to 2 weeks. 15% glycerol stocks were kept indefinitely at -80°C.

2.2.2: Bdellovibrio bacteriovorus prey-dependent (HD) strains

B. bacteriovorus host-dependant strains were grown on soft agar overlay plates of host *E. coli* cells (100 μ l per plate) consisting of YPSC bottom and an overlay containing the prey cells of semi-solid YPSC agar (0.125g/L magnesium sulphate, 0.25g/L sodium acetate, 0.5g/L Bacto peptone(Difco), 0.5g/L yeast extract, adjust to pH 7.6 using 2M NaOH. Add 0.25g/L calcium chloride dihydrate using sterile 25g/L stock after autoclaving. Bottom YPSC: add 10g/L agar, top YPSC: add 6g/L agar).

These were incubated at 29°C for 3-10 days until plaques of *B. bacteriovorus* appeared. The single plaques were then picked into 2ml Ca²⁺/HEPES (5.94g/L HEPES free acid, 0.284g/L calcium chloride dihydrate, adjust to pH 7.6 using 2M NaOH) buffer containing 150µl of overnight culture of appropriate prey cells and antibiotics as necessary, and incubated at 29°C, 200rpm shaking overnight. These lysates then resulted in a 99% pure (by microscopy) culture of *B. bacteriovorus* and could be scaled up to any volume to 1L, keeping the ratio of 3:1 prey:predator (v/v), e.g. 30ml of an overnight culture of prey (on average, approximately 1x10⁹ cells ml⁻¹) and 10ml predators (on average, 3x10⁸ cells ml⁻¹).

Lysates were kept for up to 1 week at 4°C and 15% glycerol stocks were kept indefinitely at -80°C.

2.2.2.1: Host Independent isolation and growth of *Bdellovibrio bacteriovorus*

Host-independent (HI) were isolated as described previously (Lambert *et al.*, 2006). Briefly, HI strains were isolated when required by prey-dependent strain filtration through a 0.45µm filter to separate out prey cells and then plating on rich PY media (10g/L peptone, 3g/L yeast extract, adjust to pH 6.8 using 2M NaOH. For PY agar add 10g/L agar), containing antibiotics as necessary. Filtration of the prey-dependent strains was necessary to remove prey cells which would grow faster than the newly derived HIs, which typically take 5-12 days to form single colonies at 29°C.

Growth of HI strains in liquid broth was achieved by inoculation of a single colony into 500µl PY containing antibiotics as necessary at 29°C, 200rpm. After 2 days, 500µl PY was added to the starter culture and grown under the same conditions. Larger volumes were grown by successive additions of PY broth to double the total culture volume, resulting in 1L broths in roughly 8 days. The nature of HI cells means that this is the only way of obtaining large volumes; a single colony inoculated into 50ml PY will not grow even after being left for nearly 2 weeks.

Plates of HIs were stored at room temperature for up to 3 weeks then discarded and 15% glycerol stocks were kept indefinitely at -80°C.

Antibiotic	<i>E. coli</i>	<i>B. bacteriovorus</i>
Kanamycin	50µg/ml	50µg/ml
Ampicillin	50µg/ml	N/A

Table 2.4. Typical antibiotic concentrations used for different bacterial species. All concentrations as used, unless otherwise stated for a specific strain/construct.

2.2.3: *Myxococcus xanthus*

M. xanthus strains were cultured on CYE (10g/L casitone, 5g/L yeast extract, 8mM magnesium sulphate in 10mM MOPS buffer, adjusted to pH 7.6. For CYE agar add 10g/L agar) plates incubated at 29°C for 3-5 days. Broth cultures were grown by inoculation into CYE broth, 29°C, 200rpm for 2 days. Plates were kept at room temperature for up to 2 weeks, 15% glycerol stocks were kept indefinitely at -80°C.

2.3: DNA manipulation techniques

2.3.1: Small scale isolation of plasmid DNA

For routine screening of multiple transformants to determine the most likely clones for further work, a fast version of plasmid isolation by alkaline lysis was used. 200µl of an overnight *E. coli* culture was lysed with freshly made 1% sodium dodecyl sulphate (SDS), 2M NaOH, inverted to mix, then neutralised with 3M potassium acetate, pH5.5. This mix was centrifuged for 5 min at 16,400 x g in a microcentrifuge to pellet cell debris and the supernatant removed to a new tube. Addition and mixing of 500µl 100% isopropanol removed excess salts from the plasmid DNA.

Centrifugation at 16,400 x g for 2 min pelleted the clean plasmid DNA; removal of the supernatant and drying the DNA pellet allowed resuspension in 20µl Tris-EDTA (10mM Tris-HCl, pH8.0, 2mM EDTA) and downstream screening.

Favoured clones were the re-grown from master plates in YT broth with necessary antibiotics at 37°C overnight. Plasmid DNA was prepared from these using Qiagen™ Mini-prep kits using alkaline lysis and column purification of DNA according to manufacturer's instructions.

pLOFKmgfp, used for transposon mutagenesis of *B. bacteriovorus*, is a very low copy number plasmid and is 10.8kb, just over the size cut-off for most manufactured column purification systems. Therefore, for larger scale preparations of pLOFKmgfp, necessary for Southern blotting etc, phenol chloroform extraction was used. Briefly, 1.5ml of an overnight culture of *E. coli* SM10:pLOFKmgfp was pelleted at 16,400 \times g in a microcentrifuge, resuspended in 100 μ l TEG lysis solution (25mM Tris-HCl pH8, 10mM EDTA pH8, 1% glucose) and left at room temperature for \leq 5 min. 200 μ l alkaline-SDS solution (0.2M sodium hydroxide, 1% SDS) was added, mixed gently and incubated on ice for 5 min until the solution became viscous. 150 μ l of 3M sodium acetate pH5 was added and incubated on ice for 20 min with occasional mixing to precipitate the cell debris; centrifugation at 16,400 \times g for 5 min pelleted the debris. The supernatant was decanted and mixed by vortexing with one volume of phenol/chloroform/iso-amyl alcohol [25:24:1] (Sigma), spun at 16,400 \times g for 5 min and the aqueous layer transferred to a fresh Eppendorf. This extraction was repeated twice more, then a single repeat with only chloroform to ensure full removal of the phenol. The clean supernatant was mixed with 2.5 volumes of ice cold 100% ethanol and left at -20°C for 30 min. This was centrifuged at 16,400 \times g for 5 min, the supernatant discarded and the plasmid DNA pellet washed with 70% ethanol. The final DNA pellet was resuspended in 20 μ l TE (10mM Tris-HCl, pH8.0, 2mM EDTA) and stored at -20°C for later use.

2.3.2: Large scale isolation of plasmid DNA

For midi preps of pUC19 and pSET151 –based clones, alkaline lysis and column DNA purification was carried out using either Sigma™ or Promega™ Midi prep kits according to manufacturer's instructions, typically yielding up to 5 μ g plasmid DNA.

2.3.3: Isolation of bacterial genomic DNA

Total bacterial genomic DNA was isolated using the Sigma™ Bacterial Genomic DNA mini-prep kit, according to manufacturer's instructions for Gram-negative bacteria (optimised for *E. coli* and other more usual bacteria), except for host-dependent *B. bacteriovorus* where 10ml of an overnight lysate was used and 2ml HI

cells to maximise yield of genomic DNA. Essentially, cell pellets from overnight cultures were lysed and treated with proteinase K and RNase A. Cellular proteins were precipitated but high molecular weight genomic DNA remained in solution. The genomic DNA was concentrated in columns and washed in ethanol-based wash solution. Genomic DNA was eluted in 200-25 μ l elution solution (10mM Tris-HCl, pH8.0, 2mM EDTA) and stored at 4°C until required.

2.3.4: Agarose gel electrophoresis

Agarose gel electrophoresis was carried out using 1x TBE (10.8g /L Tris-HCl, 5.5g /L boric acid, 6.0ml /L 0.375M Na₂-EDTA, pH8.0) supplemented with 0.1 μ gml⁻¹ ethidium bromide. Agarose concentrations varied depending on size of DNA fragments being sought, from between 0.8-2.0% (w/v TBE). Gels were run at a constant voltage of 100V and DNA was visualised under UV light using a BioRad™ gel documentation system. 5 μ l of ready to use GeneRuler™ 1kb DNA ladder (MBI Fermentas) (see Appendix 1 for marker sizes) was used as the molecular weight DNA marker for all gels apart from RTPCR gels (see section 2.5) when New England Biolabs 100bp marker was used to more accurately size the smaller fragments. DNA samples were loaded in 3x Orange G loading buffer (15% Ficoll (Sigma), 0.25% (w/v) Orange G dye (Sigma) in water to make 6x stock, 3x loading buffer made with 50% 6x stock and 50% glycerol (v/v)).

2.3.5: Restriction digest of DNA

Restriction endonucleases and buffers were obtained from New England Biolabs (NEB). Digests were carried out according to manufacturer's instructions using 1-10 units of enzyme for 2-6 hours at the recommended temperature (usually 37°C for most enzymes). Double digests were carried out in the buffer that gave the highest activity for both enzymes or carried out consecutively. Completion of all digests was verified by agarose gel electrophoresis.

2.3.6: Isolation of DNA fragments from agarose gels

DNA fragments to be used for cloning or as probes were excised from agarose gels using a sterile scalpel whilst visualising the DNA under UV light at 280nm. The DNA was purified from the agarose using the Qiaquick Gel Extraction Kit™ (Qiagen) according to the manufacturer's instructions. Basically, the agarose containing the desired DNA fragment was dissolved by incubation in buffer QG for 10 min at 55°C, the DNA bound to the silica column by centrifugation at 13000rpm in a benchtop centrifuge. The column and DNA were washed in ethanol and eluted in 25-50µl of low salt elution buffer (Qiagen) depending on the amount of DNA originally excised from the gel and the downstream concentration required.

2.3.7: Dephosphorylation of vector DNA

To reduce religation of vector DNA in ligation reactions, the 5' phosphate required for ligase action was removed from digested, purified vector DNA using Alkaline Phosphatase (Calf Intestinal, CIP, NEB). 1µl CIP was added to vector DNA in a reaction mix of typically 20µl in buffer 3 (NEB) and incubated at 37°C for 1 hour. The vector DNA was then purified using a QIAquick™ PCR purification Kit (Qiagen) (section 2.5.1) prior to downstream application.

2.3.8: Modification of DNA ends

Blunt-ending of DNA fragments with 5' or 3' overhangs were carried out using Cloned *Pfu* DNA polymerase (Stratagene) according to the manufacturer's instructions. Cloned *Pfu* DNA polymerase has a 3' exo-nuclease activity and 5'-3' fill-in activity so therefore can be used for blunting either 3' or 5' overhangs. Each 10-20µl reaction contained 1x cloned *Pfu* polymerase buffer, 4nM dNTPs (for fill in reactions), 2.5 units cloned *Pfu* DNA polymerase, ~100-500ng target DNA and sterile Analar™ water to the appropriate volume. The reaction was incubated at 72°C for 30 min and as cloned *Pfu* polymerase is not active at 16°C, the DNA could then be used directly in ligation reactions.

2.3.9: Ligation of restriction fragments

Ligations were performed in 10-20 μ l volumes. Reactions contained 2 units of T4 DNA Ligase (Invitrogen), 4 μ l 5x ligase buffer (Invitrogen) and a vector: insert ratio of 1:3 based upon estimates from agarose gel electrophoresis. The reaction volume was made up to the required volume using sterile distilled water. Reactions were incubated at 16°C for 16 hours or carried out at room temperature for 2 hours as necessary.

2.3.9.1: Shotgun cloning of genomic fragments

Used in finding GFP-transposon insertion sites and also for attempting to isolate the *pilA* gene from 109J. Southern blots (see Section 2.6) were carried out on total genomic DNA from the various strains, digested with an appropriate enzyme (for details, see main text) and the blots probed with either a kanamycin resistance gene isolated from pUC4K (for *B. bacteriovorus* mini Tn10*gfpKnR* mutant strains) or HD100 *pilA* (in the case of 109J). The sizes of cross-reacting bands were measured and digested genomic DNA was run on agarose gels, then sections of gel containing DNA of the appropriate size \pm 1kb was extracted. The DNA was purified and ligated to pUC19 cut with the same enzyme. The resulting ligation mix was transformed into *E. coli* DH5 α and plated on YT agar plates with the appropriate selection and screened as required (see Section 2.3.10).

2.3.10: Competence and transformation of *E. coli* with plasmid DNA

E. coli S17-1, *E. coli* DH5 α or *E. coli* DFB225 cells were made competent in batch stocks which were stored at -80°C by the following method.

5ml YT was inoculated with a single colony and grown overnight at 37°C with shaking at 200rpm as a starter culture. This was diluted 1/100 in YT broth and grown at 37°C with shaking at 200rpm to OD₆₀₀ of 0.4 to 0.5. The cells were pelleted by centrifugation at 5,000 \times g for 10 min then resuspended in 4°C TFB1 (30ml/100ml culture; 30mM potassium acetate, 10mM calcium chloride dihydrate, 50mM

manganese chloride tetrahydrate, 10mM rubidium chloride, 15% (v/v) glycerol (added after pH), pH adjusted to 5.8 using glacial acetic acid. Sterilised through a 0.2µm filter, stored at 4°C). The cells were incubated on ice for 5 min, then pelleted by centrifugation at 5,000 \times g for 10 min. The cells were resuspended in (4°C) TFB2 (4ml/100ml culture; 10mM MOPS, 75mM calcium chloride dihydrate, 10mM rubidium chloride, 15% (v/v) glycerol (added after pH). pH adjusted to 6.5 using glacial acetic acid. Sterilised through a 0.2µm filter, stored at 4°C), separated into 200µl aliquots and snap-frozen in liquid nitrogen before storage at -80°C. Each batch was tested by transformation with a control plasmid such as pUC19 and typically >1000 transformants resulted from transformation with ~50ng of control plasmid.

Transformation of competent cells was accomplished by incubating the cells with ligated vector/insert DNA for 20 min on ice; cells were then heat shocked at 42°C for 2 min, chilled on ice for 2 min, then had 1ml YT broth added and incubated at 37°C for 1 hour. The suspension was then pelleted at 16,400 \times g for 1 min, resuspended in 100µl YT and plated in necessary dilutions onto YT plates containing the necessary antibiotics. Incubation overnight at 37°C resulted in growth of transformant colonies, which were picked, streaked onto master plates and grown in YT broths to provide cultures for DNA preparation and screening of the plasmid constructs for the correct clone.

2.3.11: Conjugation of plasmid DNA into *B. bacteriovorus*

A prey culture lysate of recipient HD *B. bacteriovorus* was grown overnight at 29°C with shaking at 200rpm. 1ml of an overnight culture of donor *E. coli* S17-1 containing the desired construct was inoculated into 40ml of YT with appropriate selection and grown at 37°C, 200rpm to an OD₆₀₀ of 0.2-0.4. 10ml of the *B. bacteriovorus* cells were harvested by centrifugation at 11,950 \times g for 30 min at 4°C then resuspended in ~200µl Ca/HEPES and pipetted first for immobilisation onto a small piece (~2cm²) of Hybond-N (Amersham) nylon filter on a predried plate of PY agar. The 40ml of donor *E. coli* cells were harvested by centrifugation at 5,300 \times g for 5 min (thus avoiding shearing sex pili), resuspended in ~200µl YT and added to the filter. This resulted in approximately 10⁸-10¹⁰ *B. bacteriovorus* and 10⁷-10⁸ donor

E. coli cells, although the *E. coli* grow much more rapidly than *B. bacteriovorus* and so these numbers change throughout the experiment. The PY conjugation plates were incubated overnight (16 hours) at 29°C then the bacteria from the Hybond-N filter were resuspended in 1 ml YT by repeated pipetting.

Serial dilutions of 10^{-4} , 10^{-5} , 10^{-6} were used for growth as plaques on YPSC overlay plates supplemented with appropriate antibiotic selection and 100µl of *E. coli* S17-1:pZMR100 prey cells. As exconjugant numbers tend to be fairly low, overlay plates were also made with inoculums of 10µl, 100µl of neat YT broth suspension and the remainder of the resuspended conjugation mix as well as the serial dilutions. Numbers of exconjugants varied from $\sim 10^2$ – $\sim 10^5$ and generally represented a conjugation frequency of around 10^{-6} – 10^{-7} .

Exconjugants were then cultured into fresh lysates for 2-3 weeks daily with the appropriate antibiotic selection to encourage a double crossover event to replace the target gene. Dilutions of 10^{-4} to 10^{-6} were made and overlaid on YPSC plates, again with the appropriate prey cell and antibiotics. Plaques were then picked from these plates, grown in mini lysates for another 2-3 weeks and replated. 20 or more plaques were picked, grown in mini lysates (2ml) and then screened for a double crossover using PCR and Southern blots to screen for double recombinants and therefore gene replacement of the wild type target in the *B. bacteriovorus* genome.

2.4: DNA sequencing

1µg of dehydrated plasmid DNA template prepared using Qiagen™ DNA Mini-prep kits or 1µg of purified PCR product from genomic amplifications (see section 2.5.1 and 2.5.2) was sent for sequence analysis to MWG-Biotech Ltd, Germany. Primer concentrations were used at 100pmolµl⁻¹, or were synthesised by MWG. Each sequence run typically yielded 500-900bp of sequence of sufficient quality for confidence. Chromatograms received from MWG were examined for any possible errors in base calling and for determining which areas of the sequence data could be reliably used.

2.5: Amplification of DNA for cloning and mutant verification and RNA for use in expression studies

2.5.1: Polymerase Chain Reaction (PCR)

PCR was carried out in a ThermoHybaid gradient thermal cycler. PCR amplifications performed during this work were carried out using either Kod HiFi DNA polymerase (Novagen) or *Taq* DNA polymerase (ABGene). Kod HiFi DNA polymerase was always used for cloning work. *Taq* DNA polymerase was used for mutant screening before Southern blotting.

For Kod (Novagen) PCRs, a standard reaction mix of the following was used:

- 5 μ l 10x Kod buffer 2 (genomic DNA)
- 5 μ l Kod dNTPs (final concentration 0.2mM each)
- 2 μ l Kod MgCl₂ (final concentration 1mM)
- 1 μ l template chromosomal DNA (1-500ng)
- 2 μ l forward primer (0.2 μ M final concentration)
- 2 μ l reverse primer (0.2 μ M final concentration)
- 0.4 μ l Kod HiFi DNA polymerase
- 32.6 μ l PCR grade (sterile Analar) Water

Total reaction volume = 50 μ l

For *Taq* (ABgene) PCRs, a standard reaction mix of the following was used:

- 5 μ l 10x reaction buffer
- 5 μ l 10mM dNTPs (final concentration 0.5mM each)
- 5 μ l 25mM MgCl₂ (final concentration 2.5mM)
- 1 μ l template chromosomal DNA (1-500ng)
- 1 μ l forward primer (0.1 μ M final concentration)
- 1 μ l reverse primer (0.1 μ M final concentration)
- 1 μ l *Taq* DNA polymerase
- 31 μ l PCR grade (sterile Analar) Water

Total reaction volume = 50 μ l

Kod HiFi DNA polymerase amplifications required an extension time of 30 seconds to 1 min per kb of genomic template to be amplified. In contrast, *Taq* DNA polymerase based amplifications required an extension time of 1 min per kb of template. Specific reaction conditions for primer pairs are given as needed in the main text.

2.5.2: Purification of PCR products

PCR products were routinely analysed by agarose gel electrophoresis (section 2.3.4). Single-band fragments were purified using the QIAquick™ PCR purification kit (Qiagen) according to the manufacturers instructions. When multiple bands were observed from the PCR reaction, the desired fragment was excised from the agarose gel and purified using the QIAquick™ Gel Extraction Kit (Qiagen) (section 2.3.6) according to manufacturers instructions.

2.5.3: Reverse transcriptase PCR (RT-PCR) analysis of gene expression

2.5.3.1: Isolation of RNA from *Bdellovibrio* (carried out by Dr. Carey Lambert)

RNA was isolated as follows by Dr. Carey Lambert for use in my project. Briefly, for predatory cultures 5×10^8 - 5.6×10^9 of stationary-phase *E. coli* S17-1 were mixed with 5×10^8 - 3×10^{11} attack-phase *B. bacteriovorus* (as determined by cfu and pfu respectively) in Ca/HEPES buffer. After 15 min, samples were mixed to a final 1% (v/v) phenol and 19% (v/v) ethanol, and then the RNA extracted using Promega SV total RNA isolation kit according to the IFR published protocol (<http://www.ifr.bbsrc.ac.uk/Safety/Microarrays/protocols.html>) with the exception that RNA was eluted in 50µl rather than 100µl of sterile water. The RNA was further DNase-treated with the Ambion DNA-free kit according to manufacturer's instructions. Control infections of *B. bacteriovorus* only and *E. coli* only were also set up. For HI strains, axenic cultures were grown for 1–2 days in PY broth and then OD₆₀₀ of the cultures was matched (to 0.6) before being mixed (4ml) with phenol/ethanol and treated as for predatory cultures. Quantification of RNA was by OD₂₆₀ measurements. Samples for predatory cultures were taken at 15, 30, 45, 60, 120, 180 and 240 min post-infection (Lambert *et al.*, 2006)

2.5.3.2 Reverse transcriptase PCR (RT-PCR)

RT-PCR was performed using the Qiagen® One-Step RT-PCR kit on matched concentration RNA samples from *Bdellovibrio* predatory and HI cultures, also *E. coli* RNA as a negative control with the following conditions: one cycle of 50°C for 30 min, 95°C for 15 min, then 25 cycles of 94°C for 1 min, 48°C for 1min, 72°C for 2

min followed by one cycle of 72°C for 10 min then 4°C hold. 25 cycle amplification was used so that the PCR did not go to completion, allowing a semi-quantitative view of mRNA levels at a particular time point. Control reactions to test against the presence of contaminating *E. coli* or *B. bacteriovorus* DNA were carried out using PCR with Taq DNA polymerase (ABgene) for the same PCR conditions.

2.6: Southern Blot hybridisations

Southern blot hybridisations were carried out using the NEBlot Phototope Kit (New England Biolabs) according to manufacturer's instructions. Briefly, genomic and control DNA was digested with appropriate restriction endonucleases and resolved using agarose gel electrophoresis. DNA was transferred to a nitrocellulose membrane using capillary transfer (Sambrook and Russell, 2001), which was then probed with biotinylated DNA. Signal detection was carried out using the Phototope-Star Detection Kit (New England Biolabs) for chemiluminescent detection.

2.6.1: Transfer and immobilisation of DNA onto nitrocellulose membranes

Agarose gel electrophoresis of the digested DNA was carried out as described in section 2.3.4. 1µl of a 1/10 dilution of pre-biotinylated markers (New England Biolabs) (see Appendix 1 for marker sizes) were used in conjunction with 3µl of 1kb Generuler™ (MBI Fermentas) (see Appendix 1 for marker sizes). Agarose gels were then soaked in denaturation solution (0.5N sodium hydroxide, 1.5M sodium chloride, made up to 1L with water) for 30 min with gentle agitation, followed by two 15-min washes in neutralisation solution (1M Tris-HCl, 1.5M sodium chloride, adjusted to pH 7.5 using HCl. Made up to 1L with water). The denatured DNA was then transferred overnight to nitrocellulose membrane, pre-soaked in 2x SSC (20x SSC stock solution: 3M sodium chloride, 0.3M tri-sodium citrate, made up to 1L with water, pH to 7.0 using 10N NaOH) using 2x SSC as the transfer buffer by the capillary transfer method (Sambrook and Russell, 2001). After transfer, the membrane was allowed to dry and the DNA fixed to the membrane by UV cross-linking for 30 seconds at 50 mJoules in a BioRad GS gene linker UV chamber.

2.6.2: Synthesis of biotinylated probes

The specific DNA fragment required for probing was isolated by restriction digest (section 2.3.5), agarose gel electrophoresis (section 2.3.4) and gel purified using the Qiaquick™ gel extraction kit (Qiagen) (section 2.3.6). The DNA probe was then biotinylated according to manufacturer's instructions using the NEBlot Phototope Kit (New England Biolabs) to give roughly 350ng of probe.

2.6.3: Hybridisation

Hybridisation of biotinylated probes to immobilised DNA on membranes done according to the standard hybridisation protocol in the NEBlot Phototope Kit (New England Biolabs). Hybridisation was carried out overnight at 68°C where probe concentration was approximately 50ng/ml. After hybridisation, the membrane was washed twice in 2x SSC, 0.1% SDS at room temperature for 5 min, followed by two high stringency washes in 0.1x SSC, 0.1% SDS at 68°C for 15 min.

2.6.4: Chemiluminescent detection

Chemiluminescent detection of probe hybridisation to DNA on membranes was carried out using the Phototope-Star Detection Kit (New England Biolabs) according to manufacturer's instructions. Essentially, membrane bound biotinylated DNA is detected by first incubating the membrane in streptavidin, which binds to biotinylated DNA. Biotinylated alkaline phosphatase was added, which in turn binds the streptavidin, resulting in a conjugate between the alkaline phosphatase and the DNA bound to the membrane. CDP-Star reagent (New England Biolabs) was added; alkaline phosphatase catalyses the removal of the phosphate from the CDP-Star reagent (phenylphosphate substituted 1,2 dioxetane), giving a moderately stable intermediate, which then spontaneously decays, emitting light at 461nm wavelength. The emitted light is captured by exposing the membrane to x-ray film for 1-10 min as needed.

2.7: Protein analysis techniques

2.7.1: Sodium dodecyl sulphate polyacrylamide gel electrophoresis (SDS-PAGE)

SDS-PAGE (Laemmli, 1970) was used to check purity of flagella preps, QTOF-MS/MS analysis and prior to western blotting (see sections 2.7.3, 2.7.4, 2.7.5). SDS-PAGE gels were hand poured and prepared using the mini Protean II system (BioRad) and the BioRad Protean II xi cell for large scale SDS-PAGE gels. Unless otherwise stated, resolving gels were 12.5% acrylamide. (12.5% resolving gel: 9.475ml sterile distilled H₂O, 7.5ml 1.5M Tris-HCl, pH 8.8, 0.3ml 10% (w/v) SDS, 12.5ml 30% acrylamide/bis-acrylamide (Severn Biotech), 0.225ml 10% (w/v) (NH₄)₂S₂O₈ (ammonium persulphate), 0.015ml TEMED; 2.5% stacking gel: 14.76ml sterile distilled water, 2.54ml 1M Tris-HCl, pH 6.8, 0.2ml 10% (w/v) SDS, 2.5ml 30% acrylamide/bis-acrylamide (Severn Biotech), 0.15ml 10% (w/v) (NH₄)₂S₂O₈, 0.015ml TEMED)

Typically, 4-5µg protein, purified or whole cell extract, was run on the small SDS-PAGE gels and 8-12µg protein on larger gels. The Lowry protein concentration assay (see Section 2.7.2) was used to calculate protein concentrations; matched protein concentrations were run to enable comparison between samples. 2x sample buffer (0.6ml 0.5M Tris-HCl, pH 6.8, 1.0ml 10% SDS, 0.5ml glycerol, 0.25ml 0.5% (w/v) bromophenol blue) was added to a final concentration of 1x and the samples boiled for 5 min (with a brief centrifugation) prior to loading. The samples were then loaded onto typically 12.5% SDS-PAGE gels with a suitable molecular weight marker (BenchMark Protein Ladder [Invitrogen] for Coomassie stained gels, SeeBlue® Plus2 pre-stained standard [Invitrogen] for Western blots, see Appendix 1 for marker sizes). 1x running buffer (Tris-glycine, 9g Tris, 43.2g glycine, 3g SDS, made up to 600ml with distilled water) was prepared from a 10x stock. Gels were run at a constant 100V until the dye front was just running into the buffer.

Staining for non-western blot gels was performed overnight in Coomassie blue stain (0.1% (w/v) Coomassie brilliant blue (ICI), 30% (v/v) methanol, 10% (v/v) glacial acetic acid) and destained in 30% (v/v) Methanol, 10% (v/v) glacial acetic acid for several hours.

2.7.2: Lowry protein concentration assay

Total cell protein concentrations were determined based on the Lowry assay (Lowry *et al.*, 1951), which used SDS to improve cell lysis. Serial dilutions of protein standard, bovine serum albumin, were prepared ranging from 10-100 μ g/ml. 1ml sterile distilled water served as a blank. Cell extract samples were prepared by resuspending a cell pellet from ml culture in 125 μ l of sterile distilled water. A 50 μ l sample was combined with 3ml Solution C (Solution C: 100 solution A:1 solution B. Solution A: 2% Na₂CO₃, 0.4% NaOH, 0.16% sodium tartrate [C₄H₄O₆Na₂·2H₂O], 1% SDS. Solution B: 4% CuSO₄·5H₂O). Samples were mixed and incubated in the dark for 15 min. 0.3ml of fresh Folin's reagent diluted 1:1 with sterile distilled water was added to each sample and incubated in the dark for 45 min. 1ml aliquots were then read at the 750nm wavelength versus the blank. OD₇₅₀ versus protein concentration allowing the unknown cell sample concentration to be estimated from the standard curve. This assay was also scaled down to allow quantification of small amounts of purified protein.

2.7.3: Western blot analyses

Transfer of proteins from small SDS-PAGE gels (section 2.7.1) to a PVDF membrane support (Invitrogen) and to Hybond ECL membrane (Amersham) for larger gels was carried out using a Western blotting apparatus (Anachem) in transfer buffer (39mM Glycine, 48mM Tris, 0.037% (w/v) SDS, 20% (v/v) methanol) for 2 hours at 25V. Western blotting was carried out using the WesternBreeze Chemiluminescent Immunodetection system for anti-mouse or anti-rabbit antibodies as appropriate (Invitrogen) was carried out according to manufacturers instructions. The one adjustment made was that the membrane was incubated with primary antibody at a 1:1000 to 1:3000 dilution (depending on the antibody, as stated in main text) overnight with gentle agitation at 4°C.

2.7.4: Isolation of flagella, flagella sheath and flagella hook basal bodies (HBB) from *B. bacteriovorus*

2.7.4.1: Flagellar shearing of flagellin mutants for isolated filaments and sheath preparations

Flagellin mutants and appropriate wild type control strains were grown as standard to achieve large culture volumes. Cultures were matched to an OD₆₀₀ of 0.7 in final volumes of 2 × 300ml for HI strains, and to a cell number of 3x10⁸ cells ml⁻¹ for prey-dependent strains also in final volumes of 2 × 300ml. Cells were harvested at 4300 x g, 4°C for 45 min so as not to shear off sheath or flagella; pellets were then gently concentrated and resuspended in ice-cold 10mM HEPES pH 7.0, then combined to give a final volume of 10ml. These were passed 18 times through 30cm × 1mm cannulae (Smith Medical) on ice and centrifuged at 4300 x g, 4°C, 45 min to pellet the cell debris and leave sheath and any flagellar filaments from them in the supernatant. This supernatant was then ultracentrifuged at 115 000 x g, 90 min at 4°C and the resulting pellet resuspended in 225µl sterile TE (10mM Tris-HCl, 2mM EDTA, pH 8.0). Samples were then subject to Lowry assay for protein concentration (see section 2.7.2) and run on SDS-PAGE gels for further analysis (section 2.7.1).

2.7.4.2: Isolation of Intact Flagella with Hook Basal Bodies (HBB)

This technique was adapted for *B. bacteriovorus* from a method (Aizawa *et al.*, 1985) used in the lab of Professor S-I Aizawa, CREST Soft Nano-Machine Project, Prefectural University of Hiroshima, Japan in conjunction with S-I Aizawa and M. Kanbe. All containers (centrifuge tubes, beakers etc, were sterile).

1L of *B. bacteriovorus* lysate was centrifuged at 4°C, 15,000 x g for 30 min and resuspended in a total of 15ml of Sucrose solution (0.5M sucrose, 0.15M Tris, pH 9.5, chilled to 4°C). The suspension was stirred on ice to ensure smooth resuspension, checked microscopically. 100µl 10mg/ml 4°C freshly prepared lysozyme was added dropwise slowly over a period of 1 min; the suspension was covered and kept stirring on ice for approximately 30 min until cells had started sphaeroplasting when checked under the microscope (indicated by increasing

paleness of yellow *Bdellovibrio* cell suspension as cell walls start to break down). 1ml 20mM EDTA pH8 was added, again very slowly to chelate ion cofactors for proteases and other enzymes. After 10 min, the suspension was removed from the ice and brought quickly to room temperature by warming in hands; complete sphaeroplasting was checked by addition 2µl 10% Triton X-100 to a 20µl sample. If cells lysed, then sphaeroplasting was complete. 1ml 10% Triton X-100 was added and allowed to stir for no more than 10 min before 100µl batches of 0.1M MgSO₄ was added to provide endogenous DNase cofactors. It was found that *B. bacteriovorus* needs extra exogenous DNase (10mg/ml) added to efficiently break down DNA. Once all DNA had been degraded, 300µl 0.1M EDTA pH8 was added to stop enzyme activity. Cell debris was separated from the purified basal bodies/flagella by centrifugation at 5,200 \times g, 4°C for 25 min. Purified flagellar HBB were precipitated using 2% final concentration PEG/NaCl (20% polyethylene glycol (PEG)-3000, 1M sodium chloride) added to the cell-debris free suspension and precipitated overnight at 4°C. Rafts of flagella and basal bodies were then centrifuged at 5,200 \times g, 4°C, 30 min and resuspended in 150-250µl TE (10mM Tris-HCl, pH8.0, 2mM EDTA). Alternatively, the supernatant from the last spin was ultracentrifuged at 115,000 \times g for 2 hours at 4°C. The resulting pellet was again resuspended in 150-250µl TE (10mM Tris-HCl, pH8.0, 2mM EDTA).

Purified flagellar HBB were examined under the electron microscope (see section 2.8.2) and also by SDS-PAGE before further analysis.

2.7.5: Quantitative time of flight mass spectroscopy (QTOF-MS/MS) analysis of *B. bacteriovorus* isolated flagella/flagellar sheath

QTOF-MS/MS spectroscopic analysis of 109J HI *fliC3::Kn* and wild type HIK3, derived from 109JK (Lambert *et al.*, 2006) was carried out by Kevin Bailey from the University of Nottingham Biopolymer Analysis unit. Briefly, samples of isolated flagella/flagellar sheath were run on a 12.5% SDS-PAGE gel, lightly stained with Coomassie and briefly destained. The desired bands were excised from the gel around the predicted molecular weight of *B. bacteriovorus* flagellin (~29kD) and subject to an in-gel tryptic digest. The tryptic fragment were then analysed by QTOF-MS/MS to find flagellin peptides.

2.8: Microscopy techniques

2.8.1: Phase Contrast microscopy

Phase contrast microscopy of all bacterial strains was carried out on a Nikon Eclipse E600 microscope using the oil immersion 100x phase contrast lens. Microscope slides were prepared using 10µl bacterial culture.

2.8.2: Electron microscopy

Transmission electron microscopy (TEM) was carried out as necessary on whole bacteria and isolated flagellar proteins using carbon/formvar coated grids (Agar Scientific). Staining techniques vary from bacterium to bacterium and from structure to structure. Typically, samples were applied to grids, washed using sterile analar water if required and stained with 15µl of sample for 30 seconds to 1 min. Table 5 summarises the specific staining for different samples.

Sample	Volume sample	Stain	Grid wash?
<i>E. coli</i>	15µl	1% PTA pH7	Yes
<i>B. bacteriovorus</i> whole cell	15µl	1% PTA pH7	No
<i>B. bacteriovorus</i> pili	15µl	1% URA pH4	No
<i>Bdellovibrio</i> isolated flagella	5µl	1% PTA pH7 2% PTA pH7	No
Bdelloplasts	15µl	1% PTA pH7	No

Table 2.5: specific staining conditions for different samples for Transmission Electron Microscopy. PTA = phosphotungstic acid, URA = uranyl acetate.

In Nottingham, a JEOL JEM 1010 TEM was used with visualisation at 100kV. In Japan, a JEOL JEM 1200-EX TEM was used with visualisation at 60kV.

2.8.3: Fluorescence microscopy

Fluorescence microscopy of *B. bacteriovorus* and *E. coli* was carried out using 5µl samples which were agar mounted and examined under phase contrast and GFP (excitation 480nm) or YFP optics (excitation 500nm) as appropriate on a Nikon

Eclipse E600 epi-fluorescence microscope; images were taken using a Hamamatsu Orca ER camera and analysed using IPLab 3.6 (all supplied by Nikon UK).

2.9: Fluorescence techniques

2.9.1: Cy5 labelling of *B. bacteriovorus*

Cy5 monofunctional reactive dye (GE Healthcare/Amersham) was used to attempt to visualise pili on *B. bacteriovorus* cells using the method developed of use in *M. xanthus* (Mignot *et al.*, 2005). 10ml of *B. bacteriovorus* HD prey-dependent lysates were spun down in a Sigma benchtop centrifuge at 5200 $\times g$ at 4°C for 20 min. The pellet was washed with 1ml of room temperature labelling buffer, (50 mM K₂HPO₄/KH₂PO₄ pH 8.0, 5 mM MgCl₂, 25 μ M EDTA) by centrifugation for 10 min at 4°C, 7000rpm in a microcentrifuge. The cells were then gently resuspended in a further 1ml of labeling buffer with or without the Cy5 dye powder from one vial (the quantity used to label 1mg of protein) and incubated at room temperature for one hour. Cells were then washed twice as above to remove excess dye from the buffer to allow good visualisation. 5 μ l cells were then agar mounted and examined using GFP optics (see Section 2.8.3).

2.9.2: FM-464 labelling of bacteria

As described in section 4.3, predatory *B. bacteriovorus* HD100, 109J, an HD100 derived HI strain and *E. coli* S17-1 were labelled with FM-464, a lipophilic styryl membrane stain (Molecular Probes) in an attempt to observe the predation process. Details of specific experiments carried out are given in Section 4.3.

Cells were grown overnight as standard cultures for each species (see Section 2.2). 1ml of each bacterial culture was pelleted in a microcentrifuge and resuspended in 1ml of 10mM HEPES (free acid) pH7, 4°C. Stock FM-464 solution (1mg/ml, 4°C) was added to each to a final concentration of 5 μ g/ml and incubated on ice for 5 min. 5 μ l samples were then agar mounted and observed using the FITC (excitation 490nm) optics on a Nikon Eclipse E600 microscope using 100x magnification. More

intense staining used for HD *Bdellovibrio* strains was used at a final concentration of 100µg/ml.

2.9.3: Fluorescent assay for predatory capability of mutant strains of *Bdellovibrio*

To assess the predatory capability of the *HIpila::Kn* and *HfliC3::Kn* mutants (and also the non-*KnR* HID2 HD100-derived strain), constitutively YFP-expressing *KnR E.coli* S17-1:pSB3000 pZMR100 prey grown overnight to an OD₆₀₀ of 1.5 were challenged, on a solid PY agar surface, with the appropriate *B. bacteriovorus* mutant and merodiploid strains as necessary (experiments were tried on more dilute Luria Bertani agar but this could not support *B. bacteriovorus* viability during the experiment). The HI strains were grown for 3 days in PY Kn 50µg ml⁻¹ at 29°C to an OD₆₀₀ of 0.8 +/- 0.05; 50µl of YFP prey and 50µl *B. bacteriovorus* were mixed, spotted onto PY Kn⁵⁰ agar plates and incubated at 29°C for 24 hours. For the same test using the HID2 strain, it was grown for 3 days in PY broth only, at 29°C, 200rpm to the same optical density as for *HIpila* strains, and mixed with YFP prey that had been grown on 50µg ml⁻¹ ampicillin alone to select for the YFP-expressing plasmid (HID2 has no kanamycin resistance gene so its growth would be inhibited by the presence of kanamycin). This cell mixture was then spotted onto PY only agar plates and again incubated for 24 hours. At this time, the cells were scraped from the surface of the plate, resuspended in 1ml Ca²⁺/HEPES buffer, pelleted by centrifugation for 1 min, 16,400 x g in a microcentrifuge and resuspended in a final volume of 100µl. 5µl samples were agar mounted and examined under phase contrast and YFP optics on a Nikon Eclipse E600 microscope. *E. coli* uninfected prey and infected bdelloplasts numbers were counted (n> 2500 *E. coli* per experiment).

2.10: Bioinformatic analysis of DNA and proteins

2.10.1: BLAST analyses

BLAST analysis of proteins was carried out using the BLASTP server at NCBI www.ncbi.nlm.nih.gov/BLAST/ using the nr database and a BLOSUM62 alignment matrix using the standard NCBI default settings (gap costs existence 11, extension 1,

pairwise alignment view). NCBI protein database was also used of sequence retrieval as required.

2.10.2: Multiple alignments

Multiple protein and DNA level alignments and sequence examination was carried out using the BioEdit Sequence Alignment Editor, Version 7.0.1 © Isis Pharmaceuticals Inc. Reference: (Hall, 1999). Multiple alignments were created using ClustalW within BioEdit using the standard settings within the program, an 0% shading threshold for matching bases/amino acids and a BLOSUM62 alignment matrix. Reference: (Thompson *et al.*, 1994).

2.10.3: Plasmids maps and primer design for cloning and RT-PCR primers

Plasmid maps and theoretical restriction digests were created using Clone Manager Basic Version 8, © 1994-2005 Scientific and Educational Software.

Primers were designed either manually or using the Invitrogen OligoPerfect™ Designer at:

www.invitrogen.com/content.cfm?pageid=9716&CMP=ILC-

[OLIGOPERFECT&GPN=LAST](http://www.invitrogen.com/content.cfm?pageid=9716&CMP=ILC-OLIGOPERFECT&GPN=LAST)

Primers for PCR cloning or detection were designed with the parameters standard to the program, except the T_m changed to 55-65°C, 50% GC content and 50mM salt concentration.

Primer pairs were checked for less the 5 possible internal base-pairs between the two (which may reduce the efficiency of the PCR reaction) using the program mFold held at: www.idtdna.com/Scitools/Applications/mFold/Default.aspx/

2.10.4: Mass spectroscopic data analysis

For analysis of data files generated through Q-TOF MS/MS (see Section 2.7.5), raw data was analysed using the Matrix Science Mascot MS/MS program (recommended by Kevin Bailey at the University of Nottingham Biolpolymer Sequence Analysis Unit, QMC) to allow identification of peptide sequences generated.

www.matrixscience.com/cgi/search_form.pl?FORMVER=2&SEARCH=MIS

The parameters were as follows:

Database = NCBIInr

Taxonomy = all entries

Enzyme = trypsin

Fixed modifications = none selected

Variable modifications = carbamidomethyl (C), oxidated methionines

Peptide tolerance = +/- 1.2Da

MS/MS tolerance = +/- 0.6Da

Peptide charge = 2+ and 3+

Monoisotopic

Data format = Micromass (.PKL)

Instrument = ESI-QUAD-TOF

Reference: (Perkins *et al.*, 1999)

2.10.5: Computation of protein theoretical pI/mwt

For calculation of the predicted isoelectric point (pI) and molecular weight of proteins, sequences were inputted into the Expasy Compute pI/Mw tool held at:

www.expasy.org/tools/pi_tool.html

Reference: (Gustleiger *et al.*, 2005)

2.10.6: Image creation

Images were created and visualised/cropped for publication using either Adobe Photoshop Version 7.0.1, © 1990-2002 Adobe Systems Inc. or Microsoft ® Office Powerpoint ® 2003 (Microsoft Office Professional Edition) © 1997-2003 Microsoft Corporation.

Chapter 3: Flagella and their role in *B. bacteriovorus* predation

The aim of this work was to elucidate further the role of flagellar-mediated motility in the lifestyle of this highly motile organism, and to clarify previous research on *B. bacteriovorus* flagellar motility by application of novel techniques. My work in this area was published in (Lambert *et al.*, 2006) where I was second author, and most of the 109J work was done in collaboration with Dr Carey Lambert, with additional work by Rob Till, Laura Hobley and Michael Capeness. Their work will be briefly summarised, with my work for the paper and further characterisation described in more detail. All work done in this chapter on flagella in *B. bacteriovorus* strain HD100 was done by me. Transmission electron microscopy of 109 strains was done by me in collaboration with Professor Shin-Ichi Aizawa in Japan.

3.1: Flagella and bacterial motility – an overview

Flagella are bacterial organelles found throughout the Bacteria, in both Gram-positive and Gram-negative species. They are highly organised and complex protein structures, utilising their own specific Type III secretion system; the rotation of a rigid flagellar filament provides the motive force behind much bacterial motility. The flagellum itself can be thought of in three specific parts: the basal body, the hook and the filament, extending from the cytoplasm of the cell to the cell exterior. The best characterised flagellar systems are in the enteric Gram-negative bacteria, *Escherichia coli* and *Salmonella*, which I will review briefly, though for a more detailed review, I would recommend (Macnab, 2003).

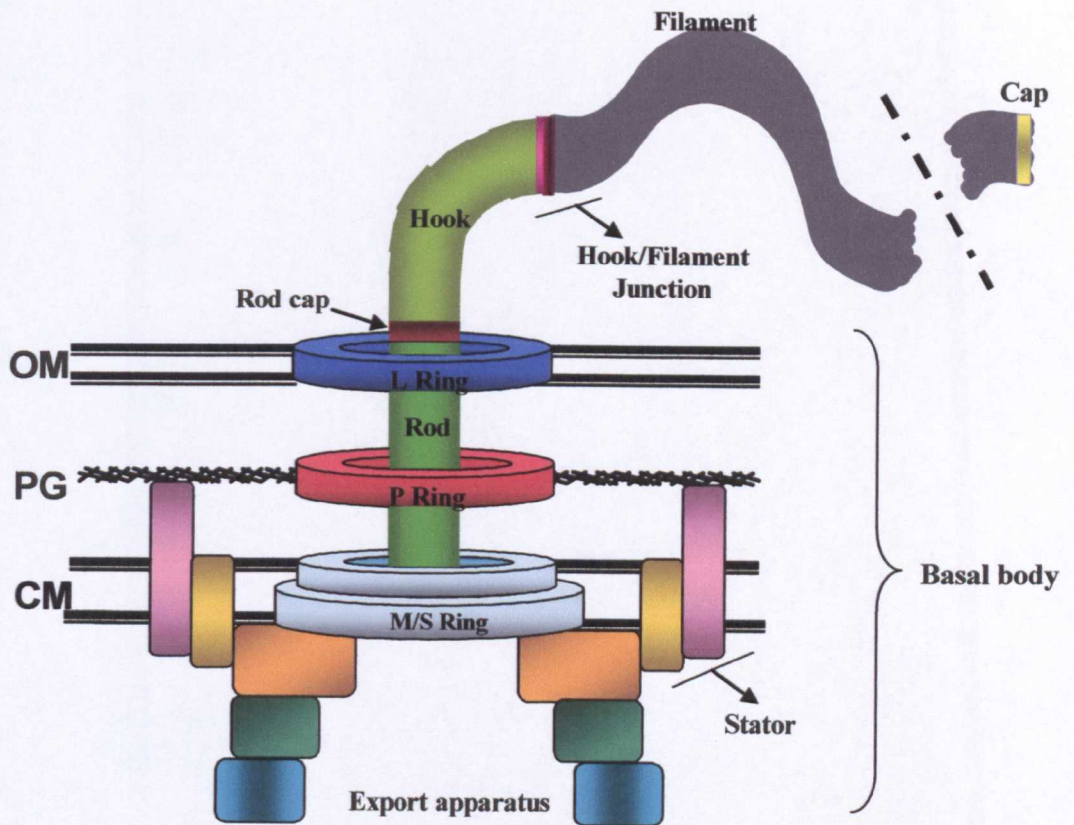


Figure 3.1: General structure of the Gram-negative flagellar complex. The following table gives the protein names and functions (colour coded). The complex extends from the cytoplasm of the bacterial cell to the exterior, with the basal body providing an anchor. This cartoon illustrates the general structure only; there are variations and uncertainties in the positioning of some of the components. Regulatory proteins and those involved in export are not shown, please refer to (Macnab, 2003) for a full review. OM = outer membrane, PG = peptidoglycan, CM = cytoplasmic membrane.

Part of Flagellar Complex	Diagram	Protein (stoichiometry in enteric bacteria)	Function	<i>B. bacteriovorus</i> gene number
STATOR		MotB (32)	Contributes to H ⁺ /Na ⁺ conductance and exerts torque against rotor/switch	MotB1 Bd145 MotB2 Bd3019 MotB3 Bd3254
		MotA (64)	Converts Na ⁺ /H ⁺ energy into torque and contributes to conductance	MotA1 Bd144 MotA2 Bd3020 MotA3 Bd3254
C RING		FliN (110)	Rotor/switch protein	Bd3327
		FliM (37)	Rotor/switch protein	Bd3328
		FliG (26)	Involved in torque generation, strong transient interactions with M/S ring	Bd3403
M/S RING		FliF (26)	Key rotor protein and mounting for rotor/switch and rod; housing for export apparatus. Interacts with and is rotated by FliG-MotAB	Bd3404
ROD		FlgB, FlgC, FlgF, FlgG (7, 6, 6, 26)	Transmission shaft for flagellar rotation	Bd3407, Bd3406, no recognisable FlgF homol. Bd0532
P RING		FlgI (24)	Part of bushing, peptidoglycan and wall anchor	Bd0535
L RING		FlgH (28)	Part of bushing, lipoprotein, outer membrane anchor	Bd0534
ROD CAP		FlgJ (5?)	Distal rod capping protein, muramidase	Bd5036
HOOK		FlgE (132)	Hook protein – universal joint	Bd3395

Table 3.1: Main structural proteins involved in the formation of the Gram-negative flagellar complex, relating to Figure 3.1 on the previous page. *B. bacteriovorus* HD100 gene homologues are given the appropriate Bd numbers. Continued on following page.

Part of Flagellar Complex	Diagram	Protein (stoichiometry in enteric bacteria)	Function	<i>B. bacteriovorus</i> gene number
HOOK/FILAMENT JUNCTION		FlgK (13)	HAP1; first hook/filament junction protein	Bd0539
		FlgL (~10)	HAP3; second hook/filament junction protein	Bd3040
FILAMENT		FliC (20,000)	Flagellar filament protein, flagellin. > 20,000 monomers	FliC1 Bd0604 FliC2 Bd0606 FliC3 Bd0408 FliC4 Bd0410 FliC5 Bd3052 FliC6 Bd3342
CAP		FliD (5)	HAP2; filament capping protein, flagellin folding chaperone	Bd0609

Table 3.1: cont. HAP = Hook Associated Protein.

The flagellar motor, consisting of the rotor C-ring protein, FliG and the stator (MotAB), drives the rotation of the rigid, helical flagellar filament via the rod proteins and the flexible hook. As the flagellar filament is rigid, rotation is converted to thrust, propelling the bacterium through aqueous environments. The motor is powered through a trans-membrane proton electrochemical gradient in neutrophilic bacteria, or through a sodium-ion gradient in alkophiles, transduced by MotAB and FliG proteins (Kojima and Blair, 2004). The flagellar motor is a small organelle, only 50nm in diameter, but can rotate at up to 300Hz (revolutions per second), illustrating the efficiency and power of this natural nano-motor. Interactions with chemotaxis proteins by FliMN modulate the rotation of the flagellum in response to tactic stimuli, altering the direction of the bacterium (Bren and Eisenbach, 2000); this has been previously shown to have a role in predatory behaviour in *B. bacteriovorus* (Lambert *et al.*, 2003). The genomic complement of *B. bacteriovorus* HD100 provides for several Mot proteins stator genes and a full set of rotor protein genes. My focus was solely on the semi-rigid propeller, the flagellar filament.

3.1.1: The flagellar filament

The flagellar filament is made up of thousands of subunits of a single protein called flagellin, or FliC. Monomers of this protein are exported outside of the cell after the hook structure (made of FlgE protein) and assembles into a hollow helical filament just under the pentameric “star-shaped” cap on the distal end, consisting of FliD (HAP2). The presence of two FliD pentamers (Yonekura *et al.*, 2000) ensures that flagellin monomers reaching the distal end of the growing filament are “caged” and retained, allowing quaternary interactions with other flagellins to continue extending the filament through self-assembly of the flagellin monomers (Macnab, 2003; Yonekura *et al.*, 2000). FliD is continuously secreted by the bacterium through the filament, meaning that if the filament breaks due to mechanical stress, FliD can reassemble and once more allow polymerisation of flagellin at the tip to extend the filament (Homma and Iino, 1985).

Bacteria display a variety of flagellar filament waveforms, lengths and numbers. The enteric bacteria, *E. coli* and *Salmonella* have several flagellar filaments, typically 4-9, scattered over the cell surface and their co-ordinated rotation counter-clockwise drives the cell forward (Berg, 2003). *Pseudomonas aeruginosa* and *Rhodobacter sphaeroides* are examples of bacteria with only a single, polar flagellar filament which drives motility; *Bdellovibrio bacteriovorus* also falls into this category.

The structure of *Salmonella enterica* serovar Typhimurium FliC, an approximately 60kD protein, was derived by X ray crystallography in 2001 (Samatey *et al.*, 2001), shown in Figure 3.2. As can be seen, the FliC protein looks like an inverted “L” shape, with the N and C termini of the protein forming the bottom of the L and the central portion of the protein being extended out.

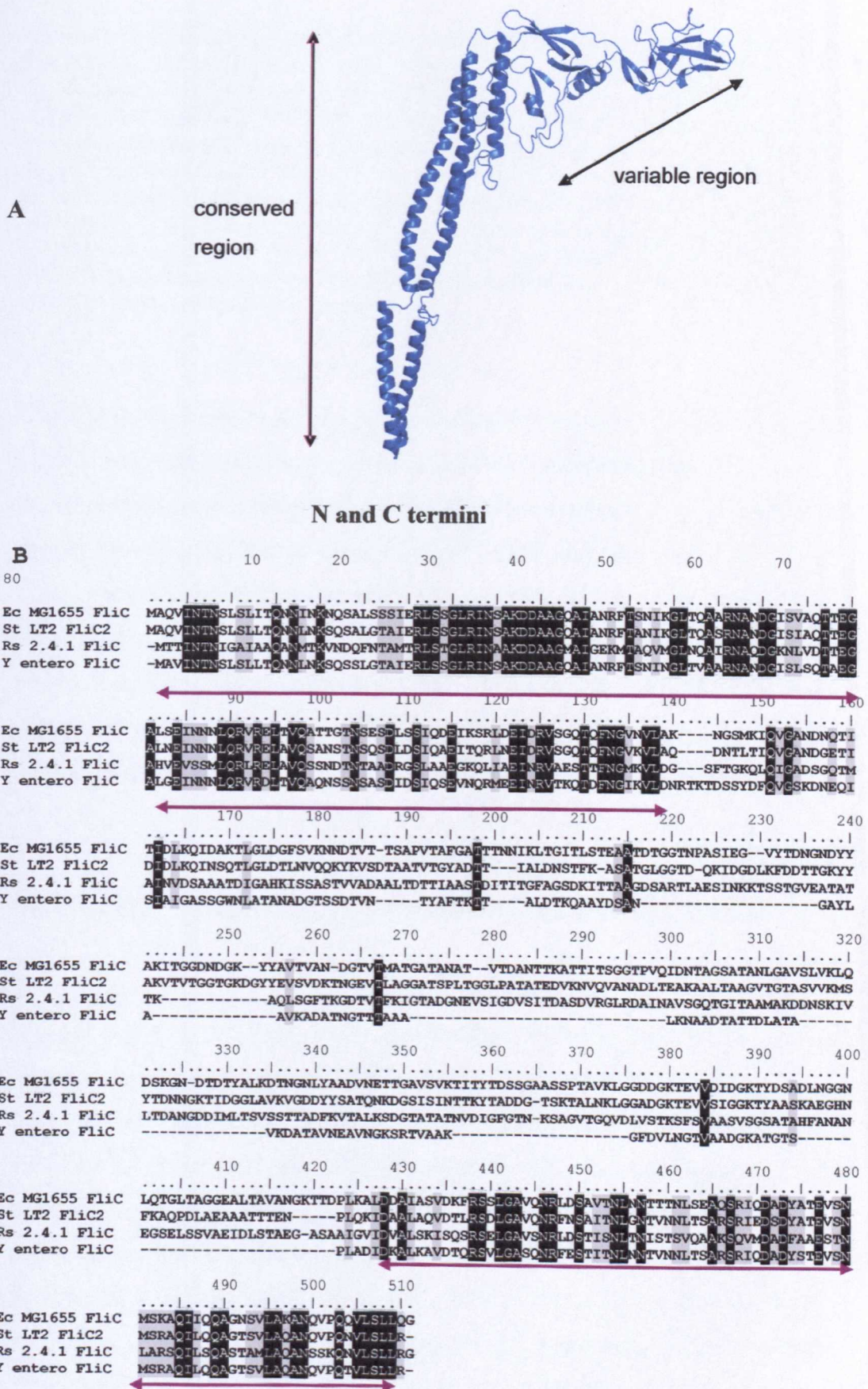


Figure 3.2: A Structural representation of *Salmonella* FliC; the inverted L shape is comprised of the N and C terminal helical domains forming the long arm, with the middle

variable region forming the short arm. The conserved regions form the inner filament core when arranged in the flagellar filament, with the central variable domain being exposed on the filament surface. Structure solved by (Samatey *et al.*, 2001), ribbon representation courtesy of R.D. Woods. **B**: Multiple protein alignment of flagellin sequences from different Gram-negative bacterial species. Underlined in purple are the conserved N and C terminal domains (corresponding to the purple line indicating the same on the structure). The N terminal domain is usually ~140 amino acids long, and the C ~90 amino acids (Beatson *et al.*, 2006). The alignment illustrates nicely the central variable region exposed on the filament surface. Created using ClustalW in BioEdit (see section 2.10). Ec = *E. coli* MG1655, St = *Salmonella enterica* serovar Typhimurium, Rs = *Rhodobacter sphaeroides* 2.4.1, Y entero = *Yersinia enterocolitica*

Throughout flagellate bacterial species, the N and C termini of the FliC protein are highly conserved, reflecting the constraints of the filament structure: 11 protofilaments are assembled via N and C-terminal interactions in a staggered helical fashion allowing quarternary interactions with other flagellins to form the flagellar filament and also to keep an approximately 3nm channel open in the middle of the filament allowing export of FliC monomers and other proteins to the FliD cap at the distal end of the filament (Kanto *et al.*, 1991; Morgan *et al.*, 1995) (Beatson *et al.*, 2006; Namba and Vonderviszt, 1997). The significance of this in relation to my work will be discussed below.

3.1.1.1: Multiple copies of the flagellin gene, *fliC*, exist in some bacterial species

Some flagellate bacteria have more than one copy of the *fliC* gene, indeed some have up to five or six copies, such as *Vibrio cholerae*, *V. parahaemolyticus*, *V. anguillarum*, *Caulobacter crescentus* and *Bdellovibrio bacteriovorus* (Ely *et al.*, 2000; Kim and McCarter, 2000; Klose and Mekalanos, 1998; McGee *et al.*, 1996; Rendulic *et al.*, 2004). Individual deletions or interruptions of these multiple *fliC* genes have different effects in different bacteria. In *V. parahaemolyticus*, individual deletions of any of the flagellins have little or no effect on the flagellar filament structure or on motility, showing no single gene product is essential for filament production (McCarter, 1995). Mutants in genes encoding the flagellins of *V. anguillarum* showed only one essential protein, FlaA, which exhibited a phenotype of reduced motility but mutant cells were still flagellate (Milton *et al.*, 1996) In *V.*

cholerae, disruption of four of the five flagellin genes present had no effect on motility or flagellar structure, but mutation of *flaA* resulted in a non-motile strain that lacked the single, polar flagellum found in the wild type; the authors hypothesised that FlaA is required as either a scaffold or a flagellar core around which the other flagellins are assembled (Klose and Mekalanos, 1998). The significance of this in the context of my work in *B. bacteriovorus* will be returned to later. One common theme amongst the studies of bacteria with multiple flagellin genes remains: no-one knows the organisation of the proteins in the flagellar filament or why some bacteria need many flagellin genes where others only have one or two. The scaffold hypothesis for filament structure mentioned above in relation to *V. cholerae* is a common one, a reservoir for phase variation or immune evasion (in pathogenic strains, or in environmental strains to avoid protozoan grazing) has also been proposed (McCarter, 2001). However, there is no single answer to this issue as yet.

3.1.2: Sheathed flagella

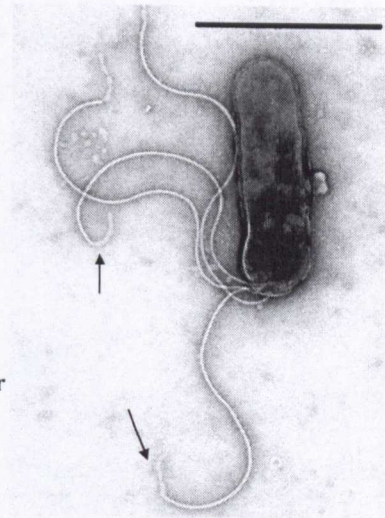
Some flagellate species also have sheathed flagella, where the flagellar filament is sheathed by an apparent extension of the cell outer membrane. Many marine *Vibrio* species, *V. cholerae*, *V. parahaemolyticus* and the gastric pathogen *Helicobacter pylori* have sheathed flagella (reviewed in (Sjoglad *et al.*, 1983)); *B. bacteriovorus* also has a sheathed flagellum, this will be discussed further in the following section.

Little is known about the synthesis or function of the flagellar sheath. In *H. pylori* (see Figure 3.3 below), the sheath has been shown to be continuous with the outer membrane, containing lipopolysaccharide and protein and seems to function in the protection of the flagella from the highly acidic environment of the stomach (Geis *et al.*, 1993). It has also been postulated in *H. pylori* that the sheath also functions to retain any secreted flagellin monomers that are potent pro-inflammatory activators of the mammalian immune system in other enteric species, such as *Salmonella* and *E. coli* (mediated by Toll-Like Receptor (TLR) 5, more will be said later on this subject) (Gerwartz *et al.*, 2004).

Figure 3.3: Transmission electron micrograph of *H. pylori* J99 wild type cell.

Polar flagella are seen, with arrows indicating sheath where the ends of the core flagellar filament have broken. Stained with 0.5% phosphotungstic acid, pH7, bar = 2 μ m.

Taken (by me) as part of work for (Wand *et al.*, 2006) involved in examining the role of the FlhB_{cc} domain in *H. pylori*. The reader is referred to this paper as it will not be discussed further as part of this thesis. (See paper bound at the back of this thesis)



In contrast to *H. pylori*, the role of the sheath in *V. anguillarum* is as a virulence determinant. *V. anguillarum* is a pathogen of fish, causing vibriosis in densely farmed fish; amongst the virulence determinants of this pathogen, VirA and VirB proteins have a role in the generation of systemic infection and these proteins are located solely on the flagellar sheath (Norqvist and Wolf-Watz, 1993).

A role for the sheath in flagellar filament assembly has also been proposed. Flagellin monomers will spontaneously form short polymers if there is a sufficiently high concentration of them (Homma *et al.*, 1986). HAP2 (FliD) mutants, where there is no cap to retain secreted flagellin monomers, of *V. parahaemolyticus* show almost wild-type flagellar filament morphologies and motility, suggesting that the sheath acts to retain the flagellin in sufficiently high local concentration for spontaneous filament polymerisation (McCarter, 1995). This work was supported by similar conclusions in *Vibrio alginolyticus*, where HAP1 and 3 mutants (hook-filament junction proteins, FlgK and FlgL) gave filament-less structures that had membrane-sheathed vesicles containing flagellin in the surrounding media, with some remnants of sheath covering the hook structure (Nishioka *et al.*, 1998). HAP1 and 3 mutants gave the same phenotype in *V. parahaemolyticus* (McCarter, 1995).

In summary, although there are clues as to some functions of the flagellar sheath, which differ throughout the Bacteria, its true function remains to be elucidated. The

main mystery still remaining is how the sheath remains undamaged during the mechanically stressful process of flagellar rotation. It is unknown whether the sheath is attached to the flagellar filament and rotates with it, or if the filament rotates freely within the sheath itself.

3.1.3: Flagella and the mammalian immune system

Bacteria have long been known to stimulate the immune system in response to bacterial infection. For example, lipopolysaccharide (LPS) of Gram-negative bacteria is recognised by Toll-Like Receptor 4 (TLR4) of macrophages when presented on the surface of mammalian cells by CD14 ; this in turn stimulates various interleukin (IL) and Tumor Necrosis Factor (TNF) production which mediate the inflammation and subsequent responses by other areas of the immune system (for a review, see (Raetz and Whitfield, 2002)).

Flagella are important in many human pathogens for colonisation of mucosal surfaces, eg *Pseudomonas aeruginosa* colonisation of the bronchial and alveolar lumen in Cystic Fibrosis patients and enteropathogenic *E. coli* adhesion to intestinal mucosa. As a consequence, evolution of the human immune system in response to bacterial pathogens has produced specific elements to specifically recognise flagellin, the protein that comprises the flagellar filament. TLR5 recognises the conserved N and C terminal domains of flagellin monomers that form the vertical part of the inverted L-shape protein structure (see Figure 3.2 in section 3.1.1) common to most, if not all, flagellate bacteria and stimulates the secretion of pro-inflammatory cytokines and chemokines necessary for further macrophage and neutrophil recruitment to the site of infection (see (Ramos *et al.*, 2004) for a full review). Flagellin monomers may be released by the bacteria through normal mechanical shearing of a flagellum, which will be repaired by formation of a new FliD cap, but secretion of FliC (flagellin) continues, releasing the monomers into the surrounding medium. Flagellin may also be released from intact flagella by proteolytic action of host enzymes. Pathogenic bacteria with a sheath, for example, *Helicobacter pylori*, retain flagellin monomers, hence reducing their exposure to TLR5-mediated immune responses (See section 3.1.2. and (Gerwartz *et al.*, 2004)).

This could have implications for future work in *B. bacteriovorus*, which also has a sheathed flagellum, and will be discussed later.

3.1.4: The *Bdellovibrio bacteriovorus* flagellum and motility



Figure 3.4: Transmission electron micrograph of *B. bacteriovorus* HD100, showing the characteristic single, polar, sheathed flagellum with a damped waveform, with the larger amplitude waveform proximal to the cell body and the smaller distal. Stained with 1% uranyl acetate, bar = 2 μ m. This thesis work.

Bdellovibrio bacteriovorus strains have a single polar flagellum that is used in the motility of this predatory bacterium. *B. bacteriovorus* swim incredibly fast for any bacterium (Records., 1991) with lab strain 109J swimming at average speeds of 35 μ m sec⁻¹ and HD100 swimming at speeds of up to 160 μ m sec⁻¹ (Lambert *et al.*, 2006) compared to average speeds of approximately 25 μ m sec⁻¹ for *E. coli*. The small size of the cells aid these high speeds; the question must be, why? Why is it necessary for these predators to have this incredible motility? This has always been the subject of some debate in the previous literature on *B. bacteriovorus*, with most researchers favouring the “drilling” hypothesis of prey entry, where flagellar-mediated motility provides a rotary force to push the predator into the prey (Burnham *et al.*, 1968).

The earliest electron microscopic observations of *B. bacteriovorus* showed that their flagella are sheathed (Seidler and Starr, 1968), but the major works on *B.*

bacteriovorus 109J flagella and their sheaths were carried out in the mid 1980s by Thomashow and Rittenberg in two papers.

In the first of these papers (Thomashow and Rittenberg, 1985b), the authors described the dampened waveform in detail. Their analysis showed that the dampened appearance (of large amplitude waveform proximal to the cell body to smaller amplitude distally, see Figure 3.5 below) was caused by a single, non-random transition between two helical structures within the filament. The first period of the filament wave is three times the amplitude of period III towards the distal end of the flagellum, with the middle period, II, resembling period I proximal to the cell and period III distally. The intersection of the two helices in period II caused a shift in the axis of the flagellar filament. Older cells show much longer flagella in a continuation of period III, indicating that certain FliC proteins continue to be synthesised and exported during attack phase. Removal of the sheath using Triton X-100 left the flagellar waveform intact, showing that it was maintained by the core filament; from these filaments SDS-PAGE of the flagellar core polypeptides showed that there were two proteins of 28kDa and 29.5kDa incorporated into the filament, with their data suggesting that they were positioned proximally and distally respectively. This was proposed as an explanation for the shift in helical axis (Thomashow and Rittenberg, 1985b).

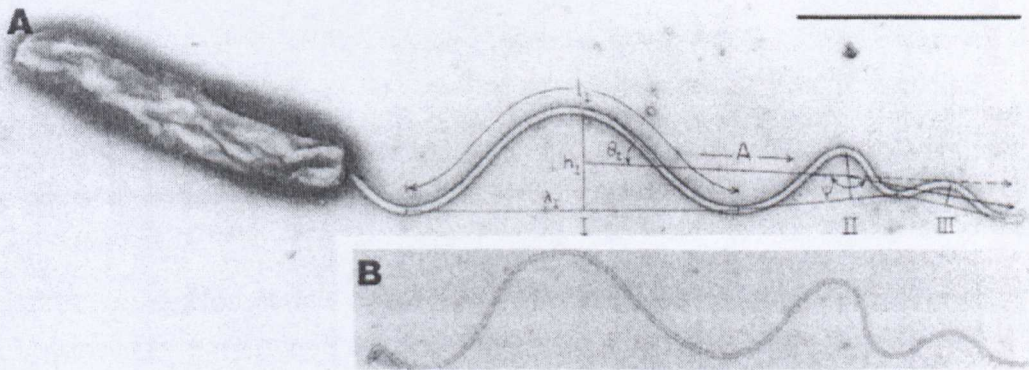
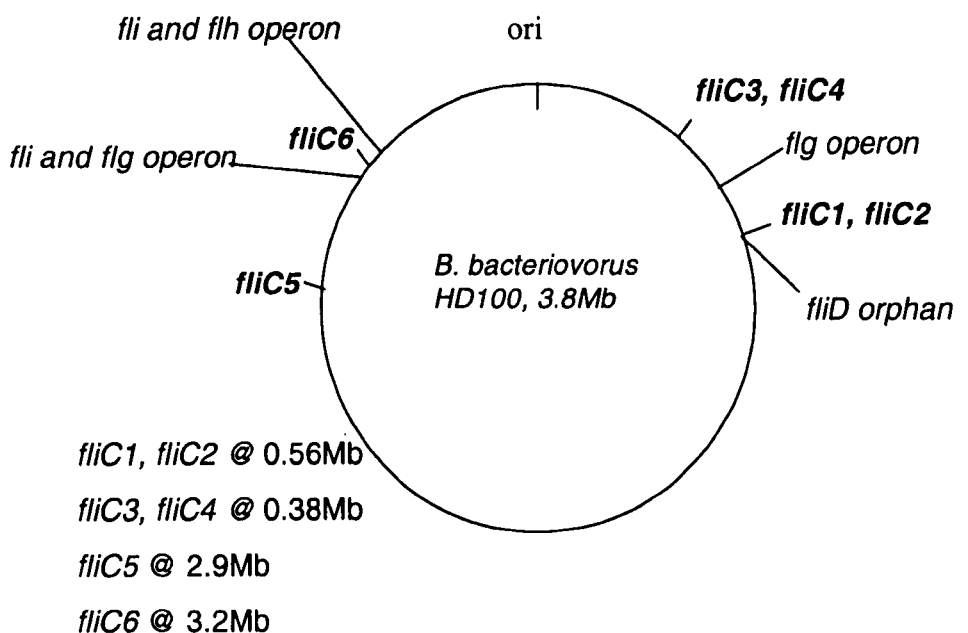


Figure 3.5: Thomashow and Rittenberg's waveform analysis of 109J. Periods I, II and III are indicated below the filament on Figure A; I is the longest and highest amplitude waveform, II forms the transitional period between proximal and distal, III is the smallest amplitude waveform that is extended as *B. bacteriovorus* cells get older. B is a core filament with the flagellar sheath removed, showing that it is the filament itself that has this dampened waveform and that it is not an artefact of the presence of the sheath. Bar = $1\mu\text{m}$, stained with uranyl acetate. For further details please refer to (Thomashow and Rittenberg, 1985b)

In the second paper, (Thomashow and Rittenberg, 1985a) *B. bacteriovorus* 109J flagellar sheaths were isolated and analysed; from this work the authors hypothesised that the flagella sheath is a stable and separate domain from that of the outer membrane, with enriched nonadecenoic acid and reduced β -hydroxymyristic acid. No further work has been carried out on *Bdellovibrio* sheaths to date, so their exact role remains unknown.

3.1.5: Genome analysis reveals that *B. bacteriovorus* HD100 has 6 flagellin genes

During the course of this project, our analysis of the HD100 genome (Rendulic *et al.*, 2004) showed that there were actually 6 copies of genes encoding flagellins (FliC proteins), much like some other species, as discussed earlier in Section 3.1.1. Like other species with multiple flagellin genes, they are not tandemly arranged in the genome, but (in common with other *B. bacteriovorus* genes that would ordinarily be found in long operons in other bacteria, see Chapter 5 for a further discussion of this in relation to *pil* genes) are scattered around the genome. Figure 3.6 below shows a cartoon of *fliC* gene positioning on the chromosome relative to the other major flagellar gene operons.



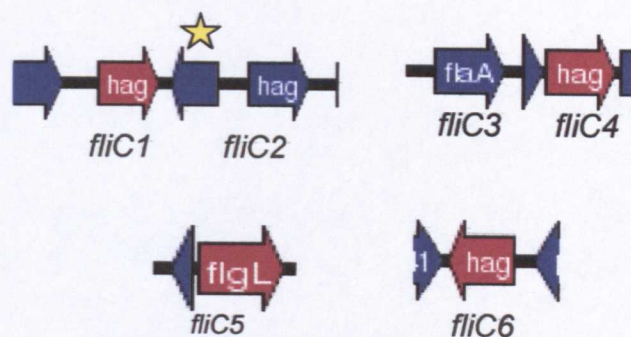


Figure 3.7: Genomic arrangement of *fliC* genes in HD100. *fliC1* and *fliC2* are tandemly arranged on the same DNA strand, with a putative transposase ORF oppositely oriented between them (starred). *fliC3* and *fliC4* are also tandemly arranged, with *fliC5* and *6* as orphans in the genome. Annotations shown as as annotated in the genome – *flic3* and *flic5* are mis-annotated as *flaA* and *flgL* respectively (Rendulic *et al.*, 2004).

Alignment of the HD100 FliC sequences showed a remarkable degree of sequence conservation between the six proteins (see Figure 3.9 below), even in the central variable domain, with only FliC1 being slightly more diverse than the rest. This again raised the question of whether all were incorporated into the flagellar filament, or whether some acted as a “spare tyre” for specialised situations, or were pseudogenes with defective promoters. Figure 3.8 below shows the classical conservation of flagellin N and C-termini between HD100 FliC3 and within the six *B. bacteriovorus* flagellins.

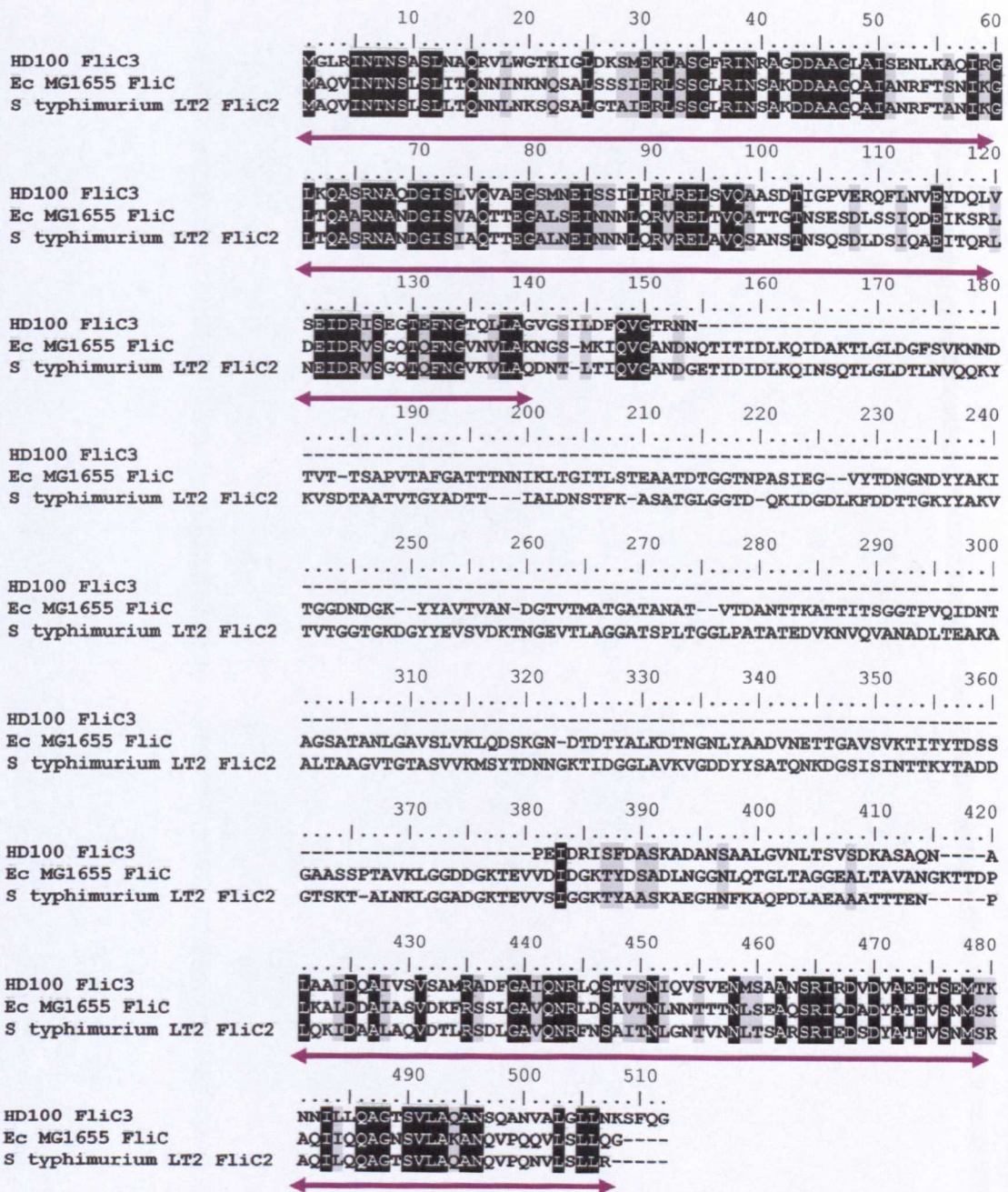


Figure 3.8: Multiple protein alignment of HD100 FliC3 with *E. coli* (Ec) and *Salmonella enterica* serovar Typhimurium flagellins, demonstrating the conserved N and C termini of the proteins (underlined in purple) and the variable region. Note that the *B. bacteriovorus* flagellin is much smaller than the others (predicted molecular weight ~29kD versus ~60kD for *Salmonella* and *E. coli*), reflected in the smaller variable domain. In relation to the published *Salmonella* FliC structure, this would mean that most of the top arm would be missing, forming a more compact structure. Alignment created using Clustal W in BioEdit, see Section 2.10.

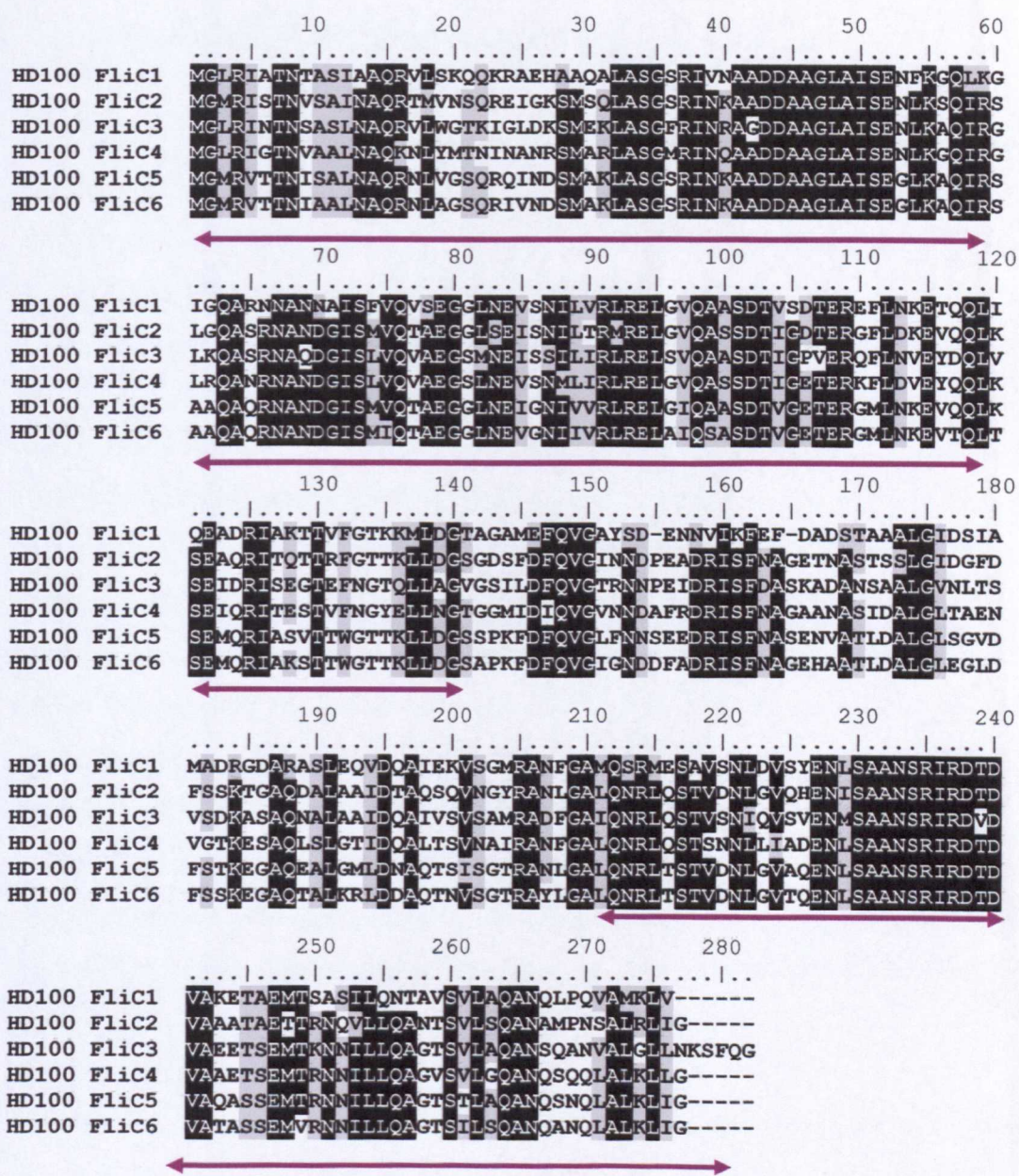


Figure 3.9: Multiple alignment of *B. bacteriovorus* HD100 FliC proteins, showing the remarkable degree of sequence conservation amongst the 6, with only FliC1 being more degenerate than the rest. Underlined in purple are the conserved N and C terminal regions, illustrating the extremely short variable region. Created using ClustalW in BioEdit (see Section 2.10)

3.2: Collaborative studies of the *B. bacteriovorus* 109J flagellins

In the course of this thesis, I, in collaboration with others, have studied and published detailed analyses of the 6 flagellin genes and proteins in *B. bacteriovorus* 109J (Lambert *et al.*, 2006). Dr Stephan Schuster kindly made available the HD100 *fliC* sequences ahead of publication and completion of the HD100 genome sequence (Rendulic *et al.*, 2004). The corresponding genes were cloned and sequenced in 109J (Dr Carey Lambert, before the start of this thesis) and work was started to insertionally inactivate each flagellin gene individually (due to constraints on antibiotic selective markers and lack of replicative plasmids in *B. bacteriovorus*, see Section 1.6). 109J, rather than HD100, was chosen for these studies due to it being, at the time, better physiologically characterised and the major flagellar studies also having been carried out in this strain (Thomashow and Rittenberg, 1985a, 1985b). In the course of this work, Dr Lambert, Rob Till and Michael Capeness did the majority of cloning and inactivation of the genes – most done before I started in the lab – and quantitative RTPCR analysis; I carried out the work on phenotyping the 109J mutant strains (by microscopy and protein analysis), with the exception of motility analysis and tracking, done by Laura Hogley. Here, I will summarise the major findings in this study, concentrating on areas of analysis carried out as part of work for this thesis.

3.2.1: Electron microscopy – optimisation and development of imaging techniques for *B. bacteriovorus*

Previous transmission electron microscopy (TEM) studies of *B. bacteriovorus* in the 1960s and 70s did much to further our knowledge of this tiny predator. Stolp and Starr started doing the earliest work, revealing attachment of *B. bacteriovorus* strains to their prey (Stolp and Starr, 1963); this work was extended by other groups with a seminal study of *B. bacteriovorus* attachment, penetration and establishment by (Burnham *et al.*, 1968) which did much to show the nature of these processes. (Abram and Davis, 1970) did much research on the effects of different stains commonly used on *B. bacteriovorus* and the resulting features of the cell

wall/membrane and were the first to properly examine non-flagellar pole ring like structures (see Section 5.3.2 for further discussion of these from my own work) and polar fibres (see Chapter 5), also looking at the flagellum and its sheath. This study led to another on prey penetration (Abram *et al.*, 1974). The final major work involving TEM was that of (Thomashow and Rittenberg, 1985b) on the structure and waveform of *B. bacteriovorus* 109J flagella, mentioned earlier in Section 3.1.4.

One thing these studies all have in common is that the vast majority of the published images come from *B. bacteriovorus* cells that had been fixed, usually in glutaraldehyde, and then stained with a variety of compounds (ranging from phosphotungstic acid to ammonium molybdate). Many of the fixed cell preparations were then sectioned, a useful tool for looking at processes that may not otherwise be seen, or subject to shadow casting. The major flaw with these preparative methods is that of distortion of the cells and the high incidence of detail being artefacts of these processes.

Perhaps one of the best examples of the examination of these methods causing a major re-evaluation of previous work in another field is that of the phenomenon of “Bayer’s Bridges”. These were originally observed in *E. coli* by Manfred Bayer in 1968 and were proposed to be relatively large areas where the inner and outer bacterial membranes were in close contact with one another, seemingly without the intervention of the peptidoglycan layer, leading to the proposition of “lipidic fusion” to allow transport of molecules from the cytoplasm to the exterior of the cell (Bayer, 1968). Work by Kellenberger, and other groups, showed that these large bridges were an artefact of the fixation and plasmolysis protocols used to image the cells; much biochemical analysis had failed to isolate Bayer’s bridges. Cryoelectron microscopy, which is less destructive due to snap-freezing of samples, and native staining of *E. coli*, along with other experimental evidence, showed that the observed Bayer bridges were an artefact of the TEM preparation methods (reviewed in (Kellenberger, 1990)).

In light of these issues, I wished to develop other techniques for *B. bacteriovorus* TEM. As the facilities for cryo-fixation were unavailable to me routinely, I concentrated on more natural sample preparation, namely letting the cells settle onto

TEM grid supports and gentle staining, with no fixation or plasmolysis. I am indebted to Prof. Liz Sockett at Nottingham and Prof. Chi Aizawa in Japan for much patience and training and helpful discussion of possible interpretations in these areas. For TEM methods, see Section 2.8.2.

Figure 3.10 below illustrates the differences seen in *B. bacteriovorus* cells stained with different compounds. The left picture (Japan) was taken using 1% phosphotungstic acid, potassium salt (PTA) pH7; using this stain, membranous protrusions from the cell body are commonly seen, the membrane appears slightly ruffled with surface protrusions of membrane material and the stain often tends to accumulate around the cell. This agrees with earlier work done by (Abram and Davis, 1970) who postulated that the formation of membrane protrusions (which is unknown in other bacteria) indicates that *B. bacteriovorus* have a distinctive cell wall/membrane composition. The right panel (Nottingham) is stained with 1% uranyl acetate (URA), pH4 (it is exceedingly difficult to alter the pH of this stain without precipitation; when made up in Tris buffer of the appropriate pH, the cells so not stain well and appear “fuzzy” when examined, not shown). URA staining does not reveal any membrane projections as PTA stains do, the cells appear dehydrated but the stain does not tend to accumulate around the cells as with PTA. The differences in these staining properties will be discussed as necessary.

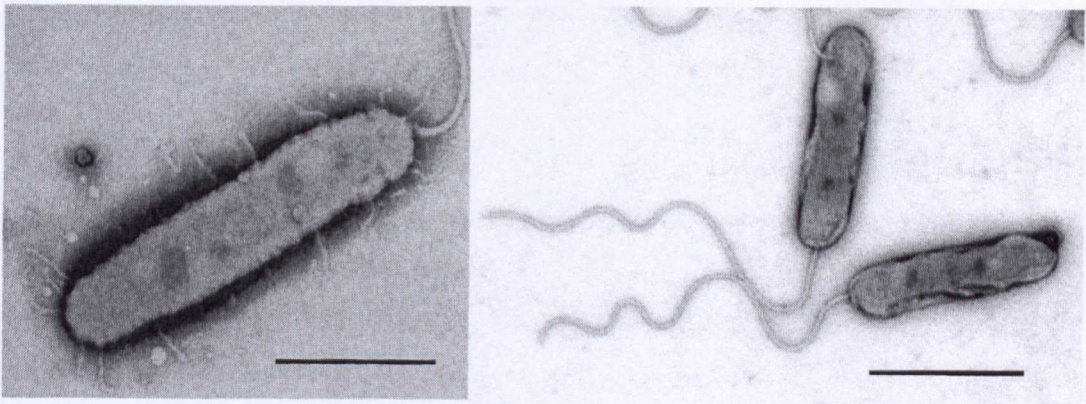


Figure 3.10: TEM of *B. bacteriovorus* 109J. Left panel, 1% phosphotungstic acid pH7 showing the membrane protrusions that are a characteristic of this stain. Right panel, 109J stained with 1% uranyl acetate pH4, no membrane protrusions are visible and the cells appear somewhat dehydrated. Uranyl acetate also enhances the flagellar filament waveform compared to phosphotungstic acid (see later). Bars = 1 μ m.

3.2.1.1: TEM observations of *B. bacteriovorus* bdelloplasts of various stages – flagella are not always shed immediately on prey penetration

As part of my work with Prof. Aizawa in Japan, I made studies of the features of the *B. bacteriovorus* life cycle using TEM, particularly the intracellular bdelloplast stages and subsequently carried on this work in Nottingham. In this section, PTA 1% pH7 was the stain of choice; it penetrates membrane layers better than URA which appears to bind to membrane residues, so PTA can be used to “see through” the outer layers of bdelloplasts. However, one URA stained bdelloplast is also included out of interest.

As can be seen in Figure 3.11, *B. bacteriovorus* 109J is attaching to its *E. coli* prey by the non-flagellar pole. In Figure 3.12, the invading *B. bacteriovorus* 109J has started to modify the prey cell wall to produce the rounded bdelloplast structure, but its flagellum is still visible (the *E. coli* strain upon which they were grown is DFB225, a non-flagellate FliG null strain, therefore any flagella observed are those of *B. bacteriovorus*). Thomashow and Rittenberg stated that flagellar shedding by the predator was an integral stage of early infection (Thomashow and Rittenberg, 1979), but my work shows that in early stage bdelloplasts (up to around 30 minutes post infection), this does not always occur. Short flagellar filaments were seen in ~ 80% of early stage bdelloplasts examined (n>100), though this figure may be an overestimate for the entire population due to the tendency of bdelloplasts to aggregate on TEM grids. Flagella originating from the *B. bacteriovorus* were never seen in more established and late stage bdelloplasts; once the bdelloplast filament has finished growing and septates, the progeny cell re-synthesise new flagella (see video DSCN1202 on accompanying CD) before lysing the remnants of the prey cell (see Section 1.3.4).

Figure 3.13, stained with URA, shows a bdelloplast with what may be a “plug” in a membrane invagination, however there is no further evidence to support this and it is only seen with this stain; again, it is a curiosity seen when TEM is applied to bdelloplasts and provides another hypothesis that is difficult to prove otherwise. Figures 3.14 and 3.15 illustrate nicely the curling of the growing *B. bacteriovorus* filament within the confines of the prey periplasm; they also demonstrate the presence of continuous prey cell membrane that forms the bdelloplasts structure and the decreasing volume of prey cytoplasm as *B. bacteriovorus* uses its contents for its own growth.

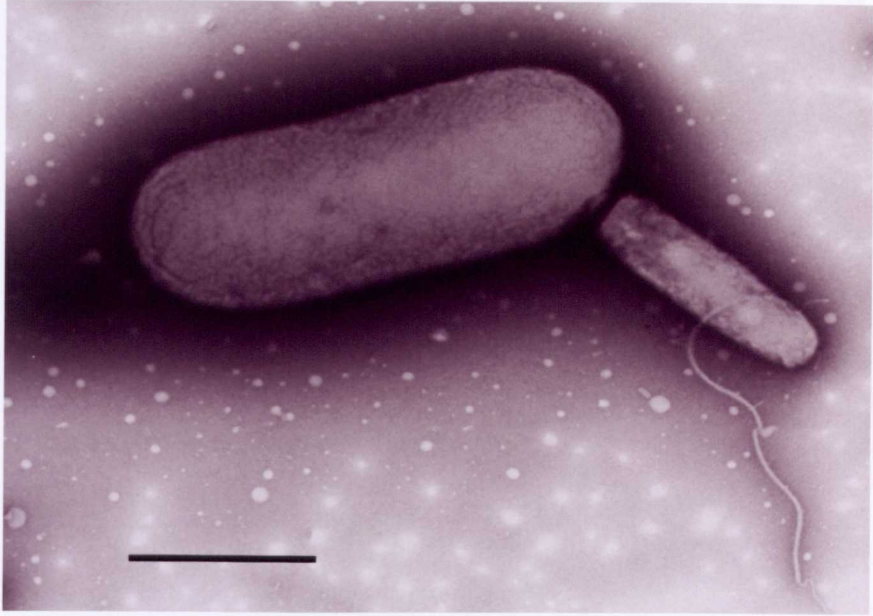


Figure 3.11. *B. bacteriovorus* 109J attaching to an *E. coli* DFB225 (non flagellate strain). Published in Nature Reviews Microbiology Vol 2(8), contents page. 1%PTA pH7, bar = 1 μ m.



Figure 3.12: 109J bdelloplast (*E. coli* DFB225). The predator has started to round up the rod shaped *E. coli*; the full length of the flagellum has not been shed yet. Please see the main text for a discussion of this phenomenon. 1%PTA pH7, bar = 1 μ m. Published in Lambert *et al* 2006.

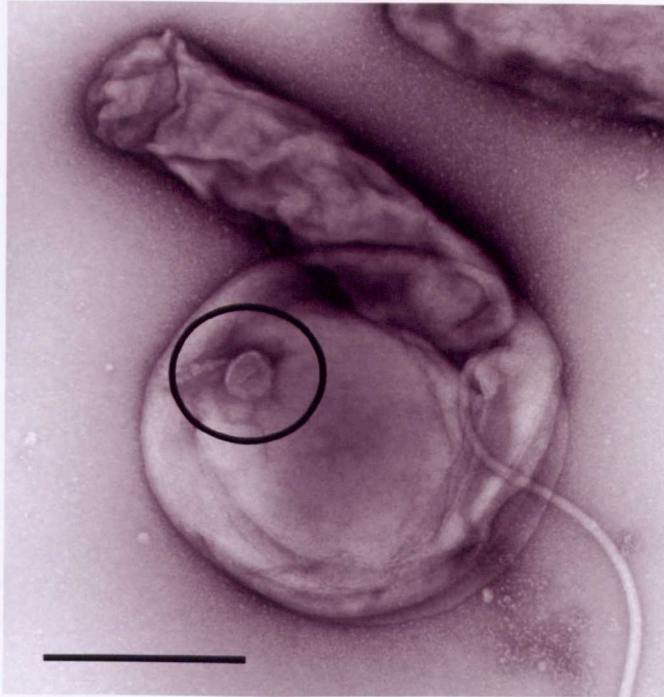


Figure 3.13. *B. bacteriovorus* HD100 bdelloplast (*E. coli* S17-1). The HD100 attack phase cell appears to be lying on top of the rounded bdelloplast and is spurious and does not appear to be associated with this bdelloplast. The bdelloplast itself has dehydrated and shrunk; it appears solid due to the nature of URA staining. However, of interest is the circled area; it may be a membrane invagination with a “plug” inserted – perhaps the area where the invading HD100 has resealed the hole it made in the membrane for prey entry? However, no further evidence has been gathered to support this hypothesis. Stained with 1% URA, pH4, bar = 0.5 μm .

Fig 3.14 : *B. bacteriovorus* HD100 bdelloplast (*E. coli* S17-1). Once the entry pore has been re-sealed and the rest of the flagellum lost, safely inside the bdelloplast, the predator starts degrading and transporting prey macromolecules into the growing predator filament. 1%PTA pH7, bar = 1 μm .

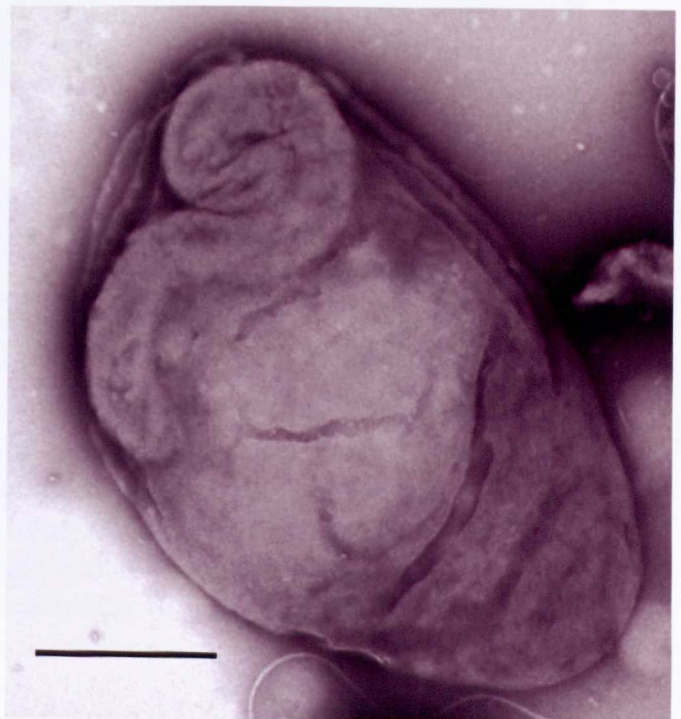


Fig 3.15 : *B. bacteriovorus* HD100 bdelloplast (*E. coli* S17-1). As more and more of the prey cell is consumed, the predator filament elongates and “twists” within the confines of the bdelloplast structure. 1%PTA pH7, bar = 1 μ m.

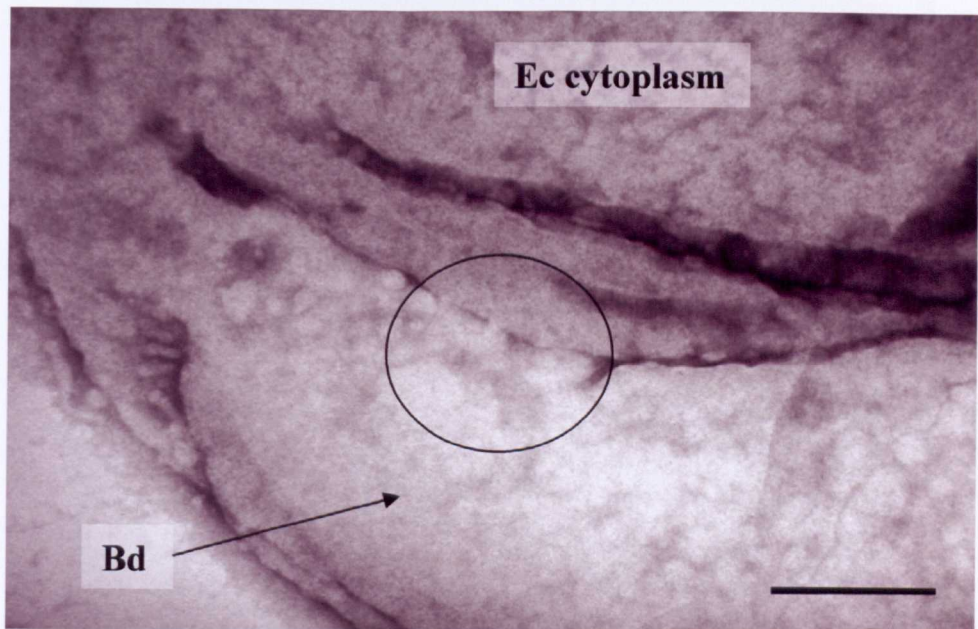


Figure 3.16: *B. bacteriovorus* HD100 bdelloplast (*E. coli* S17-1). Close examination of the regions where the predator is in close contact with the prey cytoplasm shows apparent connecting structures. However, these are only rarely seen due to technical difficulties in imaging bdelloplasts; as such the nature and function of these possible structures remains unknown. Bd = *Bdellovibrio* filament; Ec = *E. coli* cytoplasm. 1%PTA pH7, bar = 0.2 μ m.

Figure 3.17: *B. bacteriovorus* 109J late-stage bdelloplast (*E. coli* DFB225). Once the prey cell contents have been consumed and incorporated into the *Bdellovibrio* filament, septation begins. Arrow indicates a point of cell division. NB aggregates of spurious cells surrounding bdelloplasts is very common, they are nothing to do with the bdelloplast itself 1%PTA pH7, bar = 1 μ m.

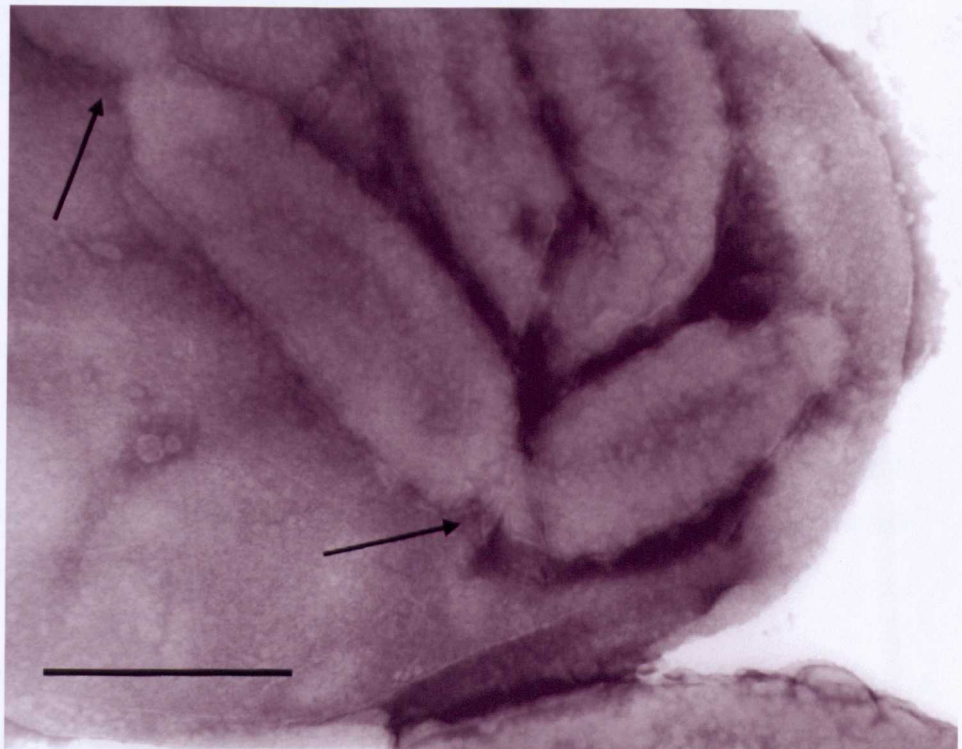
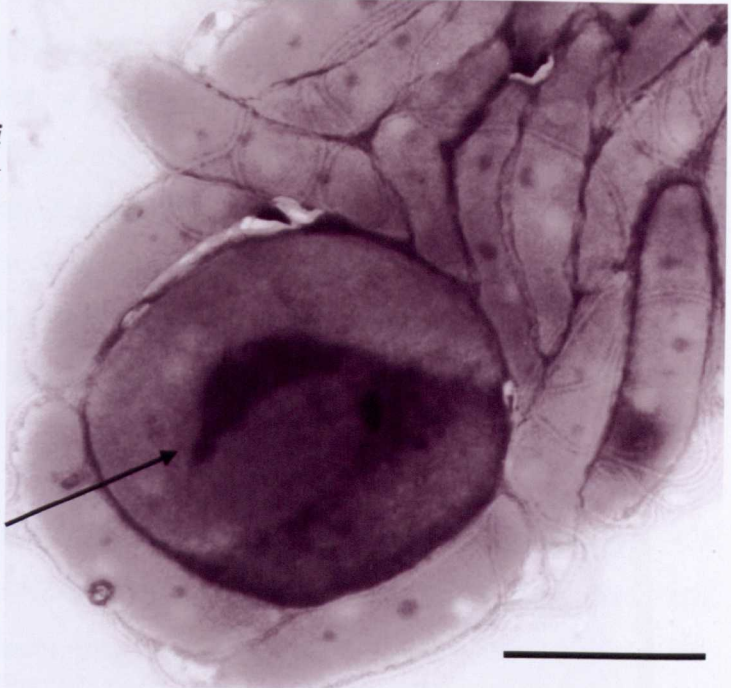


Fig 3.18 : Close up of a *B. bacteriovorus* 109J bdelloplast (*E. coli* S17-1). The *Bdellovibrio* filament has nearly finished septating, division sites are indicated by arrows. 1%PTA pH7, bar = 0.5 μ m.

Figure 3.16, an extreme close-up of the apparent attachment point between the growing *B. bacteriovorus* and the prey cytoplasmic membrane, which (from personal observation) seems to be closer at one pole (or along the length of the original invading *B. bacteriovorus*), seems to show membrane connections/possible protein transporter complexes between the two cells. However, these are extremely difficult to image, so any proposed function must remain speculative. The only way to prove their existence (or otherwise) would be immuno-TEM; however, until candidate proteins are identified and anti-sera raised, this remains outside the scope of this work.

Figures 3.17 and 3.18 show the formation of septa in the filament when the prey cell is exhausted as the *B. bacteriovorus* filaments start to divide. Imaging the final stage of *B. bacteriovorus* development, the complete septation and formation of flagellate progeny, is extremely difficult. The very short period of time between completion of septation and lysis of the prey cell ghost makes it unlikely to be caught when grids are made; despite many repeated attempts, this process was not seen.

The images shown in the figures are representative of many months of work in developing whole cell TEM imaging in *B. bacteriovorus*; other examples of the uses of electron microscopy are distributed throughout this thesis. Modifications in staining were used throughout; for example, flagella and bdelloplasts were imaged using PTA (also slight modifications in staining time), yet pili and other surface structures are imaged using URA – decreased accumulation of stain around the cell body and removal of the membranous protrusions seen with PTA are advantageous in this respect.

Imaging of flagella was done with 1% PTA pH7 throughout this work. On the advice of Prof. Aizawa, who has spent his life imaging flagella, PTA is preferable as it does not distort the natural flagellar filament as URA can do; the low pH (or high pH) can be used to characterise the helicity and transitions/conformations of flagella (Shah *et al.*, 2000) so URA staining was not used for examination of flagella.

3.2.2: Collaborative inactivation of the *fliC* genes of 109J

As this work is published (Lambert *et al.*, 2006) and done between C. Lambert and R. Till over a period of time, a brief summary only will be given here. Primer sequences and details of plasmid construction are also available in our joint publication, (Lambert *et al.*, 2006).

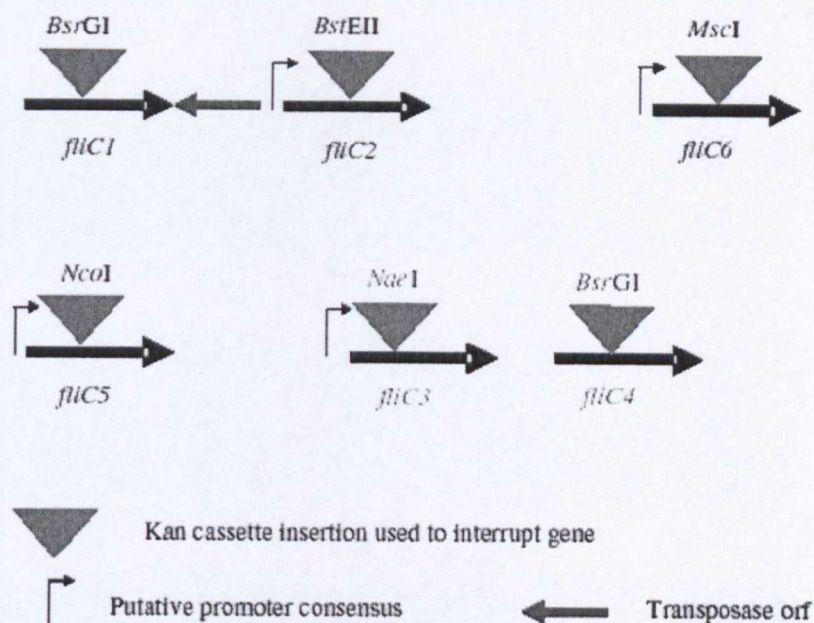


Figure 3.19: The arrangement of *fliC* genes in both HD100 and 109J; sites indicated are those within each individual flagellin gene used for inactivation by insertion of a kanamycin resistance cassette. Taken from (Lambert *et al.*, 2006).

Briefly, the HD100 sequences given to us by Dr Schuster were used to design amplification primers; the cognate genes in 109J were amplified and sequenced with the predicted translation show the same remarkable degree of sequence conservation as those of HD100 (see Figure 3.20 below). The genes were individually interrupted with kanamycin resistance cassettes (from pUC4K) and these constructs cloned into the suicide vector, pSET151, which cannot replicate autonomously in the genome but integrates into the chromosome through homologous recombination of corresponding flanking DNA either side of the target gene (Cotter and Thomashow, 1992a; Lambert *et al.*, 2003). The *B. bacteriovorus* 109J recovered from conjugation with *E. coli* S17-1 were kanamycin resistant, allowing selection for the gene interruption;

3.2.2.1: Inactivation of *fliC1,2,4* and *6* causes no gross morphological filament changes in strain 109J as examined by TEM

109JK (a wild type *B. bacteriovorus* 109J strain containing a kanamycin resistance cassette in a gene encoding a putative ABC-transporter component that is not expressed; (Lambert *et al.*, 2003), L. Hopley, unpublished results) was used as a control strain for flagellar filament mutants; predatory *B. bacteriovorus* strains were grown using the flagellar – minus (FliG null) *E. coli* DFB225 prey (Lloyd *et al.*, 1996) to ensure that any flagella seen in TEM preparations originated solely from the *B. bacteriovorus* strain under examination.

Examination of flagellar filaments from each 109J mutant strain showed that inactivation of the genes encoding FliC1, 2, 4 and 6 had no effect on filament morphologies (see Figure 3.21). All flagellar filaments from these mutants, including the 109JK control strain, had a mean length of 4.0 +/- 0.5µm and the waveform seemed to be unaffected.

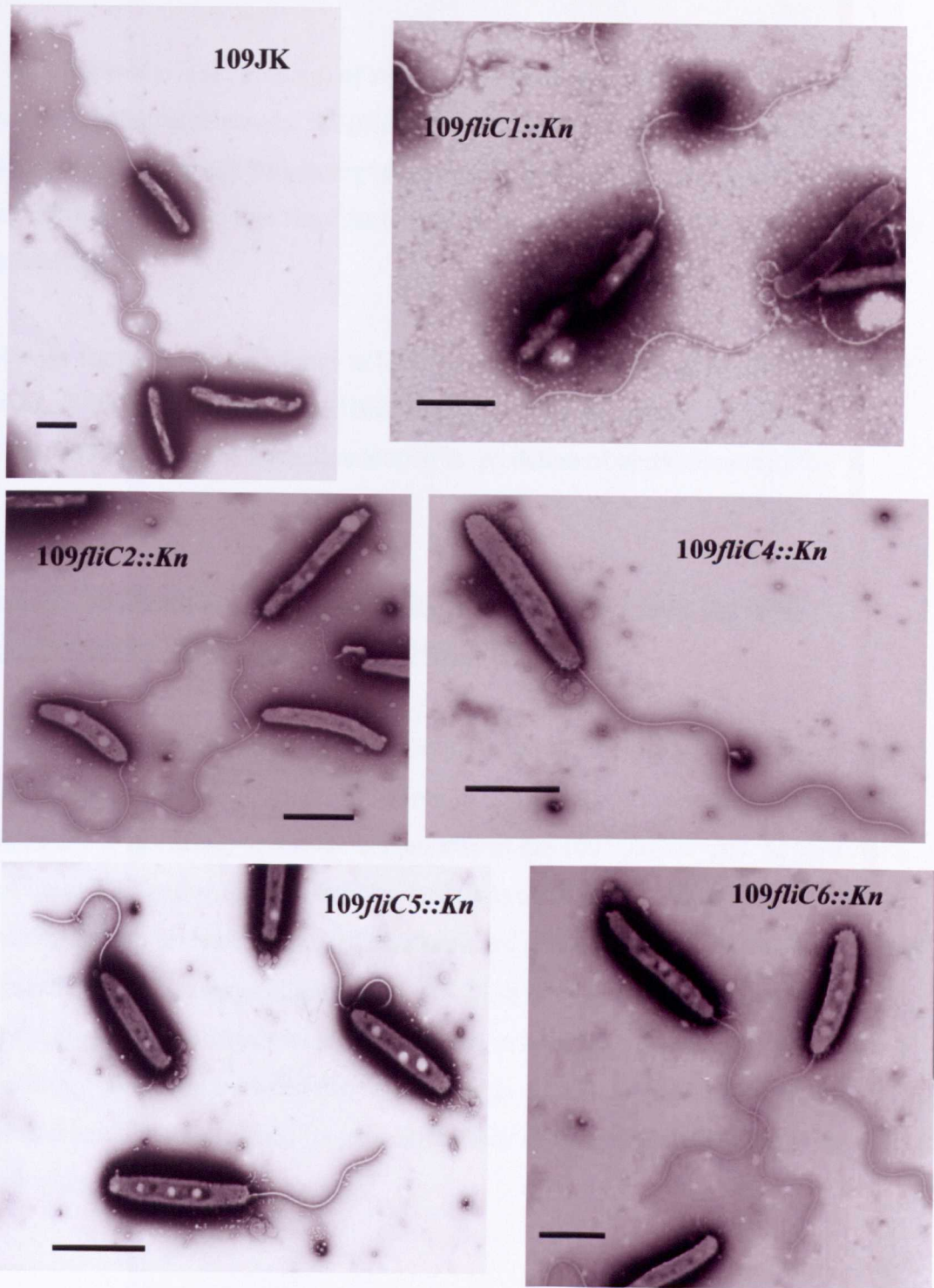


Figure 3.21 : *B. bacteriovorus* 109J *fliC::Kn* mutants. Strains are as indicated, 109JK is a kanamycin-resistant wild type strain with normal flagella. Interruption of *fliC1,2,4* and *6* have no visible effect on filament morphology. *fliC5*, however, has truncated filaments that appear to be lacking the lower amplitude, distal flagellar waveform. All stained 1% PTA pH7, bars = 1 μ m.

Tracking analysis (L. Hobley) of swimming speeds showed that although there was no morphological changes, 109J*fliC1::Kn* and 109J*fliC4::Kn* strains did show a slightly reduced mean swimming speed compared to 109JK wild type (Lambert *et al.*, 2006), indicating that flagellar length and swimming speed do not show a simple correlation.

Assays for predatory efficiency in liquid media (see (Lambert *et al.*, 2003; Lambert *et al.*, 2006) for details) showed that, from these four mutant strains, only 109J*fliC4::Kn* showed a small reduction in predation of approximately 7%.

3.2.2.2: Inactivation of the cognate *fliC* genes in HD100 gave the same phenotypes by TEM as in *B. bacteriovorus* 109J

As part of work for this thesis, I used the plasmid (pSET151 based) constructs used in 109J to interrupt the cognate *fliC* genes in HD100, the genome-sequenced strain (Rendulic *et al.*, 2004) to test the universality of the 109J phenotypes. As illustrated in Figure 3.22 below, protein level comparisons of 109J and HD100 FliCs show an extremely high level of identity (the proteins are almost identical if compared like for like rather than in a large alignment of all 12), so it was expected that the gross morphological phenotypes would be the same in both *B. bacteriovorus* strains. This homology constraint between two related strains may be related to the fact that *B. bacteriovorus* have sheathed flagella, so the lack of variation is not completely surprising.

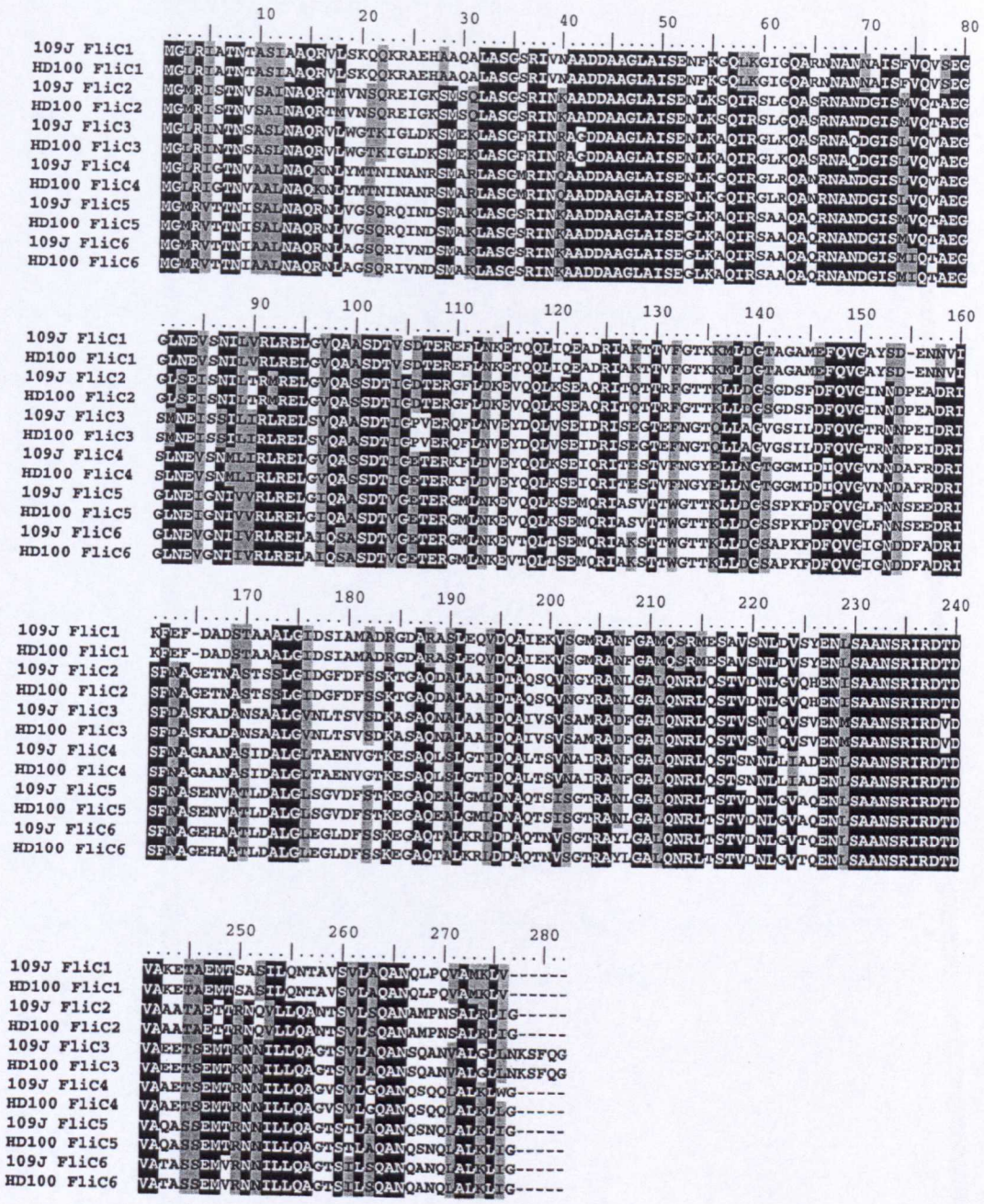


Figure 3.22: Multiple protein alignment of all 109J and HD100 flagellins; the high degree of sequence conservation is evident and is greater if the same protein pairs are considered individually. Created using ClustalW in BioEdit, see Section 2.10.

The *fliC::Kn* gene interruption constructs were conjugated into HD100 from *E. coli* S17-1 and the resulting exconjugants sub-cultured and screened for loss of the chromosomal wild-type copy of the gene and concurrent loss of the suicide plasmid vector, pSET151. Figure (i) in Appendix 3 shows the screening PCRs and confirmatory Southern blots for inactivation of *fliC3,4,5* and *6* in HD100. HD*fliC3::Kn*, like the 109J*fliC3::Kn* strain (see Section 3.2.3), had to be grown prey-independently (HI). HD*fliC2::Kn* could not be obtained during the time of this work, despite repeated attempts. HD*fliC1::Kn* was created by Dr Carey Lambert some time previously.

TEM study of the mutant strains (see Figure 3.23) obtained show the same phenotypes as 109J; HD*fliC1,4* and *6::Kn* showed no alteration in gross filament morphology or length. HD*fliC5::Kn* showed the same truncated filament as is seen in 109J*fliC5::Kn* (discussed in greater detail within this context in Section 3.2.2.3.) resulting from loss of the distal low amplitude waveform. Observation of this mutant with phase contrast microscopy also showed a visible reduction in swimming speed compared to wild type HD100 (which is highly motile, swimming at speeds of up to $160\mu\text{m sec}^{-1}$). TEM study of HD*fliC3::Kn* HI showed the same phenotypes as that in 109J; the strain had no functional flagellar filament and had a disordered sheath structure. This will be discussed in greater detail within the context of 109J*fliC3::Kn* HI in Section 3.2.3.

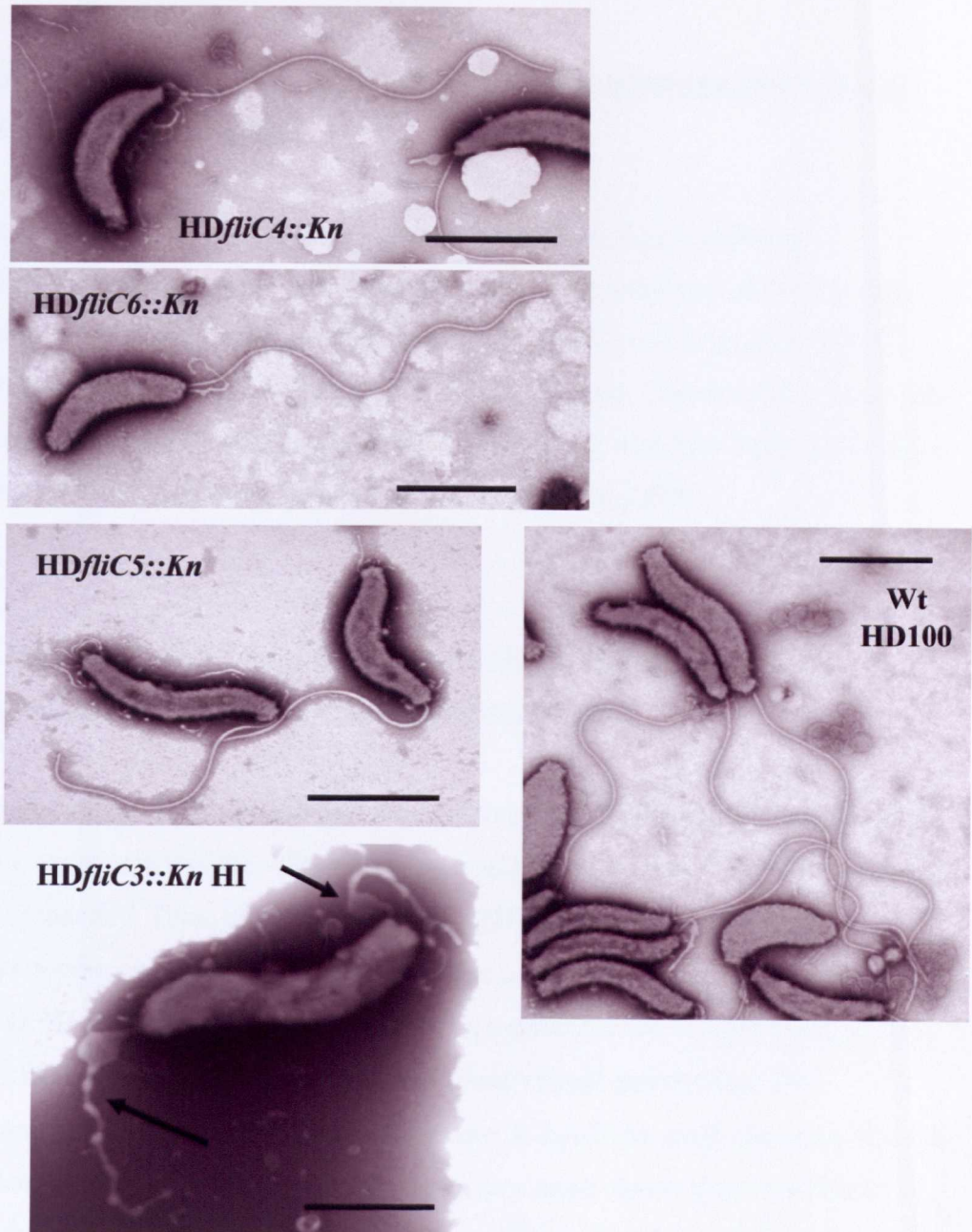


Figure 3.23: TEM of selected cognate *B. bacteriovorus* HD100 *fliC* mutant strains. Strains are as indicated. The same phenotypes as those in 109J were observed: HD*fliC1,4* and *6::Kn* do not alter in filament length or morphology compared to wild type; HD*fliC5::Kn* has truncated filaments and HD*fliC3::Kn* HI (the chromosomal interruption of *fliC3* could not be obtained in prey-dependent strains, so the host-independent growth phase of *Bdellovibrio* was used to rescue the mutant) has no intact filaments but disordered empty sheath (cell shown appeared to have a sheath present at either end of the cell; unusual but not unknown in HI *Bdellovibrio*). All stained 1% PTA pH7, bars = 1 μ m.

3.2.2.3: Inactivation of 109J *fliC5* produced truncated flagellar filaments and reduced predatory efficiency

As can be seen in Figure 3.21 earlier, inactivation of *fliC5* gave a definite morphological change to the 109J flagellum. The small amplitude waveform distal to the cell body was lost, leaving a truncated filament with a mean length of 2.3 +/- 0.5µm, a reduction of 2µm on average from the wild type. Concomitantly, there was an observed reduction in swimming speeds (80% of the wild type 35µm sec⁻¹) and a reduced predatory efficiency in this strain (Lambert *et al.*, 2006).

3.2.3: Inactivation of 109J *fliC3* produced a strain capable only of prey-independent growth with sheath but no intact filament

The most striking mutant phenotype was inactivation of *fliC3*; a double recombinant for gene replacement of the wild-type copy could not be obtained under conditions of prey-dependency. Thus, the host-independent (HI, see Section 1.4) growth mode of *B. bacteriovorus* was used to rescue the mutant so the phenotype could be examined. HIK3, an HI derivative of 109JK, was used as a control strain for this work; as can be seen in Figure 3.24, HIK3 has a diverse spiral/vibroid morphology, but importantly for this work, is normally flagellate. It should be mentioned here that due to the nature of HI growth, which tends to be very much slower than other bacteria grown on complex media (2-3 days to reach an OD₆₀₀ of ~0.8 in 1ml broth from a single colony), the flagella seen on these cells tend to be much longer than the prey-dependent strains (see Section 3.1.4, as cells age, the flagellar filament extends distally in the period III waveform).

However, the mutant 109J*fliC3*::*Kn* HI strain had no appreciable flagellar filament and was non-motile as observed by phase contrast microscopy, but did have a disordered sheath structure extending from the flagellar pole of the cell (see Figure 3.24).

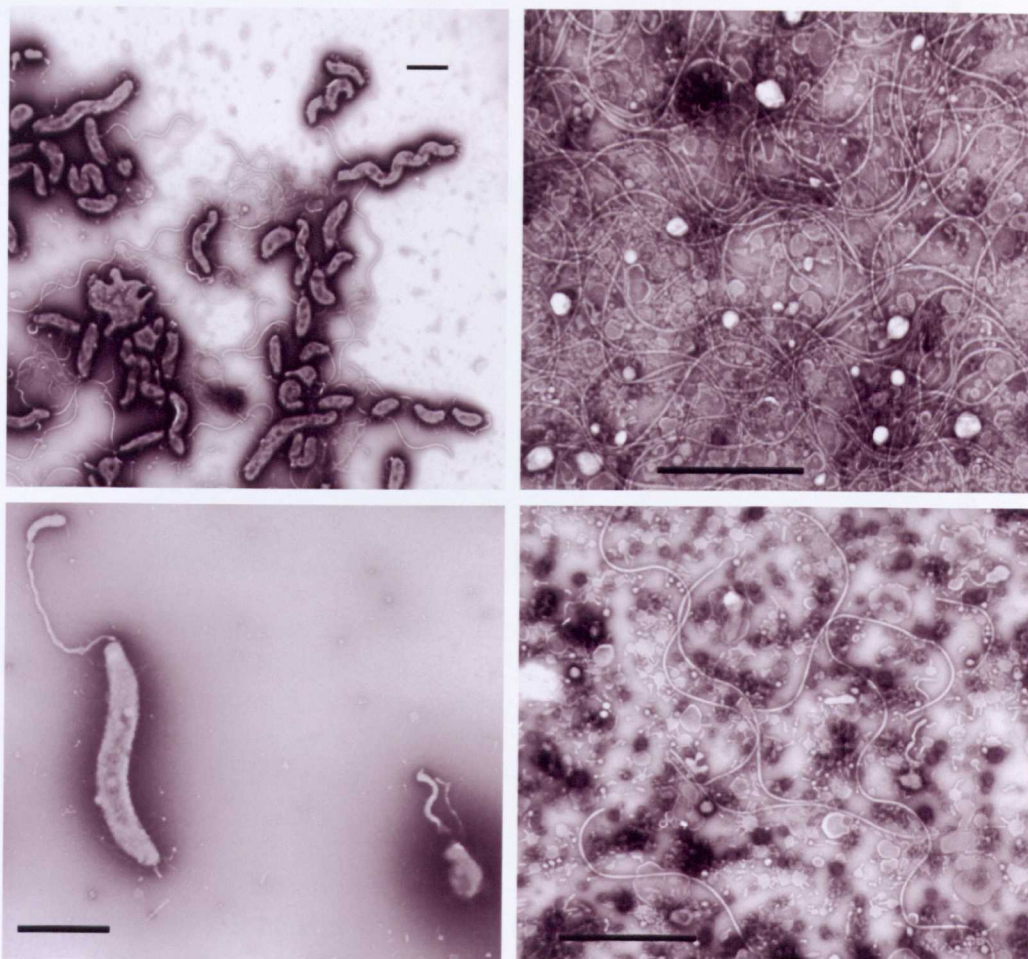


Figure 3.24: TEM images of 109JK-derived host-independent strain, HIK3 (top panels), the control strain used for HI work in this section. In common with other HI strains, HIK3 has sheathed flagella as well as the abnormal cell morphology associated with the HI phenotype. The right panel shows the result of shearing of HIK3 flagella; filaments are abundant with some lipid debris. Bottom panels, 109*fliC3::Kn* HI strain. The chromosomal interruption of *fliC3* could not be obtained in prey-dependent strains, so the host-independent growth phase of *Bdellovibrio* was used to rescue the mutant. As can be seen, the strain lacks an intact flagellar filament and has just a sheath structure, implying that flagellar motility is needed for wild-type prey dependent behaviour in *Bdellovibrio*. Bottom right panel, sheared *fliC3::Kn* sheaths reveal the presence of very few long filaments (possibly reassembled spontaneously in solution) and much more lipid debris than in HIK3, see main text for a full discussion. Stained 1% PTA pH7, bars = 1 μ m., bars = 1 μ m.

Isolation of Hook-Basal Body (HBB) structures from this mutant strain showed that the HBB was formed correctly and was not affected by the mutation in *fliC3*, as expected in the normal flagellar assembly hierarchy (see Figure 3.25 below, Method detailed in Section 2.7.4.2).

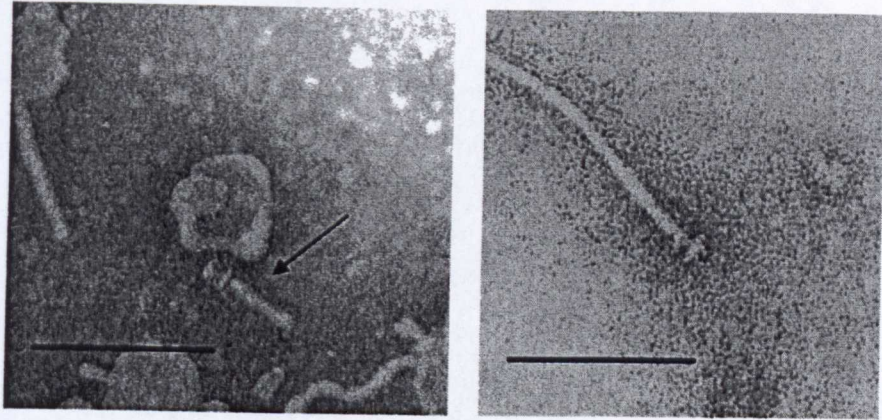


Figure 3.25: Isolated Hook-Basal Body structures from (left) 109*fliC3::Kn* HI and wild-type *B. bacteriovorus* 109J (right). The HBB structure is the same (please refer to Figure 3.1 in Section 3.1 for the general HBB structure in Gram-negative bacteria) indicating that inactivation of *fliC3* has no effect on the export and construction of the basal body of the flagellum. Stained 1% PTA pH7, bars = 0.2 μ m.

The phenotype of this mutant also implies that, despite the high degree of sequence conservation of the flagellin proteins, FliC3 has a singular function that cannot be complemented by any of the other five flagellins.

3.2.3.1: Characterisation of the *fliC3* mutant sheath-like structure – are other flagellins retained?

Studies of HAP2 (FliD) mutants of *Vibrio parahaemolyticus* which lack the filament cap to retain secreted flagellin monomers but still have the sheath, form an apparently intact, functional flagellum (McCarter, 1995) (see Section 3.1.2). To ascertain whether there were still flagellin monomers from the other five genes secreted into the sheath in the absence of FliC3, flagella shearing preparations were made of HIK3 as a control and 109*fliC3::Kn* HI strains (see Section 2.7.4.1).

As can be seen in Figure 3.24 earlier, HIK3 predictably gave abundant flagellar filaments with some lipid debris, presumably from the sheaths, as assessed by TEM. 109*fliC3::Kn* HI gave much more lipid debris, as would be expected, but also showed a few apparently intact filaments as flagellins can spontaneously reassemble into short polymers if in high local concentration (though only a tiny percentage of that of HIK3), agreeing with the previous work in other bacteria (McCarter, 1995).

Semi-quantitative reverse-transcriptase PCR analysis, carried out by C. Lambert and M. Capeness as part of collaborative work for (Lambert *et al.*, 2006), showed that in RNA samples prepared from 109*fliC3::Kn* HI and HIK3, expression levels of other flagellins were altered in the mutant strain compared to the wild type (see Figure 3.26 below)

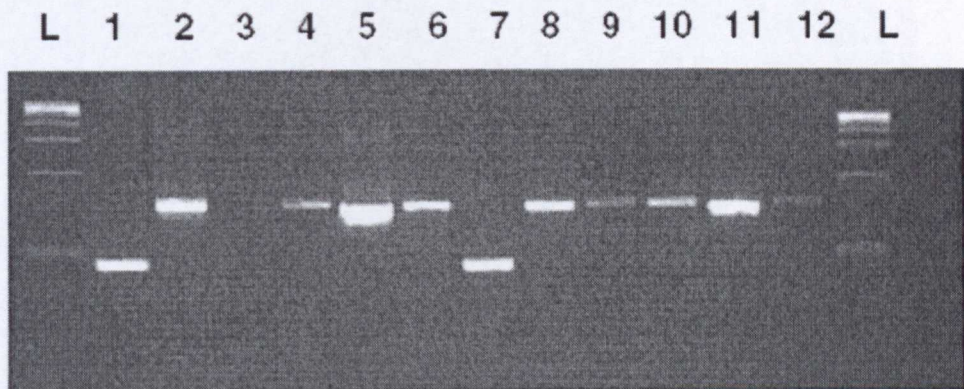


Figure 3.26: Semi-quantitative RT-PCR of flagellin genes in 109*fliC3::Kn* HI and HIK3. Lanes 1-6, *fliC1-6* primer pairs in 109*fliC3::Kn* HI, lanes 7-12, *fliC1-6* primer pairs in HIK3. Expression of *fliC3* is abolished as would be expected in the mutant strain; *fliC5,2* and *6* show an apparent increase in transcript levels compared to HIK3. (Lambert *et al.*, 2006) L = NEB 100bp ladder (see Appendix 1).

Logically therefore, there should be a difference in protein abundance of flagellins in 109*fliC3::Kn* HI compared to HIK3. I investigated this by SDS-PAGE analysis of the sheared flagellar/sheath preparations. The predicted molecular weights (from the protein sequences, calculated using the Compute pI/Mwt tool held at www.expasy.org) of both 109J and HD100 flagellin proteins are 29kD ±0.8 (see Table 3.2).

FliC	HD100 predicted mwt (kD)	109J predicted mwt (kD)
FliC1	29.09	29.09
FliC2	29.28	29.28
FliC3	29.88	29.88
FliC4	29.54	29.61
FliC5	29.21	29.21
FliC6	29.19	29.19

Table 3.2: Predicted molecular weights of *B. bacteriovorus* flagellin proteins. Predicted from protein sequence using Compute pI/Mwt held at www.expasy.org, see Section 2.10. Isolated flagella were then run on an SDS-PAGE gel to see actual flagellin sizes (see figure below)

When the flagellar shearing preparations were run on denaturing gels, flagellin bands were found distributed between 29-33kD. Thus, I carried our mass spectroscopic analysis and peptide sequencing of these altered flagellin bands, SDS-PAGE and mass spectroscopy results are demonstrated in Figure3.27 on the following page.

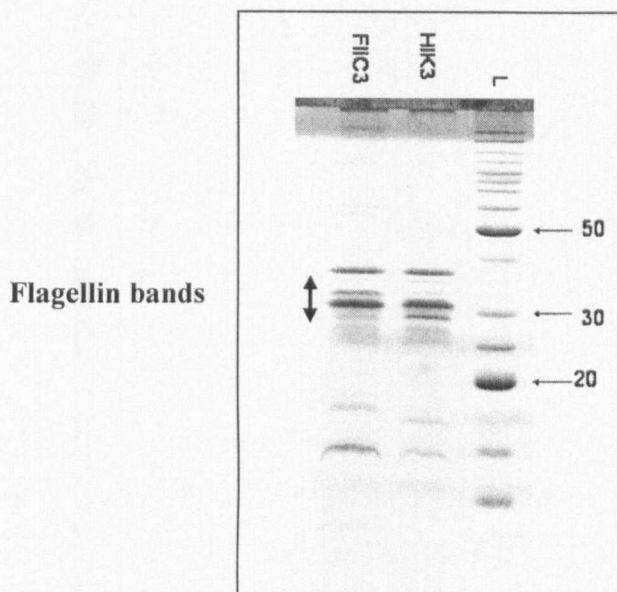


Figure 3.27: (i) 12.5% SDS-PAGE gel showing the protein profile of sheared flagella/sheath from 109*fliC3::Kn* HI and HIK3. The arrow indicates the area where flagellin proteins are according to their predicted molecular weights. Both strains contain flagellin bands between 29 and 33kD; 109*fliC3::Kn* HI shows enrichment of the band at 33kD. The dominant band in both strains is 31kD. Coomassie Blue stain, L = BenchMark protein ladder (Invitrogen) numbers on the right correspond to the molecular weight standards in kD, protein samples matched to 5µg each using the Lowry assay (see Section 2.7 for more detail).

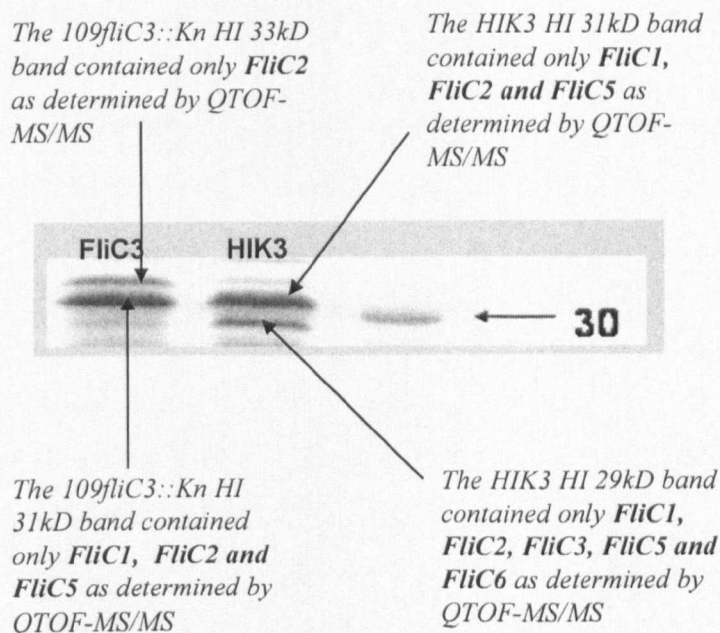


Figure 3.27(ii): Close up of flagellin region around 30kD. Mass spectroscopy results for the bands examined were as stated in the figure. Please see main text in Section 3.2.3.2 on the following page for a more detailed analysis.

3.2.3.2: Characterisation of the *fliC3* mutant sheath – Q-TOF MS/MS analysis of the dominant flagellin bands in 109*fliC3::Kn* HI and HIK3

The following experiments were carried out with Kevin Bailey from the University of Nottingham Biopolymer Sequence Analysis Unit; I am grateful for his expertise in protein mass spectroscopy and helpful hints on analysis.

The bands corresponding to 33 and 31kD in the *fliC3* mutant strain and 31 and 29kD in the HIK3 control strain were excised from a 12.5% SDS-PAGE gel and subject to in-gel trypsin digest. The 29kD band in the *fliC3* mutant strain was not sufficiently abundant to provide an accurate analysis. Quantitative Time Of Flight mass spectroscopy (see Section 2.7.5) was carried out on the samples to test for the presence of peptides unique to each of the flagellin proteins. Raw data was analysed using the Matrix Science Mascot MS/MS program to allow identification of peptide sequences generated (see Section 2.10.4, (Perkins *et al.*, 1999)). The findings are summarised in Figure 3.27(ii) above; the mass spectra and the corresponding unique flagellin peptide sequences are in Appendix 2.

As expected, no FliC3 peptides could be detected in the mutant strain; FliC3 peptides were also only rarely encountered in the wild-type HIK3 strain, indicating a possible low abundance of the protein in the wild type sample. FliC4 peptides could not be definitively found anywhere in the analysis; there was one possible fragment (data not shown) found in the HIK3 29kD sample, but the fragment was too small to reliably call as FliC4-derived. This could perhaps correspond to the low level of transcript seen in the semi-quantitative RT-PCR data (Figure 3.26) in both strains. FliC2 fragments were found in all samples tested, despite the apparent disparity in molecular weights; FliC5 and FliC1 were also found in all except the enriched *fliC3* 33kD band. FliC6 was only found in the 29kD band in HIK3; I would propose it would also be present in the faint 29kD band in the mutant strain, but this band was not sufficiently abundant for analysis.

What the protein analysis did show was that, in the absence of FliC3 in 109J, the other five flagellins are still translated and secreted; however, no rotationally functional flagellar filament is formed. Some filament-like structures are still seen in

sheath preparations of 109*fliC3::Kn*, agreeing with data from other species that high local concentration of flagellin monomers will spontaneously form short polymers (see Section 3.1.2).

3.3: Is the FliC3 mutant still predatory even though it is non-motile?

Standard predation assays used in our lab at the beginning of this work can only reliably assess the predatory capability of prey-dependent motile strains (Lambert *et al.*, 2003). As such, a new assay had to be developed for the 109*fliC3::Kn* HI mutant. The gift of pSB3000 from Dr P.J. Hill and T. Perehiec (University of Nottingham, Sutton Bonnington campus), which is a plasmid that constitutively and at high level, expresses Yellow Fluorescent Protein (YFP, excitation 500nm) when replicated in *E. coli*. Rob Till transformed this construct into *E. coli* S17-1:pZMR100 (Rogers *et al.*, 1986) (the standard prey strain for *Bdellovibrio* in our lab with pZMR100 conferring kanamycin resistance to the strain, matching that of the predator mutants under test) to produce a strain that expressed YFP and was not sensitive to kanamycin (the selection for pSB3000 was ampicillin, as mentioned in Section 1.6, *B. bacteriovorus* strains are naturally ampicillin resistant at the 50µg/ml concentration used for growth and maintenance of this strain). In collaboration with R. Till, I developed an assay to measure HI predation on immobilised fluorescent prey, detailed in Section 2.9.3.

In essence, a mixture of HI *B. bacteriovorus* and YFP-expressing *E. coli* were spotted onto a PYkan⁵⁰ agar plate to immobilise the prey (rich media supports growth of both *B. bacteriovorus* and *E. coli*) and incubated for 24 hours at 29°C. Cells were then scraped off the surface and resuspended in Ca²⁺ HEPES buffer; samples were agar mounted and examined using phase contrast and YFP optics on a Nikon Eclipse E600 microscope. The numbers of bdelloplasts formed per 1000 *E. coli* were counted (n>2500) and used as a measure of predatory capability, see Figure 3.28. In this context, it was merely to see if the 109*fliC3::Kn* strain could still predate; in Chapter 5, it was applied to compare the relative numbers of bdelloplasts formed by both control strains and mutant (see Section 5.4.2.2).

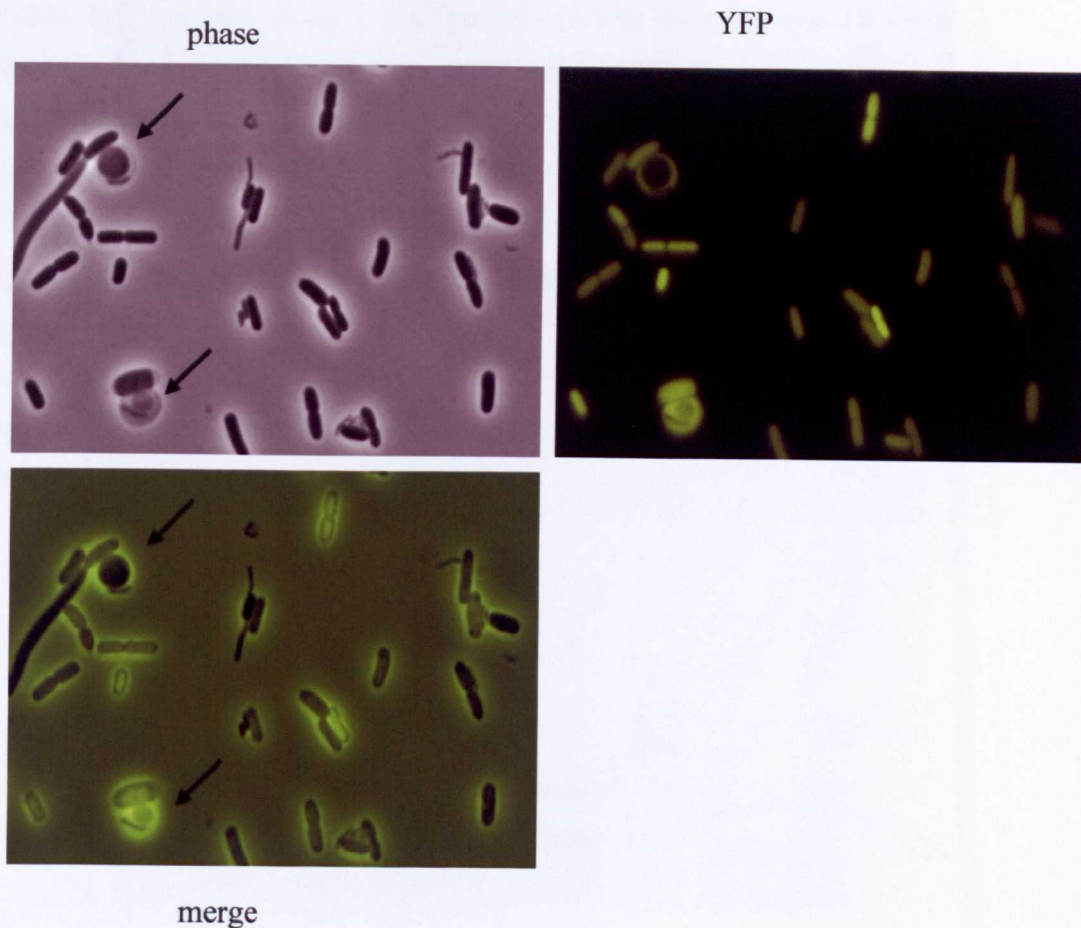


Figure 3.28: Fluorescence assay for the predatory capability of 109*flic3::Kn* HI. Arrows indicate bdelloplasts; the nature of the assay allows differentiation between the *Bdellovibrio* and *E. coli*, as only the latter express YFP, the former appear as dark cells only. These results clearly indicate that the inactivated *flic3* HI strain may be non-motile but is still capable of predatory behaviour when placed in close proximity with immobilised prey. Images taken using a Nikon Eclipse E600 microscope under 100x magnification.

The figure for the number of bdelloplasts formed per 1000 *E. coli* prey cells (unpublished data obtained later) for the 109*fliC3::Kn* HI strain is an average of 11/1000. This compares nicely to the figure of ~45/1000 for a wild-type HI strain (please see Section 5.4.2.2 for full details of this experiment). Hence, the 109*fliC3::Kn* HI is still predatory when placed in close proximity to prey, even though it is non-motile.

3.4: Comparison of the sheared flagellar protein profiles of all the 109J flagellin mutant strains

Flagellar shearing of the 109J strains, see Figure 3.29 below, showed some differences in the protein profiles.

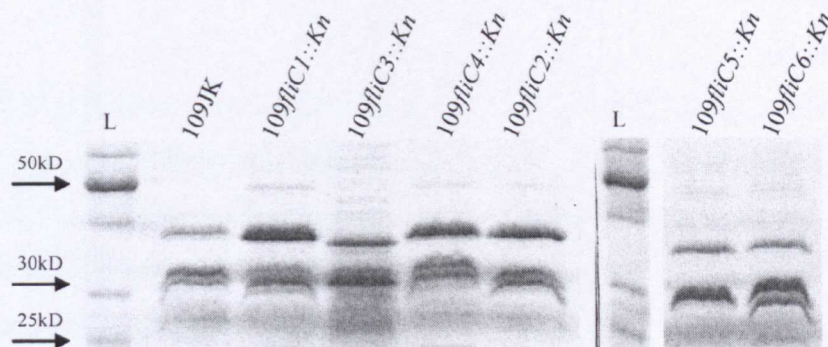


Figure 3.29: SDS-PAGE of 109J *fliC* mutant sheared flagella. Strains are as labelled. Flagellins are present in the doublet bands at approximately 30kD (as demonstrated by Q-TOF MS/MS, Section 3.2.3.2). For a full discussion, please see main text. Gels: 12.5% acrylamide, ladders (L) Benchmark protein ladder, Invitrogen, sizes are as indicated. Loaded with 4µg protein as determined by Lowry assay. Stained with Coomassie Brilliant blue and destained in 30% methanol, 10% glacial acetic acid.

As expected from the TEM phenotypes, *fliC4* and 2 do not show noticeable differences from the wild type 109JK. *fliC1* seems to show an enrichment of the lower flagellin doublet at approximately 30-31kD compared to wild type; *fliC6* seems to show an enrichment of the upper band at approximately 32kD. *fliC3*, as discussed in Section 3.2.3.2 shows a lack of the lower band at ~29kD and another band at ~33kD (more obvious on gels where the lanes have run more evenly). *fliC5*

shows only one clear band rather than two which is at approximately 30-31kD; considering the TEM phenotype where the distal small amplitude waveform of the flagellum is missing, this is unsurprising. As demonstrated in Section 3.2.3.2 (Q-TOF MS/MS) and Section 3.2.3.1 (semi-quantitative RT-PCR of the other flagellins in a *fliC3* null background), inactivation of one of the flagellin genes results in a change of expression of the others, giving a different protein profile.

3.5: Discussion

3.5.1: The entire *B. bacteriovorus* flagellum is not shed immediately upon prey entry

The observation of early stage bdelloplasts with short lengths of the predator's flagellum protruding from within showed that flagella are not entirely shed immediately upon prey entry as stated in (Thomashow and Rittenberg, 1979). The presence of short flagellar filaments outside an early stage bdelloplast therefore does not seem compromise the predatory process or integrity of the bdelloplast structure; this may be facilitated by the presence of the membranous sheath (Lambert *et al.*, 2006).

3.5.2: The role of flagellar-mediated motility in the predatory lifestyle of *B. bacteriovorus* – flagellar motility is necessary for successful predatory behaviour in liquid media but is not absolutely required for predation

Studies in 109J and HD100 show that flagellar motility affects the swimming speeds of these highly motile bacteria and (in 109J) the predatory efficiency of those mutant strains that have reduced swimming speeds. Flagellar motility is therefore important for prey encounters in liquid media. It is interesting that, despite high levels of sequence conservation between the six flagellin genes, inactivation of *flic3* resulted in a non-functional flagellar filament and a mutant strain that could not swim or predate in liquid media; FliC3 obviously has a specialised role in formation of the flagellum which cannot be predicted from its sequence nor complemented by the

continued synthesis of the other five flagellins. Other published data, where individual mutation of the five flagellin genes in *Vibrio cholerae* was carried out, showed that only one protein, FlaA, was essential for flagellar formation (Klose and Mekalanos, 1998). In the absence of FlaA, cells were non motile and had no discernable flagellar filament. This is reminiscent of the situation in *B. bacteriovorus* 109J, where inactivation of only one of the six flagellins abolished functional flagellar synthesis.

The observation, however, that the strains with non- functional FliC3 can still predate successfully when applied to immobilised fluorescent prey shows that although flagellar motility may be required for efficient prey encounters in liquid media, it is not absolutely required for predation, disproving the drilling hypothesis of (Burnham *et al.*, 1968). This led to the hypothesis of pilus-mediated prey entry, supported by the discovery of a complete set of genes potentially encoding Type IV pili in HD100 (Rendulic *et al.*, 2004), which I investigated during the course of this work (see Chapter 5). The importance of flagellar motility in normal *B. bacteriovorus* predation, however, is shown by reduction in predation efficiency and swimming speeds in the *fliC4* and *fliC5* mutant strains.

3.5.3: The *B. bacteriovorus* flagellar sheath – an enduring mystery

The slightly surprising finding that an intact, functional flagellum is not a pre-requisite for sheath formation in *B. bacteriovorus* is curious. The phenotype seen as a result of *fliC3* inactivation indicates, as in other bacteria which have a sheathed flagellum (McCarter, 2001), that sheath biosynthesis is independent of the requirement for an intact, functional flagellum (see Section 3.1.2).

The main question is does the membranous sheath rotate with the filament or is it an independent structure within which the filament moves? These are technically difficult questions to answer, especially in *B. bacteriovorus* with the lack of genetic manipulation techniques commonly available in other species. However, sequence alignments of the major *B. bacteriovorus* flagellin, FliC3, with those of other sheath-forming species (see Figure 3.30) potentially implicates certain amino acids

contained within the variable region of the flagellin in a possible sheath interaction role.

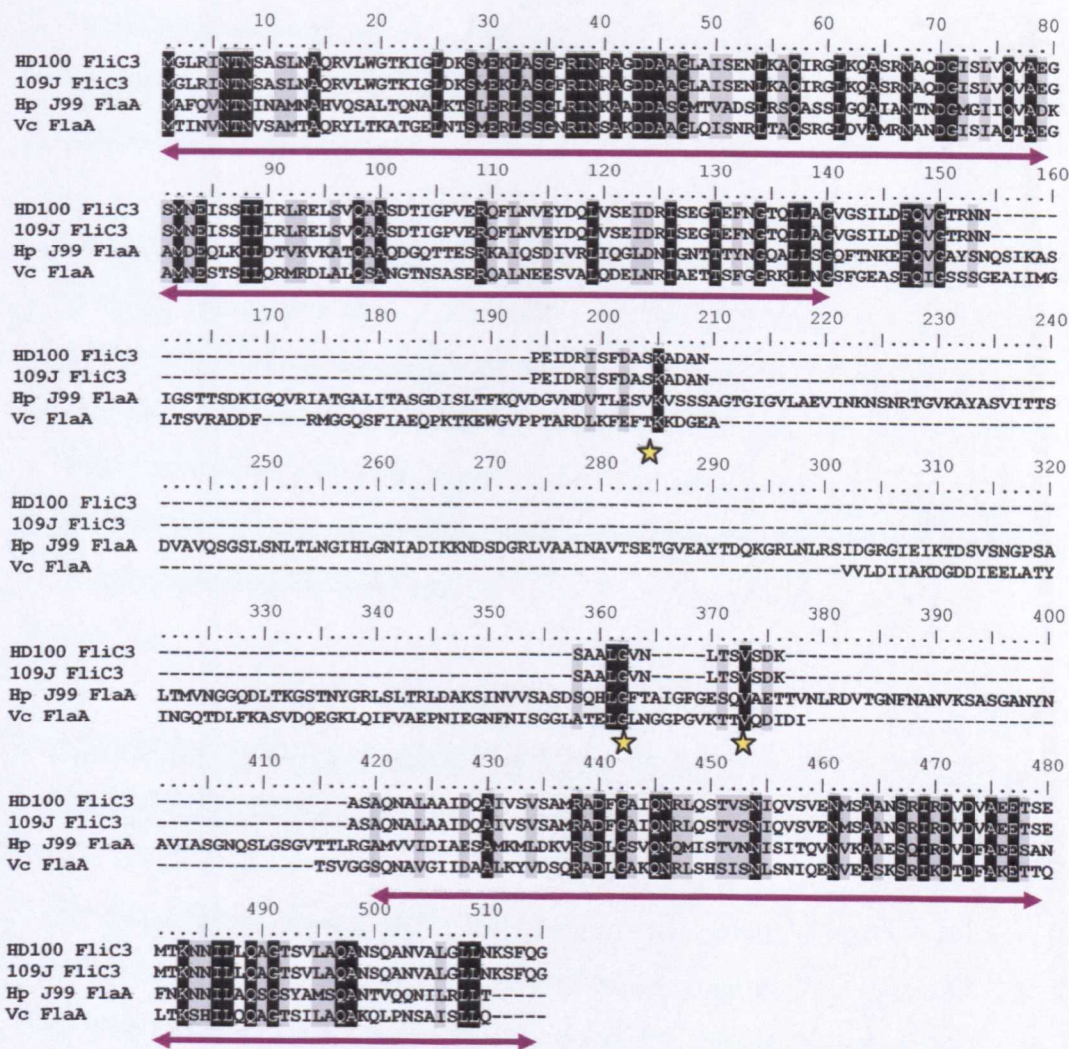


Figure 3.30: Multiple protein alignment of major flagellins in sheathed flagellate bacteria. The conserved N and C terminal regions are underlined in purple; starred residues are those conserved between the two *B. bacteriovorus* strains and the other two. The apparent conservation of the conserved (polar, charged) lysine residue in the variable region of these proteins may be significant for sheath interaction. However, this is purely speculation though may offer potential targets for future research in the *B. bacteriovorus* sheath/filament interaction. Hp = *Helicobacter pylori* J99, Vc = *Vibrio cholerae* El Tor. Alignment created using ClustalW in BioEdit, see Section 2.10.

The conservation of lysine and other residues within the variable regions of these species offers potential targets for mutation in *B. bacteriovorus*. These may or may not be significant conservations, but as *B. bacteriovorus* is found in multiple terrestrial and aquatic environments, *H. pylori* is a gastric pathogen and *V. cholerae*

is an aquatic and pathogenic bacterium implies that the one common factor is the presence of a sheath. However, this is all speculation as there has been very little work done on the sheath of any bacteria; until the development of more sophisticated genetic techniques in *B. bacteriovorus*, sheath/flagellum interaction sites must remain as speculation.

The presence of the sheath in *B. bacteriovorus* does give another boost to its potential therapeutic use. As discussed in Section 3.1.3, the *H. pylori* flagellar sheath serves to retain flagellin monomers to reduce the TLR-5 – mediated immune response to the pathogen. The *B. bacteriovorus* *fliC3* mutant also retains the other flagellins within the sheath. In conjunction with the other physical properties of *B. bacteriovorus* discussed elsewhere in this thesis (see Section 1.7), the masking of the immune-stimulatory flagellum gives hope for future therapeutic uses.

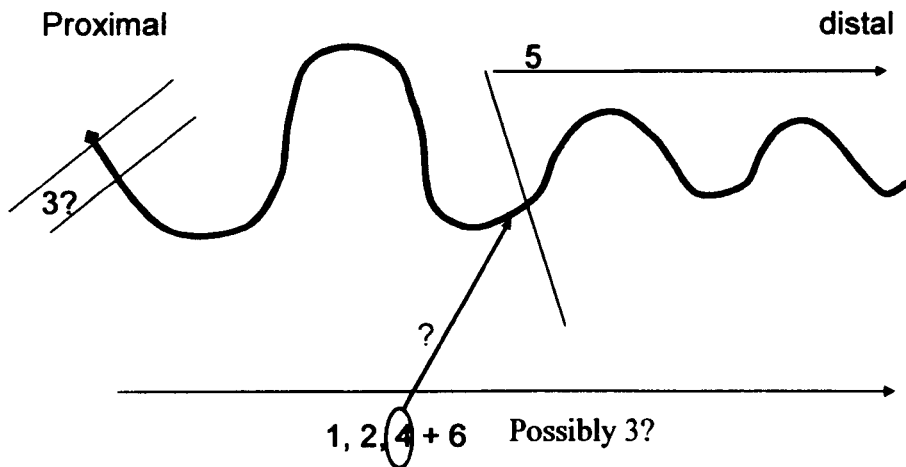
3.5.4: Does the disparate distribution of *B. bacteriovorus* flagellin proteins when examined by SDS-PAGE indicate possible post-translational modification?

The disparate distribution of the FliC proteins is curious (see Sections 3.2.3.1 and 3.4) when compared to their predicted molecular weights of 29 +/- 0.8 kD (see Table 7). This could indicate some form of flagellin post-translational modification, for example, glycosylation or phosphorylation of certain flagellin monomers, which has been shown to occur in other bacterial species such as *Campylobacter jejuni* and *Helicobacter pylori* (Guerry *et al.*, 2006; Schirm *et al.*, 2003), but this is pure speculation and further study is beyond the scope of this thesis.

3.5.5. Possible models for the arrangement of different flagellins in the *B. bacteriovorus* 109J flagellum

As discussed earlier in Section 3.1.1.1, there is no determined model for the arrangement of monomers in the flagellar filament in bacterial species that utilise multiple flagellin proteins. The main theory appears to be that of a scaffold, or core, protein that is required for correct filament formation, unless that function can be

complemented by another homologous flagellin. I agree that this is a likely model, but I propose another for the *B. bacteriovorus* flagellum, illustrated below.



The positioning of FliC3 is troublesome. The core or scaffold model would have it dispersed along the length of the filament; however, the low abundance of FliC3 unique peptides may indicate that there is less of the protein in the filament than this model would imply. I would argue for a role for FliC3 as a “junction” protein between the hook cap and the rest of the filament, which then could allow correct formation of the flagellum.

The positioning of FliC5 is somewhat more logical, as inactivation of the gene leads to loss of the distal small amplitude waveform of the flagellum. FliC1, 2 and 6, which have little discernable contribution to any measurable phenotype may well make up the rest of the filament, perhaps in a mosaic rather than in defined areas like FliC5 – otherwise their loss would be more noticeable in the mutants.

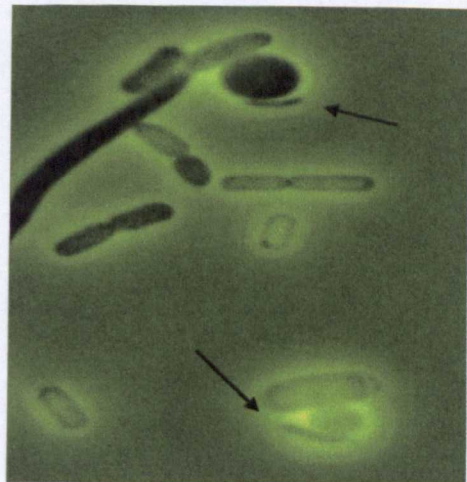
FliC4 is interesting: the mutant had no discernable morphological phenotype yet displays reduced swimming speeds and predatory capability (Lambert *et al.*, 2006). Mass spectroscopy failed to find any unique FliC4 peptides, but the gene is expressed. This indicates that possibly FliC4 is only expressed or translated at low levels. I propose that FliC4 either performs a role in perturbing the helical form in the Period II transition from large to small amplitude waveform or is distributed along the length of the flagellum in small quantities, affecting the rigidity of the filament or possibly some kind of interaction with the flagellar sheath.

Overall, it is still speculation. The most logical way to confirm the positioning of each flagellin would be immuno – electron microscopy, but the high degree of sequence conservation would make raising specific antibodies extremely difficult. Even if that was accomplished, the presence of the flagellar sheath causes its own problems for looking at flagellar proteins in intact cells. Another possible method would be individual engineering of each flagellin to express a different epitope, which could be easily detected in sheared preparations where the sheath could be removed by treatment with SDS or Triton X-100. However, the practical problems of *Bdellovibrio* genetics mean that this is currently not an option (see Section 1.6).

3.5.6: Other observations of *B. bacteriovorus* biology as a result of this study

Development and use of the fluorescence assay demonstrated findings that neatly agreed with previous research in *B. bacteriovorus*. The first is that the cytoplasmic membrane separating the cytoplasm and the periplasm of the prey cell, once rounded up into a bdelloplast by the predator, becomes permeable to small molecules while the outer membrane remains stable (Cover *et al.*, 1984; Rittenberg and Shilo, 1970). Whilst not suggesting that YFP, an approximately 27kD protein, is a small molecule, it is interesting to note the “leaky cytoplasm” of the prey cell bdelloplast – YFP is located solely in the periplasmic space of the bdelloplast (indicated by the presence of the predator), leaving the cytoplasm dark (see Figure 3.31 below).

Figure 3.31: An enlargement of the merge of Fig. 3.28 above, showing the “leaky cytoplasm” of prey bdelloplasts once infection is established. The cytoplasmic area of the prey is seen as a dark circle; the non-fluorescent predator is clearly outlined by the presence of YFP in the cytoplasm (indicated by arrows).



The other point to note is that the predator itself remains non-fluorescent. This shows that intact proteins are not taken up into the growing *B. bacteriovorus*; otherwise it too would show YFP-fluorescence.

Chapter 4: The use of fluorescence techniques to understand *B. bacteriovorus* predation

The aim of this section of work was to examine the feasibility of using GFP and other fluorophores to study development microscopically in *Bdellovibrio bacteriovorus* and also to find (before the advent of the genome sequence) differentially regulated genes between Host-Dependent and –Independent strains of the bacterium.

4.1: GFP and its application in bacteria

The development of Green Fluorescent Protein (GFP), originally isolated and characterised from the jellyfish, *Aequorea victoria* (Morise *et al.*, 1974; Ward *et al.*, 1980), as a useful tool for monitoring prokaryotic cellular processes has been particularly rapid in the last few years (for a review, see (Jansson, 2003)). The original GFP molecule has been optimised to give more useful excitation/emission spectra (Cormack *et al.*, 1996) and also to generate more stable molecules and those with different spectral properties to allow multiple fluorophore labelling of cells (for a review, see (Shaner *et al.*, 2005)).

GFP is a barrel-shaped protein with an alpha helix running down the centre (see Figure 4.1) containing the amino acids needed for its fluorescent properties through formation of a planar imidazolidone ring with conjugated double bonds. Mutations in this ring structure generate the spectral variants of GFP (excitation: 488nm, emission: 510nm), such as Yellow Fluorescent Protein (YFP, excitation: 515nm, emission: 530nm) (reviewed in (Tsein, 1998))



Figure 4.1: Schematic drawing of the structure of GFP from *Aequorea victoria*, illustrating the 11-strand β barrel and the internal α helix that forms the chromophore. Taken from (Ormo *et al.*, 1996)

GFP and its variants have been used in a wide variety of microbial fields, including the study of biofilms from both pathogenic and non-pathogenic species, bacterial cytokinesis and for environmental monitoring of specific organisms (Jansson, 2003). Genes encoding fluorescent Proteins (FPs) can be used to create tags on specific proteins on which they can be tolerated (GFP itself is a 27kD protein), for example the localisation of the polar pilus reversal regulator FrzS in *M. xanthus* (Mignot *et al.*, 2005). FPs can also be employed to create gene replacements in frame to monitor gene expression, either by targeted mutagenesis or through the use of transposons. In this study, the possibility of creating GFP *B. bacteriovorus* was explored using transposon mutagenesis with a GFP-encoding transposon, due to the lack of wide ranging antibiotic selection available in this bacterium to create targeted gene replacements without the use of antibiotic resistance.

4.1.1: GFP: Limitations and its prior reported uses in *Bdellovibrio*

There are predictable technical limitations to the use of GFP and other fluorophores in *Bdellovibrio*. The main one is the physical size of the bacterium, averaging 1 μm long by 0.5 μm wide for HD100 (see Figure 4.2) meaning that microscopy would have to be of high quality and resolution for GFP imaging in *B. bacteriovorus*.



Figure 4.2: Strain HD100 attaching to S17-1 *E. coli*. An illustration of the relatively small size of *B. bacteriovorus* compared to lab *E. coli* strains, demonstrating that very high quality and resolution imaging of GFP expression in *B. bacteriovorus* would be required. Phase contrast image taken under 100x magnification using a Nikon Eclipse 600 light microscope, bar = 1 μm .

Levels of fluorescence would be dependent on the native or exogenous promoter controlling GFP expression: some native *B. bacteriovorus* promoters would, in common with all organisms, be relatively weak or strong if the GFP were chromosomally encoded, resulting in variable levels of expression; complicating matters, there has been little or no published work on *B. bacteriovorus* promoters and their regulatory sigma factors. The predatory life cycle itself also means that there are further complications with GFP expression if under the control of a native promoter. Expression of some genes in *B. bacteriovorus* will be restricted to specific stages of the life cycle, such as prey entry/exit or filament elongation during growth.

A solution to these issues would be expression of GFP from a strong, (either *B. bacteriovorus* or non-native) promoter encoded either on the chromosome or from a plasmid capable of autonomous replication.

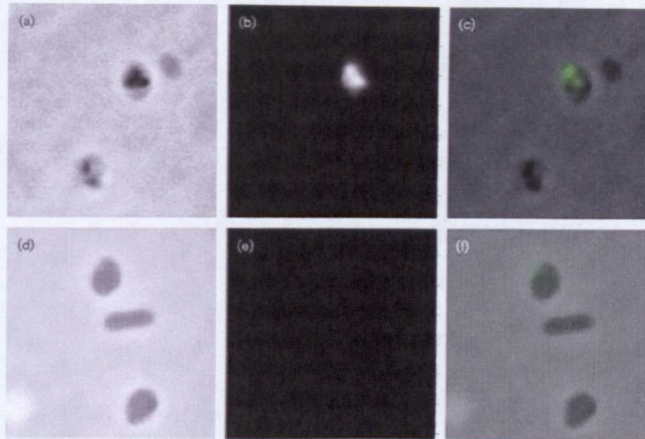


Figure 4.4: taken from (Flannagan *et al.*, 2004). Top panel, GFPpMMB206 containing 109J bdelloplast, bottom, plasmid-less 109J bdelloplast. Attempts in our laboratory to repeat this work have so far been unsuccessful.

As the preferred option for obtaining GFP *B. bacteriovorus* was unsuccessfully repeated, transposon mutagenesis was employed to create stable GFP expressing strains; this method had the benefit of possibly finding genes that were differentially regulated either throughout the predatory life cycle or between prey-dependent and – independent growth. It was decided to use a mini Tn10 transposon carrying a promoterless GFP and a kanamycin resistance gene (previously used in other bacteria, see Section 4.1.2), which had been previously successfully used in *B. bacteriovorus*.

4.1.2: pLOFKmgfp: construction and applications in bacteria.

pLOFKmgfp was created from a plasmid base that originally contained *oriT* from RP4 (allowing conjugal transfer) plasmid pBOR8 (Herrero *et al.*, 1990). This construct was ligated to an *EcoRI* insert isolated from the phage λ 1105, which contains a mini Tn10*KnR* element with the IS10R transposase encoded outside of the transposon ends (Herrero *et al.*, 1990). The resulting pLOF series of vectors has been used to isolate stable insertion mutations in a variety of bacterial species (Albertson *et al.*, 1996; Stretton *et al.*, 1998) and then further engineered to produce the final construct used in this study, pLOFKmgfp (see Figure 4.5). Stretton and co-workers introduced a promoterless *gfp* gene from pBC*gfp* into the unique *SfiI* site upstream of the *KnR* gene within the mini Tn10 ends (Stretton *et al.*, 1998), henceforth called mini Tn10*gfpKnR*.

This created a plasmid that cannot replicate in hosts that do not contain the π protein encoded by λ *pir*, could be conjugated into other bacteria from suitable hosts and encodes a mini Tn10*gfpKnR* transposon that inserts stably into the chromosome due to the IS10R transposase being plasmid encoded. Selection by Stretton *et al* for bacteria containing the insertion element was through the use of kanamycin, resistance to which is found in all exconjugants due to the *KnR* having an endogenous promoter, giving a simple screen.

This mini Tn10*gfpKnR* construct has been successfully used by groups studying gene expression in bacteria such as *Pseudoalteromonas*, *Psychrobacter* and *Vibrio*, showing promise that it may work well in *B. bacteriovorus* (Stretton *et al*, 1998). GFP fluorescence of exconjugant strains containing the mini Tn10*gfpKnR* is less frequent due to the gene not having its own promoter. Thus, GFP expression is dependent on:

- correct orientation and suitable distance with respect to the native host promoter sequences to create a transcriptional fusion
- the gene or operon interrupted not being vital for cellular survival in the stage of life being studied

Whether GFP can be visualised is also dependent on the strength of the host promoter and therefore GFP copy number. Although the transposon would not allow us to study genes vital for predatory growth, it was hoped that it may indicate the utility of GFP in *B. bacteriovorus* and potentiate further directed translational GFP fusion studies.

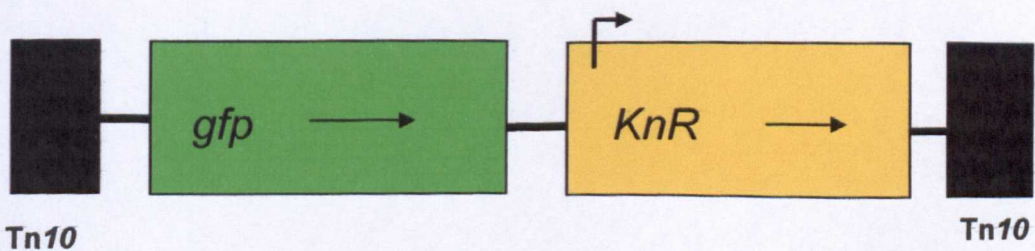
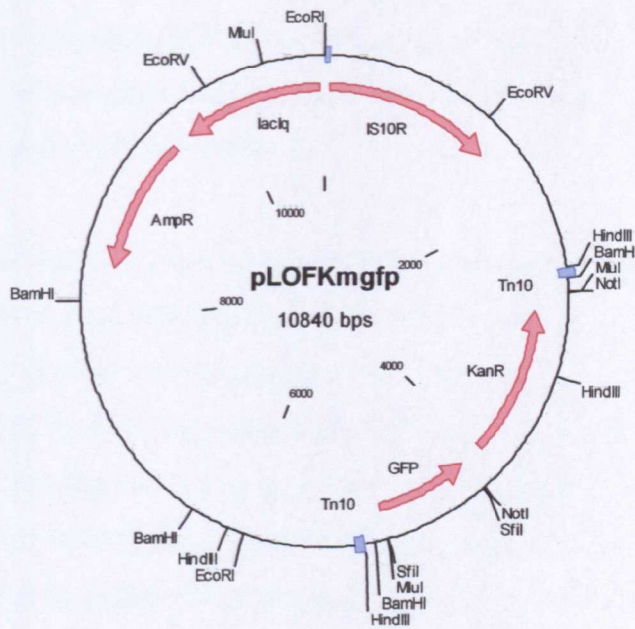


Figure 4.5: Map of pLOFKmgfp. The plasmid contains a mini Tn10 element within which are encoded a promoterless *gfp* and a kanamycin resistance gene with an endogenous promoter (mini Tn10*gfpKnR*). The IS10R transposase is encoded outside of the Tn10 ends so does not transpose into the genome with the element itself, creating a stable chromosomal mutant. Created using Clone Manager Basic Version 8. Below, expanded cartoon of transposon mini Tn10*gfpKnR*, (2.6kb).

4.1.2.1: Could pLOFKmgfp be used in *B. bacteriovorus* to deliver promoterless GFP reporter genes?

There are no previous studies that have used a suicide vector containing a transposon encoding GFP in *B. bacteriovorus*. The fact that the insertion element contains a *KnR* gene was encouraging for use in this bacterium as it is the one antibiotic to have been successfully used to create stable mutants (Lambert *et al.*, 2003; Lambert *et al.*, 2006). The plasmid pLOFKmgfp replicates at a very low copy number in *E. coli*, approximately one copy per cell, so there should only be one transposition event per *B. bacteriovorus* recipient and GFP can only be produced when the gene is under the control of a chromosomal promoter.

The aim of using this system to create a library of mutants was a proof of principle that suicide vectors can be used to deliver DNA encoding fluorophores into the *B. bacteriovorus* genome and the downstream prospects for alternatives to GFP being used if the visualisation was acceptable within *B. bacteriovorus* cells using current techniques. Another aim was to see if that random transposition could generate any fusion proteins/interruptions that had a specific subcellular or temporal expression pattern; and to see if there were any genes tagged that were differentially expressed between HD and HI states.

4.2: Construction of *B. bacteriovorus* Transposon mutants

Conjugal transfer of pLOFKmgfp from *E. coli* SM10 into *B. bacteriovorus* HD100 and 109J



Growth of exconjugants on *E. coli* S17-1:pZMR100 with Kanamycin selection on soft agar overlays to promote stable transposition into the *B. bacteriovorus* genome



100 plaques picked from both HD100 and 109J exconjugant plates and subcultured in 2ml

S17-1:pZMR100/Ca²⁺ HEPES Kan⁵⁰ cultures to give predatory lysates



Surviving Kn^R lysates screened manually using GFP optics under microscope for fluorescence



All strains, GFP+/- turned HI to screen for any differential expression of GFP-tagged genes in prey-dependent versus –independent growth



Selected strains further characterised under microscope, genomic DNA was prepared and shotgun cloned to find mini Tn10gfpKnR insertion site by DNA sequencing

	<u>109J</u>	<u>HD100</u>
<i># plaques picked after conjugation</i>	100	72
<i># plaques survived Kan⁵⁰ growth</i>	56 (4 later could not be further cultured)	23
<i># GFP+/KnR by microscopic screen</i>	37	6
<i>#GFP-/KnR by microscopic screen</i>	15	17
<i>% rescue from conjugation</i>	52 (4/56 failed to grow)	32 (23/72)

Table 4.1: Details of exconjugant numbers picked from plates, survival rate in initial lysates and percentage of GFP+ cells from those survivors. Number of plaques picked is the number of plaques obtained from 3 separate conjugations into each strain. More plaques were obtained from 109J than HD100; 109J survival and GFP expression was also higher than in HD100.

Prey-dependent 109GFP strain fluorescence scores from 20 hour predatory cultures

3	++	24	+/-
4	+	25	+/-
5	+/-	26	++
6	+	30	++
7	+	31	+/-
8	+++	32	+/-
9	++	33	+++
11	++	34	+/-
13	++	35	+
15	+	36	+
16	++	38	+++
17	+/-	39	+
18	+/-	41	++
19	++	44	+
20	+/-	45	+
21	+/-	54	+
22	+++	55	+
23	+/-	56	+

Table 4.2 Scoring of fluorescence of 109GFP strains, +++ being the brightest GFP, +/- indicating a very faint GFP. Cultures examined using GFP optics (excitation 480nm, emission 510nm) on a Nikon Eclipse E600 microscope.

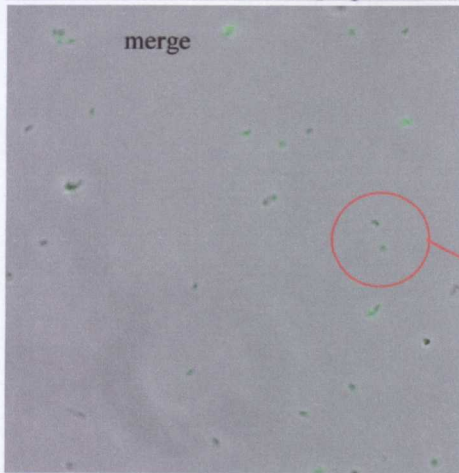
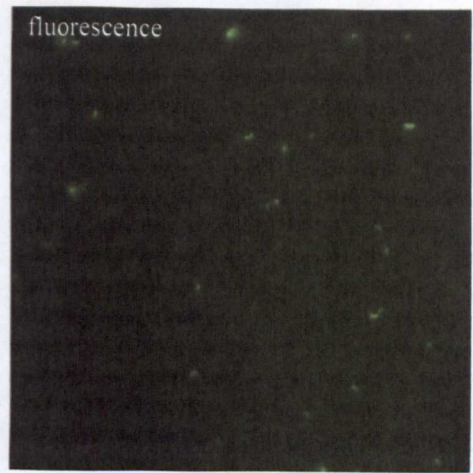
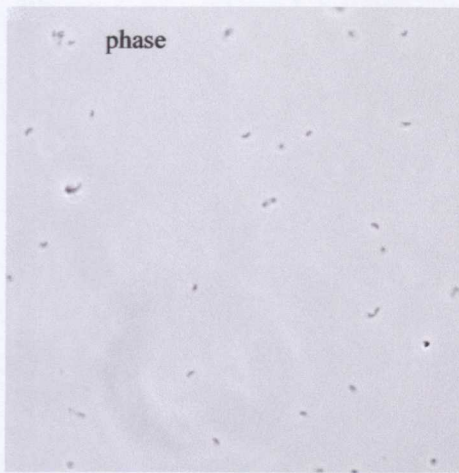
Prey-dependent HDGFP strain fluorescence scores from 20 hour predatory cultures

1	+
3	+
13	+/-
14	++
15	+/-
21	++

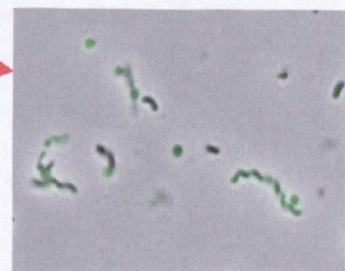
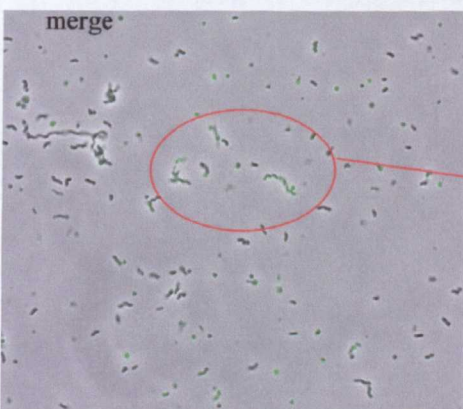
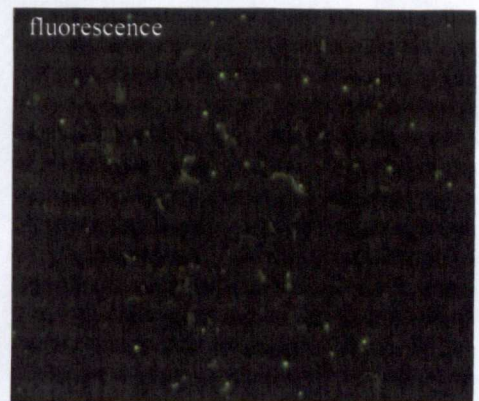
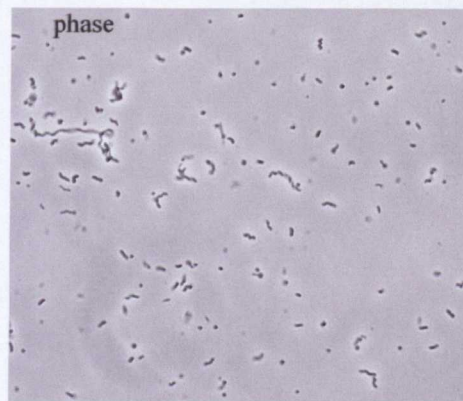
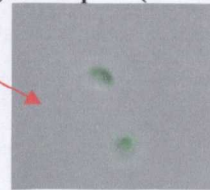
Table 4.3: Scoring of fluorescence of HDGFP strains, +++ being the brightest GFP, +/- indicating a very faint GFP. Cultures examined manually using GFP optics (excitation 480nm, emission 510nm) on a Nikon Eclipse E600 microscope.

From the screening data shown above in Tables 4.2 and 4.3, it can be seen that transposition into 109J was more efficient than into HD100, especially given that enumeration of the number of *B. bacteriovorus* going into the 3 individual conjugations into each strain averaged 4×10^8 cells for 109J and 8×10^8 for HD100. Screening of all strains was carried out manually using a Nikon Eclipse E600 microscope equipped with GFP optics and a Hamamatsu camera. 8 strains were selected to be carried forward for further analysis.

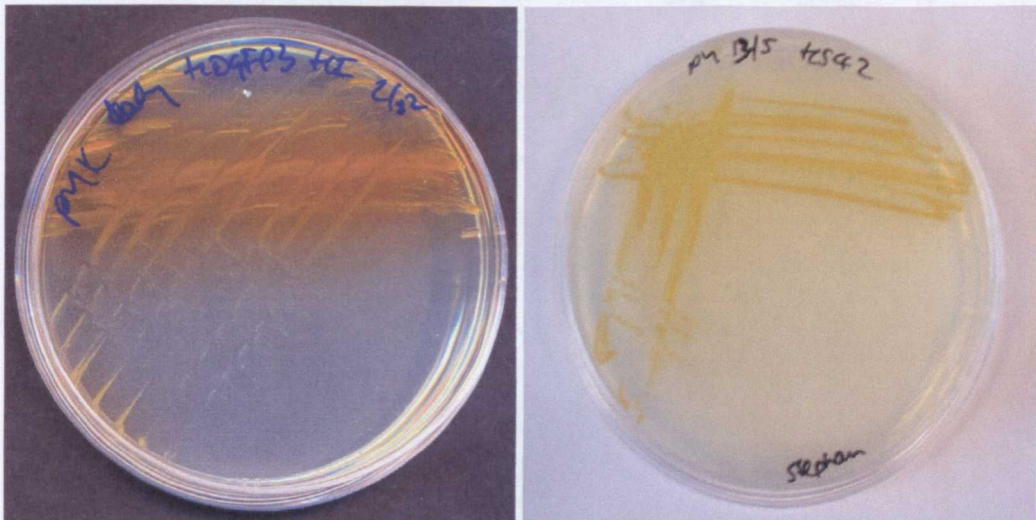
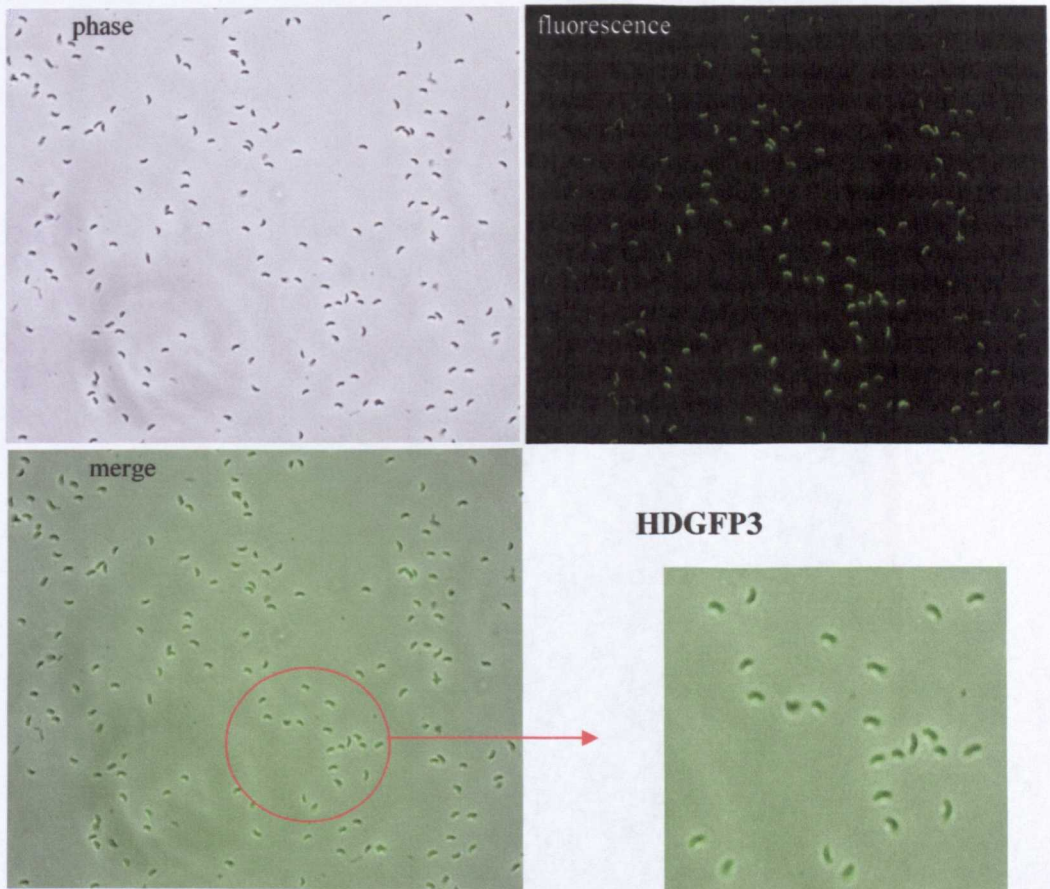
Figure 4.6 (following pages): Phenotypes of selected HD and 109 GFP+ strains. Strains are as indicated, top left panel is the brightfield image, top right is the corresponding fluorescence image, bottom right the merged image from each strain.



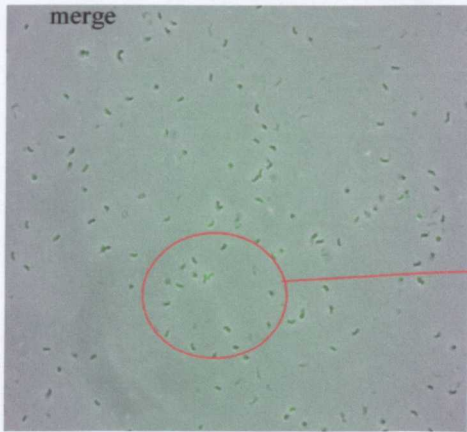
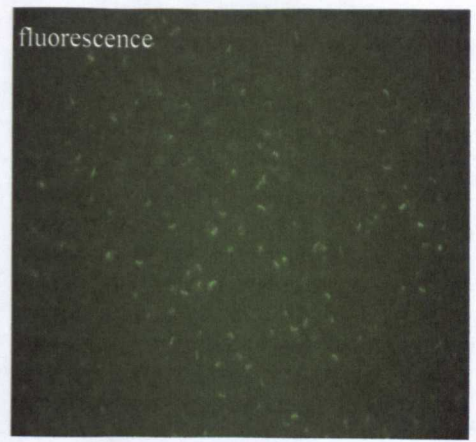
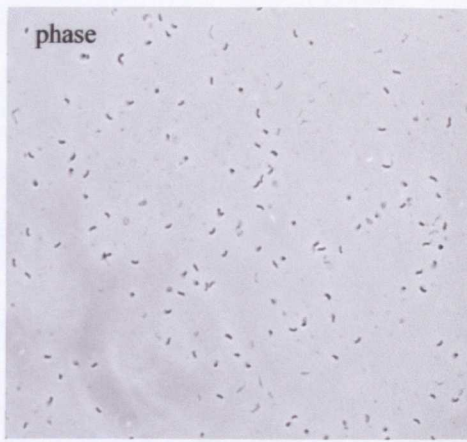
HDGFP1; phase/fluor/merge as indicated, all strains show fluorescence due to the presence of an in-frame GFP mini Tn10. Taken using a Nikon Eclipse E600 microscope, 100x magnification (cells that appear larger in images have been expanded digitally) GFP optics (excitation 480nm).



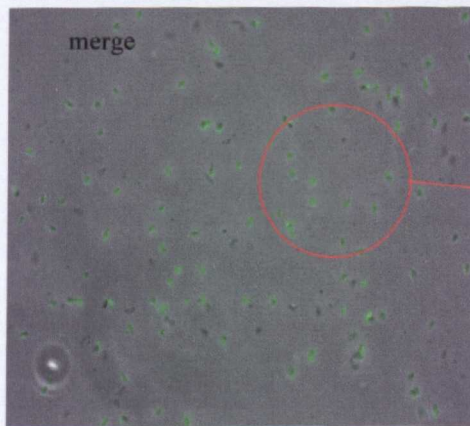
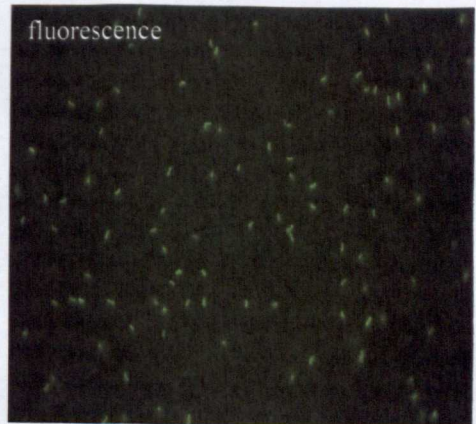
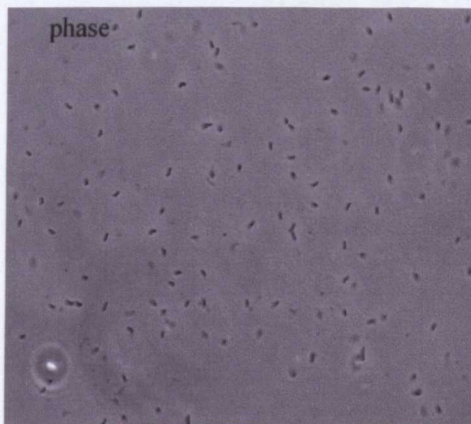
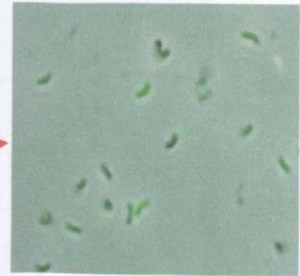
HDGFP1 HI; illustrating that there was no apparent change in fluorescence properties of any of the GFP strains that were turned HI aside from the increase associated with the larger cell size natural to HI strains.



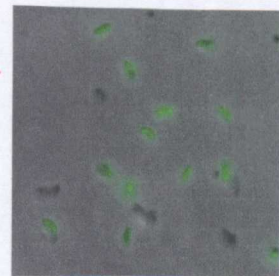
HDGFP3: this was the only strain (left hand plate) examined to have a visible change in phenotype. Cells in both HD and HI state secrete a brown pigment after a few days of growth, best illustrated by HI growth on PYKan⁵⁰ plates, left, compared to non-transposon strain HI growth, exemplified by the HS42 HI strain on the right – shown as a control for normal HI plate growth which does not exhibit the brown pigment secretion.

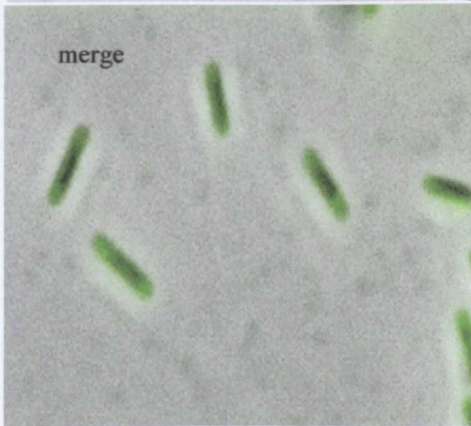
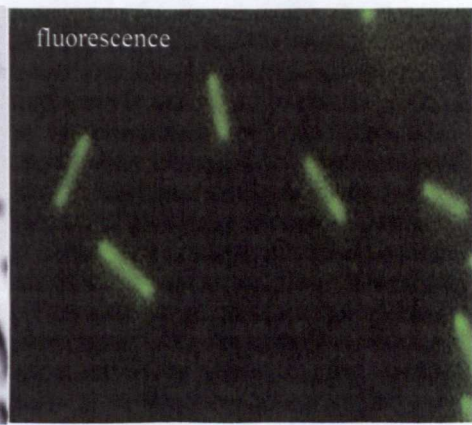
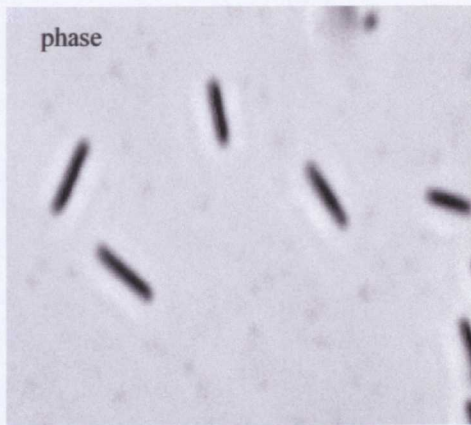


HDGFP13

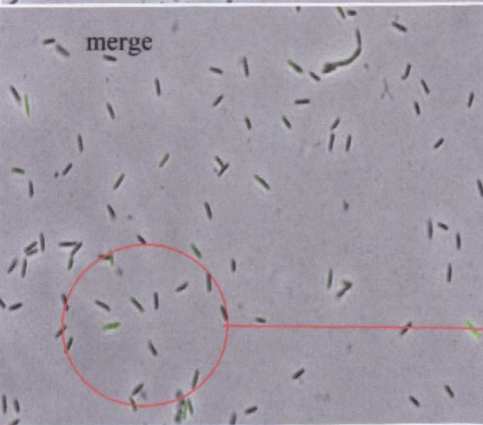
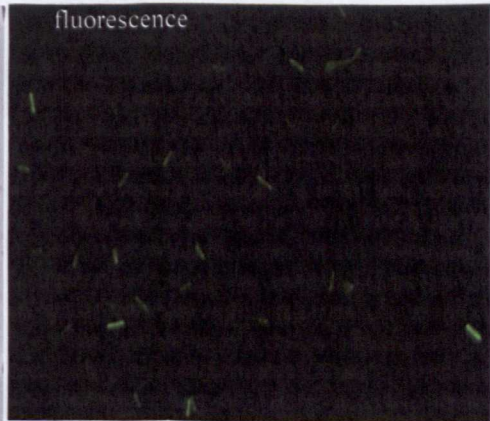
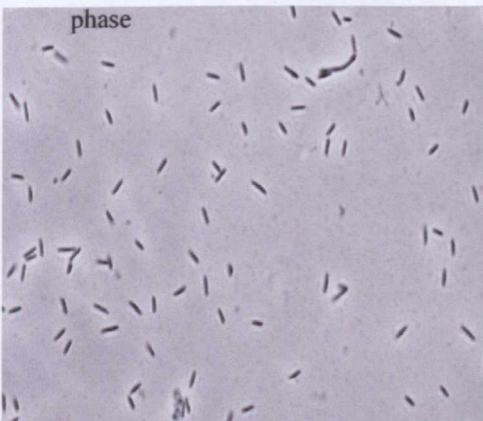


HDGFP14

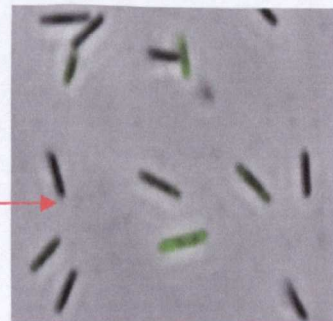


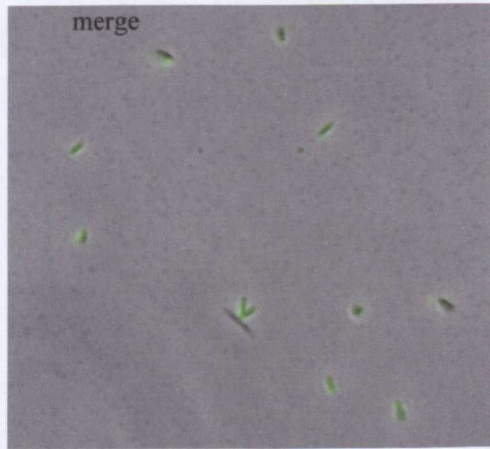
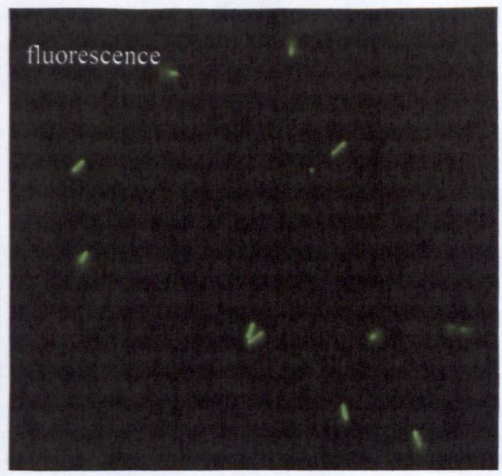
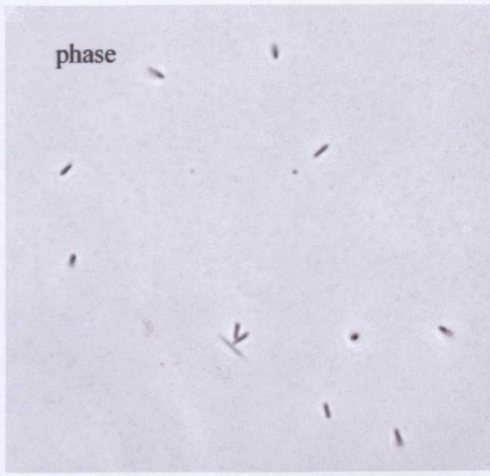


109GFP26 (taken at the same magnification (100x) as all others, but digitally zoomed in to illustrate possible nuclear exclusion or polar localisation of the GFP)

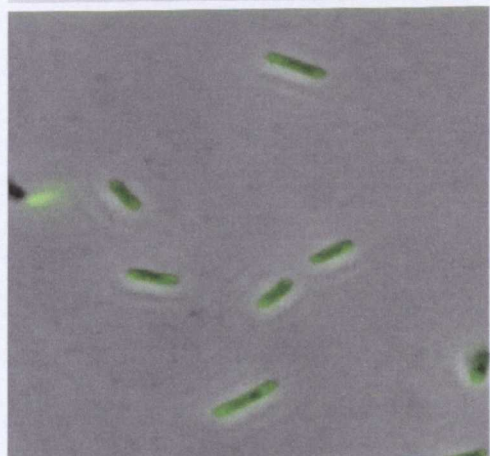


109GFP8





109GFP30



109GFP38 (taken at the same magnification (100x) as all others, but digitally zoomed in to illustrate the possible nuclear exclusion or polar localisation of the GFP)

4.2.1: Phenotypes of selected GFP expressing *B. bacteriovorus* strains

Four strains each of GFP expressing HD100 and 109J *B. bacteriovorus* were chosen for further study. All of these strains are shown in the preceding figure. Of particular interest was HDGFP3: in the prey dependent state, after 3-5 days of incubation in the absence of fresh prey, secreted a brown pigment into the media. Initially, it was thought to be some form of contamination, but plating of the strain to single plaques on soft agar overlays and re-culturing failed to remove the brown pigment. When the strain was made host-independent, the brown pigmentation of the agar surrounding the growing HI cells (see Figure 4.6 HDGFP3 above, this phenomenon was never seen in any other HI with or without the transposon insertion in the genome) confirmed that this was a by-product of this strain when faced with what was most likely to be a shortage of nutrients. However, repeated attempts at shotgun cloning the gene (see Section 4.2.2) containing the transposon insertion from this mutant failed so it is as yet unknown as to what gene has been disrupted in this strain. It is likely that it is providing a block to a biochemical pathway with a coloured intermediate which is then secreted. There are many possibilities, such as carotenoid intermediates or overexpression of iron-containing proteins but without the DNA sequence, the nature of the mutation remains unknown.

HDGFP1, 13 and 14 were all relatively bright GFP-expressing strains from the small number obtained from HD100 conjugations so were taken forward for further characterisation.

109GFP8, 26 and 38 showed to have GFP fluorescence that had a non-uniform distribution throughout the cell so were also used in further studies. 109GFP30 had no particular GFP localisation but was reasonably bright, so was also used.

All strains obtained in 109J and HD100, expressing GFP or not in the prey-dependent state, were turned prey-independent (HI, many thanks to undergraduate project student Simon King for assistance) in an attempt to find any mini *Tn10gfpKnR* insertions that proved to be differentially regulated between the prey-dependent and independent states. As illustrated in Figure 4.6 above with HDGFP1 HI, from 52 109J strains and 23 HD100 strains, none showed any discernable

differential GFP expression aside from a visible increase in GFP production due to the increase in cell length that is characteristic of all HI strains (rest of data not shown). It is also more difficult to examine low level GFP expression in HI strains due to the fact that they are inherently more autofluorescent than their parental prey-dependents; most likely this is due to increased carotenoids and due again, to increase in cell size compared to wild type HD100 and 109J.

4.2.1.1: Southern and Western blots of selected HD100 and 109J GFP-expressing strains show that strains contained different transcriptional fusions to the *gfp* gene

Southern blots with transposon-specific probes revealed that the strains were not related with regards to the transposon insertion site (see Figure 4.7 below for 109GFP strains and Figure 4.9 in Section 4.2.2 for HDGFP strains). Figure 4.8 shows Western blots which confirmed that the fluorescence seen was indeed due to transcription and translation of GFP.



Figure 4.7: Southern blot showing selected 109JGFP strain genomic DNA digested with *EcoRI*, probed with the mini *Tn10gfpKnR* cut *BamHI* from pLOFKmgfp – blot was later re-probed with the *KnR* cassette from pUC4K and gave the same bands, validating the use of the *KnR* as a probe; strains are not related with respect to mini *Tn10gfpKnR* position in the genome. All *EcoRI* digests: 109GFP8 = 6kb (lane 11), 109GFP26 = 7kb, 109GFP30 = 4kb, 109GFP38 = 3.5kb. Lanes: 1= Fermetas 1kb Generuler, 2=gap, 3=pLOFKmgfp (plasmid bearing the mini *Tn10gfpKnR* transposon) cut *BamHI* to release 2.51kb transposon fragment, positive control, 4= *E. coli* S17-1 cut *EcoRI*, negative control, 5= wild type HD100 cut *EcoRI*, negative control, 6= wild type 109J cut *EcoRI*, negative control, 7= HDpLOF11 (contains mini *Tn10gfpKnR*, but does not express GFP) cut *EcoRI*, negative control, 8= gap, 9+10= HDGFP3 cut *EcoRI* and *EcoRV* respectively, 11+12= 109GFP8 cut *EcoRI* and *EcoRV* respectively, 13+14= 109GFP26 cut *EcoRI* and *EcoRV* respectively, 15+16= 109GFP30 cut *EcoRI* and *EcoRV* respectively, 17+18 = 109GFP38 cut *EcoRI* and *EcoRV* respectively, 19= gap, 20= Fermetas 1kb Generuler.

Western blots were carried out on whole cell protein from selected 109GFP and HDGFP strains using anti-GFP antibody (Eurogentec) to confirm the presence of GFP protein and to show that the GFP seen was not autofluorescence of *B. bacteriovorus* but due to active transcriptional fusion to the *gfp* gene.

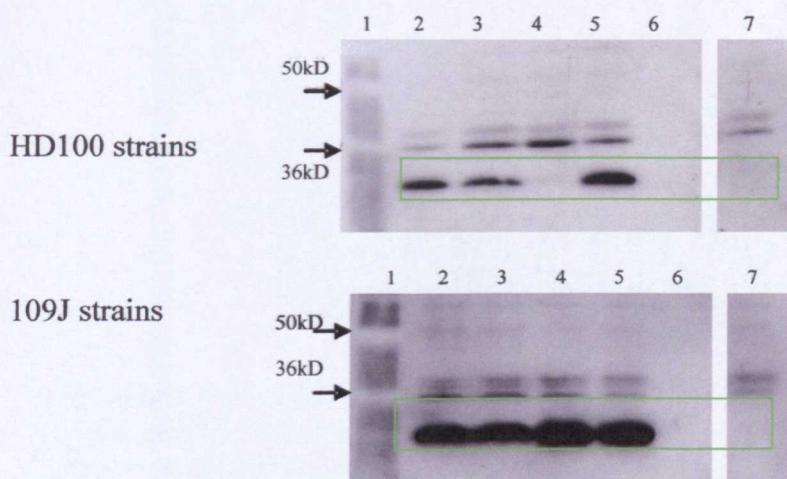


Figure 4.8 : Western blots of GFP strain attack phase *B. bacteriovorus* whole cell protein probed with anti mouse anti-GFP antibody at 1/1000 dilution (Eurogentec). GFP, at 27kD, is indicated in the strains with the green boxes strains. Lanes are as detailed below, but lane 7 on both blots are non-GFP expressing strains that contain the mini *Tn10gfpKnR* transposon (as determined by fluorescence microscopy, see tables 4.2/4.3 above) and show no GFP bands unlike the GFP expressing strains. Lane 4 HD100, HDGFP13 showed a very faint GFP band on longer exposure blots, agreeing with only the faint fluorescence seen under the microscope. All SDS-PAGE gels for blotting were run using 2 μ g of whole cell protein. **HD100GFP strains:** 1 = SeeBlue Plus2 pre-stained protein marker (Invitrogen), 2 = HDGFP1 whole cell protein, 3= HDGFP3, 4= HDGFP13, 5= HDGFP14, 6= gap, 7 = HDpLOF 5 (a non-GFP+ HD100 strain containing the mini *Tn10gfpKnR* out of frame for GFP expression). **109GFP strains:** 1 = SeeBlue Plus2 pre-stained protein marker (Invitrogen), 2 = 109GFP8 whole cell protein, 3= 109GFP26, 4= 109GFP30, 5= 109GFP38, 6= gap, 7 = 109pLOF3 (a non-GFP+ 109J strain containing the mini *Tn10gfpKnR* out of frame for GFP expression).

4.2.2 Shotgun cloning and sequencing of HD100 GFP strains

In order to determine the chromosomal insertion sites of the mini *Tn10gfpKnR* in the selected HDGFP strains, genomic DNA was prepared and cut with enzymes that would not cut within the transposon itself (ruling out *Bam*HI, *Hind*III, *Not*I, *Mlu*I and *Sfi*I, see Figure 4.5 in Section 4.1.2). The digested DNA was then subject to Southern blotting using a *KnR* probe (probing with the *Bam*HI mini *Tn10gfpKnR* fragment was also used to confirm the validity of the *KnR* probed blots and found to produce

the same size fragments. See figure 4.7 above) to determine suitable fragment sizes for shotgun cloning and sequencing. Below is shown a Southern blot of HDGFP strains using *EcoRI* digestion to identify the transposon-containing fragments.

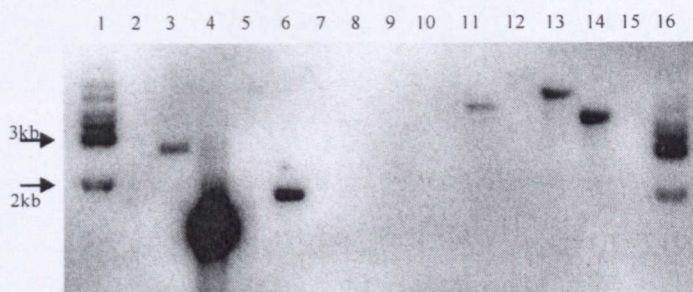


Figure 4.9: = Southern blot showing selected HD100GFP strain genomic DNA digested with *EcoRI*, probed with the KnR cassette cut *HincII* form pUC4K; strains are not related with respect to mini *Tn10gfpKnR* position in the genome. HDGFP1 (lane 11) = 5kb, HDGFP3 (lane 12) = ~8kb (band clear on over-exposed film, data not shown), HDGFP13 (lane 13) = 6kb, HDGFP14 (lane 15) = 4.5kb. Lanes: 1= Fermetas 1kb Generuler, 2=gap, 3= pLOFKmgfp (plasmid bearing the mini *Tn10gfpKnR* transposon) cut *BamHI* to release 2.51kb transposon fragment, positive control, 4= KnR cassette cut *HincII* from pUC4K, 1.25kb, 5= gap, 6= 109Jmcp::Kn (Lambert *et al*, 2003) cut *EcoRI*, positive control for KnR probe, 7= *E. coli* S17-1 cut *EcoRI*, negative control, 8= wild type HD100 cut *EcoRI*, negative control, 9+10= gap, 11-14= HDGFP1,3,13 and 14 respectively cut *EcoRI*, 15= gap, 16= Fermetas 1kb Generuler.

Mini *Tn10gfpKnR* containing *EcoRI* fragments from each strain were sized as follows: HDGFP1, 5kb; HDGFP3, ~8kb; HDGFP13, 6kb and HDGFP14, 4.5kb. *EcoRI* cut genomic DNA was subject to agarose gel electrophoresis and the region +/-0.5kb surrounding the sized region for each strain excised and purified. Ligation into pUC19, selective growth of *E. coli* DH5 α transformants on kanamycin (the transposon encodes a kanamycin resistance gene with an endogenous promoter) and subsequent restriction mapping allowed clones containing the transposon to be sent for sequencing.

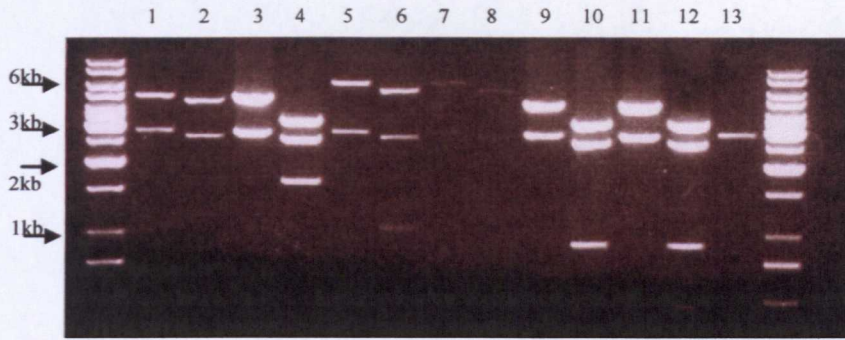


Figure 4.10: Agarose electrophoresis gel (0.8%) of restriction digests of potential mini *Tn10gfpKnR* containing clones with flanking genomic DNA in pUC19 from HDGFP1, 13 and 14. 2 potential clones from each strain were screened using *EcoRI* (E) and *BamHI* (B); the former releases the cloned insert from the vector to allow sizing and the latter releases the transposon from the genomic DNA and cuts at any other available site, allowing restriction mapping. The correct clones are seen in lanes 3 and 4 for HDGFP1; lanes 5 and 6 for HDGFP13 and lanes 11 and 12 for HDGFP14. Please see main text for details. Lanes: 1= HDGFP1.6 E, 2= 1.6 B, 3= 1.7 E, 4= 1.7 B, 5= HDGFP13.2 E, 6= 13.2B, 7= 13.4 E, 8= 13.4 B, 9= HDGFP14.4 E, 10= 14.4 B, 11= 14.5 E, 12= 14.5 B, 13= linear pUC19 cut *EcoRI* (2.68 kb). Ladders are Fermentas Generuler 1kb ladder.

The restriction digests allowed theoretical maps to be made of the constructs that were then sent for sequencing. The maps and final constructs are shown below.

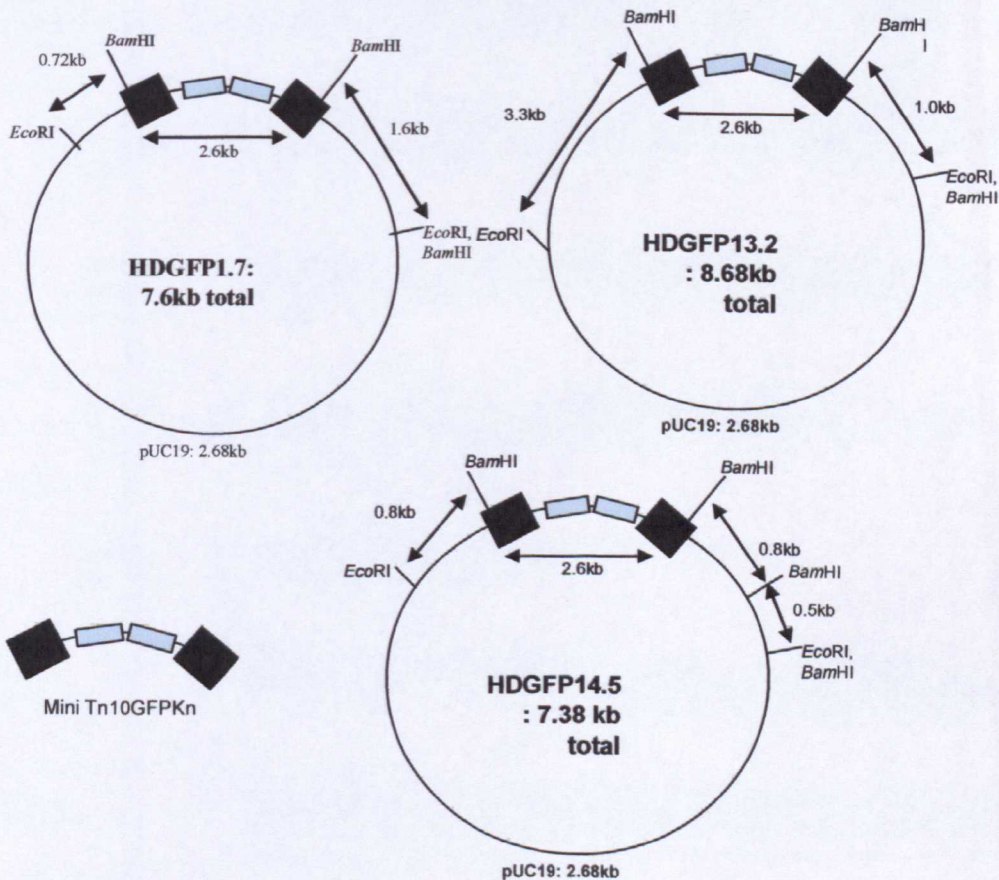


Figure 4.11: Theoretical restriction maps of HDGFP clones constructed from the restriction digests shown in Figure 4.10 above.

4.2.2.1: HDGFP1 mini Tn10gfpKnR insertion site

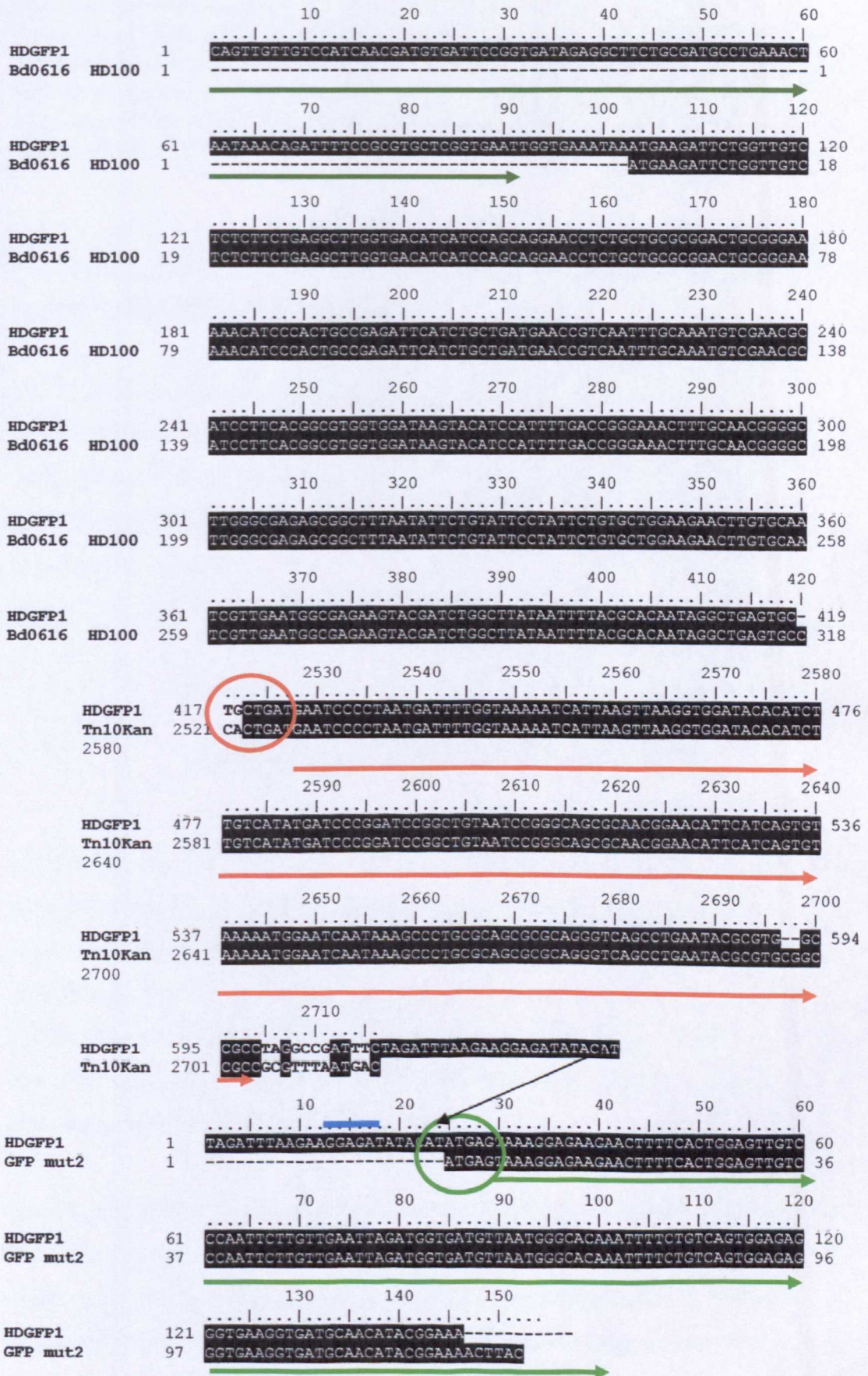
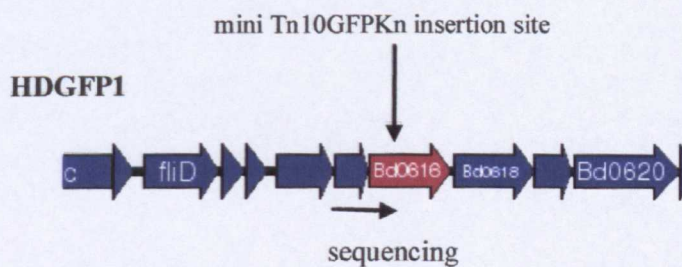


Figure 4.12: Alignment of clipped sequence data (labelled HDGFP1) with the cognate sequences from the *B. bacteriovorus* HD100 genome and the mini Tn10gfpKnR. Underlined in dark green is Bd0615, the gene prior to Bd0616 where the transposon is inserted. Circled in orange is the beginning of the miniTn10 repeat; underlined in bright green is the GFP encoded by the transposon, circled is the ATG start codon (Shine-Delgarno sequence highlighted in blue). Created using ClustalW alignments in BioEdit (see Section 2.10).

4.2.2.2: The mini Tn10gfpKnR in HDGFP1 interrupts the gene encoding an heptosyl transferase family protein

BLASTn of the sequence obtained from sequencing of the HDGFP1 shotgun clone (M13 universal -21 forward primer against the pUC19 MCS) against the *B. bacteriovorus* HD100 genome showed that the mini Tn10gfpKnR insertion site was at 318bp into Bd0616; being downstream of the promoter of this gene allowed expression of the GFP.



NCBI BLASTp of the theoretical BD0616 translation, annotated in the genome as a putative Lipopolysaccharide heptosyltransferase-I, did show homology to proteins from other bacterial species that belong to a family of lipopolysaccharide heptosyl transferases, with the annotated heptosyltransferase family protein from *Geobacter sulfurreducens* providing the top hit with an e-value of $2e-17$. *G. sulfurreducens* is also a δ -proteobacterium, so it was unsurprising that this would provide the best homologue to the *B. bacteriovorus* protein.

Heptosyltransferases are best studied in *E. coli* and *Salmonella*; Bd0616 also showed homology to *waaC* from *Salmonella*, a heptosyltransferase involved in the synthesis of the core Lipid A component of the bacterial Lipopolysaccharide (LPS) layer. WaaC aids determination of the configuration of heptose sugar residues in the core

region of Lipid A (please see Section 4.4.2.2 for a discussion of *B. bacteriovorus* LPS and Lipid A) (reviewed in detail in (Raetz and Whitfield, 2002)). Figure 4.13 shows the pathway involved in the biosynthesis of Lipid A core, with WaaC indicated.

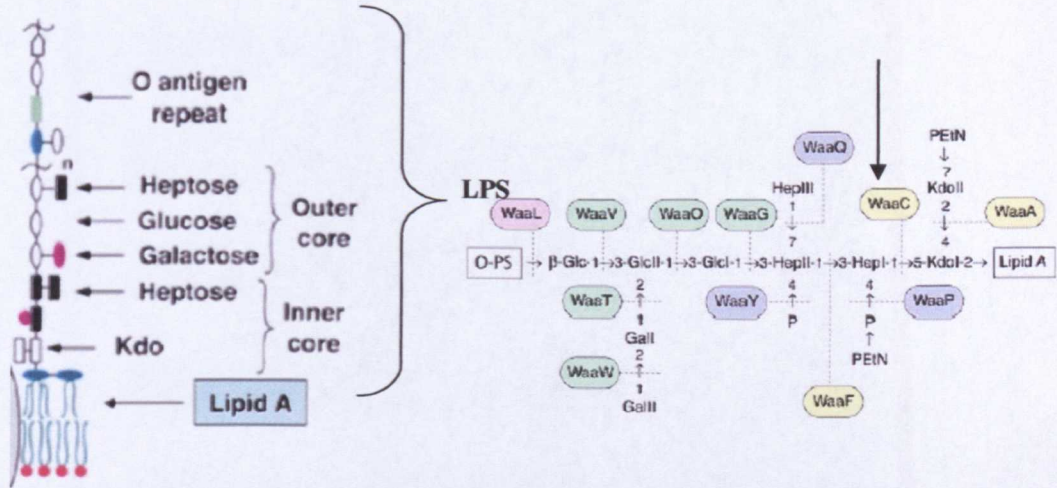


Figure 4.13: The structure of *E. coli* K12 outer membrane LPS layer (left), illustrating the relative positions of the Lipid A, core sugars and the final O antigen repeat polysaccharides. Right, schematic of biosynthesis of the core polysaccharides of bacterial LPS with WaaC indicated by the arrow. WaaC is involved in the heptose sugar configuration of the inner core polysaccharides (O-PS is O polysaccharide). Modified from (Raetz and Whitfield, 2002).

HDGFP1 showed no apparent gross alteration in predatory efficiency or timing when examined by phase contrast microscopy alongside other HD100 strains containing mini *Tn10gfpKnR* insertions and wild type HD100 cells. No other gross phenotype, such as motility, showed any discernable difference to wild type HD100 cells.

4.2.2.3: HDGFP14 transposon insertion site

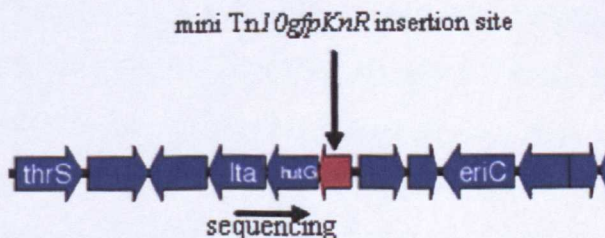
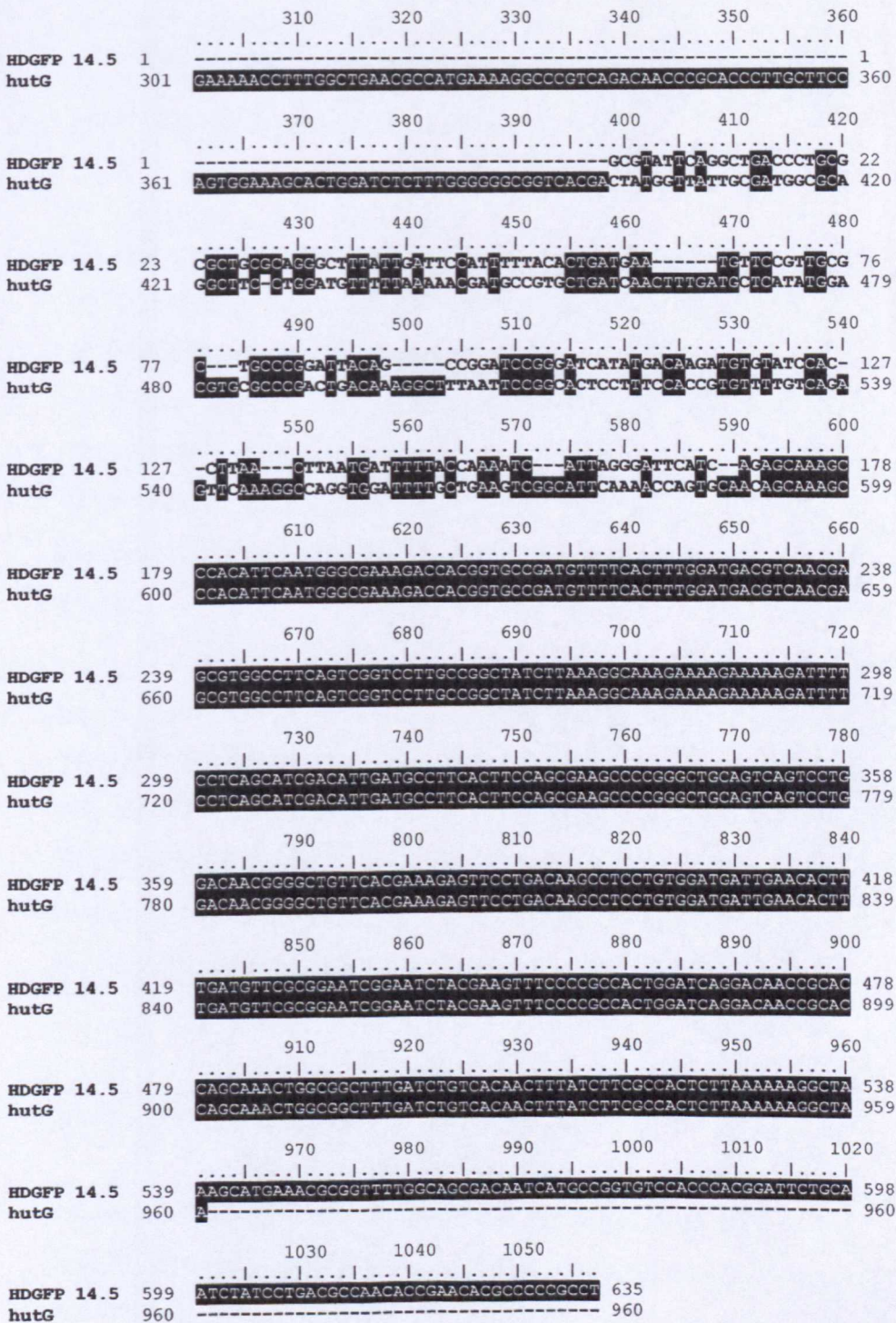


Figure 4.14: Alignment of the reverse complement of the DNA sequence obtained from the HDGFP14.5 construct using the universal pUC19 forward primer. The sequence corresponds to *hutG* in the HD100 genome but does not pick up the mini Tn10*gfpKnR* ends, which was estimated as indicated on the lower diagram to be in Bd1813 from the restriction map generated (see Figure 4.11) above. Alignment created using ClustalW in BioEdit, see Section 2.10.

BLASTn of the sequence data obtained from the HDGFP14 construct against the HD100 genome showed that the chromosomal DNA corresponded to *hutG* (which encodes a formimidomyglutamase) but did not pick up the transposon ends. Restriction mapping allowed deduction of the mini Tn10*gfpKnR* insertion site from the sequence data obtained. From where the sequence ends, there was another ~0.7db DNA to the transposon insertion; from the data, there was another 368bp of *hutG* to the end of the coding sequence, placing the transposon in Bd1813 as illustrated above.

BLASTp of the NCBI nr database with the hypothetical translation of BD1813 showed that it had no known homologues; only very few weak homologies were seen and these to other conserved bacterial hypothetical proteins. As such, the function of Bd1813 remained unknown; also HDGFP14 had no discernable phenotype with regards to predation or motility when observed in comparison to other HD100GFP/nonGFP strains or wild type.

4.2.2.4: HDGFP13 transposon insertion site

Unfortunately, both forward and reverse universal pUC19 primers gave sequencing that aligned only with the transposon ends, indicating that there was very little, if any, DNA contained within the HDGFP13 construct. This was at odds with the restriction map generated from digestion patterns, which showed that there should have been at least 4kb of *B. bacteriovorus* genomic DNA contained within the clone. Time limitations meant that the shotgun cloning of genomic DNA from this strain could not be repeated; sequencing using the upstream DNA of the *gfp* gene from the transposon was not possible due to primer design constraints (data not shown).

4.3: Other fluorescence work in *B. bacteriovorus*

Cy5, another fluorescent dye, was also used in an attempt to visualise pili on the surface of *B. bacteriovorus*; please see Chapter 5 Section 5.2.4.

4.3.1: FM4-64 membrane staining

FM4-64, (*N*-(3-triethylammoniumpropyl)-4-(6-(4-(diethylamino)phenyl)hexatrienyl)pyridinium dibromide, Molecular Probes), is a lipophilic styryl membrane stain commonly used in eukaryotic cells to visualise plasma membranes (see Molecular Probes website, <http://probes.invitrogen.com/lit/bioprob34/section12.html> for more information on the use of FM4-64 in eukaryotes). It has also been successfully used in a variety of bacteria; for example, to aid visualisation of engulfment in *Bacillus subtilis* sporulation (Pogliano *et al.*, 1999) and to clarify membrane location with respect to fluorescently-labelled oscillating FrzS in *Myxococcus xanthus* (Mignot *et al.*, 2005). FM4-64 is easily monitored using FITC optics on a fluorescence equipped microscope.

The original idea for using FM4-64 in *B. bacteriovorus* was to monitor prey invasion, establishment and filament elongation of stained predator on unstained prey. This would reveal areas of new membrane synthesis in the *B. bacteriovorus* filament due to the protection afforded by the bdelloplast environment: FM4-64 only binds to membranes directly exposed to the dye, thus freshly synthesised outer membrane within the bdelloplast would not stain.

4.3.2: FM4-64 staining of *B. bacteriovorus* strains and *E. coli*

Technical considerations meant that dye loading and predation monitoring had to be carried out in 10mM HEPES free acid buffer, pH7 as the calcium found in normal *B. bacteriovorus* Ca²⁺/HEPES suspension buffer interferes with dye loading into membranes. Initial light microscopic observation of *B. bacteriovorus* predation of *E. coli* S17-1 as a standard lysate in 10mM HEPES pH7 showed no discernable effect on the expected predation process (data not shown).

Typically, 5µg/ml FM4-64 is loaded into bacterial cells to allow clear membrane visualisation (Pogliano *et al.*, 1999). 5µg/ml FM4-64 labelled *B. bacteriovorus* HD100 buffered in 10mM HEPES were agar-mounted and observed using the FITC (excitation 490nm) optics on a Nikon Eclipse E600 microscope using 100x magnification. Compared to an *E. coli* S17-1 control labelled in the same way, HD100 showed extremely poor dye loading that was virtually invisible (see Fig. 4.15A). Higher concentration (100µg/ml) FM4-64 in both HD100 and 109J was used to see if it was a concentration-dependent effect (see Fig. 4.15B). This gave better membrane labelling, but at concentrations of dye 20 times that normally used in bacteria which was still relatively poor compared to *E. coli*.

To ensure that poor visualisation was not an artefact of the small size of *B. bacteriovorus*, Host-Independent (HI) cells derived from HD100 prey dependent strains were also loaded with 5µg/ml FM4-64 (see Fig. 4.15C). As HI cells are generally longer than their prey-dependent parents, if physical cell size was the cause of poor staining/ability to see dye loading, the HIs would be brighter. As shown in Fig 4.15C, there was no appreciable difference in fluorescence intensity between the *B. bacteriovorus* strains.

4.3.3: Predation of FM4-64 labelled *Bdellovibrio* on unlabelled *E. coli*

As there was reasonable dye-loading at 100µg/ml in *B. bacteriovorus* HD100, the cells were washed twice in 10mM HEPES to remove excess stain and then inoculated into a 2ml lysate in HEPES containing 50µl unlabelled S17-1 and 100µl labeled HD100. V/v ratio was changed from the usual 3:1 prey:predator ratio due to the need to observe the culture over short periods of time and also due to loss of some *B. bacteriovorus* during the washing steps. The culture was incubated at 29°C, 200rpm shaking and samples taken at the standard time points of 15 minutes, 30 minutes, 45 minutes and 1 hour; these correspond to attachment, invasion, bdelloplast formation and establishment.

The experiment was,unsuccessful due to residual FM4-64 present in the HD100 sample, despite the washing steps, which was of a sufficient concentration to also label the *E. coli* S17-1. Labelling of both strains meant that no accurate observation of the predation process could be carried out.

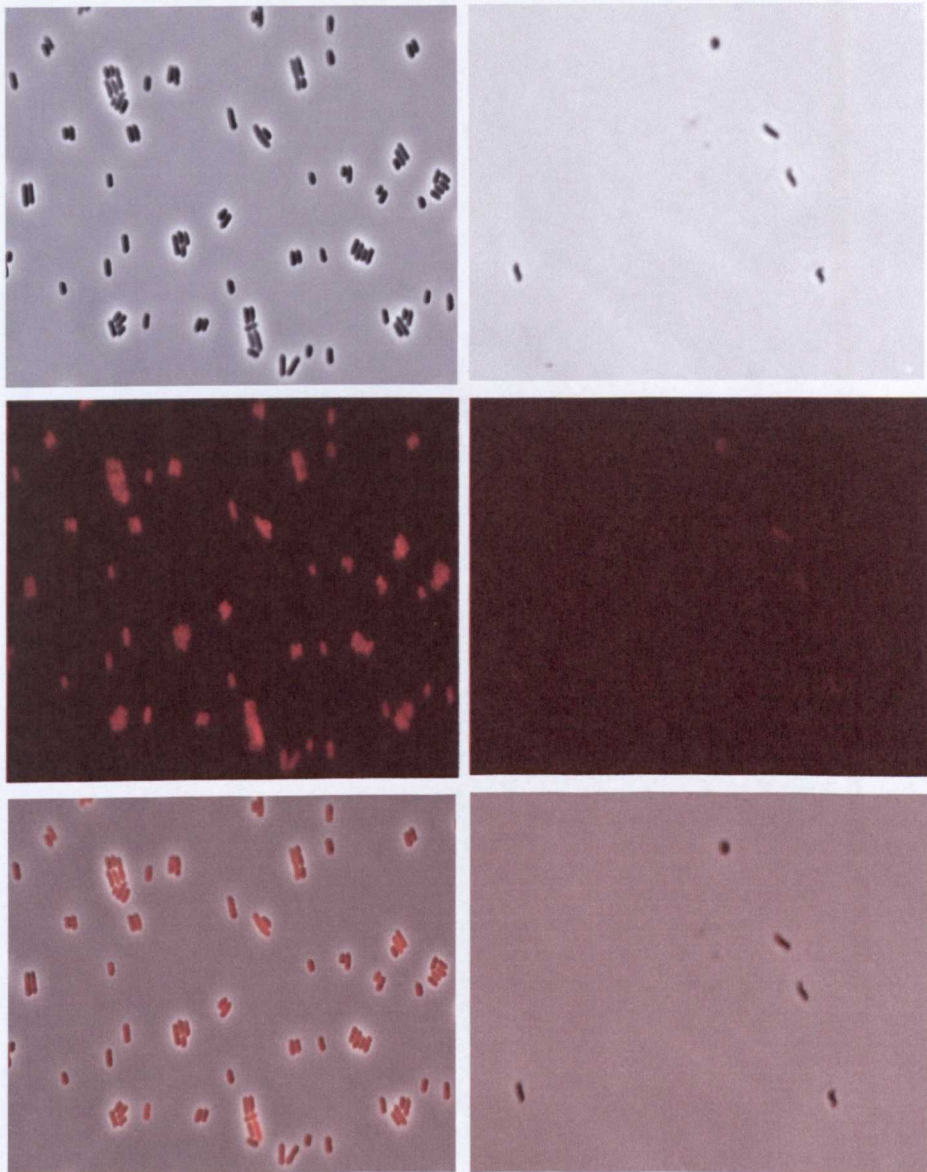
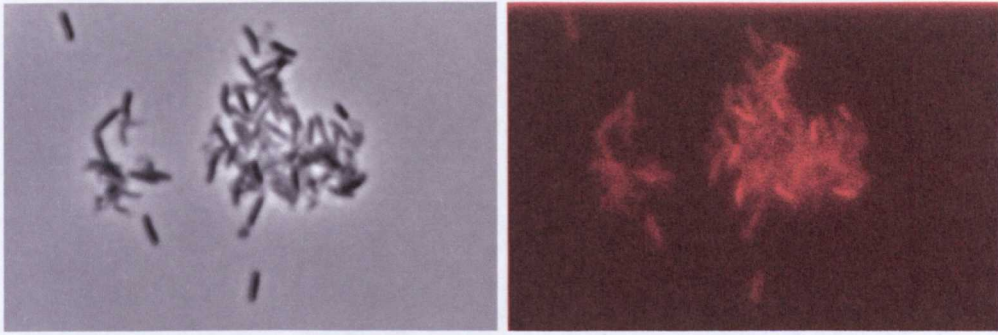
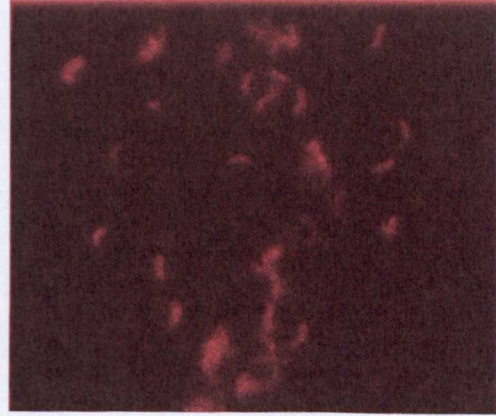
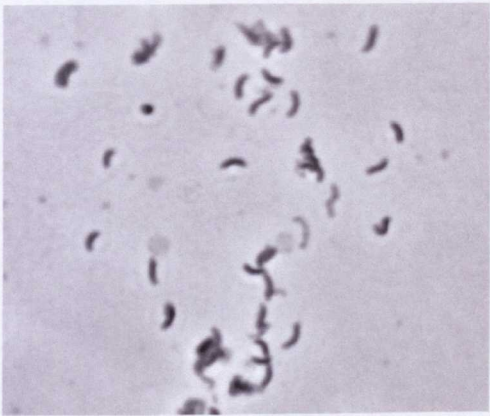
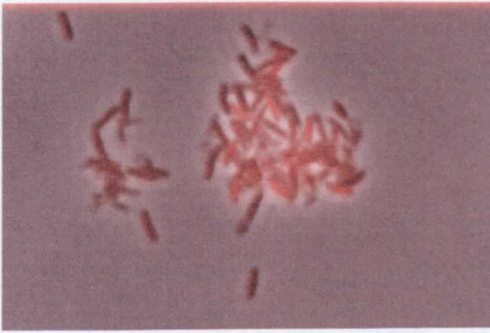


Figure 4.15 A. Right hand panels: *B. bacteriovorus* stained with FM4-64 at concentrations used previously in other bacteria (Sharp and Pogliano, 1999) of 5 μ g/ml. Fluorescence is extremely faint, images digitally zoomed in. In contrast, *E. coli* S17-1 stained with the same concentration (left hand panels) gives an even, intensive stain, much brighter than that of *B. bacteriovorus* strains (see below). All images in this figure taken under standard FITC optics on a Nikon Eclipse E600 microscope at 100x magnification. Images processed using IPLab software. Top to bottom: brightfield view, fluorescence view, merged image.



(i) *B. bacteriovorus* 109J



(ii) *B. bacteriovorus* HD100

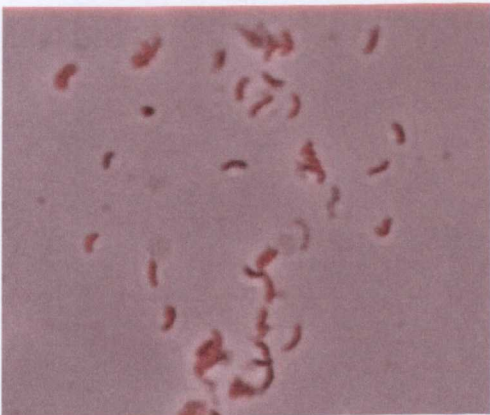


Figure 4.15 B. Higher, excess concentration stained 09J and HD100, 100ug/ml FM4-64. Staining is improved but is still very poor compared to that of *E. coli* in both *B. bacteriovorus* strains.

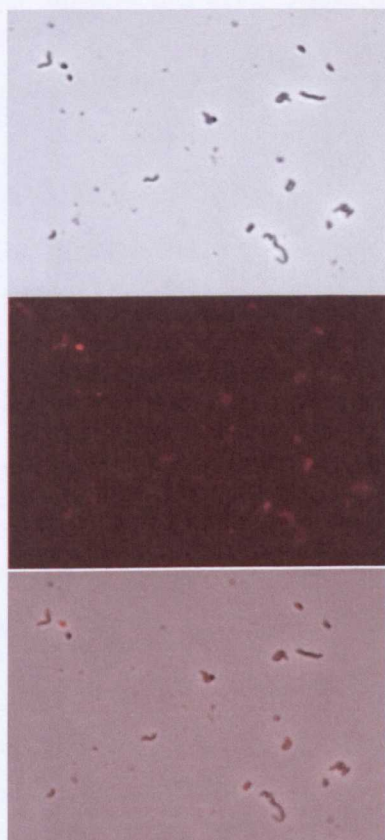


Figure 4.15 C. In an effort to determine whether the lack of visible FM4-64 uptake in prey-dependent strains was a result of cell size, *B. bacteriovorus* being extremely small, HI cells derived from HD100 were also stained with 5ug/ml FM4-64. As can be seen in the panels, even the larger HI cells are still not fluorescing much brighter than prey-dependent HD100. This indicates that it is more to do with membrane absorbance of the stain in *B. bacteriovorus* rather than physical cell size.

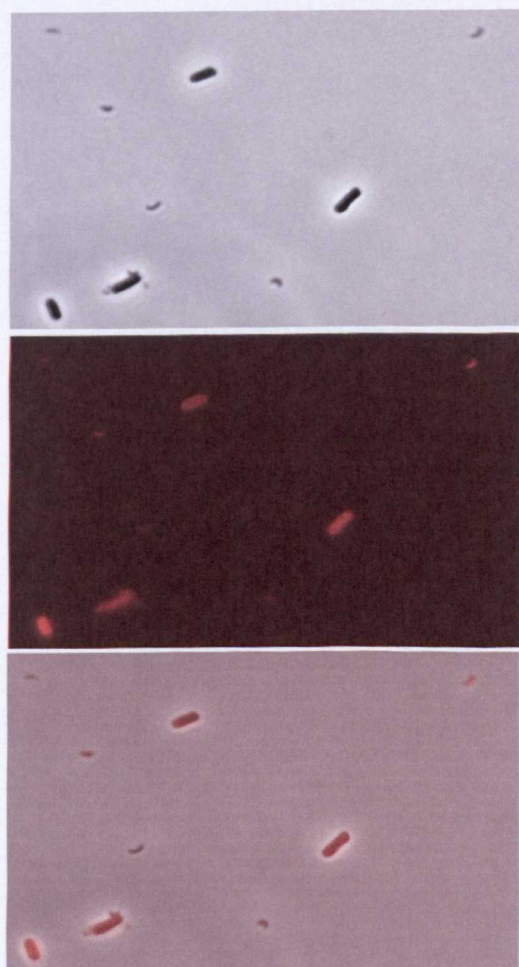


Figure 4.15 D. Attempts made to predate *B. bacteriovorus* HD100 stained with 100ug/ml FM4-64 on unlabelled *E. coli* S17-1. After 30 minutes of co-incubation in HEPES buffer (see Chapter 2), the S17-1 was observed to have absorbed the residual stain from the HD100 buffer despite washing of the cells to remove excess stain.

4.3.4: Predation of FM4-64 labelled *E. coli* by *B. bacteriovorus*

As there was no prospect of being able to conduct the original experiment to monitor *B. bacteriovorus* outer membrane synthesis with labelled predator, the converse experiment was carried out. Labelled prey cells being predated by unlabelled *Bdellovibrio* would show at what point in the predatory life cycle that the outer membrane of the bdelloplast would start to be degraded, corresponding with loss of dye and decrease in fluorescence.

E. coli S17-1 was labelled with 5µg/ml FM4-64, giving average fluorescence typified by the left hand panel of Fig 4.15A. A lysate of 2ml HEPES, 100µl unlabelled *B. bacteriovorus* HD100 and 50µl labelled S17-1 was incubated at 29°C, 200rpm and samples taken at the standard time points of 15 minutes, 30 minutes, 45 minutes and 1 hour; these correspond to attachment, invasion, bdelloplast formation and establishment.

As observed previously, predation using unlabelled bacteria in 10mM HEPES pH7 is within normal parameters. However, samples taken at 15 minutes showed no sign of attachment of *B. bacteriovorus* to its prey. At 30 minutes, attachment was observed, but extremely rarely (see Fig. 4.15E(i)), where $n > 1000$ cells examined. After 1 hour, when HD100 lysates are usually established in the bdelloplast, evidence of only 1 bdelloplast was seen over repeated examination of samples, again $n > 1000$. Additionally, the S17-1 were not surviving well in the presence of the dye; many *E. coli* cells were observed to be losing membrane integrity and lysing, corresponding with the increase in cell transparency compared to normal and decrease in fluorescence (see Fig. 4.15E(ii)).

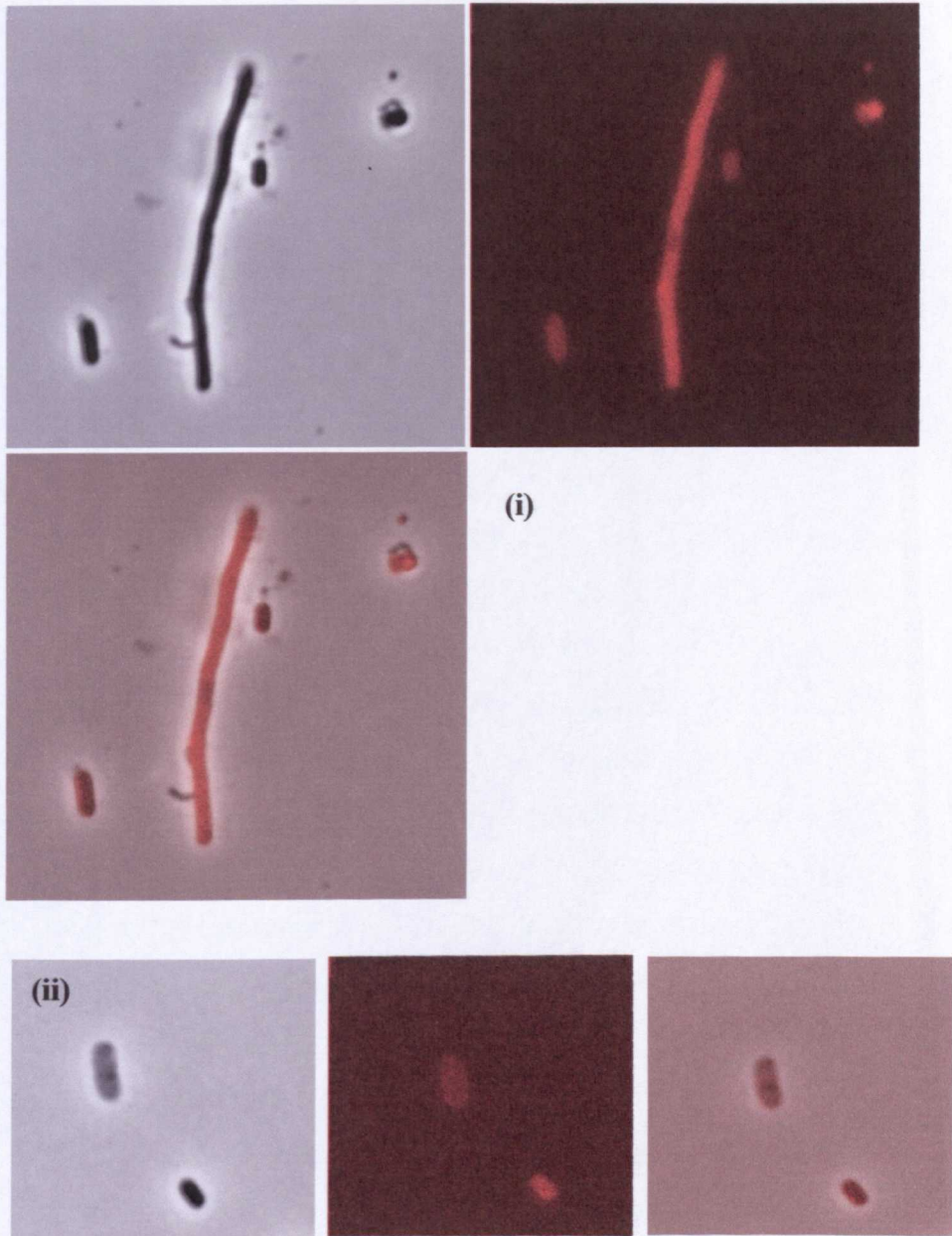


Figure 4.15 E. (i) Unlabelled HD100 co-incubated with S17-1 labelled with 5 μ g/ml FM4-64, 45 minutes post-infection. An example of one of the rare occurrences of predator attachment to prey ($n > 1000$ cells). In a normal, unstained infection, most of the prey cells would be invaded and the predator establishing stable bdelloplasts at this time. (ii) S17-1 after 1 hour incubation with HD100. Many *E. coli* cells were observed to be losing membrane integrity and lysing, corresponding with the increase in cell transparency compared to normal and decrease in fluorescence.

4.4: Conclusions from fluorescence work in *B. bacteriovorus*

4.4.1: GFP transposon mutagenesis

The first use of transposon mutagenesis of *Bdellovibrio bacteriovorus* has provided some promising results. Initially, this work has shown that the mini Tn10GgfpKnR from pLOFKmgfp can be successfully used in *B. bacteriovorus* to produce GFP transcriptional fusions; secondly that GFP itself can be expressed and visualised in this bacterium from chromosomal basis rather than from a plasmid. This work provided a small-scale preliminary experiment into the feasibility of Tn10 transposon screening of *B. bacteriovorus* to examine genes that may be differentially expressed between prey-dependent and –independent variants. It is encouraging that none of the strains analysed here were genetic “siblings”, indicating that in *B. bacteriovorus*, the mini Tn10GgfpKnR apparently shows no particular preference for any native chromosomal sequence in regards to insertion into the chromosome (this is not the case for all transposons, some of which hotspot in *B. bacteriovorus*, R. Till, L. Sockett, personal communication). Though I failed to find any differential expression here, a full saturation screen of *B. bacteriovorus* genes is now possible and would form the basis of a full project in its own right especially with transposons delivering translation fusions. This would allow assessment of any phenotypes produced from the predicted genes in the genome that cannot be assigned any function through homology searches, in relation to predation, motility or development throughout the predatory life cycle and during prey-independent growth.

Further work is needed to characterise fully the mutants generated in this screen, particularly the pigment-producing HDGFP3 and the LPS mutant HDGFP1. Full phenotyping for predation efficiencies would be optimal; for HDGFP3, repeated attempts at shotgun cloning should be done again, though it is curious that many attempts were made and were unsuccessful during the course of this work. It may well be that there is a gene contained in the genomic DNA flanking the transposon insertion site that interferes with *E. coli* DH5 α growth; perhaps another cloning strain could be tried. Shotgun cloning and sequencing of the 109GFP strains already characterised would also be desirable as part of wider work on this project.

4.4.2: Conclusions from FM4-64 work

The hypothesis and direction of the original experiment depended on FM4-64 being able to label the *B. bacteriovorus* membrane to allow visualisation of the growing filament in the bdelloplast; this type of membrane labelling in other bacterial species having been successfully carried out previously, e.g. (Mignot *et al.*, 2005; Pogliano *et al.*, 1999). However, *B. bacteriovorus* strains seem to be refractory to this particular membrane dye, as shown by poor loading seen at concentrations many times higher than used in other species. This could possibly be due to the nature of *B. bacteriovorus* lipopolysaccharide (LPS); analysis of the LPS structure was undertaken by Schwudke and co-workers who showed that *B. bacteriovorus* HD100 has an unusual Lipid A characterised by the absence of negatively charged groups found in other Lipid A's (Raetz and Whitfield, 2002; Schwudke *et al.*, 2003), which will be discussed further below. The precise action by which FM4-64 binds its targets is unknown, but it is a lipophilic, hydrophobic dye that binds membranes (Haughland, 2002), so is presumably charged or at least a polar molecule; charged Lipid A moieties found in most bacteria would be an ideal target for this dye to bind to.

4.4.2.1: Conclusions from FM4-64 work – implications for *B. bacteriovorus* predation

The observation that *B. bacteriovorus* could only very rarely predate (1/1000) FM4-64 stained *E. coli* prey under conditions that would usually produce >90% bdelloplast formation at the same time point is interesting. The only difference in prey is the presence of the dye bound in the membrane. Previous studies in *B. bacteriovorus* indicated that there were differences in predation efficiencies of rough and smooth LPS mutants of *Salmonella* and *E. coli* (rough being those lacking O-antigen side chains of LPS, smooth being those with the O-antigen) with rough mutants providing a better attachment of *B. bacteriovorus* 109J at 20 minutes than smooth (Varon and Shilo, 1969). The authors in this study hypothesised that the core LPS layers, exposed in the rough mutants, provided the possible receptor for *B. bacteriovorus* attachment to prey and that the presence of O-antigen in the wild type smooth cells merely presented a barrier.

With regard to FM4-64 – mediated inhibition of predation, the presence of the dye in the membrane may almost completely preclude predator attachment by obscuring the potential receptor sites for *B. bacteriovorus* attachment. However, there is no mention in the available literature about the precise mode or nature of FM4-64 binding to membranes, except that it is thought to integrate into the outer leaflet of membranes (Haughland, 2002). Further study of this molecule in combination with various prey LPS mutants in relation to dye loading of prey and *B. bacteriovorus* predation efficiency may provide a better insight into the nature of *B. bacteriovorus* attachment to prey cells.

4.4.2.2: Conclusions from FM4-64 work – further evidence for the unusual nature of the *B. bacteriovorus* membrane

Previous work on the *B. bacteriovorus* membrane has revealed that it has several unusual characteristics that are not found in other bacterial species. As noted elsewhere in this thesis, staining of *B. bacteriovorus* with certain dyes used for visualisation of cells in electron microscopy (for example, phosphotungstic acid, see Section 3.2.1) produce membranous protrusions/perturbations of the membrane that are easily detached from the cell (this work, (Abram and Davis, 1970)) which the Abram and Davis suggested were evidence for an unusual outer membrane in this bacterium compared to others. Incidental experiments from other work on the effects of penicillin on 109J by Thomashow and Rittenberg showed that *B. bacteriovorus* is unusually sensitive to lysozyme, unlike other Gram-negative bacteria that need to be pre-treated to alter their outer membranes to allow the enzyme access to its substrate peptidoglycan; they also noted, as I have seen in my own work (data not shown), that *B. bacteriovorus* strains are also unusually sensitive to detergent treatment, inducing cell lysis at concentrations that are used in *E. coli* for outer membrane purification (Thomashow and Rittenberg, 1978a). All of these data indicate an unusual outer membrane biochemistry.

More recent work on *B. bacteriovorus* membranes has confirmed this. The presence of sphingophosphonolipid molecules in the related strain, *Bacteriovorax stolpii* UKi2, is another indication of the odd biochemistry found in *Bdellovibrionaceae*:

sphingophosphonolipids are only rarely found within the Bacteria but are ubiquitous in eukaryotic species and the authors hypothesised that there may be a role for sphingolipids and their derivatives in predatory behaviour (Jayasimhulu *et al.*, 2007). Perhaps what is most interesting in relation to work in FM4-64 that showed that the dye (also Cy5, another membrane dye, please see Section 5.2.4) did not effectively bind the membranes was the discovery that *B. bacteriovorus* HD100 Lipid A lacks the phosphate groups usually present in the polar headgroup (Schwudke *et al.*, 2003). They also showed that the fatty acid groups in Lipid A were less acylated than in other bacteria, which they hypothesised would lead to a more fluid and permeable outer membrane.

The alteration of Lipid A in *B. bacteriovorus* to a more neutral, fluid species could possibly account for some membrane stains that bind in other bacteria not staining *Bdellovibrio* species well, if at all. A larger range of dyes needs to be employed to find those that can be used in *B. bacteriovorus*.

Chapter 5: The role of Type IV pili in *B. bacteriovorus* predation

If flagella are not absolutely required for predatory behaviour, as shown in Chapter 3, then there should be another mechanism used to enter prey. Previous EM studies have shown the predator squeezing through a small pore in the prey outer membrane, a pore smaller than the physical width of the *B. bacteriovorus* (Abram *et al.*, 1974; Burnham *et al.*, 1968). The sequencing of the *Bdellovibrio bacteriovorus* HD100 genome showed that the predator has a full set of genes to potentially encoding Type IV pili structures, which were hypothesised by the lead authors and myself in the HD100 genome paper to mediate prey entry (Rendulic *et al.*, 2004). It can be seen on electron micrographs of invading *B. bacteriovorus* ((Burnham *et al.*, 1968) and in work from my thesis, Fig 5.1) that the pore formed in the outer membrane is small and a “tight fit” for the invading predator. Thus a significant force may be required for prey entry by the predator. Type IV pili in other bacterial species have been shown to be capable of exerting forces of up to 100pN under tension to pull the cell body to the point of pilus attachment (Maier *et al.*, 2002a; Merz *et al.*, 2000), see section 5.1. Attachment of *B. bacteriovorus* to prey cells could not be disrupted by vortexing nor brief sonication (Burnham *et al.*, 1968), indicating a strong interaction between predator and prey. These observations led me to investigate the possible role(s) of Type IV and/or Flp pili in the *B. bacteriovorus* predatory life cycle. In this chapter, Type IV pili and their roles in different bacterial species will be introduced, followed by the results gained from my work in *B. bacteriovorus*. Again, electron micrographs from my work are included.

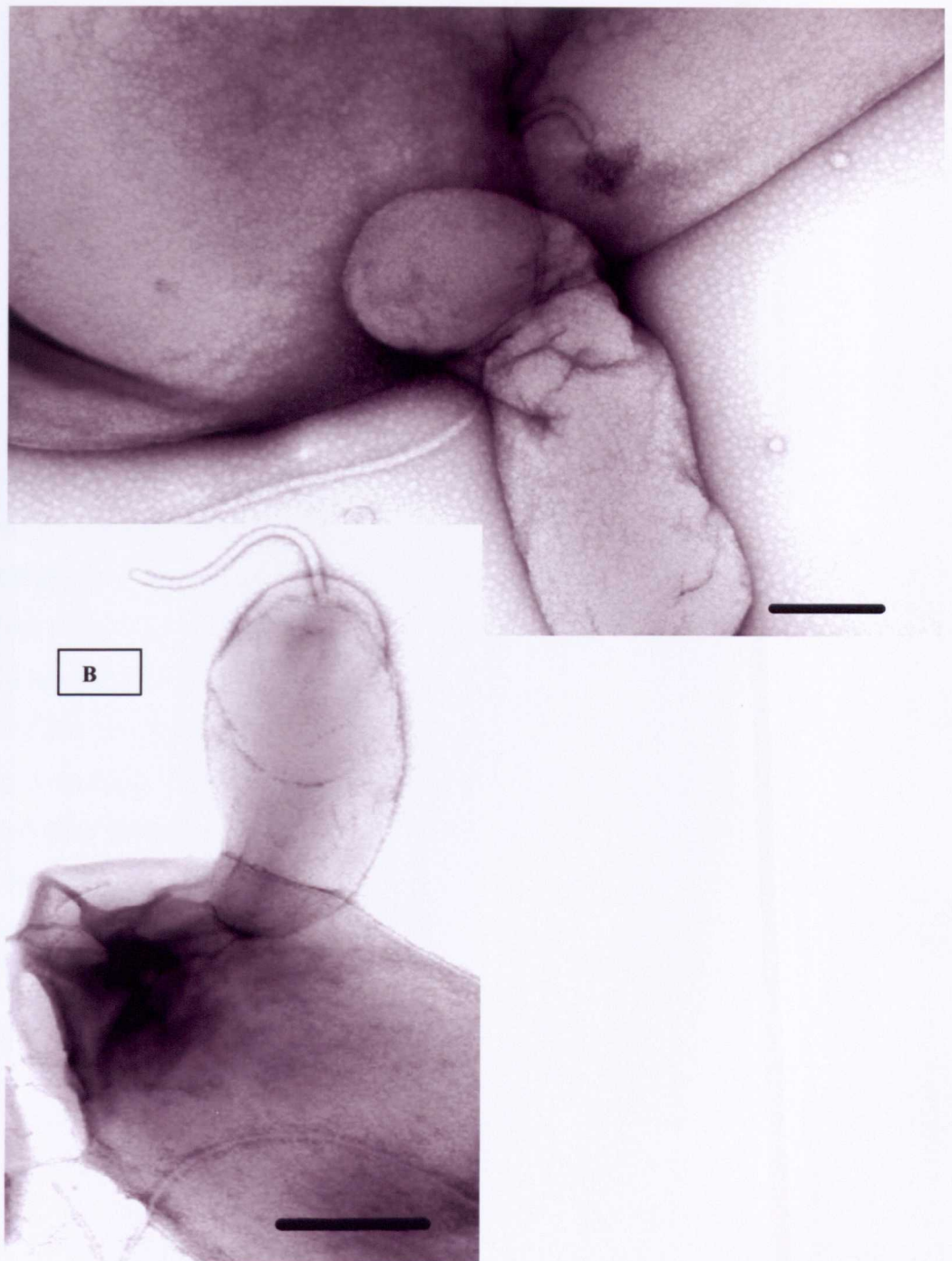


Figure 5.1: Transmission electron micrographs showing prey invasion. **A,B** show wild type HD100 *B. bacteriovorus* invading *E. coli*, demonstrating that the pore generated in the prey outer membrane by the predator is smaller than the predator itself. Stained with 1% uranyl acetate, bars = 0.2 μ m. (This thesis work)

5.1:What are Type IV pili?

Type IV pili (tfp) are adhesive, polar organelles found in a wide range of Gram-negative bacteria from pathogens such as *Neisseria gonorrhoea* and *Pseudomonas*

aeruginosa in adherence to host cells, to environmental species such as *Myxococcus xanthus* for fruiting body formation and social gliding motility (extensively reviewed in (Craig *et al.*, 2004; Mattick, 2002). Tfp are used for, amongst other things, a form of bacterial translocation called twitching motility, which is distinct from flagellar-rotation-mediated swimming and also swarming motility, mediated by peritrichous flagella in species such as *Proteus mirabilis*.

Twitching motility is mediated by retraction of the pilus fibre, which is extruded through the outer membrane of the bacterium. Merz and co-workers showed in an elegant set of experiments that it is the retractile force of the tfp filaments in *Neisseria* that provide the motive for twitching (Maier *et al.*, 2002a; Merz *et al.*, 2000). Their experiments using laser tweezers holding a latex bead in an optical trap, tethered to immobilised *Neisseria* cells, showed that the cells pulled the bead towards them, out of the trap, with forces in excess of 80pN, proving that retraction of the pilus fibre is necessary for tfp-mediated motility. In *Pseudomonas aeruginosa*, Skerker and Berg directly observed extension, attachment of pili to the quartz slide, force exertion and then retraction of tfp fibres using Cy3 fluorescent dye-labelled pili (Skerker and Berg, 2001).

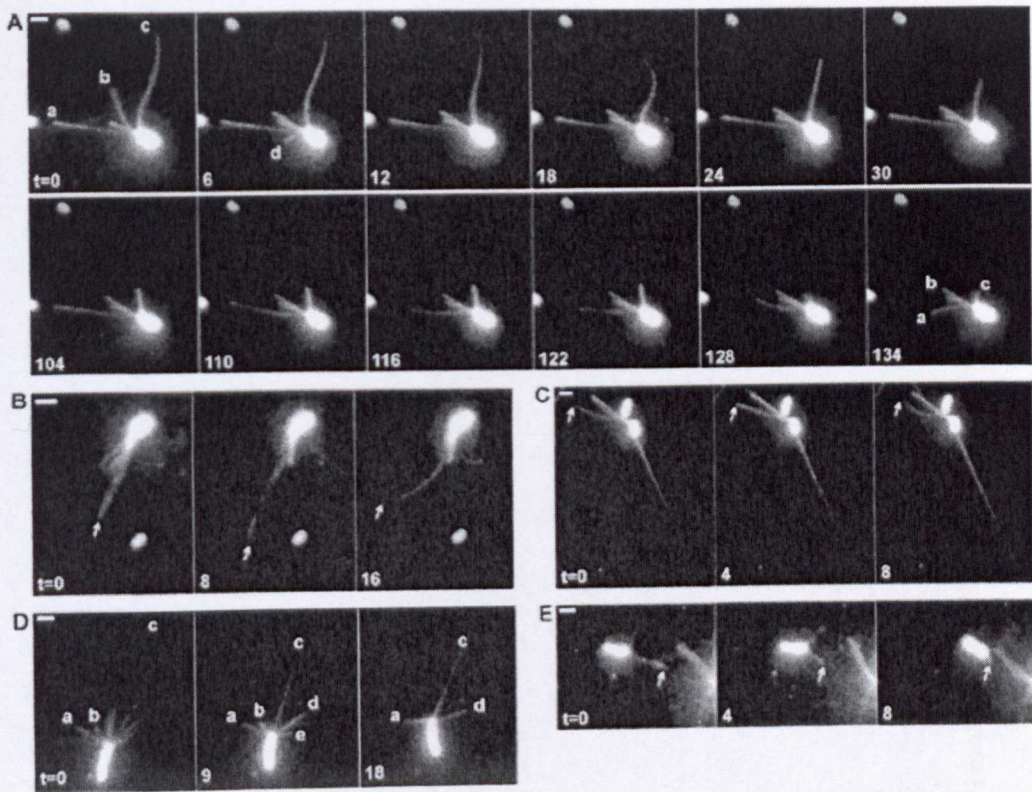


Fig 5.2 Taken from Skerker and Berg 2001. **A** and **B**: extension and retraction of pili in *Pseudomonas aeruginosa*. **C** Pilus fibres under tension, anchored away from the cell body. **D** and **E** show cell movement towards point of attachment indicated by the arrow, **E** time elapsed = 8 sec. Bars 2 μ m.

In summary, type IV pili are used for a range of purposes in diverse bacteria, but share common themes of working by extension from the cell pole, attachment to a substrate and retraction of the pilus fibre, pulling the cell body toward the point of attachment. Thus, they could be candidates for *B. bacteriovorus* entry into the prey periplasm.

5.1.1 General structure of the Gram-negative bacterial Type IV pilus

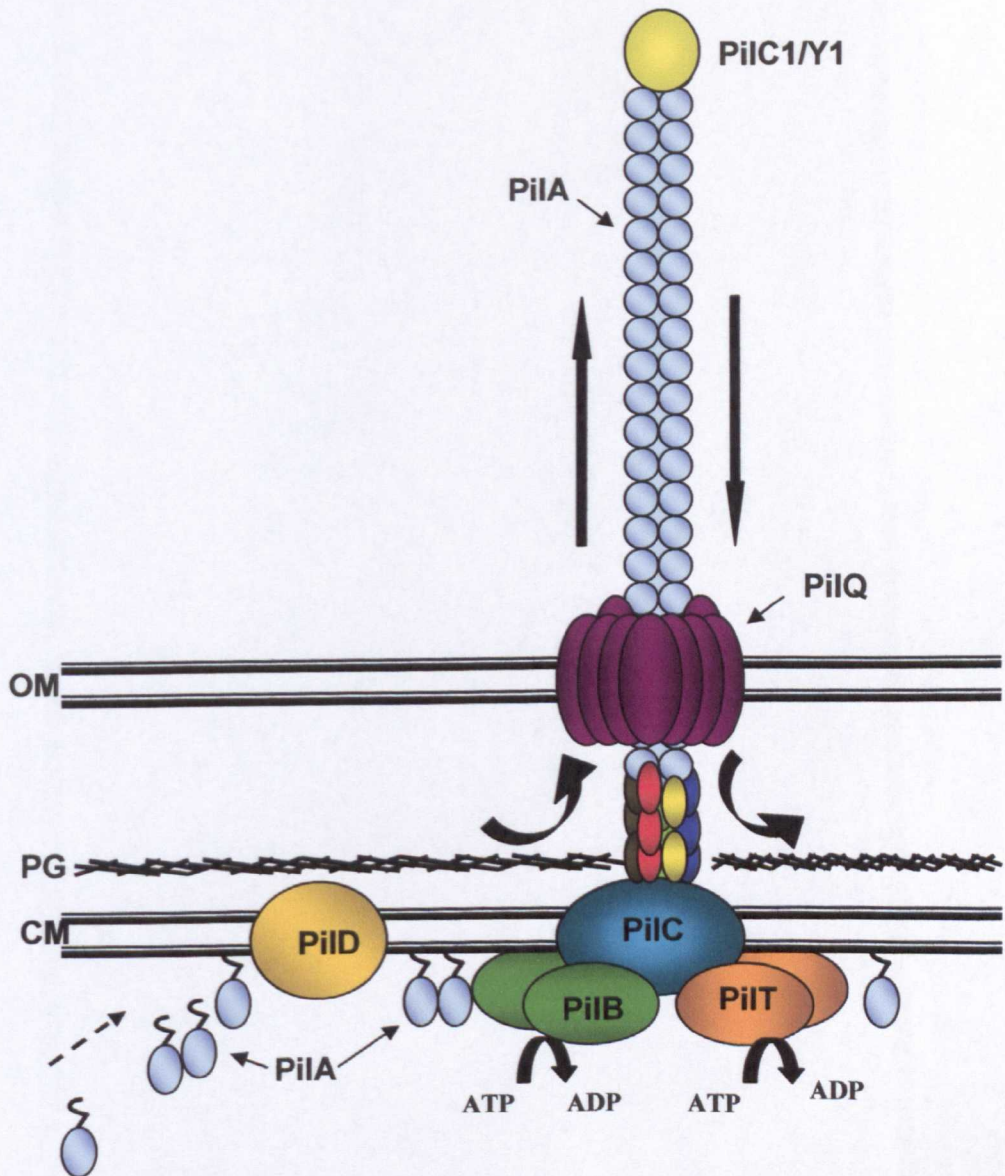


Figure 5.3. Cartoon representing the general structure of the Gram-negative bacterial Type IV pilus as found in *Neisseria* and *Pseudomonas*. See Table 5.1 for details of protein functions. OM = outer membrane, PG = peptidoglycan, CM = cytoplasmic membrane. Essentially, immature PilA is held under the CM, processed by the pre-pilin peptidase, PilD and assembled into helical fibres by the action of the PilB extrusion ATPase. PilC anchors the base of the pilus in the CM and PilQ allows it to pass through the OM to the exterior of the cell. PilT ATPase provides the force necessary for helix disassembly and hence pilus retraction. After Mattick, 2002.

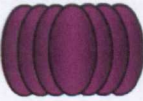
PROTEIN	FUNCTION	DIAGRAM REPRESENTATION
PilB	ATPase, pilus extrusion	
PilT	ATPase, retraction	
PilC	Polytopic membrane protein required for pilus biogenesis	
PilA	Pilus fibre protein, immature protein is held under the cytoplasmic membrane	
PilE, V, W, X FimU	Minor pilins	
PilD	Pre-pilin peptidase	
PilQ	Outer membrane multimer complex needed for PilA fibre extrusion.	
PilC1/Y1	Tip invasin/adhesin found in some species	

Table 5.1: Key to general diagram of the bacterial type IV pilus. After (Mattick, 2002), see Fig 5.3

5.1.1.1: Roles of the Type IV pilus proteins in pilus formation: knowledge from other species

From extensive studies amongst the three main model organisms (*M. xanthus*, *P. aeruginosa* and *N. gonorrhoeae*), there has emerged a general consensus about the mechanism and common structure of tfp, the latter being illustrated in Fig 5.3 For extensive reviews, see (Mattick, 2002) and (Craig *et al.*, 2004). Essentially, the

immature fibre protein, PilA, is synthesised and held under the cytoplasmic membrane and is processed to form mature PilA through cleavage of the leader sequence by the pre-pilin peptidase and methylase, PilD. Mature PilA is assembled into polymers in a helical fashion through the action of an ATPase, PilB, responsible for fibre extrusion and due to the action of the polytopic cytoplasmic membrane anchor protein PilC. The helical fibre is polymerised into a three-start helix and extruded through the peptidoglycan layer via the action of an unknown (probable) lytic transglycosylase and out to the exterior of the cell body through a dodecameric multimer of PilQ. PilQ multimers (secretin homologues of the *gspD* superfamily, (Peabody *et al.*, 2003) are found in the outer membrane of the cell and form a gated pore through which the typically 5-7nm diameter PilA fibre can pass (Nudleman *et al.*, 2006; Wolfgang *et al.*, 2000). Once the pilus fibre attaches to its substrate, it is disassembled through the action of multimers of the PilT ATPase, held under the cytoplasmic membrane like its antagonist, PilB. PilT removes PilA monomers from the base of the fibre; coincident with the adhesion of the pilus tip, this action pulls the cell body towards the point of attachment. Thus, type IV pili work through cycles of extrusion, attachment and retraction, in a ratcheting mechanism (reviewed in (Mattick, 2002).

5.1.2: The genetics of Type IV pilus biogenesis

5.1.2.1: *Myxococcus xanthus* as a model for studying *B. bacteriovorus* Type IV pili

M. xanthus, along with *P. aeruginosa* and *N. gonorrhoeae*, is one of the most extensively studied organisms in relation to type IV pili. For the purpose of studying *B. bacteriovorus*, *Myxococcus* is perhaps the most logical model to use as it is also a member of the δ -proteobacteria. As such, it would be expected that there would be a higher degree of conservation at the gene/protein level between the two species better than *Pseudomonas*, a γ - and *Neisseria*, a β -proteobacterium.

Another reason for using *Myxococcus* as a model for *Bdellovibrio* study is that the *Myxobacterales* are also predatory (for a review, see (Rosenberg and Varon, 1984).

Myxococcus, however, is a “pack hunter” in that swarms of cells secrete lytic and other biocidal enzymes into the surrounding environment to lyse any other bacteria and then take up the resulting nutrients. Predation is dependent upon genes and their protein products associated with signalling and A-motility (the alternative Myxobacterial motility system, associated with gliding, rather than Social, tfp-dependent motility, see (McBride, 2001) for a review of motility systems in *Myxococcus*) and the predatory process itself may represent part of the ecological balance in soil bacterial communities (Pham *et al.*, 2005).

5.1.2.2: *M. xanthus* Type IV pili and mutant phenotypes

Early work by Dale Kaiser showed that *M. xanthus* social motility is correlated with the presence of pili (Kaiser, 1979). Mutants in Social motility genes showed a lack of pili when examined under the electron microscope or were defective in non-dispersed growth, a feature of *Myxococcus* strains with functioning pili.

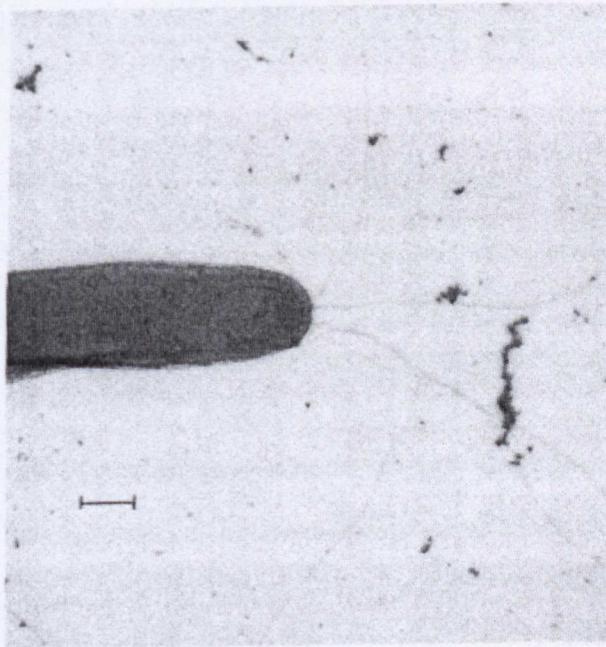


Figure 5.4: Transmission electron micrograph of wild type *M. xanthus* showing polar pilus fibres. Stained with uranyl acetate, bar = 0.5 μ m. Taken from (Kaiser, 1979).

Work by Rosenbluh and Eisenbach confirmed Kaiser's early observations, when mechanical shearing/removal of pili from *M. xanthus* A-motility defective but S-motility normal strains showed a total loss of cell movement (Rosenbluh and Eisenbach, 1992).

Transposon mutagenesis has long been used as a tool to probe Myxobacterial motility. Initial experiments, again from the Kaiser lab, found three genes involved in biosynthesis of pili, *pilS*, *pilR* and *pilA* (Wu and Kaiser, 1995). The authors proposed that due to the sequence homology of the PilA fibre protein to other known type IV pilus proteins in *Pseudomonas* that *Myxococcus* pili belong to the type IV group. Since this foundation, the type IV pilus genes of *M. xanthus* have been identified and mainly all characterised (reviewed in (Kaiser, 2003; Wall and Kaiser, 1999).

5.1.2.3: Conservation of Type IV pilus genes between *Myxococcus* and *B. bacteriovorus*

The recent sequencing of both the *Bdellovibrio bacteriovorus* HD100 (Rendulic *et al.*, 2004) and *Myxococcus xanthus* DK1622 genomes (TIGR, <http://pathema.tigr.org/tigr-scripts/CMR/GenomePage.cgi?org=gmx>) has enabled proper comparisons of the motility systems in these δ -Proteobacteria for the first time. The main difference between the two bacteria is in the use of flagella motility: *Myxococcus* is a non-flagellate top-soil bacterium (Henrichson, 1972) whereas *B. bacteriovorus* uses a single polar flagellum for motility through liquid environments (Lambert *et al.*, 2006). Both species, however share genes for apparently conserved Type IV pilus systems which are used for S-motility in *Myxococcus* (Kaiser, 2003) and which are proposed to be involved in the prey-cell-entry characteristic of the predatory *B. bacteriovorus* (Rendulic *et al.*, 2004). The relevant genes are listed in the Table below:

Table 5.2: Genes shown to be required for tfp biogenesis in *M. xanthus* and their homologues from *B. bacteriovorus* HD100 as found through BLASTP analysis.

GENE	FUNCTION	HD100 homologue	HD100 GENE #	REFERENCE
<i>pilB</i>	ATPase, pilus extrusion	<i>pilB</i>	Bd1509	(Turner <i>et al.</i> , 1993)
<i>pilT</i>	ATPase, retraction	<i>pilT</i> (2 annotated, best homologue)	Bd3852	(Wu and Kaiser, 1997)
<i>pilC</i>	Polytopic membrane protein required for pilus biogenesis	<i>pilC</i>	Bd1511	(Mattick, 2002; Nunn <i>et al.</i> , 1990)
<i>pilS</i>	Negative regulator <i>pilA</i> expression, 2 component system with PilR	<i>pilS</i>	Bd1512	(Wu and Kaiser, 1997)
<i>pilR</i>	Regulates <i>pilA</i> expression, 2 component system with PilS	<i>pilR</i>	Bd1513	(Wu and Kaiser, 1997)
<i>pilA</i>	Pilus fibre protein	<i>pilA</i>	Bd1290	(Wu and Kaiser, 1995)
<i>pilG</i>	Part of ABC transporter required for pilus biogenesis with PilHI	Bd1291	Bd1291	(Wu <i>et al.</i> , 1998)
<i>pilH</i>	Part of ABC transporter required for pilus biogenesis with PilGI	annotated <i>phnC</i> , upstream of <i>pilI</i>	Bd0860	(Wu <i>et al.</i> , 1998)
<i>pilI</i>	Part of ABC transporter required for pilus biogenesis with PilGH	<i>pilI</i>	Bd0861	(Wu <i>et al.</i> , 1998)
<i>pilD</i>	Pre-pilin peptidase	<i>pilD</i>	Bd0862	(Nunn <i>et al.</i> , 1990)
<i>pilS2/R2</i>	Homologues PilSR in <i>Myxococcus</i>	No definite homologues	N/A	(Jelsbak and Kaiser, 2005)
<i>pilM</i>	Required for pilus biogenesis, FtsA/MreB homology	<i>pilM</i> (better homologue) <i>pilM</i>	Bd0863 Bd1585	(Martin <i>et al.</i> , 1995)
<i>pilN</i>	Involved in pilus biogenesis	<i>pilN</i>	Bd0864	(Martin <i>et al.</i> , 1995; Mattick, 2002)

GENE	FUNCTION	HD100 homologue	HD100 GENE #	REFERENCE
<i>pilO</i>	Involved in pilus biogenesis	<i>pilO</i>	Bd0865	(Mattick, 2002)
<i>pilP</i>	Lipoprotein needed to stabilise PilQ multimer formation	<i>pilP</i>	Bd0866	(Drake <i>et al.</i> , 1997; Nudleman <i>et al.</i> , 2006)
<i>pilQ</i>	Outer membrane multimer complex needed for PilA fibre extrusion.	<i>pilQ</i> (most convincing homologue of 3 annotated)	Bd0867	(Wall and Kaiser, 1999)
<i>tgl</i>	Lipoprotein with TPR protein interaction domains that is required for PilQ multimer formation	most likely candidate annotated <i>pilF</i> in genome	Bd3829	(Rodriguez-Soto and Kaiser, 1997a, 1997b)

Homology searches using reciprocal NCBI BLASTPs (Altschul *et al.*, 1997) and ClustalW protein alignments (Thompson *et al.*, 1994)(see Methods Section 2.10) show that *B. bacteriovorus* has conserved homologues of *Myxococcus* genes encoding Type IV pili (Table 10). Additional *pil* genes, eg the minor pilins *pilE, V, W, X* and *fimU* found in other piliated species such as *Pseudomonas* were not found in *B. bacteriovorus*. Both δ -Proteobacteria have the same *pil* gene order as is seen within the *Myxococcus* operon (see Figure 5.5 below) but *B. bacteriovorus* seems to have undergone genomic rearrangements which have scattered parts of the operon to different areas of the genome. Certain *Bdellovibrio* genes will be discussed in greater detail later (see Section 5.3.4 and 5.3.5) due to more than one homologue being found in the HD100 genome.

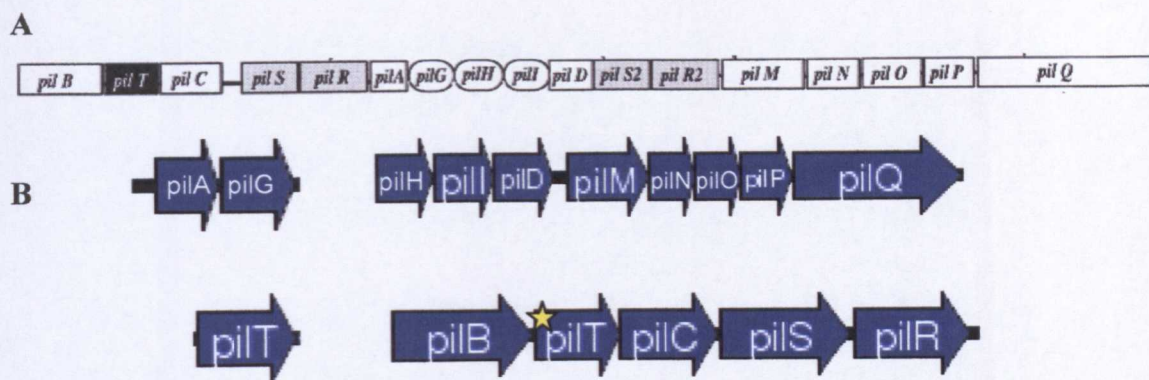


Figure 5.5: Comparison of the operon structure of *pil* genes in *Myxococcus* and *B. bacteriovorus* **A:** organization of *Myxococcus pil* genes, taken from Wall and Kaiser, 1999. **B:** *pil* genes are scattered around the HD100 genome, but the ancestral organization can be seen with the gene order being conserved. The starred annotated *pilT* within the operon is a good homologue, but Bd3852 on the left is a better homologue, suggesting a duplication event. *B. bacteriovorus* does not have convincing homologues of *pilR2/S2*. Also see (Evans *et al.*, 2006) – in press.

Gliding motility genes are implicated in *Myxococcal* motility, but these systems seem to be not present in *B. bacteriovorus*, or made redundant so long ago that the genes involved are no longer recognisable as such. My protein-level homology searches found no significant homologues of *Myxococcus* genes involved in gliding (Youderian *et al.*, 2003). The most obvious example of such a gene is the *mglA* gene, the protein product of which in *Myxococcus* is absolutely required for both A and S motility (Hartzell and Kaiser, 1991b) and is present in *B. bacteriovorus* (Bd3734) but its counterparts in *Myxococcus* that are only required for gliding, such as *mglB*, *cglB* and *aglZ* (Hartzell and Kaiser, 1991a; Rodriguez and Spormann, 1999; Yang *et al.*, 2004), are absent from the *B. bacteriovorus* genome.

Nor does *B. bacteriovorus* appear to have the *frz* gene system that is used in *Myxococcus* for switching the pole at which pili are extruded during social motility (Reviewed in (Ward and Zusman, 1999). The pole-switching *Myxococcus frzS* gene (Mignot *et al.*, 2005) has no significant homologues in the *B. bacteriovorus* genome, and the other *frz* genes only show partial homology to general MCP or 2-component sensor-regulators, likely required for flagellar motility or unrelated processes. Biologically, this makes sense as *Myxococcus* uses the pilus pole-switching for reversal of the direction of cell motility as a non-flagellate soil-surface bacterium (Mignot *et al.*, 2005). *B. bacteriovorus* on the other hand uses flagellar-mediated

motility through liquid environments and has a single pole dedicated to housing the flagellum. It follows, therefore, that there would never be a requirement for FrzS-mediated switching of the piliated pole in *B. bacteriovorus* as in this bacterium pilus-like structures are at the non-flagellate pole where prey cell entry occurs.

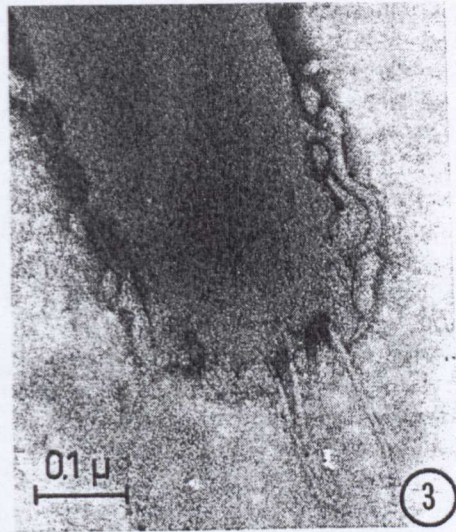
Taken together, the conclusions are that there is a conserved cell movement pathway between the two bacteria in the form of Type IV pili, where the genes may be ancestral to both. After the speciation and divergence of these predators, *Myxococcus* retained gliding genes and developed slow surface motility behaviours, feeding socially and co-operatively on prey, in rich soil/dung environments, by external enzymic hydrolysis. *B. bacteriovorus* retained/acquired the genes necessary for flagella motility and forsook slow gliding/twitching motility for rapid, lone, seeking of distant prey across more dilute areas of water within soil, sediment and aquatic environments.

5.1.3: Previous *B. bacteriovorus* work on pilus-like fibres and hypotheses for holdfast structures

As shown above, the HD100 genome encodes a set of genes that could potentially form tfp structures; what follows is a summary of the previous published evidence for and pilus-like protein fibres seen in *B. bacteriovorus*.

B. bacteriovorus attachment to its prey is always from the anterior, non-flagellate pole. Since its discovery in 1963 (Stolp and Starr, 1963), intensive electron microscopy studies have been employed to find the mechanism of prey cell entry by the predator. Shilo in 1969 observed “*spike-like filaments which may play a role in the attachment and penetration of prey*” in *B. bacteriovorus* 109J (Shilo, 1969) through studies of 109J incubated with *E. coli* B (Figure 5.6)

Figure 5.6: Transmission electron micrograph of *B. bacteriovorus* 109J showing anterior fibres, hypothesised by the authors to be involved in prey entry. Stained with 2% phosphotungstic acid, bar = 0.1 μm . Taken from (Shilo, 1969).



Burnham and co-workers, through another intensive EM study, proposed a “holdfast structure” at the anterior pole of *B. bacteriovorus* (see Figure 5.7 (2)) when looking at predator-prey interaction, though it is unclear as to whether this is a defined structure or an artefact of the staining preparation techniques employed, with glutaraldehyde fixation and acetone dehydration after negative staining being a fairly harsh treatment of bacterial cells (Abram and Davis, 1970; Burnham *et al.*, 1968). Further work by Abram and Davis also showed anterior fibres on *B. bacteriovorus* cells in uranyl acetate stained preparations (see Figure 5.7 (35)); they proposed that these fibres could be used to form a strong interaction between predator and prey and also noted that if the fibres were formed after initial predator attachment, then the chances of seeing many on free-swimming *B. bacteriovorus* would also be rather small (Abram and Davis, 1970).

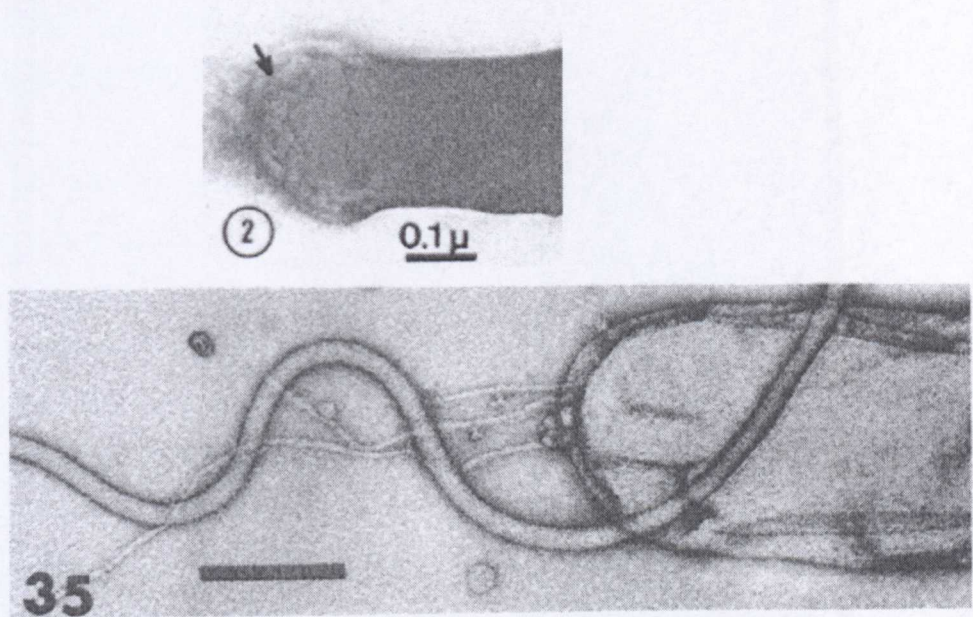


Figure 5.7: 2 taken from (Burnham *et al.*, 1968) showing the proposed “holdfast “ structure at the anterior pole. **35** taken from (Abram and Davis, 1970), showing anterior fibres that the authors proposed could be used to mediate a strong interaction between predator and prey, bar = 0.2 μ m. The large wavy filament that can be seen is the *B. bacteriovorus* flagellar filament.

5.2: Hypothesis and my evidence for *B. bacteriovorus* expressing and using Type IV pili for prey entry

Immense forces can be generated by the ratcheting mechanism of Type IV pili (Maier *et al.*, 2002b), needed to squeeze the predator through a small opening in the prey against the forces that would be produced as the periplasmic and cytosolic contents of the prey push against the invading *B. bacteriovorus*. I propose that Type IV pili are the only known bacterial external organelle that would be capable of doing this, with a potential solid surface providing the anchor for the ratchet being the prey peptidoglycan.

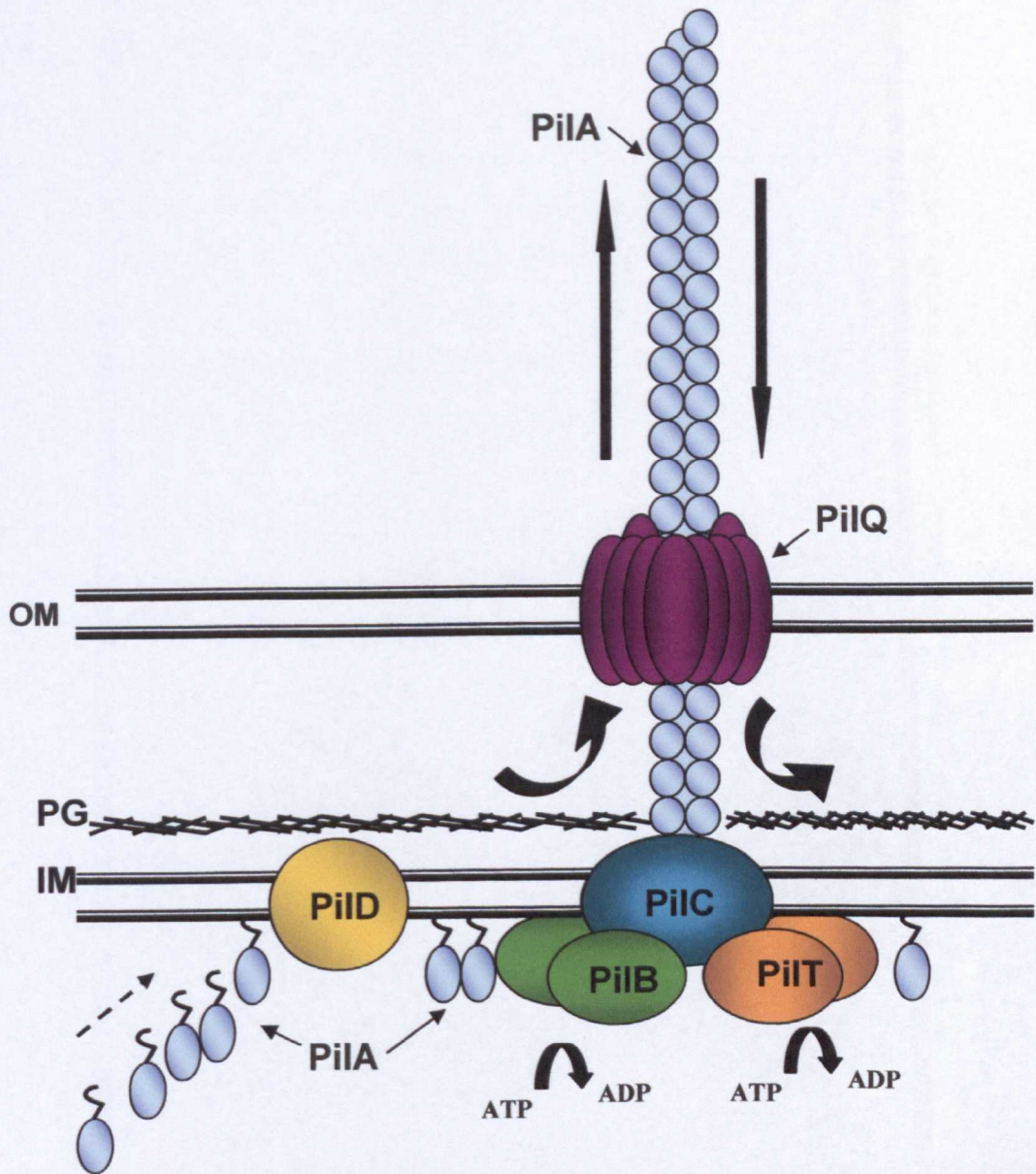
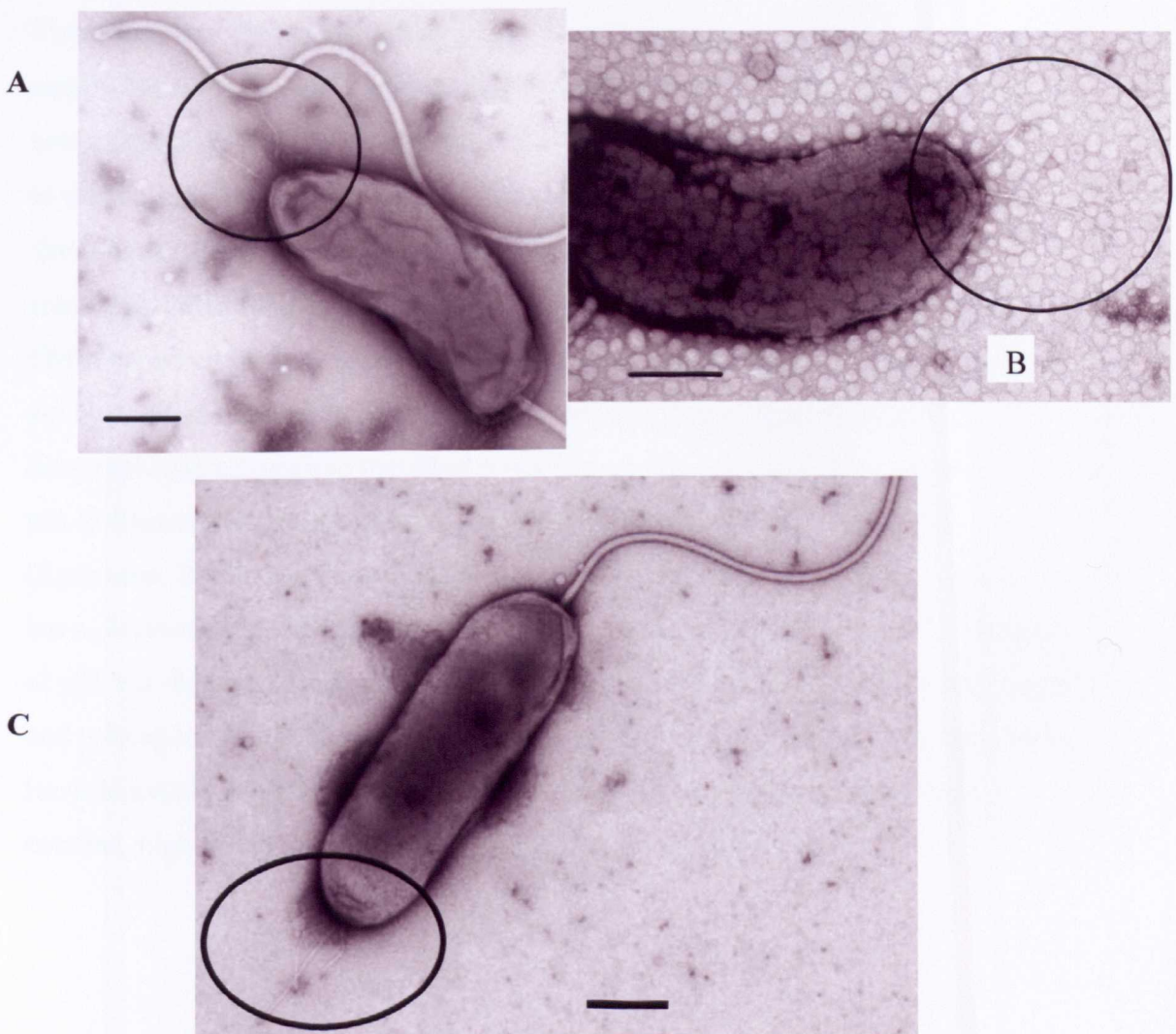


Figure 5.8. Cartoon representing my proposed structure of the *B. bacteriovorus* HD100 Type IV pilus based on the general structure of Gram-negative bacterial pili and the *pil* genes found in HD100 through BLASTP searches (see Table XX and Section 2.10). See Table 5.1 for details of protein functions. OM = Outer membrane, PG = peptidoglycan, CM = cytoplasmic membrane. After Mattick, 2002. NB: This is only a very basic model, as the exact function and localisation of other proteins involved in pilus formation, eg PilGHIMNOP, are still under investigation as of Feb 2007.

5.3: Electron microscopic analysis of *Bdellovibrio bacteriovorus* to ascertain the presence of pilus-like fibres on the cell surface.

Pili may however have many other adhesive roles in the lifestyle of an aquatic or terrestrial bacterium, such as attachment to abiotic surfaces (reviewed in(Craig *et al.*, 2004; Mattick, 2002). Thus to ascertain whether Type IV pili were expressed in attack phase predatory *B. bacteriovorus*, electron microscopic (EM) observations of both HI grown *B. bacteriovorus* and those freshly liberated from host-dependent predatory growth were carried out using uranyl acetate staining (Figure 5.9).

Figure 5.9: Transmission electron micrographs of attack phase *B. bacteriovorus* freshly liberated from prey cells. **A and B:** Wild Type HD100 pilus-like fibres. **C:** Wild type 109J pilus like fibres. All stained 1% uranyl acetate, bars = 0.2 μ m



5.3.1: Observation of pilus-like fibres on the non-flagellar pole of *B. bacteriovorus* HD100 and 109J

My EM studies confirmed the early work of Shilo (1969) and Abram and Davis (1970) where small, polar fibres were shown on *B. bacteriovorus*. I visualised pilus-like fibres, measuring on average $8\text{nm} \pm 1\text{nm}$ in diameter and ranging from $0.2\mu\text{m}$ to $0.35\mu\text{m}$, were seen in approximately 30% of host dependent HD100 cells (Fig 5.9 AB) in uranyl acetate stained preparations. Similar fibres with the same dimensions were also seen in uranyl acetate stained preparations of 109J (see Fig. 5.9, C). Agreeing with Abram and Davis (1970), broken fibres were often seen lying in close proximity to the cells, indicating that the shear forces associated with staining seems to affect the proportion of *B. bacteriovorus* seen with intact fibres.

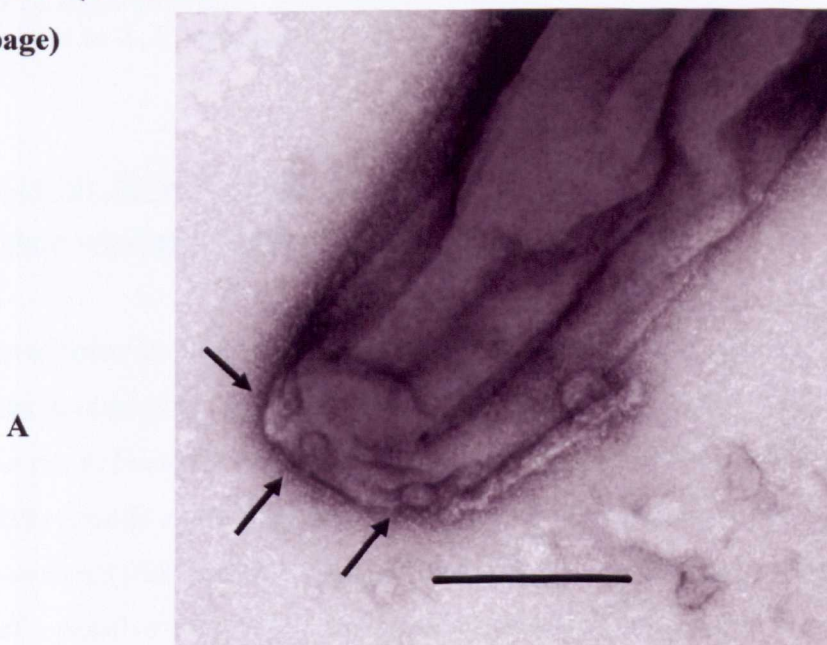
There were and are also technical difficulties in imaging pili, which are by their very nature, helical polymers. Small diameter helical polymers such as pili, aside from being extremely difficult to crystallise, can be refractory to electron microscopy due to the fact that they tend to exist in multiple forms at any one time, so showing disorder and heterogeneity. These factors combine to produce a weak electron scattering, which makes these thin fibres extremely difficult to see as the nature of EM is based on electron scatter to produce a clear image (Egelmann, 2000). There are high resolution techniques aided by vast computational power available to get fine resolution images and therefore structural models of thin helical polymers, like pili or filamentous phage, such as iterative helical real space reconstruction (Egelmann, 2000), but these are beyond the facilities available to me on a routine basis. Atomic Force Microscopy (AFM) may offer an alternative option for imaging of pili, but this is also technically extremely difficult; AFM studies of 109J by Nunez and colleagues (Nunez *et al.*, 2005) did not show any pilus-like fibres, but their work focused mainly on 109J predation in whole bacterial communities rather than detailed, high magnification studies of the poles of individual cells.

5.3.2: Observation of ring-like structures on the anterior pole of HD100

High resolution EM studies also confirmed the presence of ring-like structures on the anterior pole of *B. bacteriovorus* (see Figure 5.10 A, B below). These ring-like structures are never seen on the flagellar pole (see Figure 5.10 C below). These were first seen by Abram and Davis, who hypothesised that the rings would be “differentiated sites of association between the [pilus-like, previously noted] fibres and the cell wall... and may be related to *Bdellovibrio* parasitic activity” (Abram and Davis, 1970).

My initial interpretation of these structures was that they may be multimers of the pilus outer-membrane secretin, PilQ. *N. meningitidis* PilQ forms dodecameric ring structures, which have been shown by high resolution electron microscopy and single particle analysis to have a diameter of 16.5nm and an internal cavity diameter of 6.5nm (Collins *et al.*, 2001). However, the stained ring-like structures on the anterior pole of *B. bacteriovorus* measure approximately $44\text{nm} \pm 4\text{nm}$ in diameter, which makes it unlikely that they are PilQ multimers. They could be some other structure involved in the predation process, made likely by their polar localisation. However, until candidate proteins are found, there is no way of knowing what these structures may be.

**Figure 5.10 (continued
next page)**



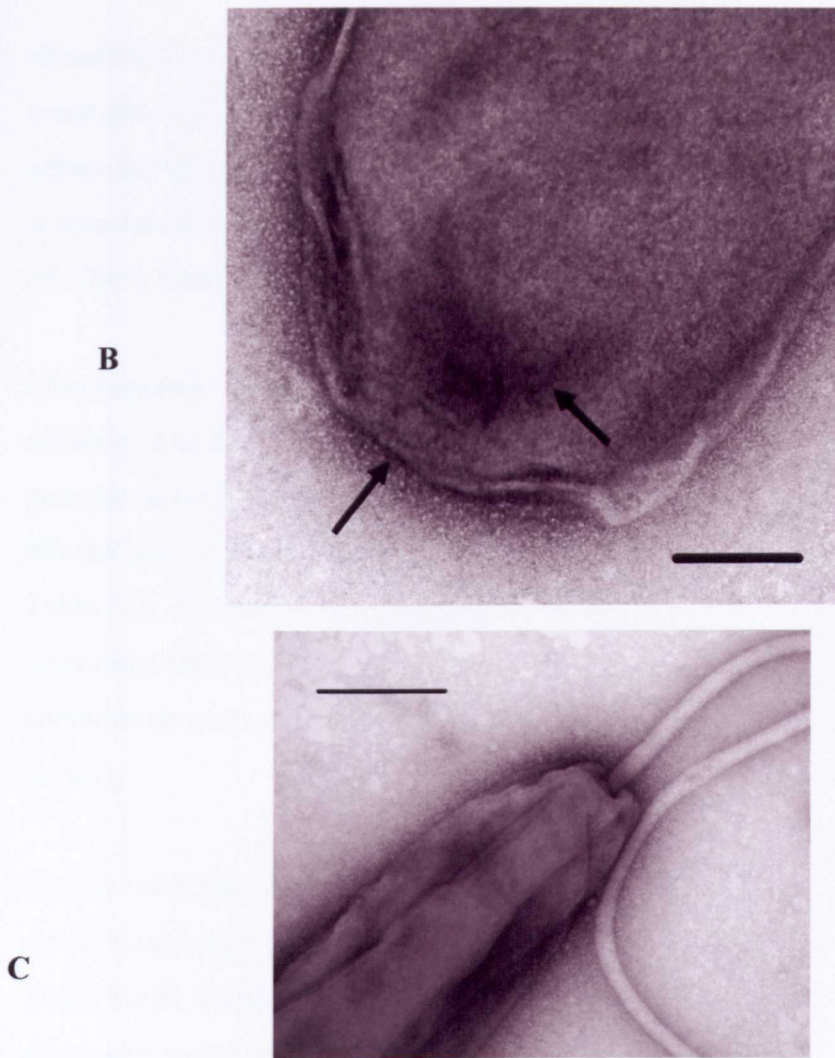


Figure 5.10 High resolution EM of wild type HD100 *B. bacteriovorus*. **A**, **B** arrows indicate the ring-like structures found on the anterior pole of the bacteria. **C** shows the lack of these structures on the flagellar pole of the cell. Stained 1% uranyl acetate, bars in **A**, **C** = 0.2 μ m, **B** = 0.1 μ m.

5.3.3: Are the fibres Type IV pili or Flp pili? The HD100 genome encodes an incomplete set of genes requires for Flp pilus formation

As shown earlier in Section 5.1.2.2, the *B. bacteriovorus* HD100 genome contains all the genes necessary in *M. xanthus* for tfp formation. However, there are also some genes in the *B. bacteriovorus* HD100 genome that others have stated that could potentially encode another set of pilus-forming genes. In a recent study, Schwudke and co-workers (Schwudke *et al.*, 2005) noted varying expression, over a predatory cycle, of a putative TypeIVb *flp-1* gene homologue in *B. bacteriovorus* HD100

(Rendulic *et al.*, 2004), which encodes the pilus fibre of Flp pili. In other bacteria these are a specific subset of Type IVb pili (Kachlany *et al.*, 2001), used for tight adherence to surfaces, and are best characterised in *Actinobacillus actinomycetemcomitans*, the causative agent of juvenile periodontitis ((Henderson *et al.*, 2003; Kachlany *et al.*, 2001).

I investigated this possibility by BLAST analysis and I believe that Flp pili are unlikely to be functional in *B. bacteriovorus* HD100 as the analysis of the HD100 genome showed that while there are a full set of genes that would encode Type IV pili (*pil* genes), there are only **some** of the genes that would encode Flp pili (see Table 11). Furthermore, the proteomic approaches employed by Schwudke and coworkers (Schwudke *et al.*, 2005) failed to find any Flp-1 protein in cell envelope preparations of *B. bacteriovorus* HD100, but did find PilA, the Type IVa pilus fibre protein.

Protein-level Blast homology searches of the HD100 genome also revealed that there are no homologues of the *tadV*, *rcpC*, *rcpB*, *tadZ*, *tadE*, *tadF* and *tadG* genes. RcpB, TadZ, TadE, TadF and TadG are **required** for Flp fimbrial formation in *A. actinomycetemcomitans* as shown by individual gene replacement with a spectinomycin-resistance cassette (Wang and Chen, 2005). Point mutation of the gene encoding the conserved aspartate residues of the pre-pilin peptidase, TadV, (which is also lacking in *B. bacteriovorus* strain HD100), also stopped production of Flp pili and showed accumulation of unprocessed Flp-1 pilin and the TadE and TadF pseudopilins (Tomich *et al.*, 2006). Recent work in *Pseudomonas aeruginosa* identified a Flp pilus operon and another aspartate pre-pilin peptidase, FppA, again which has no identifiable *B. bacteriovorus* homologue. Deletion of *fppA* in *Pseudomonas aeruginosa* again resulted in accumulation of the immature Flp pre-pilin (de Bentzmann *et al.*, 2006). Crucially, *P. aeruginosa* also has *pilD*, the Type IV pre-pilin peptidase, as does *B. bacteriovorus*; in an *fppA* mutant background, PilD was unable to process Flp pre-pilin (de Bentzmann *et al.*, 2006). Taken together, the 2006 work by various groups and my bioinformatic analysis of the HD100 genome, seem to indicate that there is an insufficient Flp pilus gene complement, in *B. bacteriovorus*, to form functional Flp-pilus structures. This then leaves the complete

set of genes with Myxococcal homologues encoding Type IV pili as the sole, complete candidate gene set (See Table 10 above).

GENE	FUNCTION	BDELLOVIBRIO HOMOLOGUE?	NCBI BLAST
<i>flp-1</i>	Pilus subunit	No	other Flp-1 from characterised species
<i>flp2</i>	Duplication <i>flp-1</i>	No	low scores to other characterised flp species
<i>tadV</i>	non-methylating prepilin peptidase	No	CpaA homology, all proteins found in flp species
<i>rcpC</i>	unknown	no	weak cpaB homology, few hits, all in flp species
<i>rcpA</i>	Secretin	yes, GspD and PilQ, not surprising dues to OM/secretin homology	RcpA/GspD/PilQ/Type II/III secretin
<i>rcpB</i>	secretin/OM protein	No	only RcpB from flp species
<i>tadZ</i>	unknown, possible extracellular secretion vesicles	No	tadZ from Flp species, weak ATPase domain
<i>tadA</i>	ATPase	yes, TadA (e-100) Bd0111 hit locus, also CpaF (7e-76) Bd0793	TadA, secretion NTPases, CpaF
<i>tadB</i>	pilC like	TadB (2e-08)C terminal homology Bd0110, hit region	TadB, Type II secretion homologues
<i>tadC</i>	pilC like, adherence to surfaces	TadC (2e-09) Bd0470, also TadB hit region again	TadC/Type II/IV secretion
<i>tadD</i>	required for production fimbriae	AgIT (7e-09) Bd0833, Bd0225 (3e-04), TPR repeat protein	TadD, TPR domain protein
<i>tadE</i>	pseudopilin	No	TadE flp species
<i>tadF</i>	pseudopilin	No	TadF flp species, ATP/GTP binding site A motif
<i>tadG</i>	possible anchor for fimbriae, control of matrix material secretion	no	only TadG from flp species

Table 5.3: Genes required for Flp pilus formation in *Actinobacillus actinomycetemcomitans* (Kachlany *et al.*, 2001; Wang and Chen, 2005) BLASTP against the *B. bacteriovorus* HD100 genome and the NCBI database. Not all the genes required for Flp pilus formation are found in the genome.

There are, however, some candidates for duplicated Type IV pilus genes in HD100 which I will describe subsequently and have studied by Reverse Transcriptase – PCR.

5.3.4: Bioinformatic analysis to identify prospective Type IV pilus genes: multiple *pilQ* homologues are found in the HD100 genome

I have demonstrated in Section 5.1.2.3 that the *B. bacteriovorus* HD100 genome contains all the genes necessary in *M. xanthus* for Type IV pilus formation. However, certain genes showed multiple homologues within the genome sequence; *pilQ* was one.

The *pilQ* gene product in other bacteria forms a dodecameric multimer of the GspD family of secretins (Peabody *et al.*, 2003) that is inserted into the outer membrane of poles carrying pili (see Figure 5.3) allowing export of the pilus fibre to the exterior of the cell through a gated channel (Collins *et al.*, 2001; Mattick, 2002). 3 annotated *pilQ* genes are present in the genome of HD100: Bd0112, Bd3306 and Bd0867.

Protein level homology searches against the NCBI database and reciprocal BLASTs against the *B. bacteriovorus* genome show that Bd0112 had more homology to CpaC proteins (logical, as the Bd0112 gene is directly upstream of an annotated *cpaF* gene in the HD100 genome) and other secretins than to known PilQs; unsurprising as most secretins share C-terminal sequence similarity (Collins *et al.*, 2001; Peabody *et al.*, 2003). Bd 3306, another annotated PilQ shows more homology with other general Type II and III secretion proteins than known PilQs.

Bd0867 on the other hand shows excellent homologies to other PilQ proteins, bringing up *M. xanthus* PilQ with an e value of $7e-74$ in an NCBI BLASTP (see section 2.10) and is also found in an operon with other *pil* genes (see Figure 5.5, section 5.1.2.3), making this the most likely candidate for the *B. bacteriovorus* PilQ homologue. BLASTP searches also bring up other δ -proteobacterial PilQs and those from *P. aeruginosa* and *N. gonorrhoeae*. An alignment Bd0867, hereafter referred to as PilQ, with *M. xanthus* is shown below in Figure 5.11.

```

M xan PilQ 1 MLEESA VTRGK WMLAAAWAVVLV GARVHGAELN LTRGLDVSRTGSGAQVVVVTGRPPTFT 60
Bd0867 1 ----- 1

M xan PilQ 61 VFRLSGPERLVLDLSSADATGKIGHHEGSGPVSQFSDQRASVGRVLLALDKASQY 120
Bd0867 1 -----MNGFTRLVLLSAMIASLT 18

M xan PilQ 121 DVRADGNRVVLSVDGTSQSVDAKRAETPARTERMTASVEAKPHPVAAQAPAKVVKAESAA 180
Bd0867 19 SCASRPVEDDLSDGMDSSADVTSADESAPAADSASDDFAEFDEIDNQQPAQAESQAAPA 78

M xan PilQ 181 VP-KAALPENVAAREADEREVSNEPAQHITAMSFADDTL SIRADGDIARYEVLELADPPRL 239
Bd0867 79 DDQDLALEEEVNEAGGQEQVADAPAPAPEETSPTEDPFADSSVADVP-----AQTPEP 131

M xan PilQ 240 AVDLFGVGLATRAPRVKSGALRDVVRVGAHADKVLRLVLDVVRGTM PAYRVD RANRGLLEVVLG 299
Bd0867 132 TVTETTPDPFADQEPVSEPA----- 152

M xan PilQ 300 RAVARTWRRPLRPRAVVASVAEVEPLRQTPVKSDASPVVEVKDVRFEESSSGGRIVMRLS 359
Bd0867 152 -----APVTEPIAAVPSGAPANITDLKFRANETGGTIVIVQGD 189

M xan PilQ 360 GTSGWKVDR-PDPRSAVLTLDNARLPKPFERSLDTSA LDTPVKMLSAF SVPGAGGKVRILV 418
Bd0867 190 RPLTYTTRTNPDLRQFLIEVDNANLPDRLKRS LTKDKGSGVGAIDAVQNP GS-ATARFV 248

M xan PilQ 419 VAADGALPEKVSQASAGT LSWRLDVKGVKTEEVAVAQRTAGFTT---EAPAYAEGAPQQA 475
Bd0867 249 IQMREGLGEPMVQEQGNLLIVASGSAPAEAMEVTDVSTAMEDNNILPSQNLTEFLAGNT 308

M xan PilQ 476 RYRGRKRVSEFEFKDIDTQNLRRVIAELSKKNTIVADDVSGKVTIRLRNVPWDQALDLVLR 535
Bd0867 309 KFYGKKISLETSNMDIRDALNFTIEESGVNML SEDVRGAVSLKLRQVPWDQALVVIMKA 368

M xan PilQ 536 KALGKEEFGNIIRIAPLKTLEEARLRQERKKS LQQCEDLMVNL LPVNYAVAADMAARVK 595
Bd0867 369 KKLGYTROGNVIRIAPLQDLKAEEDDATKLAQARKNLEPLKVRMFPVSYAKVDELEKLIK 428

M xan PilQ 596 DVLSEKRSVTVDORTNVLLVVKDVRNTERARSLVRS LDTQTPQVILIESRIVEANTSFERS 655
Bd0867 429 DELGDRGRVVDVRTNALVVDTEENLERAARL IASLDTQPAQVSIECKIVEAKESFTRN 488

M xan PilQ 656 LGVQWGGQARAGQATGNSTGLIFENMLAVTGGVTGTCAGLPDNPNFVNLPTGTGQGVGG 715
Bd0867 489 LGVNW SATGAPIKLGSTARG---EVMNPSFNVNQSAGSSGALNENLVGQLD----- 539

M xan PilQ 716 AMGFTFGSAGGALQLNRLSAAENEGSVKTI SAKVITLDNNTARINQGVSTPFSQ TSAQ 775
Bd0867 539 ----IFGLSAAALN-----ESEEQVKIISAPRIMT LSNERADINQTEVPVRQVTQN 589

M xan PilQ 776 GVN----TTFVEARLSLEVTPHITODGSVLM S LNASNNQP-DPSSGTGANGQPSTQRKEAN 830
Bd0867 590 GTATQETPFQKPLTLKLEVTPOVADGSVIMKLVN RQFRGADVSSAGQCAFVANSREAN 649

M xan PilQ 831 TVLVKQCDTIVIGGIYVRRGATQVNSVPELSRTEPVLGLL FKNNSSETDTRQELLIFFLTPR 890
Bd0867 650 TRVLVKNGQNAVIGGIYQSDATDGEVGVPEFREL PFVSYLFRFKNISKEKSELLIFFLTPR 709

M xan PilQ 891 TLNRQTIAQTL----- 901
Bd0867 710 IMGQIDNNAGNPTTDF 726

```

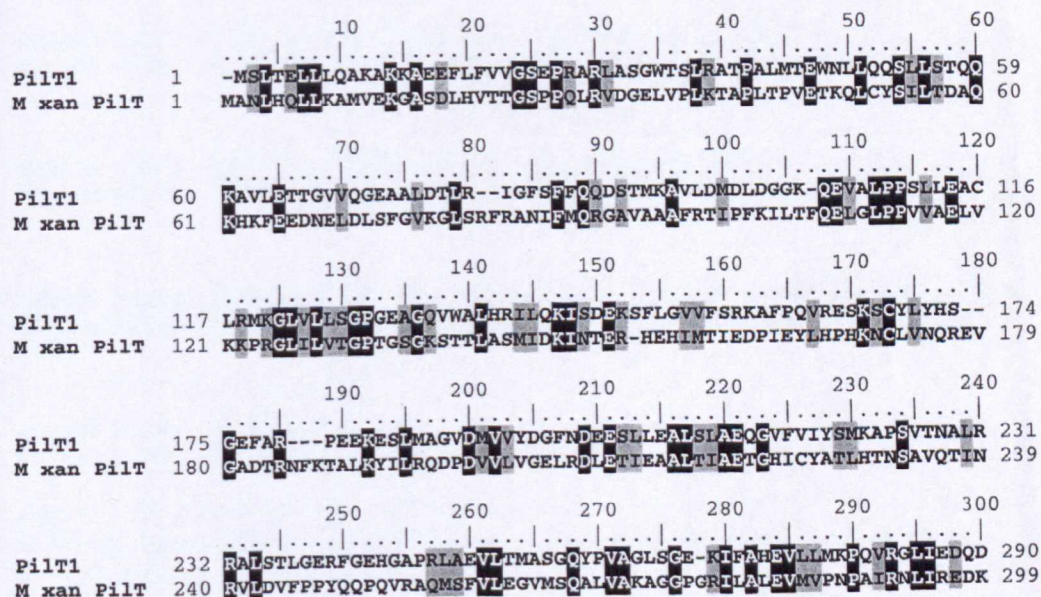
Figure 5.11: Alignment of *B. bacteriovorus* best PilQ homologue with the *Myxococcus xanthus* PilQ. Alignment made using ClustalW in BioEdit (See Methods Section 2.10).

Having identified the most likely candidate *pilQ* gene, incidentally the *pilQ* annotated gene with the highest Frequency of Preferred codons (Henry, Sharp and Sockett, manuscript in preparation), making it more likely to be more highly expressed than the other annotated *pilQs*, all further work on *pilQ* was done on this gene.

5.3.5: Bioinformatic analysis to identify prospective Type IV pilus genes: multiple *pilT* homologues are found in the HD100 genome

pilT also has 2 homologues annotated in the *B. bacteriovorus* HD100 genome. PilT protein functions in pilus fibre retraction through dissociation of the PilA fibre protein polymers: mutants in *pilT* in *M. xanthus* are still piliated but deficient in pilus-mediated S-motility (Wu *et al.*, 1997); *pilT* mutants in *P. aeruginosa* are deficient in pilus-mediated twitching motility and are also hyperpiliated, yet resistant to pilus-specific phage infection (Whitchurch *et al.*, 1991); *pilT* mutants in *N. gonorrhoeae* were unable to pull cells out of an optical trap using Type IV pili whereas the wild-type could (Merz *et al.*, 2000). PilT proteins are members of a diverse group of Type II secretion NTPases (Whitchurch *et al.*, 1991). NCBI BLASTPs with the annotated *B. bacteriovorus* PilT sequences and reciprocal BLASTP against the HD100 genome sequence showed that both *pilT* genes could potentially encode PilT.

Bd1510 sits in an operon with other *pil* genes and the predicted encoded protein has good homology to other known PilTs, with the highest e value being 3e-14 to another δ -proteobacterium, *Geobacter sulferruducens*. Thus, Bd1510 was designated *pilT1*. An alignment with the Myxococcal PilT is shown below in Figure 5.12 below (continued on following page).



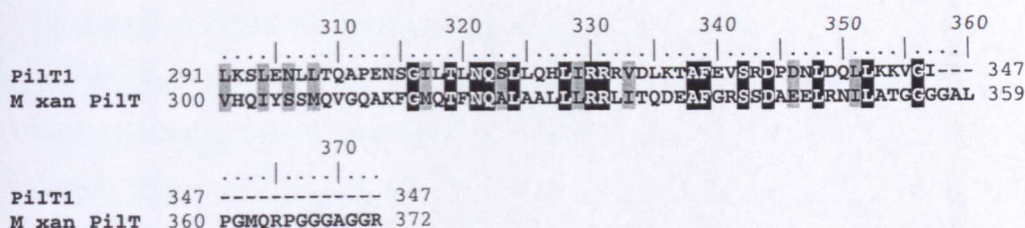


Figure 5.12: Alignment of *M. xanthus* PilT with *B. bacteriovorus* PilT1. Created using ClustalW in Bioedit (see Methods Section 2.10)

Bd3852, an orphan in the genome showed even stronger homologies to other PilTs along the whole length of the protein, with e values of 9e-113 to the δ -Proteobacterium *Pelobacter propionicus* DSM 2379. Bd3582 was designated *pilT2* and seems the more likely candidate for the true PilT homologue in HD100. An e-value of 3e-95 picked out the *M. xanthus* pilT. Alignment with *M. xanthus* PilT (Figure 5.13 below) shows the high degree of sequence conservation between the two proteins.

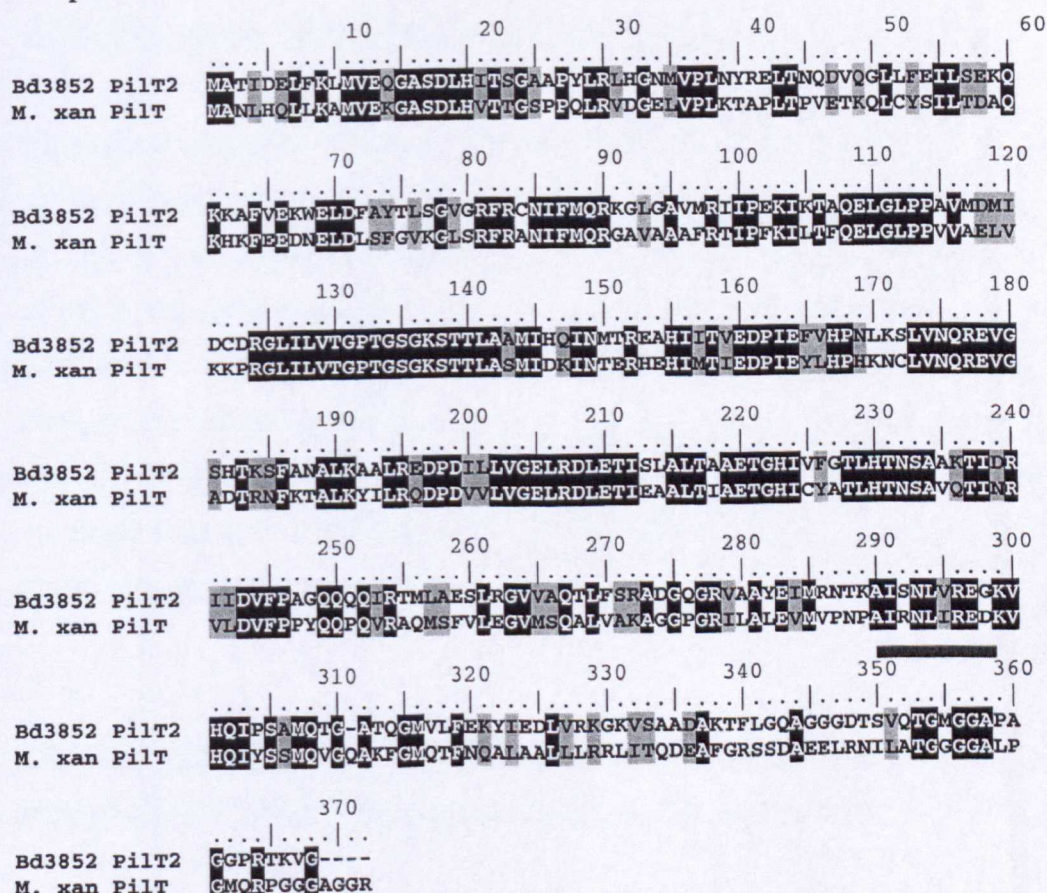


Figure 5.13: Alignment of *M. xanthus* PilT with *B. bacteriovorus* PilT2. Created using ClustalW in BioEdit (see Methods Section 2.10). Underlined is the AIRNLIRE motif shown to be critical for PilT function, discussed below.

As shown in Figure 5.13, both *M. xanthus* and *B. bacteriovorus* PilT2 proteins show a characteristic C-terminal motif, AIRNLIRE (the motif is not found in PilT1 of *B. bacteriovorus*), though in HD100, the arginine residue has been replaced with a serine. This motif (underlined in alignment) has been proposed by Aukema and co-workers (Aukema *et al.*, 2005) to form an amphipathic 2-turn α helix which is not directly involved in the catalytic NTPase activity of PilT, nor oligomerisation to form a ring structure shown to be characteristic of this protein (Forest *et al.*, 2004). Aukema *et al* propose that the AIRNLIRE motif is involved in either protein-protein interactions, possibly with PilA, or a role in maintaining the correct positioning of the protein's C-terminus relative to the catalytic core (Aukema *et al.*, 2005). The fact that this motif has been shown to be functionally important for PilT and is conserved in *B. bacteriovorus* PilT2 adds further confidence to *pilT2* being the true PilT in HD100.

5.3.6: PilA and its biogenesis, structure and function

There are three logical targets for mutagenesis and functional disruption of Type IV pili in *B. bacteriovorus*: interruption of *pilQ*, which would not allow pilus extrusion through the outer membrane; interruption of *pilT*, which would allow the production of pili on the cell surface but not pilus retraction; and interruption of *pilA*. PilA is the protein that makes up the pilus fibre – absence of that protein would automatically abrogate and pilus-mediated function in *B. bacteriovorus*. Due to there being multiple homologues of *pilT* and *pilQ*, the safest mutational option seemed to be *pilA* – a single copy gene. A more detailed analysis of PilA follows and then details of my mutational analysis of the *B. bacteriovorus* HD100 *pilA* gene.

5.3.6.1: PilA from other species – the crystal structures and sequence characteristics of Type IVa pilins shared by *B. bacteriovorus* PilA

PilAs, or pilins, are the fibre forming protein of the Type IV pilus; they can be subdivided into two distinct groups: type IVa and IVb: Type IVb pilins include those found in *Vibrio* species (eg *V. cholerae* TcpA), pathogenic *E. coli* species and

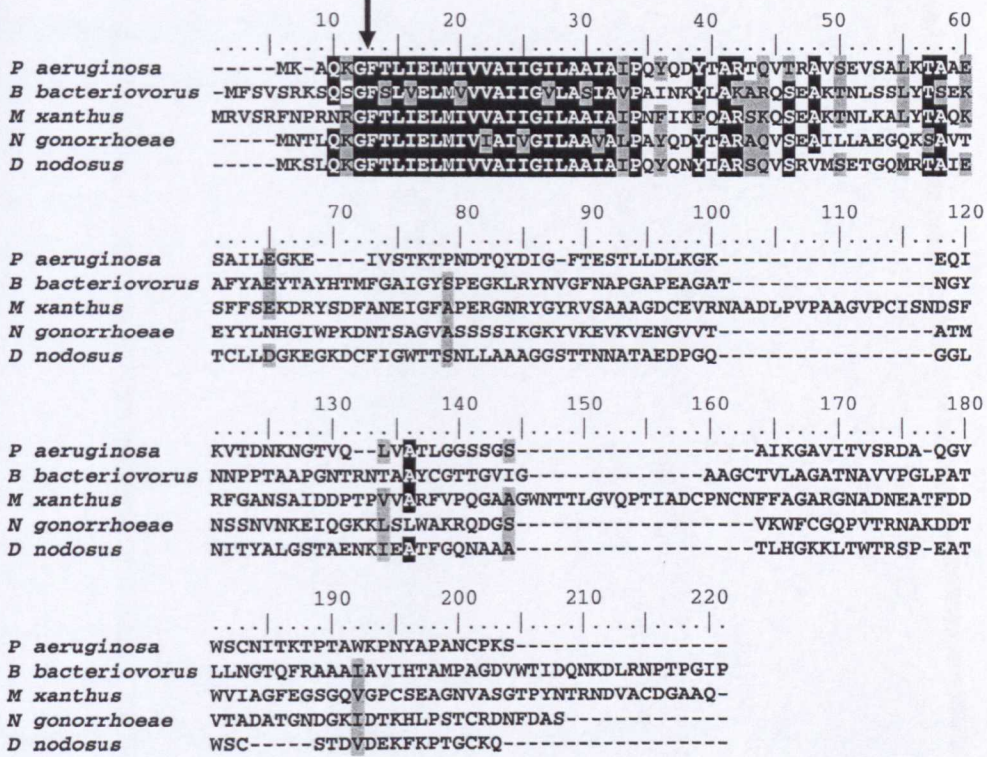
Salmonella species – IVb are found almost exclusively on bacteria that colonise the human intestinal tract; Type IVa pilins include those found in *Neisseria*, *Pseudomonas* and *Myxococcus* species (Craig *et al.*, 2004). Table 12 below summarises the main differences between IVa and IVb types.

Characteristic	Type IVa	Type IVb
Length leader peptide	5-6 amino acids	15-30 amino acids
Average length of mature protein	150 amino acids	190 amino acids
N-methylated N terminal residue	Phenylalanine	Methionine, leucine or valine

Table 5.4: Summary of the characteristics of Type IVa vs IVb pilin proteins. After (Craig *et al.*, 2004).

Examination of the *B. bacteriovorus* HD100 PilA homologue shows it is a Type IVa pilin, which is not entirely unexpected as this is the class into which δ -proteobacterial *M. xanthus* PilA falls. Figure 5.14 below shows ClustalW (through BioEdit) multiple alignments of HD100 PilA with both Type IVa and IVb pilins. Indicated by the arrow is the point of cleavage (see Section 5.3.6.2) of the immature protein to expose the conserved phenylalanine residue, which is then methylated and the pilus fibre subunits polymerised to form pili.

A



B

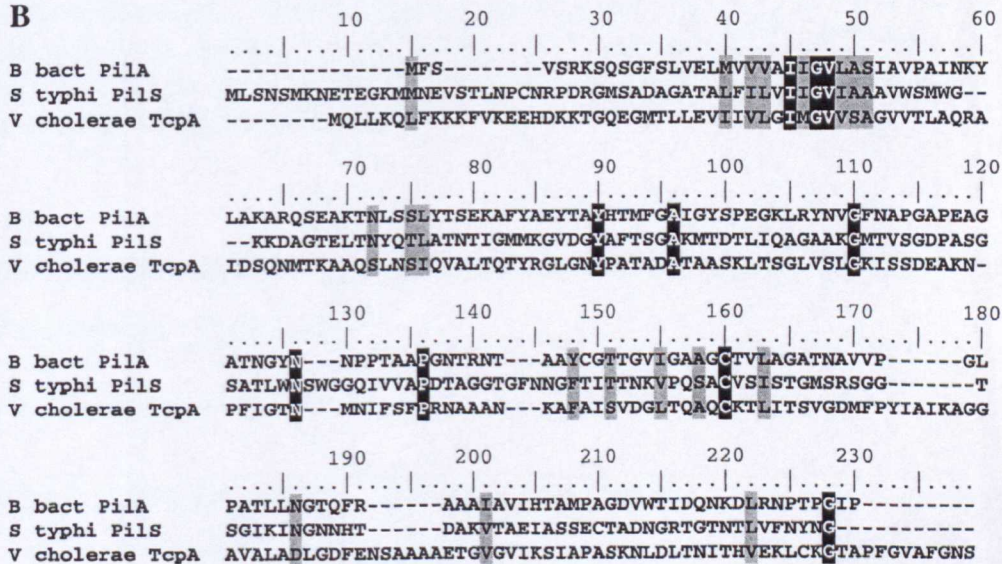


Figure 5.14: Alignment of *B. bacteriovorus* HD100 PilA with **A** other characterised Type IVa pilins and **B** with Type IVb pilins. HD100 PilA shows more extensive homology with IVa, showing the normal highly conserved N-terminus and divergent C-terminus, also the GF cleavage point, indicated by the arrow. Thus, it is designated a Type IVa pilin. See main text for further discussion Section 2.10 Methods for details of alignments.

One of the characteristics of Type IVa pilins is the highly conserved hydrophobic N-terminal region. Crystal structures have been obtained for *P. aeruginosa* (Craig *et al.*, 2003; Hazes *et al.*, 2000) and *N. gonorrhoeae* (Parge *et al.*, 1990) Type IVa pilins and show remarkable structural conservation, as shown in Figure 5.15 below:

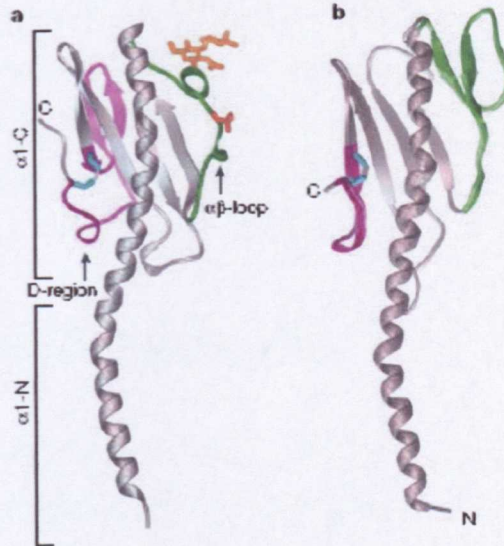


Figure 5.15: The structures of **a:** *N. gonorrhoeae* GC pilin and **b:** *P. aeruginosa* PAK pilin. The conserved hydrophobic N terminal region of IVa pilins forms an alpha-helix which is buried in the core of the pilus fibre. The surface exposed region comprises of beta-sheets; the variation in the C terminal region of pilin proteins is explained by the need for antigenic variation on exposed bacterial extracellular structures. Taken from (Craig *et al.*, 2004).

Sequence analysis and homology alignments therefore show that the HD100 PilA homologue is a Type IVa pilin.

5.3.6.1.1: How do Type IV pili bind to their target?

Type IV pili can bind to a wide range of surfaces from metals and plastics to tissue and other bacteria. In some pathogenic species, eg *Neisseriaceae*, there are specific proteins, PilC1 and PilC2 that mediate adhesion of Type IVa pili to epithelial cells in pathogenic species (Rudel *et al.*, 1995). There are no homologues of genes encoding these proteins that can be found in the HD100 genome. However, the C-terminal region of PilA in *Pseudomonas aeruginosa*, specifically exposed disulphide bonds formed by C-terminally located cysteine residues, have been implicated in the

binding of *P. aeruginosa* to glycosphingolipids (Hazes *et al.*, 2000; Lee *et al.*, 1994). Site directed mutation of these Cys residues in *P. aeruginosa* PilA resulted in a huge reduction in cellular pilin levels and resultant loss in the formation of pili (Burrows, 2005). *B. bacteriovorus* HD100 also has C-terminally located cysteine residues, Cys 121 and Cys 132, which, in the absence of adhesin/invasin homologues in the genome, could potentially be used for pilus adhesion. However, the limitations of *B. bacteriovorus* practical genetics preclude the possibility of site directed mutagenesis of these cysteine residues in the time-course of my project.

5.3.6.2: The role of PilD in PilA maturation

For assembly into mature Type IVa pili in other bacteria, the immature pre-pilin protein is cleaved at the conserved N-terminal glycine-phenylalanine motif by the pre-pilin peptidase/ N-methylase, PilD. PilD has a cytoplasmic membrane location (Nunn and Lory, 1991); immature PilA is also likely held under the cytoplasmic membrane to be available for processing. Mature PilA cleaved by PilD lacks the immature N terminal signal sequence and is N-methylated on the new N-terminal residue, phenylalanine (Strom and Lory, 1992).

5.3.6.3: PilA in 109J – pilus-like fibres are seen on the pole of the *B. bacteriovorus* cell

As demonstrated in Figure 5.9 (see section 5.3), *B. bacteriovorus* strain 109J also has polar, pilus-like fibres, but, as yet, has no available genome sequence. In the HD100 sequence, there are C-terminal cysteine residues that have implications for pilus attachment (see section 5.3.6.1.1). For comparison to HD100 PilA, I decided to try and isolate the *pilA* gene in the non-sequenced 109J strain in an attempt to see if the cysteine residues were also present in the 109J PilA, lending credence to the hypothesis that these amino acids may be involved in pilus attachment.

5.3.6.3.1: Attempts using PCR to clone 109J *pilA*

The most logical step to isolating *pilA* in 109J was to use the original HD100 *pilA* cloning primers; *pilAF* and *pilAR* (see section 5.4.1 for more detail) which produce a 2.37kb band in HD100 (see figure 5.16 below) with *pilA* in the middle of the product.

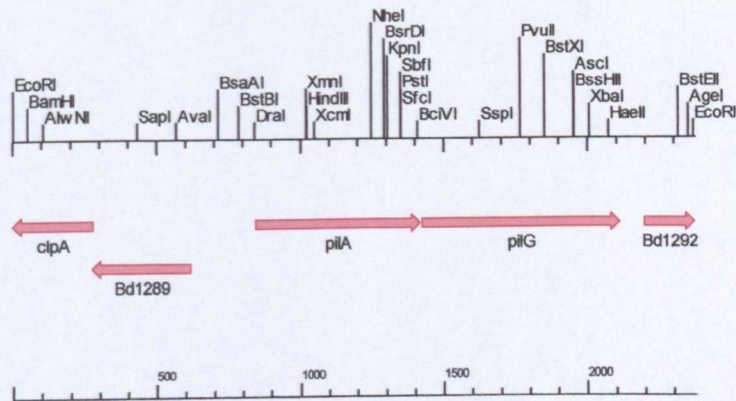


Figure 5.16: PCR fragment produced in HD100 using *pilAF* and *pilAR* cloning primers, 2.37kb. Produced using Clone Manager Basic V. 8 (see methods section 2.10)

A gradient PCR using cycles of: 95°C for 1 minute x 1, 30 cycles of 95°C 1 minute, 50-65°C 1 minute, 72°C for 2 minutes, 1 cycle of 72°C for 10 minutes and a 4°C hold was carried out on 109J genomic DNA using Kod HiFi polymerase (Novagen) with controls of HD100 genomic DNA and no template. Reactions were the standard 50ml as stated in section 2.5.1. The 2.37kb product is observed in HD100 PCRs at an annealing temperature of 65°C.

Figure 5.17 below shows that this primer pair did not amplify the same region of 109J DNA as it does in HD100, demonstrated by the lack of a 2.3kb band in the 109J PCRs, despite a low stringency annealing temperatures. Therefore, new primers had to be designed to be more specific to the *pilA* region.

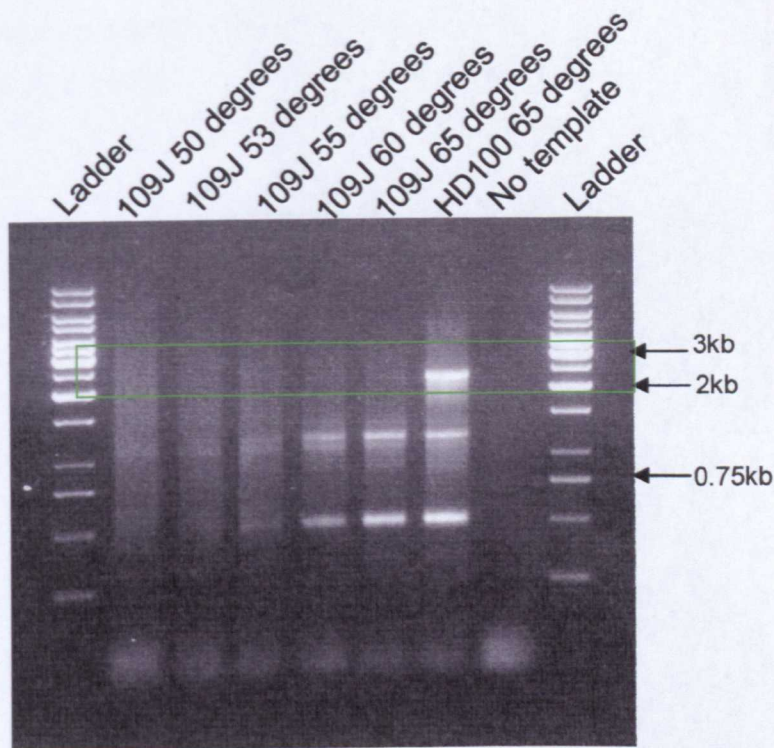


Figure 5.17: 0.7% TBE agarose gel showing attempts to PCR the 2.37kb fragment obtained in HD100 (highlighted in green box) from 109J using pilAF and pilAR (see primer table 2.3 in methods). Low to high stringency Kod polymerase gradient PCR on 109J genomic DNA failed to amplify the corresponding fragment. Ladder is 1kb Generuler (MBI Fermentas).

5.3.6.3.1.1: Attempts using PCR to clone 109J *pilA* – primers designed to conserved regions of *pilA* and *pilG*

As the HD100 cloning primers did not pick up a corresponding band in 109J genomic DNA, primers were designed specifically within *pilA* and gene *pilG*, which lies directly downstream of *pilA* in the HD100 genome. The reasoning behind this was that although *pilAG* are removed in the genome from the rest of the *pil* operon (see section 5.1.2.2), *pil* genes seem to show association and conservation in gene order; therefore in 109J, *pilG* should be likely downstream of *pilA* in the genome sequence. With this in mind, regions of the PilA and PilG proteins in HD100 that showed good conservation with the same proteins found in other species were

identified. The cognate stretches of DNA from HD100 were then used to design primers with either *Bam*HI or *Eco*RI ends to facilitate cloning of any amplified product from 109J DNA.

PilA

	10	20	30	40	50	60
<i>P aeruginosa</i>	-----MK-AQNGFTLIELMIVVAITGILAAIAIPEQYQDYTARTQVTRAVSEVSALKTAAE					
<i>B bacteriovorus</i>	-----MFSVSRKSSGFSIWEELMIVVAIIIGVLAATAVPAINKYLAKARQSEAKTNLSSLYTSEK					
<i>M xanthus</i>	-----MRVSRFNPRNGFTLIELMIVVAITGILAAIAIPEQYQDYTARAQVSEAILLAEGQKSAVT					
<i>N gonorrhoeae</i>	-----MNTLQKNGFTLIELMIVVAITGILAAIAIPEQYQDYTARAQVSEAILLAEGQKSAVT					
<i>D nodosus</i>	-----MKSLQKNGFTLIELMIVVAITGILAAIAIPEQYQDYTARAQVSEAILLAEGQKSAVT					

PilG

	10	20	30	40	50	60
Bd1291 PilG	MDSVLTN-----LTHLQTKIPSVLLGIFALLMVCSTVNYNFSSTPAHQRLI					48
<i>M xanthus</i> PilG	MSSGGSTVLRAALPQEGGLSQFYNPRLMRSVVLCLAVCAIAVMAEKPAKPLRTKDGPII					60
<i>A dehalogens</i> PilG	MSLGR-----OKVGLAALLAAGACALAAARLPVAAQRAYDLGPV					40

	70	80	90	100	110	120
Bd1291 PilG	49 APPFMVEHLSFGYQEATANILWIRAVQDFDYCDREIADRVCINNNSWLYKMLDAITNLSEH					
<i>M xanthus</i> PilG	61 PRREFLEIVGAAQKPLLAIFYWLSIQQVGRANTDT-----EYRDVFFYADLAADLDPK					
<i>A dehalogens</i> PilG	41 PTSAALRWASFGHPTLANLWLRVQYMGDPRADQR-----GWEKLFPPALDLVTDLDEA					

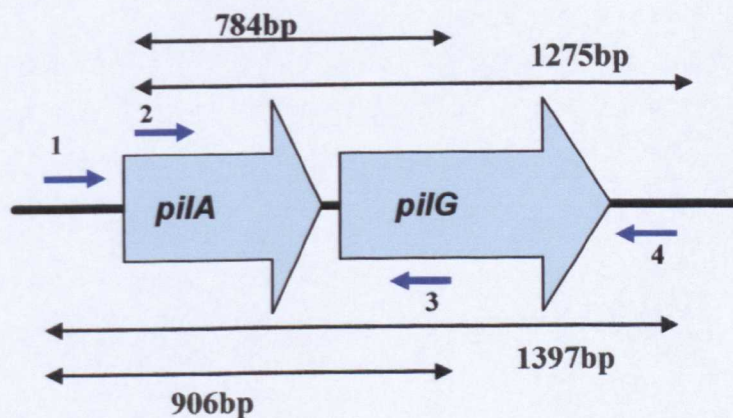


Figure 5.18: underlined are the regions most conserved at the protein level between PilAs and PilGs from different species. *A. dehalogens* = *Anaeromyxobacter dehalogens*. These were then correlated with the coding DNA of HD100 and primers designed to the most conserved regions. Primers and their positions are indicated by the dark blue arrows. Primer 1 = pilAup1_4, primer 2 = pilAcon1_1, primer 3 = pilGcon1_2, primer 4 = pil11. Expected product sizes from different primer combinations are as indicated.

Standard Kod HiFi DNA polymerase reactions (Section 2.5.1) were set up using both HD100 and 109J genomic DNA as templates and a no template negative control for each primer combination. The following gradient PCR conditions were used for all reactions: 1 cycle of 95°C for 5 minutes, 30 cycles of 95°C for 30seconds, 50-65°C

for 30sec, 72°C for 1 minute, 1 cycle of 72°C for 10 minutes and a 4°C hold. Primer combinations and expected product sizes are shown in the table below.

Reaction #	Primer combination	Expected product size (bp)	Restriction site ends
1	pilAup1_4 (1) pilGcon1_2 (3)	906	<i>Bam</i> HI
2	pilAup1_4 (1) pil11 (4)	1397	<i>Bam</i> HI/ <i>Eco</i> RI
3	pilAcon1_1 (2) pilGcon1_2 (3)	784	<i>Bam</i> HI
4	pilAcon1_1 (2) pil11 (4)	1275	<i>Bam</i> HI/ <i>Eco</i> RI

Table 5.5: Primer combinations used in both HD100 and 109J to try and amplify the *pilAG* genes. Numbers in brackets correlate with the primers indicated on the diagram in Fig 5.18 (previous page). Expected product sizes in bp and cloning ends on the primers are shown.

0.8% TBE agarose gels run with 10µl of the completed PCR reactions were run. The HD100 template PCRs gave the correct size bands for each primer combination; the 109J PCRs were less successful. Only primer combinations 2, 3 and 4 at varying stringency temperatures gave any possible correct products. The gels were re-run to eliminate unsuccessful PCRs with HD100 correct sizes next to the cognate 109J PCRs to show better any useful products, shown in Figure 5.19..

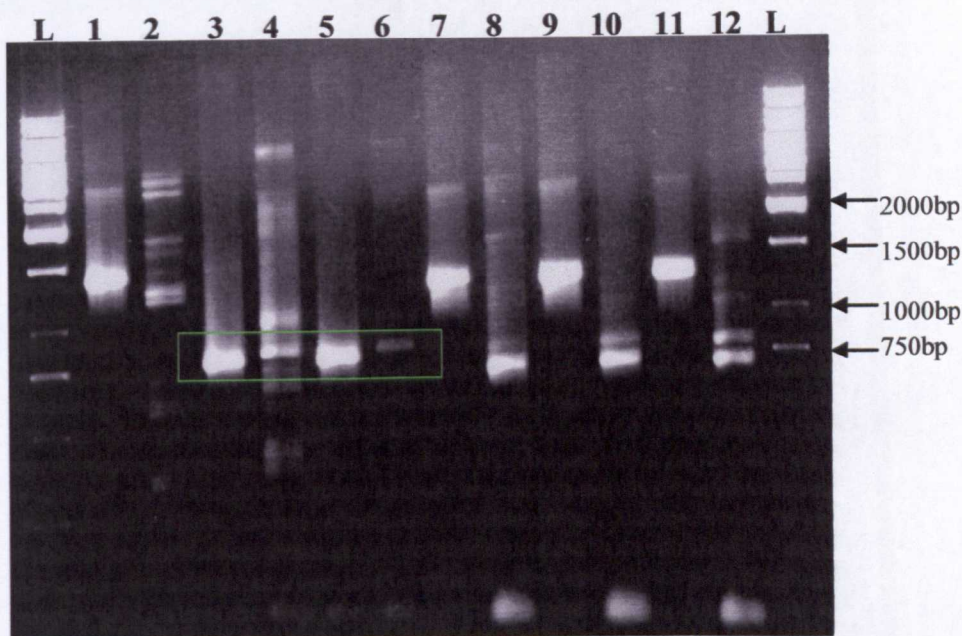


Figure 5.19: Agarose gel of promising PCRs to amplify 109J *pilA* using potential conserved primers from HD100 sequences. L = 1kb Generuler (Fermentas), sizes as indicated. 1=HD100 rxn2 65°C, 2=109J rxn2 65°C, 3=HD100 rxn3 60°C, 4=109J rxn3 60°C, 5=HD100 rxn3 65°C, 6=109J rxn3 65°C, 7=HD100 rxn4 55°C, 8=109J rxn4 55°C, 9=HD100 rxn4 60°C, 10=109J rxn4 60°C, 11=HD100 rxn4 65°C, 12=109J rxn4 65°C. The only 109J PCR that correlates with the expected band size in HD100 (lanes 3 and 5) was given by PCR using primer pair 3, *pilAcon1_1* and *pilGcon1_2*, giving bands of 784bp (indicated on gel by green box, lanes 4 and 6 are the 109J products). This was chosen for further study.

As the only primer combination to give the same size product in HD100 and 109J, *pilAcon1_1* and *pilGcon1_2* (reaction 3, lanes 4 and 6 on gel), the remainder of both the HD100 and 109J PCRs were run out and the 784bp fragments gels purified. As this particular primer combination both had engineered *Bam*HI ends, which do not cut in the native HD100 genomic sequences of *pilAG*, the purified fragments were cut with *Bam*HI and ligated into pUC19 cut with the same enzyme and dephosphorylated. The ligations were transformed into DH5α *E. coli* for blue white screening to check for the presence of insert and quick plasmid minipreps were made (see Section 2.3.1). Promising plasmid clones of both HD100 (as a control) and 109J were then purified using the Qiagen™ plasmid Mini-prep kit according to manufacturer's instructions.

5.3.6.3.1.2: Sequencing of putative HD100 and 109J *pilAG* sequences

The HD100 clone of *pilAG* using primer pair 3 in pUC19 gave the construct shown below, which was sent for DNA sequencing using M13 universal primers. The sequence showed that the construct did actually contain the HD100 *pilAG* sequences (See Appendix 2 for sequencing alignments and chromatograms), validating the method used for its isolation.

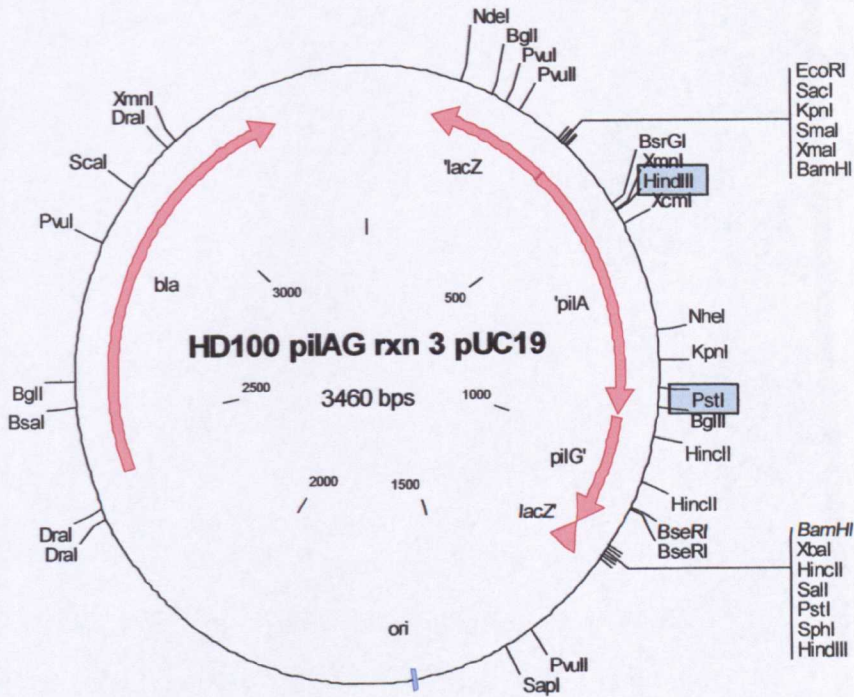


Figure 5.20: Plasmid map of the HD100 *pilAG* fragment cloned into pUC19. Highlighted are the unique *HindIII* and *PstI* sites used in Section 5.3.6.3.2. Created using Clone Manager Basic V. 8 (see section 2.10 for details).

The most promising clone obtained from the 109J PCR reaction using primer pair 3 was digested with *HindIII* and *BamHI*. With the latter, the 2.6kb pUC19 fragment and the 0.78kb *pilAG* fragment was released, the correct sizes for this analysis. In the HD100 *pilAG* DNA sequence, a *HindIII* site near the 5' end of *pilA* gave the orientation relative to the pUC19 multiple cloning site; in the 109J construct, only a linear product of approximately 3.4kb was obtained, indicating that the *HindIII* site was not conserved in the 109J sequence, as shown in Figure 5.21 below.

Figure 5.21: 0.8% TBE agarose gel showing the results of digestion of the putative 109J *pilAG* clone with *Hind*III and *Bam*HI. Size marker = 1kb Generuler (Fermentas), sizes and lanes as indicated.



This construct was sent for sequencing, which showed that it was not the 109J *pilAG* genes, but BLASTN searches against the *B. bacteriovorus* HD100 genome indicated that it was homologous to *drrB*, which encodes a permease component of an ABC transporter (see Appendix 2).

Obviously, even though the primer pairs used were carefully designed to anneal to only the most conserved regions of *pilA* and *pilG*, this approach was unsuccessful in 109J, perhaps due to some genomic rearrangement or divergent DNA sequence to that of HD100. Therefore, shotgun cloning was attempted to try and isolate the 109J *pilA* sequence.

5.3.6.3.2: Southern blots of 109J genomic DNA using the HD100 *pilA* sequence as a probe

In another attempt to isolate the 109J *pilA* homologue, Southern blots of whole 109J chromosomal DNA digested with a variety of standard cloning restriction enzymes (see Figure 5.22 below for details) were run, with a control of HD100 genomic DNA cut with the *Hind*III and *Pst*I (this will liberate a 340bp fragment, the sites are

positioned within *pilA* as indicated in Figure 5.16, Section 5.3.6.3.1.2). The blots were probed with the HD100 *pilA* fragment cut from the pUC19 construct containing the HD100 *pilAG* sequences, using *KpnI* which contained 438bp of the verified HD100 *pilA* sequence (see Section 5.3.6.3.1.2, this probe was used for inclusion of the coding DNA for the conserved N terminus of PilA). Figure 5.22 below shows the resulting blot, with the 109J cross-hybridising bands. As the *BamHI* fragment was approximately 3.2kb, it was used as the basis for shotgun cloning to obtain the 109J *pilA* sequence.

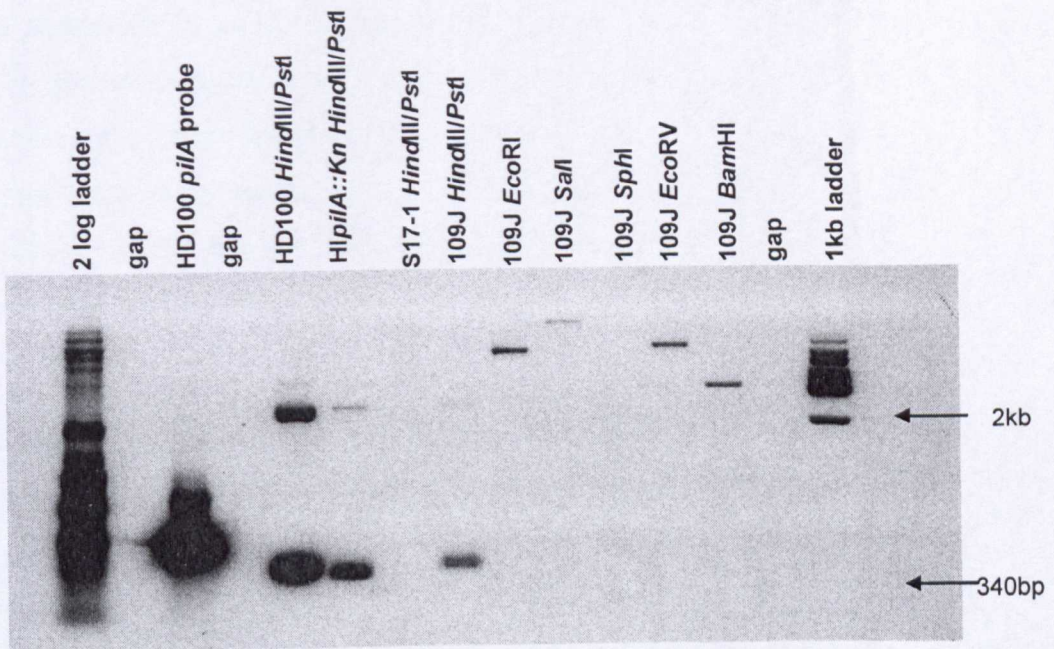


Figure 5.22: Southern blot to find bands in 109J genomic DNA cut with different restriction enzymes that cross-hybridised to the HD100 *pilA* probe. *KpnI*-cut *pilA* probe was run as a positive control (438bp); HD100 and HIpilA knockout strain (see subsequent sections) genomic DNA was cut with *HindIII* and *PstI*, the 340bp band corresponds to the size of fragment liberated from within the native *pilA* sequence (the presence of a larger band may indicate an incomplete double digest of the genomic DNA). *E. coli* S17-1 DNA cut with the same enzymes was included as a negative control. Restriction enzymes used are as indicate in the lane labels; 2 log ladder = NEB Biotinylated 2-log DNA ladder; 1kb ladder = Fermentas 1kb Generuler. At approximately 3.2kb, the *BamHI* hybridising fragment was chosen to work with.

5.3.6.3.3: Shotgun cloning of the 109J to find *pilA* and the resulting sequences

Having identified the band in 109J genomic DNA that hybridised to the HD100 *pilA* sequence probe, the remaining 109J *Bam*HI genomic digest was run out on a 0.8% agarose gel and the fragment sizes corresponding to 3kb +/- 1kb were excised and purified. The resulting mix of fragments was ligated to de-phosphorylated pUC19 vector, also cut with *Bam*HI, the mix transformed into *E. coli* DH5 α and subject to blue/white screening for vector inserts. 30 clones were obtained and the plasmid DNA was prepared using the Qiagen™ plasmid DNA mini-prep kit. 3 μ l of each purified plasmid DNA were then spotted directly onto Hybond -N membranes and subject to Southern hybridisation, probed with the same HD100 *Kpn*I *pilA* fragment used in the original blots. Controls of 0.5 μ l of HD100, 109J and S17-1 genomic DNA were included, as were the *pilA* probe, NEB 2-log Biotinylated DNA ladder (to check efficiency of the chemi-luminescent detection) and pUC19 as a negative control for probe hybridisation were also included. Figure 5.23 below shows a “dot-blot” of 30 potential clones.

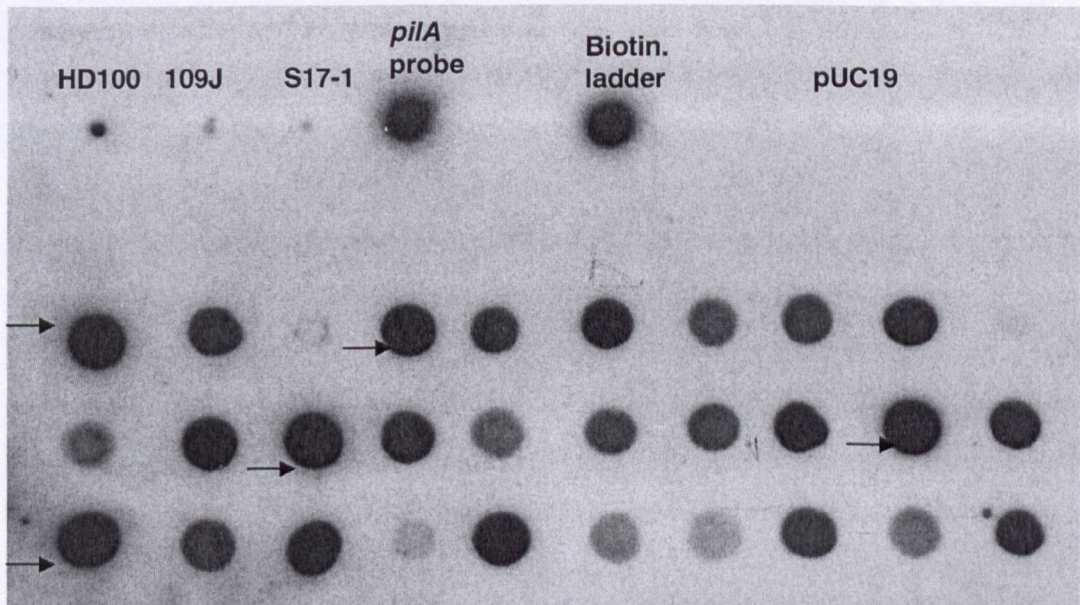


Figure 5.23: “Dot-blot” of potential 109J *pilA* – containing clones, probed with the HD100 *pilA* gene. Controls are as labelled, potential clone were numbered 1-30 top left to bottom right. Curiously, even though the background hybridisation of the probe to pUC19 was very low, almost all the plasmid DNA preps hybridised. Clones 1, 4, 13, 19 and 21 were chosen for further analysis (indicated by arrows).

As indicated by the dot blot, even under stringent Southern conditions, there was a high level of hybridisation to most of the plasmid clones tested; as such a true Southern blot of plasmid DNA cut with *Bam*HI (to liberate the insert of 109J DNA) were performed and probed in the same way. Again, virtually every clone hybridised (data not shown). As such, clones 1, 4, 13, 19 and 21 were chosen for further analysis. Restriction digestion using *Bam*HI showed that clones 13 and 21 had an insert size closest to the 3.2kb shown on the original Southern (see Figure 5.22 previously) and were sent for DNA sequencing using pUC19 universal primers.

Clone 13 was again, not the 109J *pilA*; sequence alignment with the HD100 genome showed it was homologous to Bd1444 in HD100, a serine protease. Clone 19 also disappointed, with sequencing showing it was homologous to Bd2872, which has no known function, but is predicted to have weak homologies to cell wall surface anchor family proteins. See Appendix 2 for sequencing data.

I then decided to abandon this strategy and concentrate on the HD100 *pilA*.

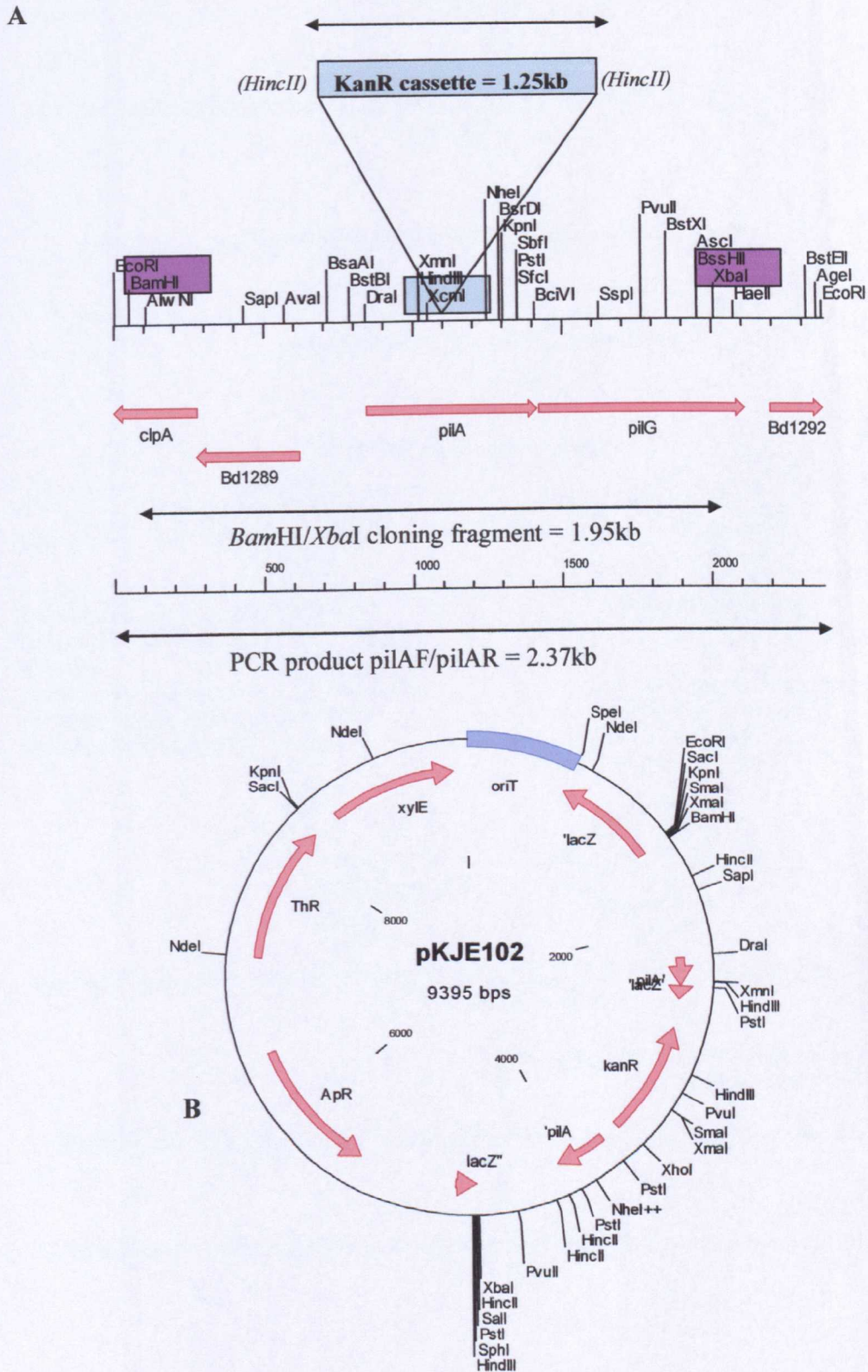
5.4: HD100 *pilA* inactivation – the rationale

In *B. bacteriovorus* HD100, to make a non functional Type IV pilus system to test any involvement in the predatory life cycle, *pilA* was targeted for gene interruption with a kanamycin resistance cassette. *pilQ* or *pilT* interruption would have given non-functional pili also from work done in other species, see (Mattick, 2002) for an overview. However, due to the fact of there being multiple homologues of these genes in HD100, *pilA*, the single copy gene encoding the pilus fibre protein was chosen. If PilA was non-functional, then there could be no pili produced. Therefore, *pilA* was inactivated and the resulting mutant strains phenotyped for predatory behaviour.

5.4.1: The strategy for *pilA* inactivation

The wild-type *pilA* gene (CAE79186, Bd1290) was amplified from HD100 genomic DNA by PCR, using KOD Hi-Fi DNA polymerase (Novagen) in buffer 2 for genomic DNA, in a standard reaction (see Section 2.5.1) using the following conditions: 1 cycle of 95°C for 5 minutes, 30 cycles of 95°C for 1 minute, 65 °C for 1 minute, 72 °C for 2 minutes, 1 cycle of 72 °C for 10 minutes and a 4 °C hold. The full length gene was cloned with 1kb flanking DNA either side using *pilAF* and *pilAR* cloning primers (see Table 3, Chapter 2). The resulting 2.3Kb fragment was gel purified and digested with *Bam*HI and *Xba*I using unique sites within the genomic sequence then ligated into pUC19 digested with the same enzymes to produce pKJE100. A 1.25kb kanamycin resistance cassette, released from pUC4K (Vieira and Messing, 1982) by digestion with *Hinc*II, was gel purified and blunt-ligated into a blunted *Xcm*I unique site 204bp into the coding sequence of *pilA* and flanking regions in pUC19 (pKJE100) to create pKJE101. *Bam*HI and *Xba*I digestion of pKJE101 liberated the interrupted *pilA* and flanking regions, which was then sub-cloned into conjugative plasmid pSET151 (Bierman *et al.*, 1992) digested with the same enzymes to produce pKJE102 and used to insertionally inactivate the cognate *pilA* gene in the HD100 genome through conjugation from an S17-1 donor strain containing pKJE102 into HD100 ((Lambert *et al.*, 2003), summarised in Fig 5.24).

Figure 5.24: Summary of the cloning strategy used to inserttionally inactivate *pilA* in the Hd100 genome. **A**, PCR fragment obtained and sites used for DNA manipulation. Sizes in kb are as indicated. The *HincII*-cut *KnR* cassette from pUC4K was ligated into the blunted unique *XcmI* site (Blue) 204bp into the coding sequence of *PilA* contained in the 1.95kb *BamHI/XbaI* (purple) cloning fragment. **B** plasmid map of the final construct, pKJE102: pSET151 suicide vector containing the *KnR* interrupted version of *pilA* used for conjugation into *Bdellovibrio*. Both produced using Clone Manager Basic Version 8 and Microsoft PowerPoint (see Methods section 2.10).



5.4.1.1: Scheme showing the screening protocol for *B. bacteriovorus* mutant strains.

Transformation of interrupted *pilA* construct in plasmid pSET151 (pKJE102) into *E. coli* S17-1



Conjugation of plasmid construct from early log phase *E. coli* S17-1 into fresh, wild-type HD100 attack phase cells



Growth of exconjugant plaques, selecting for Kanamycin resistance on *E. coli* S17-1 pZMR100 soft agar overlays at 29°C



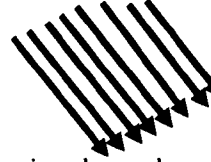
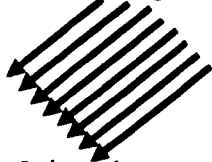
4 individual plaques picked into 2ml predatory cultures on *E. coli* S17-1 pZMR100 prey



Sub-cultured for 7 days, 29°C, 200rpm shaking

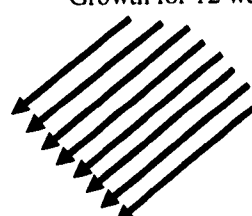


Each of the 4 original predatory cultures split into 2 to give 8 strains



8 strains turned Host-Independent (HI) on PY KnR selection (12). Continued plaquing and picking of 3 individual colonies per strain, giving rise to 24 strains, 1.1 through 8.3. Growth for 12 weeks.

Continued prey dependent growth on S17-1 pZMR100. Continual and picking of 3 individual plaques followed by predatory growth, giving Rise to 24 strains, 1.1 through 8.3. Growth for 12 weeks.



Taq PCR screen of 24 HI and 24 HD strains using original *pilA* cloning primers to detect size change caused by *KnR* interruption



Merodiploid strains were cultured for a further 6 weeks and then re-screened

Southern blot of genomic DNA of putative mutant strains using pSET151, *pilA* and *KnR* probes



Confirmation of correct mutation by amplification and sequencing of the interrupted *pilA* gene from *pilA* mutants

5.4.2: Characterisation of the resulting mutant strains

Screening for double recombinant strains, ie where the wild type copy of *pilA* had been replaced by the *KnR* interrupted copy, was carried out initially by Taq PCR . Shown in Figure 5.25 below are screening PCRs of all HI and HD lines of transconjugants after 12 weeks of appropriate sub-culturing under appropriate conditions and kanamycin selection. Controls of genomic DNA isolated from HD100 and one of no DNA were included. A standard reaction mix for Taq PCR (Abgene) (see Section 2.5.1 methods) was used with 1ul of culture from each strain as a template; the primers were the original cloning primers (*pilAF* and *pilAR*) which amplify a 2.36kb region of the HD100 genome, including the *pilA* gene. PCR cycles were as follows: 95°C for 5 min once, 30 cycles of 95°C for 30sec, 70°C for 30sec and 72°C for 4 min, one cycle of 72°C for 10 min and a 4 °C hold. Merodiploid strains were expected to show 2 bands, one of 2.36kb, indicating the presence of the wild type copy of *pilA*, and one of 3.8kb generated by the *pilA::KnR* interrupted gene. The gels showed that there were 9 likely mutant strains, all from HI derivatives, with the other 14 HI and all 24 HD strains still being merodiploid. 6 prospective *pilA*- strains were taken forward for Southern blotting.

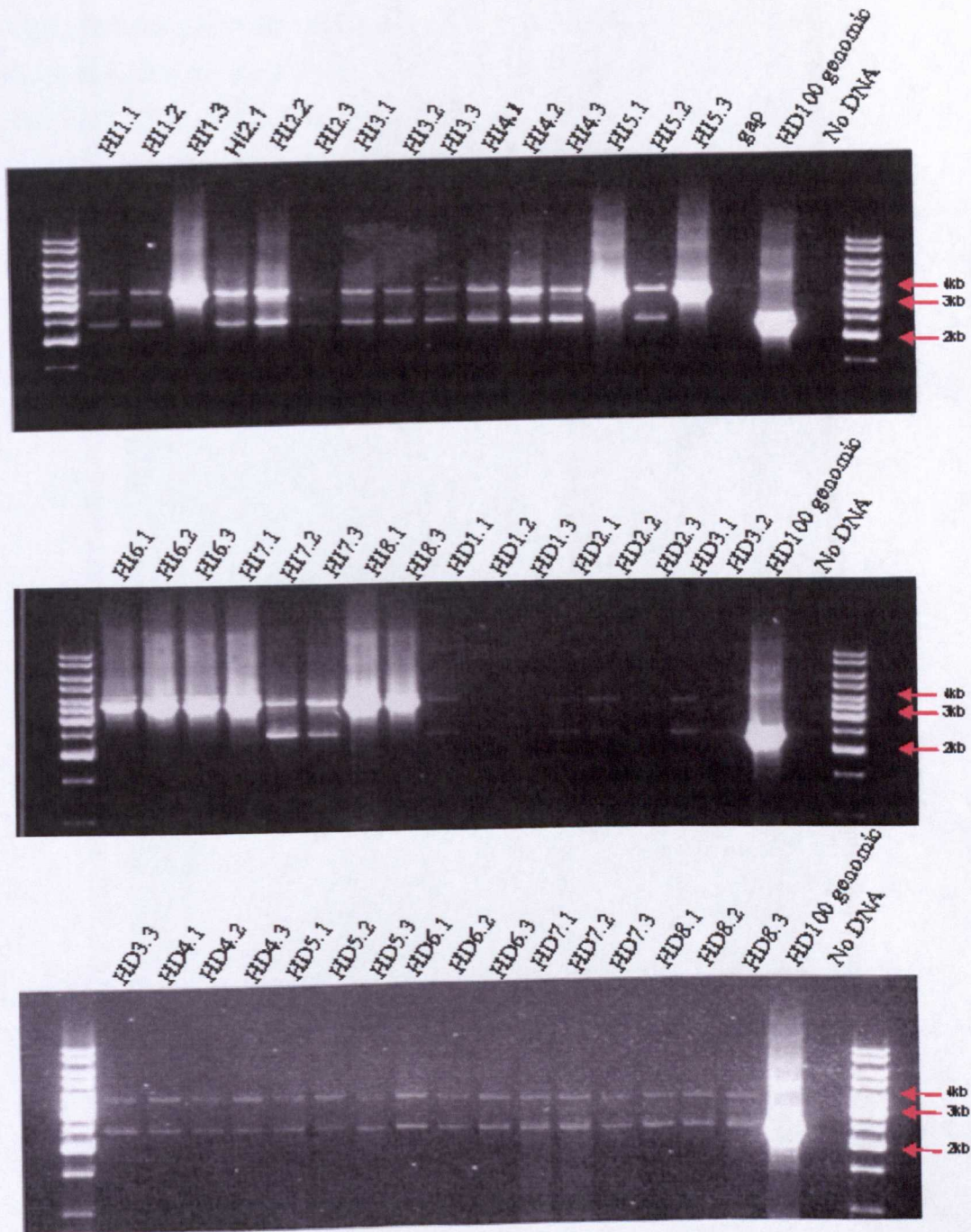


Figure 5.25: PCR screens of HI and HD lines of *pil::KnR* exconjugants to find double recombinants. Strains are as indicated (HD = prey dependent, HI = host-Independent), Taq PCR carried out using *pilAF* and *pilAR* original cloning primers. Merodiploid strains (eg lane HI1.1) show 2 bands, one of 2.36kb, indicating the presence of the wild type copy of *pilA*, and one of 3.8kb generated by the *pilA::KnR* interrupted gene (KnR cassette = 1.25kb). Double recombinants show only the 3.8kb mutant band indicating loss of the wild type gene. Ladders are Generuler™ 1kb DNA ladder (Fermentas).

Genomic DNA preparations (Sigma mini genomic DNA kit, see section 2.3.3) were made from 6 of the likely mutant strains. These were digested with *HincII*, as were pKJE102 (*pilA::KnR* in pSET151) and pUC4K (to liberate the 1.25kb *KnR* cassette). pSET151 was digested with *EcoRI* to give a 6.28kb linear fragment. The blots were probed with linear pSET151 and the *KnR* cassette; the *KnR* blot was then stripped and re-probed with HD100 *pilA* 1.98kb *EcoRI/XbaI* fragment from pKJE100 to confirm that the *KnR* hybridising bands corresponded with the *pilA* hybridising bands.

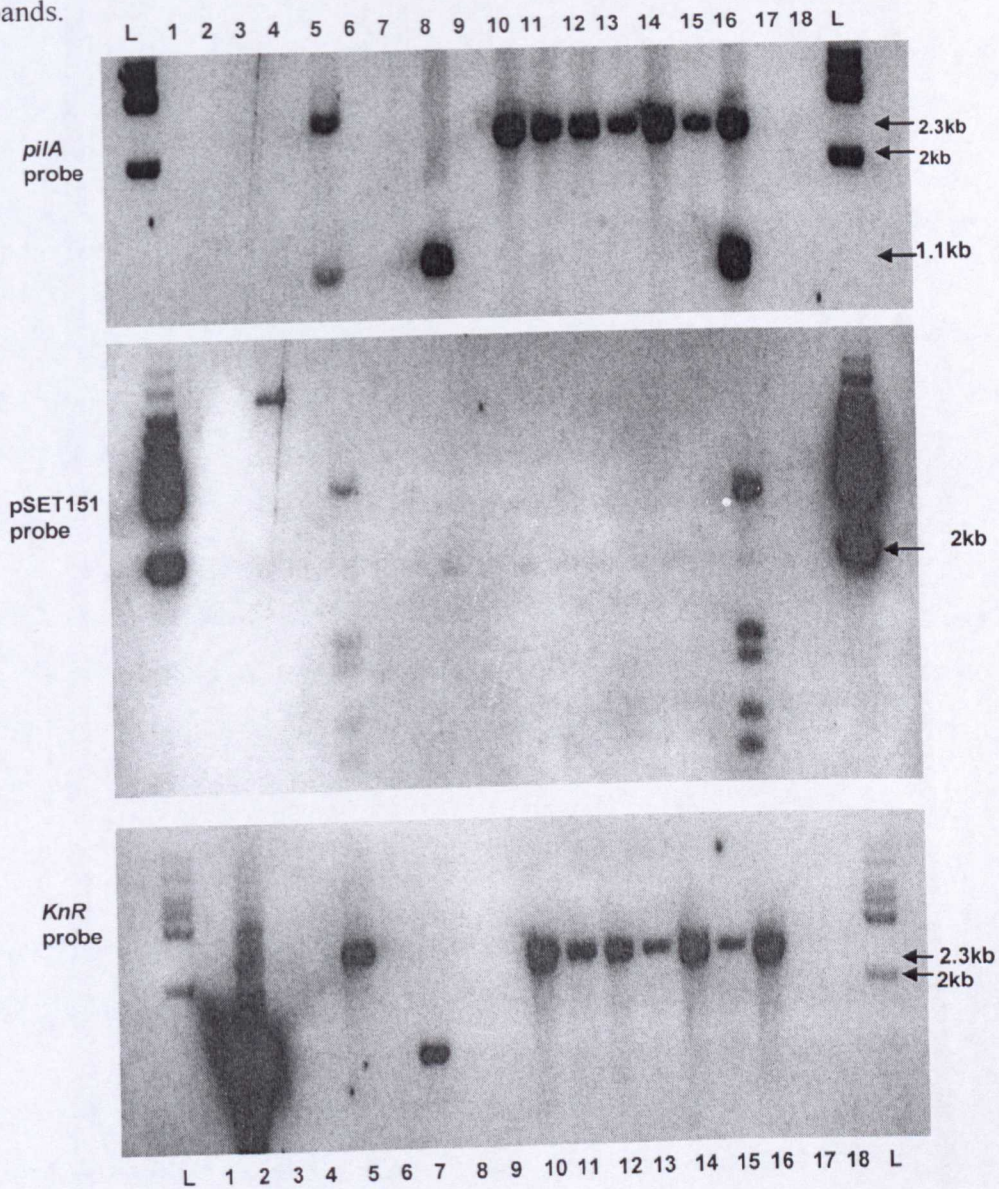


Figure 5.26: Southern Blots confirming the HI*pilA::KnR* mutants. Lane order is as follows on all blots: L = Generuler™ 1kb DNA ladder [Fermentas], 1 = gap, 2 = *KnR* 1.25kb cassette, 3 = linear 6.28kb pSET151, 4 = gap, 5 = pKJE102, 6 = gap, 7 = *B. bacteriovorus* 109J *mcp2::KnR* (16), 8 = wt HD100, 9 = gap, 10 = HI*pilA*1.3, 11 =

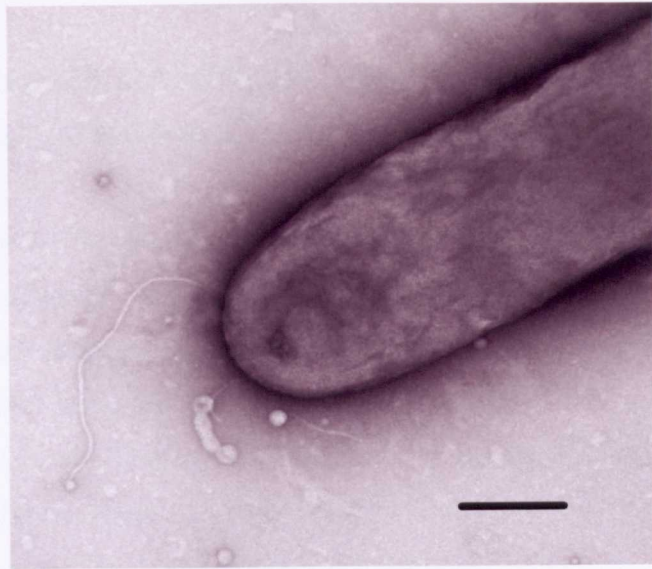
HI*pilA*5.3, 12 = HI*pilA*6.1, 13 = HI*pilA*6.2, 14 = HI*pilA*6.3, 15 = HI*pilA*8.1, 16 = HI*pilA* merodiploid 7.1, 17 = gap, 18 = gap, 19 = Generuler™ 1kb DNA ladder. All genomic DNA preparations were digested with *HincII*, were pKJE102 and pUC4K (to liberate the *KnR* cassette). pSET151 alone was digested with *EcoRI* to give a 6.28kb linear fragment.

The prey-dependent merodiploid strains were subject to further sub-culturing and screening (see flow chart, section 5.4.1.1), but the mutant *pilA* interruption could not be obtained under prey-dependent growth conditions. The HI state is a useful tool for culturing and subsequent analysis of mutations that have adverse effects on predation, which would be lethal in the Host-Dependent (HD) state. All the six *pilA::KnR* mutant strains obtained were all host-independent, in line with the hypothesis that functional PilA is required for the predatory process. Screening of prey-dependent (HD) merodiploid strains was continued for a further six weeks, but double recombinants were never obtained.

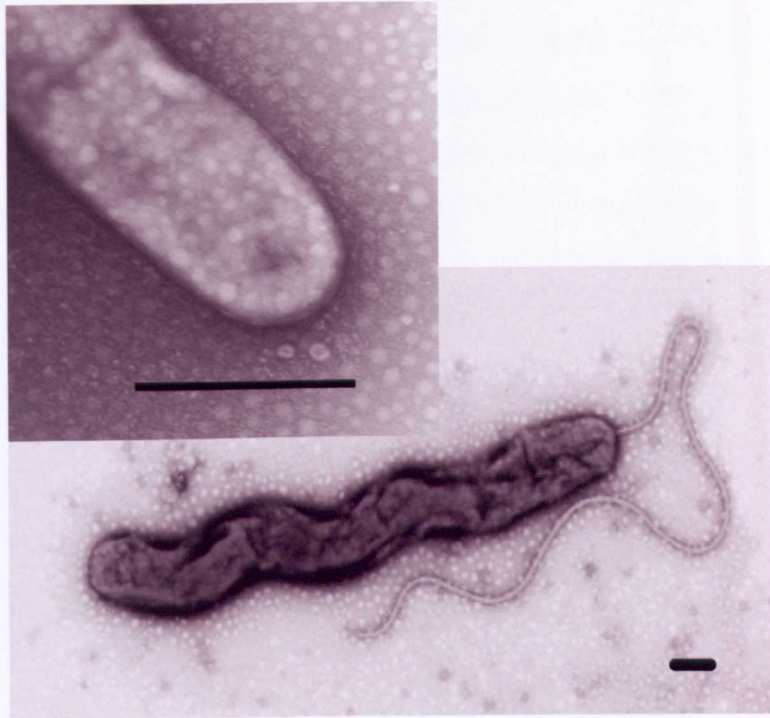
Due to the nature of HI growth, in the following experiments were carried out using the parental merodiploid strains as controls; this was a fair control as each had been subject to the same culture regime as the mutant lines, yet still carried the wild type *pilA* gene (see flow chart, section 5.4.1.1).

5.4.2.1: No pilus fibres were seen on HI*pilA::KnR* strains under the electron microscope.

High resolution TEM studies of the 6 mutant stains and the parental merodiploid strains revealed the presence of pili on the merodiploid HI strains at roughly the same percentage as that seen in prey-dependent cells, 30% (see Section 5.3.1.). However, pilus-like fibres were never seen in the HI*pilA::KnR* mutants (n >1000)



A



B

Figure 5.27: TEM characterisation of merodiploid and mutant *HIpilA::Kn* strains. **A** shows a merodiploid *HIpilA/pilA::Kn* strain displaying pilus fibres on the cell poles at roughly the same frequency as wild-type prey-dependent HD100 (30%). **B** shows 2 individual isolates of *HIpilA::Kn* mutant strains. No pili were ever seen on the poles of these cells; the lower TEM shows a characteristic HI morphology, all cells were polarly flagellate as expected. The top TEM shows a typical closer view of the cell pole. Cells stained with 1% uranyl acetate, bars = 2.0 μ m.

5.4.2.2: No predatory capability was seen in the *pilA::Kn* HD100 HI strains: growth on *E. coli* overlays and use of the fluorescent prey assay

The classical test of host-independent predation on *E. coli* is to inoculate liquid HI culture onto soft agar overlays of the appropriate host strain and incubate at 29°C for 6 days to see any areas of lysis, indicating that the HI strains are predatorily active upon the *E. coli*. Non-predatory strains will only show growth on top of the overlay with no areas of lysis. This test was employed to further characterise the mutant and merodiploid H*pilA* strains. A single colony of each HI strain was inoculated into PY broth and pre-grown for 3 days at 29°C, 200rpm to a final volume of 2ml. 10ul of culture was spotted onto soft agar overlays of kanamycin-resistant S17-1:pZMR100 *E. coli* prey and incubated at 29°C for 7 days. Figure 5.28 shows that H*pilA/pilA::Kn* merodiploid strains formed zones of clearing where they were spotted onto the prey cell lawn, whereas the H*pilA::Kn* mutant strains did not, showing that PilA is required for predatory growth on immobilised prey.

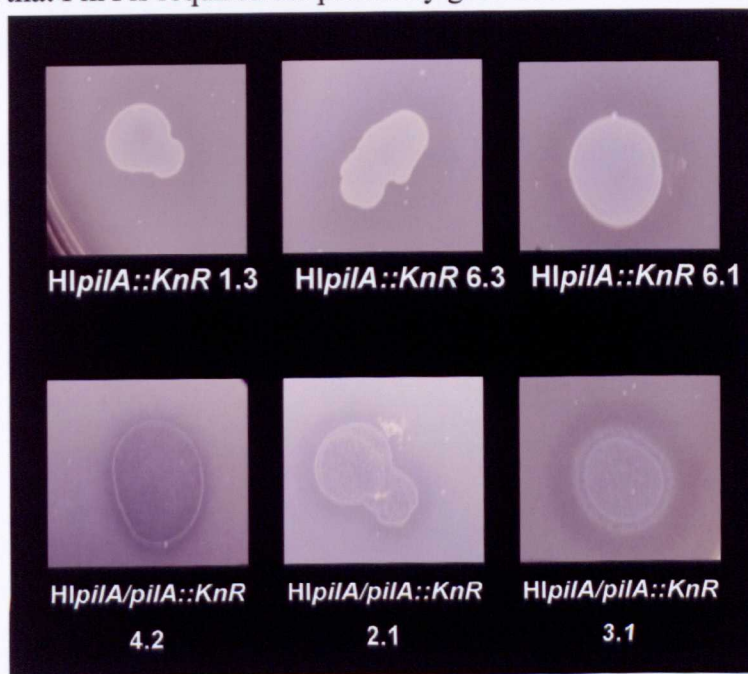


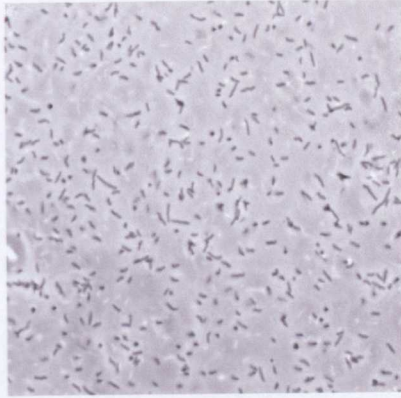
Figure 5.28: H*pilA::Kn* mutant strains and H*pilA/pilA::Kn* strains were grown on lawns of *E. coli* S17-1 pZMR100 (KnR) soft agar overlays. H*pilA/pilA::Kn* merodiploid strains formed zones of clearing where they were spotted onto the prey cell lawn, whereas the H*pilA::Kn* mutant strains do not, agreeing with the hypothesis that *pilA* is required for predatory growth on immobilised prey.

The other assay used in our laboratory to determine the predatory capabilities of mutant strains is challenging constitutively YFP-expressing *E. coli* S17-1 (S17-1:pSB3000pZMR100) on a solid PY agar surface with mutant and merodiploid HI strains (see section 2.9.3, (Lambert *et al.*, 2006). The YFP-expressing prey allows examination of any bdelloplast formation on the immobilised host and also allowed easy distinction between prey and predator.

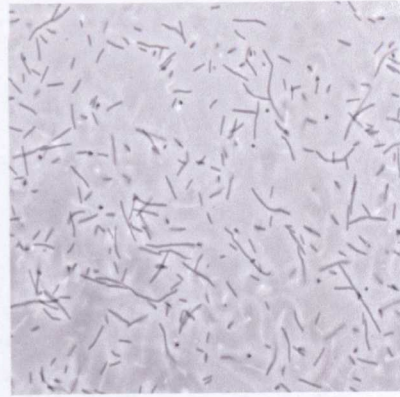
Replicate experiments were carried out using independently derived HI *pilA::Kn* mutant strains, paired with their merodiploid parental strains and chosen for their diverse morphologies (see Figure 5.29). The “wild-type” HID2 strain (HD100 derived), which had no kanamycin resistance was also tested in a slightly modified experiment (see Section 2.9.3) to show numbers of bdelloplasts given by a non-mutant strain under these assay conditions. The idea of this approach was that, as the HI phenotype is not precisely defined by anyone in the *Bdellovibrio* field, and may involve phenotypic variation in different HI derivatives, I wished to test the effects of *pilA* interruption in the most morphologically diverse HIs that had been derived. If a common phenotype was seen for all, this was due to the *pilA* mutation rather than another mutation or combination of mutations that are found in the generation of the HI phenotype.

Figure 5.29 (following page): (i) - Varying morphologies of individually derived HI *pilA::Kn* strains then used in fluorescent predation assays. Taken under phase contrast at 100x magnification. (ii) show predation tests of HI *pilA::Kn* (A), HI *pilA/pilA::Kn* (B) and HID2 (C) on immobilised YFP-labelled *E. coli* S17-1. The HI *pilA::Kn* mutant was seen to be non-predatory, while the merodiploid HI *pilA/pilA::Kn* and HID2 strains showed rounded bdelloplasts containing *Bdellovibrio* and thus normal predation C HID2. N > 2500 *E. coli* observed per strain. Images taken using YFP optics on a Nikon Eclipse E600 microscope at 100x magnification.

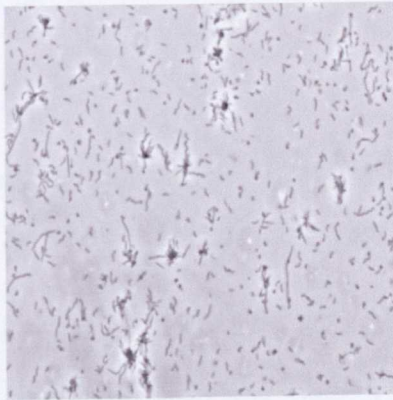
(i)



HlpilA::Kn 1.3, short, straight cells.



HlpilA::Kn 6.1, long, kinked cells



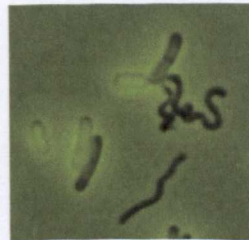
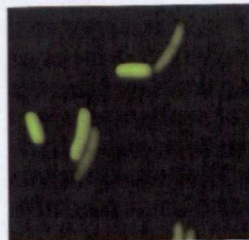
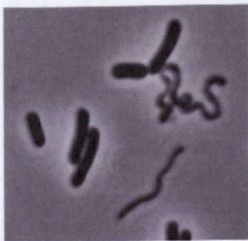
HlpilA::Kn 6.3, curly, branched cells

(ii)

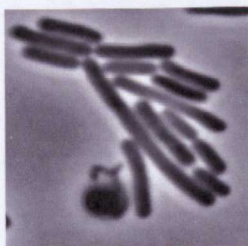
Phase

fluorescence

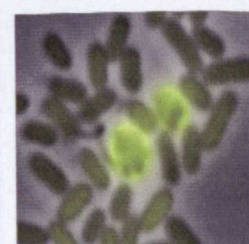
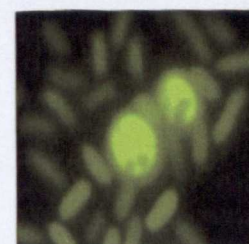
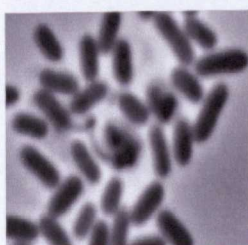
merge



A



B



C

As can be seen in the preceding figure, *HIpilA::Kn* strains used in these assay did indeed have extremely diverse morphologies. The final results show, over several independent replicate experiments (carried out both by myself and Dr Carey Lambert), that on average, the parental merodiploid *HIpilA/pilA::Kn* strains gave, on average, 44 bdelloplasts/1000 *E. coli*, versus the mutant *HIpilA::Kn* strains which were never observed to form bdelloplasts (n > 2500 *E. coli* examined per experiment). HID2, the non-KnR HD100 “wild-type” HI strain gave, on average, 45 bdelloplasts/1000 *E. coli*, which showed that the parental merodiploid *HIpilA/pilA::KnR* strains gave “wild type” levels of predatory activity in this assay.

5.4.2.3: Attempts to use immunology to study the PilA protein: *B. bacteriovorus* PilA does not cross react with the Myxococcal anti-PilA antibody

Correspondence with Pascal Bolon at Eurogentec showed that there would only be one possible weakly antigenic region on the native *B. bacteriovorus* HD100 PilA, underlined in the alignment with the Myxococcal PilA below (Figure 5.30, P. Bolon, personal communication). This region approximately corresponds to the first beta turn of the *P. aeruginosa* PilA crystal structure (Hazes *et al.*, 2000) shown in Figure 5.30, indicated by the purple line.

	10	20	30	40	50
<i>M. xanthus</i> PilA	MRVSRFNPRNRGFLIIELMIVVAIIIGILAAATAIENFIRFOARSKQSEAKT			
<i>B. bacteriovorus</i> PilA	-MFSVSRKKSQSQSGSLVELMIVVAIIIGVLASIAVPAINKYLAKARQSEAKT			
	60	70	80	90	100
<i>M. xanthus</i> PilA	NLKALYTAQKRFSEKDRMSDFANEIGFAPERGNRYGYRVSAAGDCEVR			
<i>B. bacteriovorus</i> PilA	NLSSLYTSEKAFYAEYTAHTMTMFGAICYSPEGKLRYNVGFNAPG-APEAG			
	110	120	130	140	150
<i>M. xanthus</i> PilA	NAADLPVPAAGVPCISNDSFRFGANSAIDDPPTVVARFVPGGAAGWNTTL			
<i>B. bacteriovorus</i> PilA	ATNGYNNPPTAAEGNTRNTAAAYCGTTGVIG-----AAGCTVLA			
	160	170	180	190	200
<i>M. xanthus</i> PilA	GVQPTIADCPNCNFFAGARGNADNEATFDDWVIACFEFGSGQVGPCSEAGN			
<i>B. bacteriovorus</i> PilA	CATNAVVPGLPATLLNGTQFRAAATAVVIHTAMPAG--DVWTIDQNKDLRN			
	210	220			
<i>M. xanthus</i> PilA	VASCTEYNTNRNDVACDGAAG			
<i>B. bacteriovorus</i> PilA	PTPCIP-----			

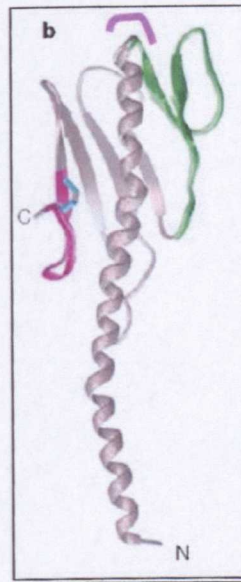


Figure 5.30: Alignment of HD100 PilA with *M. xanthus* PilA. A higher degree of conservation along the length of the protein is seen than with other proteobacterial PilAs, which is unsurprising as both bacteria are δ -proteobacteria. Underlined is the possible antigenic region of the HD100 PilA, approximately corresponding to the region highlighted on the crystal structure of *P. aeruginosa* PilA (Hazes *et al.*, 2000).

It was therefore decided not to synthesise a peptide antibody to HD100 PilA, but to try and use the previously generated *M. xanthus* anti-PilA antibody, which was made from purified Myxococcal PilA (Wu and Kaiser, 1997) (with grateful thanks to Mitch Singer at UC Davis for the kind gift of antiserum) as there would be a good chance of cross reaction with the HD100 PilA protein. BLAST of the HD100 genome with the *M. xanthus* PilA sequence revealed no significant stretches of homology with other *B. bacteriovorus* proteins, giving hope that this approach might

work. Immunological proof of the absence of the PilA protein in *HlpilA::Kn* strains would be absolute.

As such, Western blots (see section 2.7.3, 2.7.1) of whole cell protein of wild type, mutant *HlpilA::Kn* and merodiploid *HlpilA/pilA::Kn* *B. bacteriovorus* strains, with wild type *M. xanthus* DK1622 as a control were performed. A typical blot is shown in Fig. 5.31.

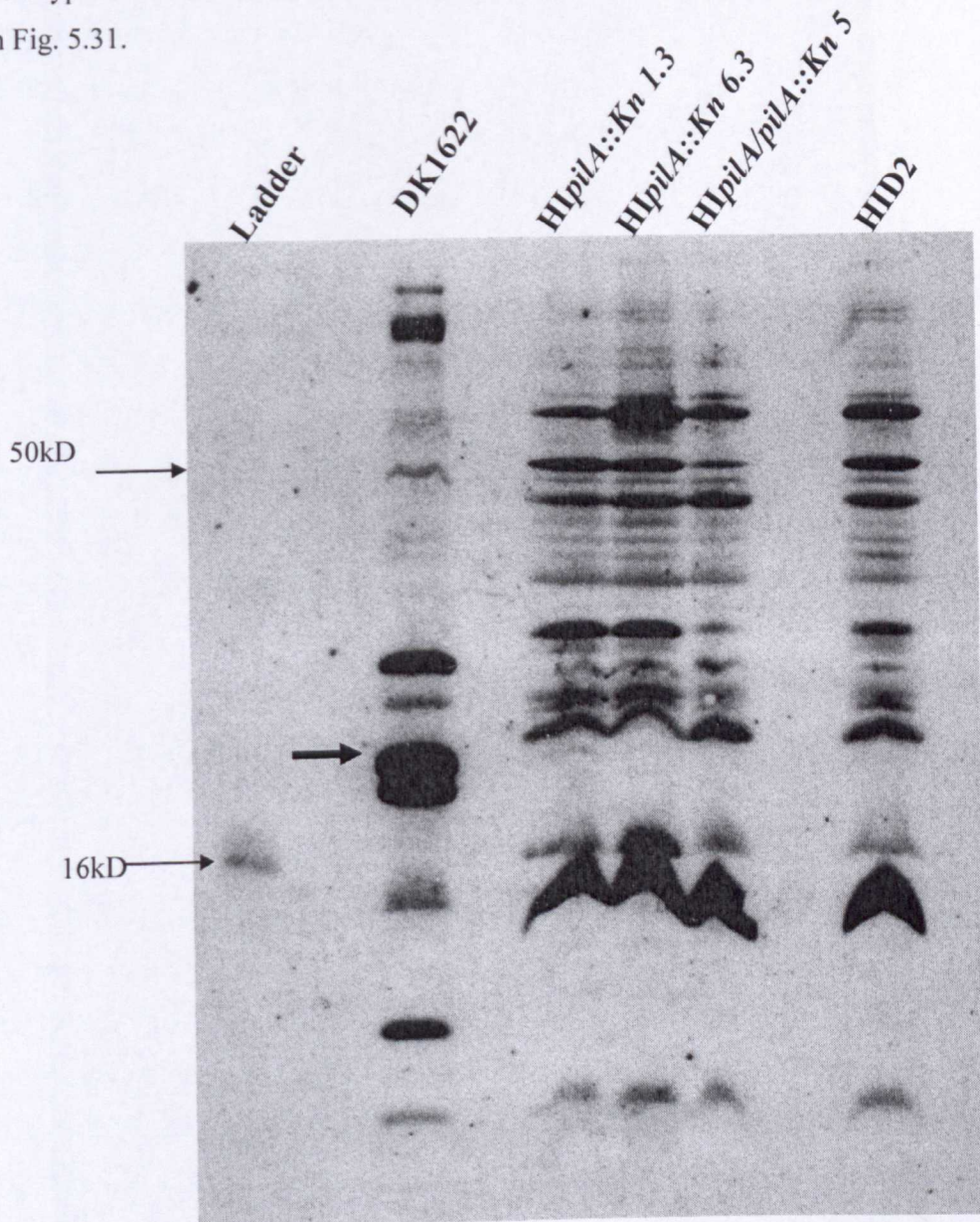


Figure 5.31: Western blot of whole cell proteins using the *Myxococcus xanthus* anti-PilA antibody at 1:3000 dilution. **Please see main text for a full discussion of this blot.** Ladder = 10 μ l SeeBlue Plus2 (Invitrogen) sizes as indicated (original blot transfer with prestained markers used to size where antibody not detected them), DK1622 = *M. xanthus* wild type strain (4 μ g protein), *HlpilA::Kn* 1.3 and 6.3 =

HD100 derived HI strains with an interrupted *pilA* gene, HI*pilA/pilA::Kn 5* = merodiploid HD100 derived HI strain with interrupted and wild type copies of *pilA*, HID2 = HD100 derived HI strain with only the wild type copy of *pilA* (all *B. bacteriovorus* strains 8µg protein). Arrow indicates the size that should correspond to *M. xanthus* PilA.

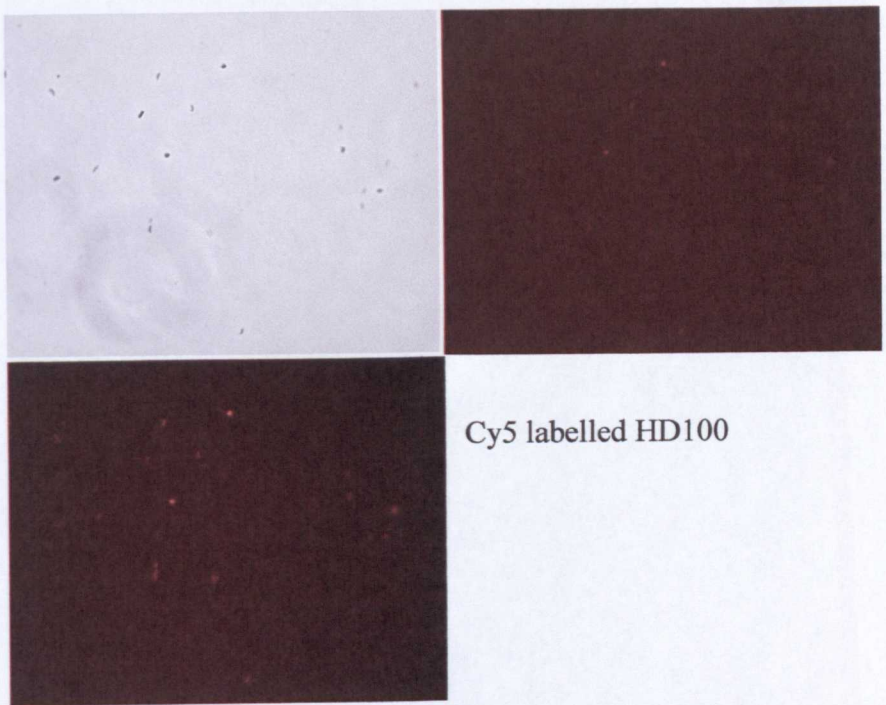
As can be seen, the antibody cross reacts with a great deal of *M. xanthus* whole cell proteins, making identification of even the *Myxococcus* PilA very difficult. The size of PilA in *M. xanthus* is 25kD from the published literature (Wall *et al.*, 1998) and so could be one of the dominant bands starred on the blot in the above Figure. The predicted molecular weight of the mature *B. bacteriovorus* PilA is approximately 20kD (predication made from the protein sequence using Compute pI/Mw held at Expasy, see Section 2.10 for details). However, the high degree of cross-reaction of this antibody with many *B. bacteriovorus* proteins and the “smiles” on the lanes make it impossible to pick out which, if any, the HD100 PilA could be. Attempts to resolve these issues were made over many repeats of this experiment, but no conditions could be found in which the blot improved.

5.4.2.4: Attempts to visualise pili on the surface of *B. bacteriovorus* HD100 cells using Cy5

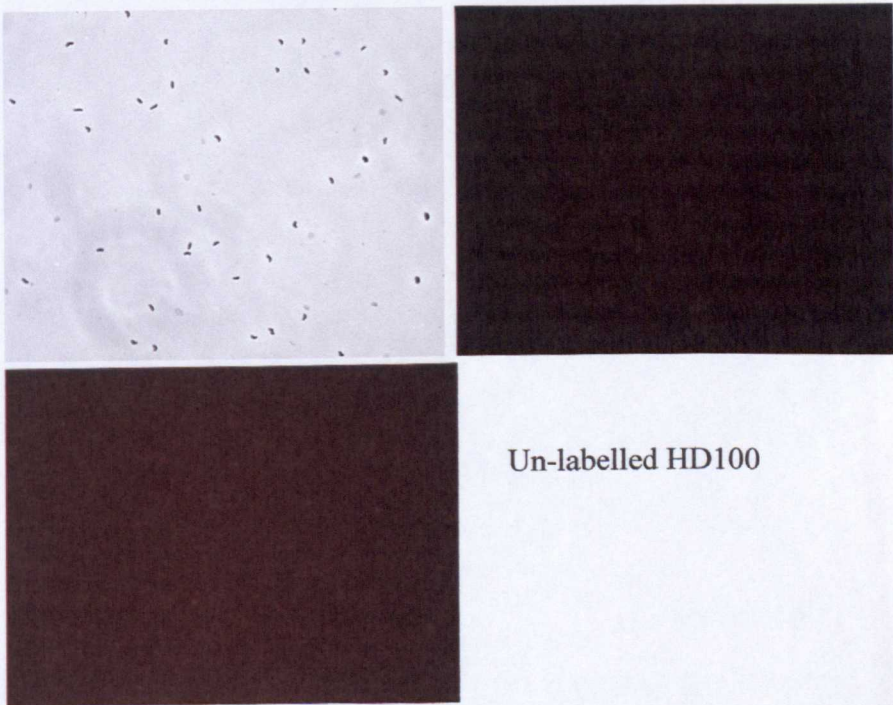
In the absence of a functional antibody, another way to confirm the presence of pili seen on *B. bacteriovorus* cell poles aside from electron microscopy was desirable. In other studies, notably in *P. aeruginosa* and *M.xanthus*, Cy3 or Cy5 monoreactive dyes (Amersham/GE Healthcare) have been used to microscopically demonstrate the presence of pili on bacterial cells by fluorescence (Mignot *et al.*, 2005; Skerker and Berg, 2001), also see Figure 5.2 earlier. Mignot *et al* successfully showed the presence of pili on *Myxococcus* cell poles using Cy5, which labels proteinaceous extracellular structures, so this experiment was tried in *B. bacteriovorus* HD100. HD100 was grown on the flagellar-minus strain DFB225 *E. coli* to ensure that any remaining prey cells would not have labelled flagella which could mask *B. bacteriovorus* structures. The absence of flagella in *Myxococcus* ensured that any labelled extracellular structures were pili; *B. bacteriovorus* does have a single, polar

flagellum – this is however sheathed by membrane and at the opposite pole to that used for prey attachment, so there were no concerns about the Cy5 labelling the flagella and being mistaken for pili.

However, as discussed in Chapter 4, (see Section 4.3.1), labelling with dyes that function in other bacteria once again proved very difficult in *B. bacteriovorus*. As demonstrated in Figure 5.32, the dye loading of the cells was very poor, again like the FM4-64 tried in Chapter 4. As with the FM4-64, the prey strain *E. coli* were labelled much better (data not shown). This approach therefore was not successful for labelling *B. bacteriovorus* pili.



Cy5 labelled HD100



Un-labelled HD100

Figure 5.32: Cy5 labelling experiments using HD100. As can be seen, the agar mounted Cy5 labelled cells were only marginally more fluorescent than the unlabelled control. This was insufficient to demonstrate the presence of pili in HD100. Images taken under GFP optics on a Nikon Eclipse E600 microscope, 100x magnification.

5.5: Reverse Transcriptase PCR of *pilA* and other associated *pil* genes across the HD100 life cycle

As immunological and dye-based approaches were unsuccessful, further analysis of the role of Type IV pili across the *B. bacteriovorus* life cycle was carried out using semi-quantitative 25 cycle Reverse-Transcriptase PCR (RT-PCR, see Section 2.5.3.2, (Lambert *et al.*, 2006). *pilA* expression was examined, along with other selected *pil* genes whose products function in pilus extrusion and retraction in other species, and the Bd0108 gene within the *hit* locus – a region containing four ORFs shown to be mutated in some host-independent strains of *B. bacteriovorus* thought to be associated with that phenotype (Barel and Jurkevitch, 2001; Cotter and Thomashow, 1992b).

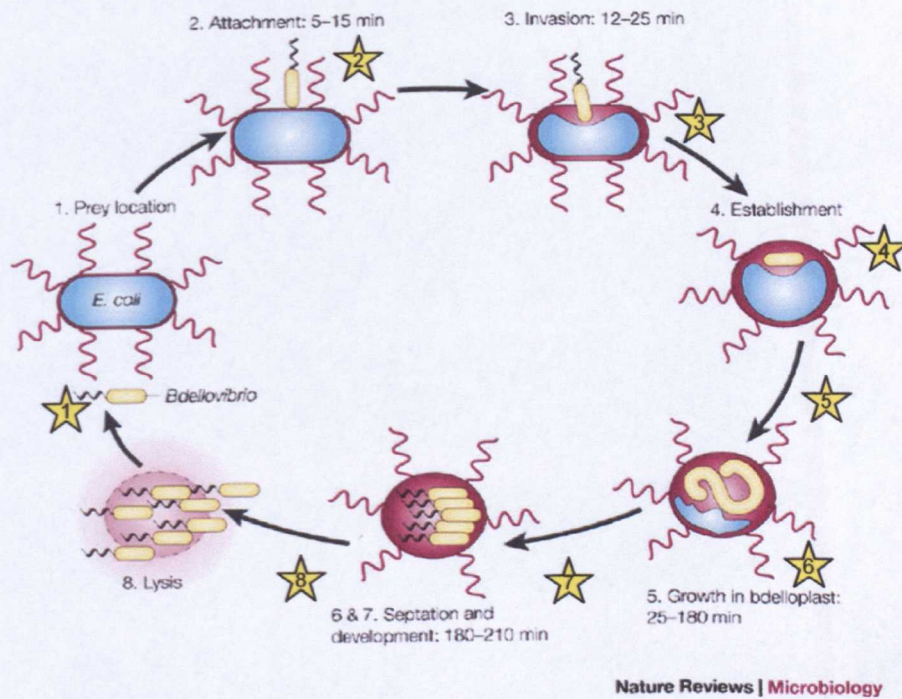


Figure 5.33: Stars on the life cycle of predatory *B. bacteriovorus* give a visual representation of the stages at which cultures were sampled and RNA prepared to enable transcript profiling at different stages of *B. bacteriovorus* growth. 1 = attack phase, 2 = 15 minutes post-infection, 3 = 30 min, 4 = 45 min, 5 = 1 hr, 6 = 2 hr, 7 = 3 hr, 8 = 4 hr. RNA sampling carried out by Dr Carey Lambert, modified from (Sockett and Lambert, 2004) with kind permission.

For a published version of this work, please refer to Evans, K.J., Lambert, C. and Sockett R.E. (2007) Predation by *B. bacteriovorus* requires Type IV Pili. *J. Bact.* 189:4850-4859. Reference added post viva.

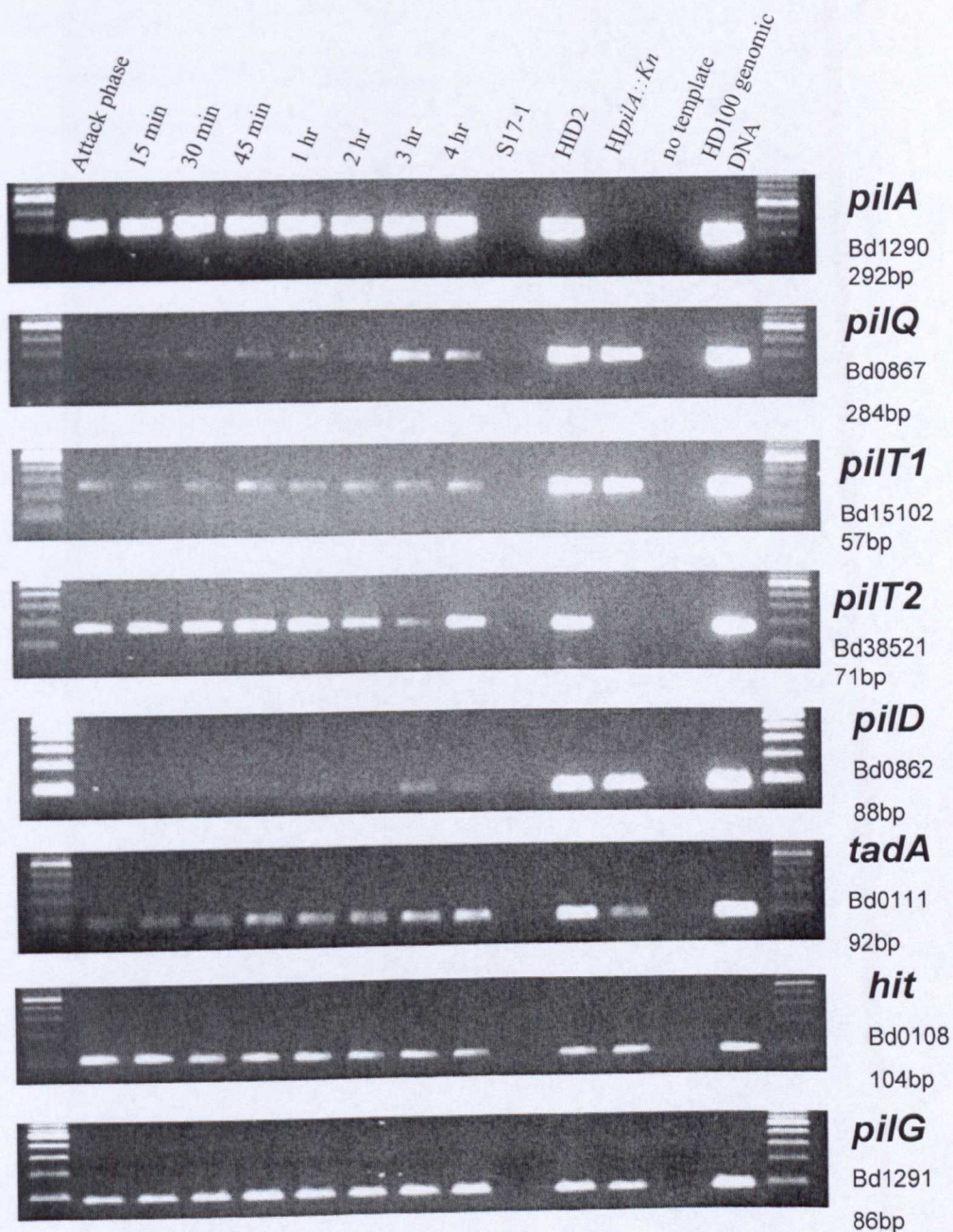


Figure 5.34: Semi-quantitative reverse-transcription PCR of RNA from *B. bacteriovorus* predatory cultures, timepoints were as indicated on the previous figure – taken at defined points in the predatory life cycle; also taken from matched OD₆₀₀ cultures of host-independent strains of HIpilA::Kn (strain 6.1) and HID2. Genes whose expression was examined are as stated to the left of the panels; RTPCR product sizes are as stated. Gels were 2% TBE agarose, size markers on the extreme left and right were NEB 100bp ladder (see Appendix 1 for sizings), control lanes were *E. coli* S17-1 RNA to exclude primer cross-reaction with any prey RNA, no template and HD100 genomic DNA. Taq PCRs done under the same conditions were also carried out to ensure no DNA contamination of the RNA samples; all were negative (data not shown).

As demonstrated in Evans, K.J., Lambert, C. and Sockett R.E. (2007) Predation by *B. bacteriovorus* requires Type IV Pili. *J. Bact.* **189**:4850-4859, due to the nature of the *B. bacteriovorus* HD100 predatory life cycle, internal mRNA level controls commonly used in other bacteria such as sigma factors or ribosomal RNA genes are massively regulated and change expression upon prey entry and predator growth within the periplasm (C. Lambert, C-Y. Chang, R.E. Sockett, unpublished data). This is logical in the context of *B. bacteriovorus* as the predator does not replicate in the host-dependent phase outside of the prey periplasmic environment, so expression of genes related to replication would be unnecessary in the attack phase of the life cycle. The variation in expression levels of the commonly used control genes means that they are unsuitable for this use in *B. bacteriovorus* HD100. As such, there are limitations to this analysis even though RNA levels for each extraction timepoint were quantified by nano-drop (C. Lambert); however, in Evans *et al* (see reference above added in proof), we demonstrated the validity of the semi-quantitative RT-PCR data using Quantitative RT-PCR, carried out by Dr C. Lambert. Please refer to the above publication for data.

5.5.1: *pilA* expression

The *pilA* gene showed constitutive expression at all time points across the *B. bacteriovorus* life cycle. Attack phase cell levels of *pilA* mRNA did not decrease during bdelloplast formation and maturation. As all predatory cycle RNA preparations were made from cultures that began with the inoculation of identical numbers of predatory *B. bacteriovorus* equivalent to those in the attack-phase only sample, it was possible to compare expression patterns of one gene across the predatory life-cycle. Consistent transcript levels showed abundance of the *pilA* mRNA, which would facilitate rapid protein synthesis of a supramolecular fibre structure as necessary in the predatory life cycle. *pilA* is also expressed in the HD100-derived, predatorily competent, HI strain, HID2; *pilA* mRNA expression was abolished in the HI*pilA::Kn* mutant strain, as expected.

5.5.2: *pilQ*, Bd0867, expression

As shown in Section 5.3.4, Bd0867 was the most convincing *pilQ* homologue of the 3 *pilQ* genes annotated in the HD100 genome. *pilQ* showed lower expression in attack phase than in later bdelloplast stages. This could be interpreted as the beginning of

septation of the growing *B. bacteriovorus* filament within the bdelloplast and the formation of new cell poles with completed pilus basal structures (including PilQ); pilus fibres have only been observed to be polar rather than lateral (see Section 5.3). This also means that *pilQ* could be useful as a marker for late bdelloplast stages and filament septation. In the HI strains tested, HID2 wild-type and the HI*pilA::kn* mutant, *pilQ* transcripts were present, indicating that the basal pilus structures are probably also present in HI *B. bacteriovorus* strains .

5.5.2: *pilT1*, Bd1510, expression

B. bacteriovorus pilT1 (see Section 5.3.5) showed a steady level of expression throughout the developmental cycle from attack phase through to late bdelloplast. Like the *pilQ*, transcripts are present in both HID2 and HI*pilA::Kn* strains, indicating a mixed population of HI.

5.5.3: *pilT2*, Bd3852, expression

In its expression pattern, *pilT2* was somewhat unusual, confirmed by multiple repeats both on the same set of RNA and one made at a different time (courtesy of Dr C-Y Chang, data not shown). The gene showed expression in attack phase cells, which increased slightly in the early bdelloplast stages, with a peak of expression between 45 minutes and 1 hour, which then dropped slightly at 2 hours, reaching its lowest level at 3 hours and then returning to an increased level at 4 hours. Interestingly, *pilT2* expression was apparently low in the *pilA* knockout strain compared to *pilA* wild type HID2 although a direct comparison cannot be made from semi-quantitative data. As mentioned above in Section 5.3.5, PilT provides the retractile force of the Type IV pilus motor, being a hexameric ATPase of the AAA⁺ family (Herdendorf *et al.*, 2002) which is held at the base of the Type IV pilus under, and probably in association with, the cytoplasmic membrane. The dip in expression at 3 hours, as the poles are probably starting to form, is somewhat difficult to explain, but the RTPCR data showed that its expression possibly responds to that of the *pilA* gene. There has been no previous published work on any aspect of *pilA/pilT* interaction in gene regulation.

5.5.4: pilD expression

PilD, the pre-pilin peptidase that cleaves and methylates the immature PilA fibre protein so it can be exported and polymerized, is associated with the cytoplasmic membrane of bacteria that utilize Type IV pili (reviewed in (Mattick, 2002)). *B. bacteriovorus pilD* showed virtually no expression in attack phase cells when compared to later stages of bdelloplast formation. The expression pattern of *pilD* is reminiscent of that of *pilQ* (Section 5.5.1) which seems logical, with the peak of expression of both these genes apparently coinciding with the beginning of cell pole formation.

5.5.5: tadA, Bd0111 expression

tadA in *Actinobacillus actinomycetemcomitans* and *Pseudomonas aeruginosa* encodes the traffic NTPase required for the formation of Flp pili (Bhattacharjee *et al.*, 2001; de Bentzmann *et al.*, 2006). As shown earlier (see Section 5.3.3), the HD100 genome encodes an incomplete set of genes required for Flp pilus formation, but does encode a TadA homologue which has an *e* value of $3e-95$ to the *A. actinomycetemcomitans* protein; however it has better mid- to C-terminal homology to other proteins that are not TadA homologues, most of which are GspE family Type II secretion proteins. The N terminal 300 amino acids show good homology to NTP binding domains involved in Flp-pilus formation. Like PilT, TadA is a member of the secretion NTPase (GspE) family, and forms a distinct subfamily that is widespread amongst the Bacteria and Archaea (Kachlany *et al.*, 2001). *tadA* has lower level of expression in attack phase *B. bacteriovorus* than in the bdelloplast stages. The functionality of TadA in *B. bacteriovorus* is unknown; however, if it is involved in a Type II secretion function for molecules associated with the predatory process after PilA-mediated prey cell entry, then lack of *pilA* may affect its expression in that fashion through an unknown signalling mechanism.

5.5.6: *hit*, Bd0108 expression

This gene associated with the *hit* locus was chosen for expression studies as it the same as used in the analysis of (Schwudke *et al.*, 2005), who performed quantitative RTPCR studies of the *hit* region of HD100 and found that over a time course of 5 hours that there was a dip in *hit* gene expression at 90 minutes, followed by a rise to initial levels at 3 hours post infection. My semi-quantitative 25 cycle RTPCR of *hit* locus gene Bd0108 does not lend strong support to this finding. If anything, the amount of *hit* transcript produced seemed to decline slightly over the infection time course from wild type levels in these experiments but it must be remembered that these levels are only relative. In addition, *hit* transcripts were still produced in HID2, the HD100-derived HI strain and also the HI*pilA::Kn* mutant strain, indicating that in these HI strains, *hit* locus gene expression has not been affected by the HI phenotype, suggesting that changes elsewhere in the genome account for the HI growth.

5.5.7: *pilG* expression

PilG forms part of an ABC-type transporter required for PilA export and functional pilus biogenesis in *M. xanthus*, with these genes having no known homologues in other Type IV pilus-producing species, indicating a possible restriction to the δ -proteobacteria (Wu and Kaiser, 1995). *B. bacteriovorus* HD100 has good homologues of all three genes, *pilGHI* (Bd1291, Bd0860 and Bd0861 respectively). Wu *et al* concluded that PilGHI may be required for OM localization/export of PilA as mutants do not shed PilA into the surrounding medium, but do not produce functional pilus fibres. This may account for the lack of *B. bacteriovorus* gene homologues for minor pilin proteins, which may perform such a role in other bacteria. For example, *Pseudomonas aeruginosa pilE, V, W, X* and *fimU* genes have no counterparts that can be found through homology searches of both the *B. bacteriovorus* and *M. xanthus* genome sequences. The *pilE, V, W, X* and *fimU* genes are required for pilus assembly in *P. aeruginosa* (reviewed in (Mattick, 2002) just as *pilGHI* do in *M. xanthus* and would be expected to do in *B. bacteriovorus*. The *pilG* gene was chosen for transcriptional assay as it lies directly downstream of *pilA*. Expression profiling in the mutant HI*pilA::Kn* strain showed that there was no polar

effect on *pilG* transcription caused by insertion of the kanamycin-resistance cartridge into *pilA*.

Data presented above shows that type IV pilus genes are expressed in *B. bacteriovorus*; however, a full quantitative Real-Time PCR analysis would show absolute expression levels. The semi-quantitative analysis, like work previously published in (Lambert *et al*, 2006), gives an indication of relative levels of gene expression across the predatory life cycle.

5.6: Discussion

In this section of work, I have demonstrated that the PilA fibre-forming protein of Type IV is used to mediate *B. bacteriovorus* prey entry and/or establishment in the bdelloplast. Electron microscopy of wild-type attack phase predators showed pilus fibres on the non-flagellar pole; it also showed the presence of ring-like structures on the piliated pole, but their function remains, as yet, unknown. Interruption of the *pilA* gene in HD100 gave a strain that could not predate, even when placed in close proximity to prey cells. Reverse-transcriptase PCR of Type IV pilus genes showed that they are expressed in *B. bacteriovorus*; conversely, bioinformatic analysis of the HD100 genome showed that Flp-pili are probably not functional in *B. bacteriovorus*.

Interestingly, in the recently sequenced genome of a related member of the *Bdellovibrionaceae*, *Bacteriovorax marinus* (shotgun sequencing completed at the Sanger Centre, Cambridge, UK, available for BLAST searches at http://www.sanger.ac.uk/Projects/B_marinus/) there appears to be a homologue of *B. bacteriovorus* PilA. TBLASTN search of the *Bacteriovorax* genome produced a predicted protein homologue of PilA with an e value of 7.0e-22. Retrieval of the nucleotide sequence and translation of the DNA sequence into protein (Translate tool at Expasy, http://www.expasy.org/cgi-bin/dna_aa) followed by alignment with HD100 PilA produced the following:

		10	20	30	40	50	60	
B mar transl	1	-FMKSEKNEEGFTLVELMVVVAIIGLDSAVATPNFRKYOAKTKTSEAKLQLSSHYSAETA	59					
HD100 PilA	1	MFVSRKRSQSGFSLVELMVVVAIIGVLSIAVEPAINKYLAKARQSEAKINLSSLYTSEKA	60					
		70	80	90	100	110	120	
B mar transl	60	LQSDFDAYASCLTDAGYLPFRGGNYVAVGFPDSDTGGISTVT SNGGTCGGAGNTGGPSN	119					
HD100 PilA	61	FYAETAYHTMFGAIGYSP-ECKLRNNGFNAPGAPEAGATNGYNNPPAAPGNTARN--T	117					

```

                130      140      150      160      170      180
B mar transl  120 KTVACKSAADCDLGFILVK-TTAGLSQSSNSVEADGLGFVAGAVGYTDSKAKANVADLW 178
HD100 Pila   118 AAYCGTTGVICAAAGCTVLAGAANAVVPLPATLLNGTQERRAAIAVHTAMPAG---DVM 174

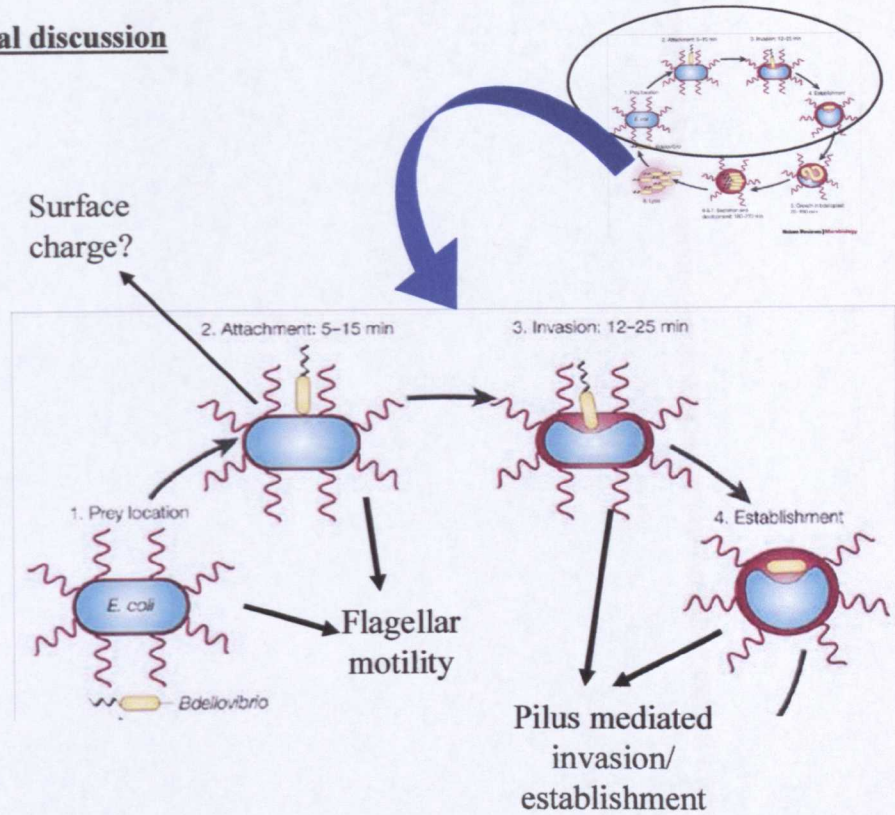
                190
B mar transl  179 AIDENKNI----- 186
HD100 Pila   175 TIDONKDLRNPTPGIP 190

```

The alignment shows not only the characteristic N-terminal homology shared by Type IVa pilins, but also a high degree of predicted sequence conservation along the length of the protein.

This gives evidence that the use of Type IV pili in *Bdellovibrio* species may be widespread; failure to clone the 109J *pilA* sequence was offset by the observation of pilus fibres on the poles of 109J cells. However, until the genome of 109J is sequenced, then this hypothesis is still speculative.

Chapter 6: Final discussion



6.1: Summary of research findings: the role of surface structures in the predatory lifestyle of *B. bacteriovorus* and implications of techniques developed

This work has examined the role of general bacterial surface structures within the context of *B. bacteriovorus* predation. Prior to this, the role of *B. bacteriovorus* cell surface structures was mainly limited to (a now superseded consideration of the role) of flagella, with only speculation about pilus-like fibres. What has been demonstrated in this thesis through the use of gene inactivation and other, novel, techniques is that flagellar-mediated motility is extremely important in the predatory lifestyle of *B. bacteriovorus*, in both strain HD100 and 109J, but is not absolutely required for prey entry as inactivation of the key flagellin gene, *fliC3*, does not abolish predatory behaviour when the *B. bacteriovorus* are placed in proximity to immobilised prey. Other surface structures, Type IV pili, have been demonstrated to be the mediators of predation. Abolition of expression of the fibre forming protein, PilA, produced strains that were incapable of penetrating and growing on prey, even when placed in close proximity.

The importance of flagellar motility has always been speculated upon before the development of genetic techniques for gene interruption in this bacterium, but here

that role has been more clearly defined. The publication of the *B. bacteriovorus* HD100 genome (Rendulic *et al.*, 2004) allowed identification of six individual *fliC* genes contributing to the flagellar filament and that they were all present and have a role in filament formation in both HD100 and 109J. Individual inactivation of these genes showed that, despite their apparent sequence conservation, one (*fliC3*) is absolutely essential for flagellar motility and predation in liquid media, and that two (*fliC4* and *fliC5*) others have an essential role in the correct formation of the flagellum. Without *FliC4* and *FliC5*, flagellum length, swimming speeds and predation are reduced. These results demonstrate that having multiple flagellin genes cannot compensate instantly for loss of essential ones and that a reduction of motility can affect predation rates in liquid environments.

Further analysis of these mutants, at the protein level, show that loss of one flagellin protein seems to affect the expression, or at least the quantities of other flagellins produced. Protein analysis also demonstrated that despite having extremely similar predicted molecular masses, the flagellins migrate differently on denaturing gels, with (in the *FliC3* mutant and the HIK3 wild type backgrounds) some flagellins being found in different size fractions simultaneously. This gives a possibility of post translational modifications being made to the proteins, but indiscriminately (as against just one flagellin being modified all the time). This could perhaps indicate some role for phosphorylation or glycosylation along the length of the filament in interactions with the *B. bacteriovorus* flagellar sheath. This remains, at present, merely speculation, as does the role of the sheath in general and how it survives the intense mechanical stresses involved in the high speeds attained by motile *B. bacteriovorus* (see Chapter 3 for more detailed discussion).

Type IV pili have been shown to be the mediators of prey entry/establishment in this work. Once the entry pore in the prey outer membrane has been generated, electron microscopy has shown the *B. bacteriovorus* squeezing through the small hole and confirmed the presence of polar fibres at the opposite end to the flagellum where the predator is always seen to attach to the prey. We and co-authors proposed in our analysis of the HD100 genome that Type IV pili could provide the means for prey entry; analysis carried out as part of work for this thesis showed that not only does the HD100 genome encode a full set of genes for Type IV pili but does not have the

necessary genes required for Flp pilus formation. RT-PCR studies of selected Type IV pilus genes shows that they are expressed; mutation of *pilA* resulted in a strain that could not produce pilus fibres or, importantly, be predatory even if placed in close proximity to prey.

The use of the HI phenotype of *B. bacteriovorus* in providing a rescue for mutants that affect the predatory capabilities of the bacterium has also been explored in this work. Development of a standard protocol for multiple isolations of strains containing the same mutation has overcome the doubt about the validity of using HI derivative of prey-dependent *B. bacteriovorus* for mutational analysis. The novel use of fluorescently labelled prey (in conjunction with R. Till) has proved a useful assessment of predation in HI cells that cannot be tested in other methods standard in our laboratory. Exploration and initial development of other fluorescence techniques within this work have shown that GFP can be used to label *B. bacteriovorus*, but full use of the potential for fluorescence studies in this bacterium needs refinement of the technologies employed for visualisation due to the small physical size of the cells and hence the apparent faintness when observed using the facilities available on a routine basis to me. I have also shown that membrane stains, such as FM4-64 and Cy5, that are commonly used in other bacteria are not universal in their applications in *Bdellovibrio*, raising interesting questions about the uniqueness of the *B. bacteriovorus* membrane structure and the implications of this (see Section 4.4 for a fuller discussion).

In this work, different ways of examining the physiology and morphology of *B. bacteriovorus* throughout the life cycle using whole cell stained electron microscopy preparations have also been studied, particularly in the bdelloplast stages. The resulting images often raise more questions than they answer, but provide some possible clues to the intracellular stages of the predatory life cycle without damaging the cells through fixation procedures. Microscopy techniques employed have confirmed previous research and disproved other hypotheses, such as that flagella are not always shed immediately on prey entry (see Section 3.2.1.1) and that the prey cytoplasmic membrane becomes leaky during the bdelloplast stages when the predator is established in the periplasm (see Section 3.5).

6.2: Further questions from this work and directions for future research

With respect to the *B. bacteriovorus* flagellum and its role, some questions have been raised through work in this project and with others. The role of the sheath is still a mystery; work on this structure would be an aid in the field of flagella in general a little is known about it. There may be some clues as to sheath interaction residues in the sequence of FliC3 when compared to other sheathed flagellate bacteria (see Section 3.5.3). The question of post translational flagellin modification should also be addressed, perhaps using the glycosylation systems that are partially characterised in *H. pylori*, which has a sheathed flagellum, as a model. Truncation of the flagellum in the FliC5 mutants should be further explored, as in older *B. bacteriovorus* cells the flagellum carries on elongating in the small amplitude distal waveform (Thomashow and Rittenberg, 1985b); if FliC5 is the main or sole component of the distal filament, no elongation should occur. My personal observations of these cells indicate that it does not, but a properly controlled study should be carried out (underway, L. Hobley and L. Sockett). Continued elongation of the filament also means that the sheath must also be continuously synthesised. Sheath biosynthesis, as shown in the FliC3 mutants, is independent of an intact, functional flagellum, but as all *B. bacteriovorus* flagella are sheathed, the biosynthesis is likely to in some way share a regulatory genetic pathway with one aspect of flagellar biosynthesis. This would again be of interest to others in the field. Individual epitope tagging of each flagellin gene would provide positional information of flagellin location within the flagellum, which is currently unknown in any of the bacteria containing multiple flagellin genes.

Further studies of the Type IV pilus system in *B. bacteriovorus* would also be highly informative. Mutation of the true orthologues of *pilQ* and *pilT* would provide non-piliated and hyperpiliated cells respectively if analogous systems in other bacteria are used as a model (Mattick, 2002). A *pilT* mutation in particular would be beneficial as a hyperpiliated phenotype would potentially allow mechanical shearing of pili, used extensively in *M. xanthus* (Wall *et al.*, 1998) resulting in native protein for raising antisera. In wild-type *B. bacteriovorus*, pili are only present on approximately 30% of free-living attack phase cells as seen by intensive TEM study, so shearing of cells to produce native pilin is not feasible (this was tried as a part of this work, insufficient pili for analysis were obtained as examined by SDS-PAGE and TEM,

data not shown). An antibody to native PilA would allow immuno-electron microscopy to show the precise timing of pilus extrusion. My hypothesis is that pili are extruded into the periplasm of prey once the entry pore has been created in the prey outer membrane, as pili may be damaged by the predator's own lytic enzymes during pore generation.

Abolition of predation by mutation of *pilQ* or *pilT* would also independently confirm the result obtained through the inactivation of *pilA*. Further exploration of the role of PilA itself would also be interesting. The HD100 genome does not encode any homologues of known adhesins/invasions that cap the tip of Type IV pili in some other species, but within the sequence of PilA there are two mid to C-terminal cysteine residues that may be able to form a disulphide bond. As discussed in Section 5.3.6.1.1, these have been implicated in the mechanism of pilus tip adhesion in other bacteria so mutagenesis of these residues may abolish the ability of *B. bacteriovorus* pili to bind to whatever their target is, most likely in my view the prey peptidoglycan (a rigid structure that should provide an anchor to pull the cell body into the prey periplasm). A full crystal structure of PilA would be extremely informative in both raising peptide antibodies but also as to whether these potential disulphide bond-forming residues are actually exposed at the tip of the pilus.

Further development and use of different microscopic techniques is invaluable to the continued study of this organism. As mentioned in Chapter 1, the Subramaniam lab at NIH Bethesda is currently starting to study *B. bacteriovorus* using 3D electron tomography (Narasimha *et al.*, 2006) which will provide a wealth of information about the structures inherent in the predator that cannot be seen using conventional techniques. It would again be confirmatory of the use of Type IV pili in *B. bacteriovorus* as the technique should be able to visualise PilQ outer membrane multimers and possibly immature PilA pools being held under the cytoplasmic membrane next to the rest of the Type IV pilus machinery.

Scanning electron microscopy of *B. bacteriovorus* has been used previously in other areas of research, for example, predation of biofilms (Kadouri and O'Toole, 2005), but a more focused study of bdelloplasts and the invasion process would be fascinating. This would be the same with atomic force microscopy, though my

personal view is that this technique is perhaps less suited to *B. bacteriovorus* predation than other microscopic avenues.

Development of fluorescence microscopy and detection techniques for use in *B. bacteriovorus* is a little more complex as cell size and fluorescence intensity stretch the sensitivity of current widely available microscopes. Confocal microscopy may be an answer, but again, the dimensions of the cells may prove something of a hindrance to spatial resolution. Deconvolution microscopy has been successfully used in other bacterial fluorescence applications, for example in *Bacillus subtilis* (Pogliano *et al.*, 1999), so this may provide good resolution of GFP or other fluorescent reporter foci if a target protein has been tagged. However, as techniques evolve rapidly and equipment becomes more readily available, their applications in *B. bacteriovorus* will be extensive.

The immediate focus of any further experimentation in this organism needs to be expansion of the repertoire of genetic techniques to overcome the limitations currently experienced as discussed in Section 1.6. The ability to experiment with multiple antibiotic selective markers, complement loss of gene function from an autonomously replicating plasmid and create point mutations in key residues of proteins of interest would result in a massive expansion of information gathered about this organism. Many of the experiments suggested above would require one or other of these techniques, so as yet, they are not possible to carry out; however work has started in our lab to try and resolve some of these issues, beginning with the question of useful antibiotic resistances (R. Till, L. Sockett).

One area that shows promise within the near future is that of comparative genomics. The sequencing of the genome of *B. bacteriovorus* strain W that forms bdelloccysts, a resting stage allowing survival of the *Bdellovibrio* for long periods of time under harsh conditions or the absence of prey (Tudor and Conti, 1977) is currently being undertaken by Dr John Tudor and colleagues. Sequencing of the closely related marine *Bdellovibrio*, *Bacteriovorax marinus*, is nearing completion at the Sanger Centre (www.sanger.ac.uk) and, as seen in Section 5.6, may provide useful information on genes important to predation, though the data currently are not in a completed nor readily usable format. These genomes, in combination with that of *B.*

bacteriovorus HD100 may well give further clues to conserved genes specific to these predators, useful as nearly a third of the genes in the HD100 genome remain hypothetical as they have no homologues in the public databases (Rendulic *et al.*, 2004).

Perhaps the ultimate aim of research into predatory bacteria is their potential as “living antibiotics”. With the emergence of more and more pathogenic bacterial strains that are resistant to mainstream antibiotics and a decrease of new antibiotics being discovered, it is more important than ever to explore other avenues for treatment of serious Gram-negative bacterial disease. Initial experiments in our laboratory show some promise, but further research is vital. Key to this is our understanding of the predatory process itself: this knowledge will hopefully lead to clinical trials of *B. bacteriovorus* as a therapeutic agent. This work has contributed to the understanding of the early stages of predation by *Bdellovibrio bacteriovorus*, particularly the roles of the surface structures of pili and flagella, so forms a starting point for future work on this novel and fascinating microbial predator.

REFERENCES

- Abram, D., and Davis, B.K. (1970) Structural properties and features of parasitic *Bdellovibrio bacteriovorus*. *J Bact* 104: 948-965.
- Abram, D., Castro e Melo, J., and Chou, D. (1974) Penetration of *Bdellovibrio bacteriovorus* into host cells. *J Bact* 118: 663-680.
- Aizawa, S.I., Dean, G.E., Jones, C.J., Macnab, R.M., and Yamaguchi, S. (1985) Purification and characterization of the flagellar hook-basal body complex of *Salmonella typhimurium*. *J Bact* 161: 836-849.
- Albertson, N.H., Stretton, S., Pongpattanakitsote, S., Ostling, J., Marshall, K.C., Goodman, A.E., and Kjelleberg, S. (1996) Construction and use of a new vector/transposon, pLBT::mini-Tn10:lac:kan, to identify environmentally responsive genes in a marine bacterium. *Fems Microbiology Letters* 140: 287-294.
- Altschul, S.F., Madden, T.L., Schaffer, A.A., Zhang, J., Zhang, Z., Miller, W., and Lipman, D.J. (1997) Gapped BLAST and PSI-BLAST: a new generation of protein database search programs. *Nucleic. Acids. Res.* 25: 3389-3402
- Aukema, K.G., Kron, E.M., Herdendorf, T.J., and Forest, K.T. (2005) Functional Dissection of a Conserved Motif within the Pilus Retraction Protein PilT. *J Bact* 187: 611-618.
- Baer, M.L., Ravel, J., Chun, J., Hill, R.T., and Williams, H.N. (2000) A proposal for the reclassification of *Bdellovibrio stolpii* and *Bdellovibrio starrii* into a new genus, *Bacteriovorax* gen. nov. as *Bacteriovorax stolpii* comb. nov. and *Bacteriovorax starrii* comb. nov., respectively. *Int J Syst Evol Microbiol* 50 Pt 1: 219-224.
- Barel, G., and Jurkevitch, E. (2001) Analysis of phenotypic diversity among host-independent mutants of *Bdellovibrio bacteriovorus* 109J. *Archives of Microbiology* 176: 211-216.
- Bayer, M.E. (1968) Areas of adhesion between wall and membrane in *E. coli*. *J. Gen. Micro* 53: 395-404.
- Beatson, S., Minamino, T., and Pallen, M. (2006) Variation in bacterial flagellins: from sequence to structure. *Trends Micro* 14: 151-155.
- Berg, H.C. (2003) The rotary motor of bacterial flagella. *Ann Rev Biochem* 72: 19-54.
- Beveridge, T. (1999) Structures of Gram-negative cell walls and their derived membrane vesicles. *J Bact.* 181: 4725-4733.
- Bhattacharjee, M.K., Kachlany, S.C., Fine, D.H., and Figurski, D.H. (2001) Nonspecific Adherence and Fibril Biogenesis by *Actinobacillus actinomycetemcomitans*: TadA Protein Is an ATPase. *J Bact* 183: 5927-5936.
- Bierman, M., Logan, R., O'Brien, K., Seno, E.T., Rao, R.N., and Schoner, B.E. (1992) Plasmid cloning vectors for the conjugal transfer of DNA from *Escherichia coli* to *Streptomyces* spp. *Gene* 116: 43-49.
- Bren, A., and Eisenbach, M. (2000) How signals are heard during bacterial chemotaxis: protein-protein interactions in sensory signal propagation. *J Bact.* 182: 6865-6873.

- Burnham, J.C., Hashimoto, T., and Conti, S.F. (1968) Electron microscopic observations on the penetration of *Bdellovibrio bacteriovorus* into gram-negative bacterial hosts. *J Bact* 96: 1366-1381.
- Burrows, L.L. (2005) Weapons of Mass Retraction. *Mol Microbiol* 57: 878-888.
- Collins, R.F., Davidsen, L., Derrick, J.P., Ford, R.C., and Tonjum, T. (2001) Analysis of the PilQ Secretin from *Neisseria meningitidis* by Transmission Electron Microscopy Reveals a Dodecameric Quaternary Structure. *J Bact* 183: 3825-3832.
- Cormack, B.P., Valdivia, P.H., and Falkow, S. (1996) FACS-optimised mutants of the green fluorescent protein (GFP). *Gene* 173: 33-38.
- Cotter, T.W., and Thomashow, M.F. (1992a) A conjugation procedure for *Bdellovibrio bacteriovorus* and its use to identify DNA sequences that enhance the plaque-forming ability of a spontaneous host-independent mutant. *J Bact* 174: 6011-6017.
- Cotter, T.W., and Thomashow, M.F. (1992b) Identification of a *Bdellovibrio bacteriovorus* genetic locus, hit, associated with the host-independent phenotype. *J Bact* 174: 6018-6024.
- Cover, W.H., Martinez, R.J., and Rittenberg, S.C. (1984) Permeability of the boundary layers of *Bdellovibrio bacteriovorus* 109J and its bdelloplasts to small hydrophilic molecules. *J Bact* 157: 385-390.
- Craig, L., Taylor, R.K., Pique, M.E., Adair, B.D., Arvai, A.S., Singh, M., Lloyd, S.J., Shin, D.S., Getzoff, E.D., Yeager, M., Forest, K.T., and Tainer, J.A. (2003) Type IV Pilin Structure and Assembly: X-Ray and EM Analyses of *Vibrio cholerae* Toxin-Coregulated Pilus and *Pseudomonas aeruginosa* PAK Pilin. *Mol Cell* 11: 1139-1150.
- Craig, L., Pique, M.E., and Tainer, J.A. (2004) Type IV pilus structure and bacterial pathogenicity. *Nat Rev Microbiol* 2: 363-378.
- de Bentzmann, S., Aurouze, M., Ball, G., and Filloux, A. (2006) FppA, a Novel *Pseudomonas aeruginosa* Prepilin Peptidase Involved in Assembly of Type IVb Pili. *J Bact* 188: 4851-4860.
- Donze, D., Mayo, J.A., and Diedrich, D.L. (1991) Interrelation among the *Bdellovibrios* revealed by partial sequences of 16S Ribosomal RNA. *Current Microbiology* 23: 115-119.
- Drake, S.L., Sanstedt, S.A., and Koomey, M. (1997) PilP, a pilus biogenesis lipoprotein in *Neisseria gonorrhoeae*, affects expression of PilQ as a high-molecular-mass multimer. *Mol Microbiol* 23: 657-668.
- Egelmann, E.H. (2000) A robust algorithm for the reconstruction of helical filaments using single particle methods. *Ultramicroscopy* 85: 225-234
- Ely, B., Ely, T., Crymes, W., and Minnich, S. (2000) A family of six flagellin genes contributes to the *Caulobacter crescentus* flagellar filament. *J Bact* 182: 5001-5004.
- Evans, K.J., Hogley, L., Lambert, C., and Sockett, R.E. (2006) *Bdellovibrio*: lone hunter cousins of the pack hunting Myxobacteria: ASM, in press.
- Falagas, M., and Bliziotis, I. (2007) Pandrug-resistant Gram-negative bacteria: the dawn of the post-antibiotic era? *Int. J. Antimicrob. Agents* E-pub ahead of print.
- Flannagan, R.S., Valvano, M.A., and Koval, S.F. (2004) Downregulation of the motA gene delays the escape of the obligate predator *Bdellovibrio bacteriovorus* 109J from bdelloplasts of bacterial prey cells. *Microbiology* 150: 649-656.

- Forest, K.T., Satyshur, K.A., Worzalla, G.A., Hansen, J.K., and Herdendorfs, T.J. (2004) The pilus-retraction protein PilT: ultrastructure of the biological assembly. *Acta Cryst D60*: 978-982.
- Fratamico, P.M., and Whiting, R.C. (1995) Ability of *Bdellovibrio bacteriovorus* 109J to lyse gram-negative food-borne pathogenic and spoilage bacteria. *Journal of Food Protection* 58: 160-164.
- Geis, G., Suerbaum, S., Forsthoff, B., Leying, H., and Opferkuch, W. (1993) Ultrastructure and biochemical studies of the flagellar sheath of *Helicobacter pylori*. *J. Med. Micro* 38: 371-377.
- Gerwartz, A., Yu, Y., Krishna, U., Isreal, D., Lyons, S., and Peek, R. (2004) *Helicobacter pylori* flagellin evade Toll-Like Receptor 5 - mediated innate immunity. *J. Infect. Disease* 189: 1914-1920.
- Gray, K.M., and Ruby, E.G. (1989) Unbalanced growth as a normal feature of development of *Bdellovibrio bacteriovorus*. *Archives of Microbiology* 152: 420-424.
- Guerry, P., Ewing, C., Schirm, M., Lorenzo, M., Kelly, J., Pattarani, D., Majam, G., Tibault, P., and Logan, S. (2006) Changes in flagellin glycosylation affect *Campylobacter* autoagglutination and virulence. *Mol. Micro.* 60: 299-311.
- Gustleiger, E., Hoogkind, C., Gattiker, A., Duvaud, S., Wilkins, M., Appel, R., and Bairoch, A. (2005) Protein Identification and analysis tools on the ExPASy server. Humana Press.
- Hall, T.A. (1999) BioEdit: a user-friendly biological sequence alignment editor and analysis program for Windows 95/98/NT. *Nucleic Acids Symposium Series* 41: 95-98.
- Hanahan, D. (1983) Studies on transformation of *Escherichia coli* with plasmids. *Journal of Molecular Biology* 166: 557-580.
- Hartzell, P., and Kaiser, D. (1991a) Upstream Gene of the *mgl* Operon Controls the Level of MglA Protein in *Myxococcus xanthus*. *J Bact* 173: 7625-7635.
- Hartzell, P., and Kaiser, D. (1991b) Function of MglA, a 22-Kilodalton Protein Essential for Gliding in *Myxococcus xanthus*. *J Bact* 173: 7615-7624.
- Haughland, R. (2002) Handbook of fluorescence probes and research products. Molecular probes.
- Hazes, B., Sastry, P.A., Hayakawa, K., Read, R.J., and Irvin, R.T. (2000) Crystal Structure of *Pseudomonas aeruginosa* PAK Pilin Suggests a Main-chain-dominated Mode of Receptor Binding. *J Mol Biol* 299: 1005-1017.
- Henderson, B., Nair, S.P., Ward, J.M., and Wilson, M. (2003) Molecular pathogenicity of the oral opportunistic pathogen, *Actinobacillus actinomycetemcomitans*. *Ann Rev Micro* 57: 29-55.
- Henderson, I., Owen, P., and Nataro, P. (1999) Molecular switches - the ON and OFF of bacterial phase variation. *Mol. Micro.* 33: 919-932.
- Henrichson, J. (1972) Bacterial surface translocation: a survey and a classification. *Bacteriol. Rev.* 36: 478-503.
- Herdendorf, T.J., McCaslin, D.R., and Forest, K.T. (2002) *Aquifex aeolicus* PilT, Homologue of a Surface Motility Protein, Is a Thermostable Oligomeric NTPase. *J Bact* 184: 6465-6471.
- Herrero, M., de_Lorenzo, V., and Timmis, K.N. (1990) Transposon vectors containing non-antibiotic resistance selection markers for cloning and

- stable chromosomal insertion of foreign genes in gram-negative bacteria. *J Bact* 172: 6557-6567.
- Homma, M., and Iino, T. (1985) Excretion of unassembled hook-associated proteins by *Salmonella typhimurium*. *J Bact* 164: 1370-1372.
- Homma, M., Iino, T., Kutsukake, K., and Yamaguchi, S. (1986) In vitro reconstitution of flagellar filaments onto hooks of filamentless mutants of *Salmonella typhimurium* by addition of hook associated proteins. *PNAS* 83: 6169-6173.
- Horowitz, A.T., Kessel, M., and Shilo, M. (1974) Growth cycle of predacious *Bdellovibrios* in a host-free extract system and some properties of the host extract. *J Bact* 117: 270-282.
- Jansson, J.K. (2003) Marker and reporter genes: illuminating tools for environmental microbiologists. *Current Opinion in Microbiology* 6: 310-316.
- Jayasimhulu, K., Hunt, S., Kaneshiro, E., Watanbe, Y., and Giner, J.-L. (2007) Detection and identification of *Bacteriovorax stolpii* UKi2 shpingophosphonolipid molecular species. *J. Am. Soc. Mass Spectrom.* 18: 394-403.
- Jelsbak, L., and Kaiser, D. (2005) Regulating Pilin Expression Reveals a Threshold for S Motility in *Myxococcus xanthus*. *J Bact* 187: 2105-2112.
- Jurkevitch, E., Minz, D., Ramati, B., and Barel, G. (2000) Prey range characterization, ribotyping, and diversity of soil and rhizosphere *Bdellovibrio* spp. isolated on phytopathogenic bacteria. *Applied and Environmental Microbiology* 66: 2365-2371.
- Kachlany, S.C., Planet, P.J., DeSalle, R., Fine, D.H., Figurski, D.H., and Kaplan, J.B. (2001) *flp-1*, the first representative of a new pilin gene subfamily, is required for non-specific adherence of *Actinobacillus acintomycetemcomitans*. *Mol Microbiol* 40: 542-554.
- Kadouri, D., and O'Toole, G.A. (2005) Susceptibility of biofilms to *Bdellovibrio bacteriovorus* attack. *Appl Environ Microbiol* 71: 4044-4051.
- Kaiser, D. (1979) Social gliding is correlated with the presence of pili in *Myxococcus xanthus*. *PNAS* 76: 5952-5956.
- Kaiser, D. (2003) Coupling cell movement to multicellular development in Myxobacteria. *Nat Rev Microbiol* 1: 45-54.
- Kanto, S., Okino, H., Aizawa, S.-I., and Yamaguchi, S. (1991) Amino acids responsible for flagellar shape are distributed in terminal regions of flagellin. *Journal of Molecular Biology* 219: 471-480.
- Kellenberger, E. (1990) The "Bayer Bridges" confronted with results from improved electron microscopy methods. *Mol. Micro* 4: 697-705.
- Kim, Y.-K., and McCarter, L. (2000) Analysis of the polar flagellar gene system of *Vibrio parahaemolyticus*. *J Bact* 182: 3693-3704.
- Klose, K., and Mekalanos, J. (1998) Differential regulation of multiple flagellins in *Vibrio cholerae*. *J Bact* 180: 303-316.
- Kojima, S., and Blair, D. (2004) The bacterial flagellar motor: structure and function of a complex molecular machine. *International Rev. Cytology* 233: 93-134.
- Kutuzova, G., Albrecht, R., Erikson, C., and Qureshi, N. (2001) Diphosphoryl lipid A from *Rhodobacter sphaeroides* blocks the binding and internalisation of lipopolysaccharide in RAW 246.7 cells. *J. Immunol.* 167: 482-489.

- Laemelli, U. (1970) Cleavage of structural proteins during the head assembly of the bacteriophage T4. *Nature* 227: 680-685.
- Lambert, C. (2002) A genetic approach to predator-prey interactions in *Bdellovibrio bacteriovorus*. PhD Thesis, Nottingham University
- Lambert, C., Smith, M.C.M., and Sockett, R.E. (2003) A Novel assay to monitor predator-prey interactions for *Bdellovibrio bacteriovorus* 109J reveals a role for methyl-accepting chemotaxis proteins in predation. *Environmental Microbiology* 5: 127-132.
- Lambert, C., Evans, K.J., Till, R., Hobley, L., Rendulic, S., Schuster, S.C., Aizawa, S.-I., and Sockett, R.E. (2006) Flagellar motility is not essential for bacterial prey-penetration by *Bdellovibrio bacteriovorus*. *Mol Microbiol* 60: 274-286.
- Lee, K., Sheth, H., Wong, W., Sherburne, R., Paranchych, W., Hodges, R., Lingwood, C., Krivan, H., and Irvin, R. (1994) The binding of *Pseudomonas aeruginosa* pili to glycosphingolipids is a tip-associated event involving the C-terminal region of the structural pilin subunit. *Mol. Micro* 11: 705-713.
- Lenz, R., and Hespell, R.B. (1978) Attempts to grow *Bdellovibrios* micurgically-injected into animal cells. *Archives of Microbiology* 119: 245-248.
- Lloyd, S., Tang, H., Wang, X., Billings, S., and Blair, D. (1996) Torque generation in the flagellar motor of *Escherichia coli*: evidence of a direct role for FliG but not for FliM or FliN. *J Bact* 178: 223-231.
- Lowry, O.H., Rosebrough, N.J., Farr, A.L., and Randall, R.J. (1951) Protein measurement with the folin phenol reagent. *J Biol Chem* 193: 265-275.
- Macnab, R.M. (2003) How bacteria assemble flagella. *Annual Reviews of Microbiology* 57: 77-100.
- Maier, B., Potter, L., So, M., Seifert, H.S., and Sheetz, M.P. (2002) Single pilus forces exceed 100pN. *PNAS* 99: 16012-16017.
- Martin, P.R., Watson, A.A., McCaul, T.F., and J.S., M. (1995) Characterisation of a five-gene cluster required for the biogenesis of type 4 fimbriae in *Pseudomonas aeruginosa*. *Mol. Micro.* 16: 497-508.
- Mattick, J.S. (2002) Type IV pili and twitching motility. *Annual Review of Microbiology* 56: 289-314.
- McBride, M.J. (2001) Bacterial gliding motility: multiple mechanisms for cell movement over surfaces. *Annual Review of Microbiology* 55: 49-75.
- McCarter, L. (1995) Genetic and molecular characterisation of the polar flagellum of *Vibrio parahaemolyticus*. *J Bact* 177: 1595-1609.
- McCarter, L. (2001) Polar flagella motility of the *Vibrionaceae*. *Micro. Mol. Biol. Rev.* 65: 445-462.
- McGee, K., Horstedt, P., and Milton, D. (1996) Identification and characterisation of additional flagellin genes from *Vibrio anguillarum*. *J Bact* 178: 5188-5198.
- Merz, A.J., So, M., and Sheetz, M.P. (2000) Pilus retraction powers bacterial twitching motility. *Nature* 407: 98-102.
- Mignot, T., Merlie, J.P., and Zusman, D.R. (2005) Regulated Pole-to-Pole Oscillations of a Bacterial Gliding Motility Protein. *Science* 310: 855-857.
- Miller, V.L., and Mekalanos, J.J. (1988) A novel suicide vector and its use in construction of insertion mutations: osmoregulation of outer membrane proteins and virulence determinants in *Vibrio cholerae* requires toxR. *J Bact* 170: 2575-2583.

- Milton, D., O'Toole, R., Hoerstedt, P., and Wolf-Watz, H. (1996) Flagellin A is essential for the virulence of *Vibrio anguillarum*. *J Bact* 178: 1310-1319.
- Morales, V.M., Backman, A., and Bagdasarian, M. (1991) A series of wide-host-range low-copy-number vectors that allow direct screening for recombinants. *Gene* 91: 39-47.
- Morgan, D., Owen, C., Melanson, L., and DeRosier, D. (1995) Structure of bacterial flagellar filaments at 11Å resolution: packing of the alpha-helices. *J. Mol. Biol* 249: 88-110.
- Morise, J.G., Shimomura, O., Johnson, F.H., and Winant, J. (1974) Intermolecular energy transfer in the bioluminescent system of *Aequorea*. *Biochem* 13: 2656-2662.
- Namba, K., and Vonderviszt, F. (1997) Molecular architecture of the bacterial flagellum. *Q. Rev. Biophys.* 30: 1-65.
- Narasimha, R., Aganj, I., Borgnia, M., Sapiro, G., McLaughlin, S., Milne, J., and Subramaniam, S. (2006) From gigabytes to bytes: automated deionising and feature identification in electron tomograms of intact bacterial cells. *Institute for Mathematics and its Applications* pre-print series.
- Nishioka, N., Furano, M., Kawagishi, I., and Homma, M. (1998) Flagellin-containing membrane vesicles excreted from *Vibrio alginolyticus* mutants lacking a polar-flagellar filament. *J. Biochem.* 123: 1169-1173.
- Norqvist, A., and Wolf-Watz, H. (1993) Characterisation of a novel virulence locus involved in expression of a major surface flagellar sheath antigen of the fish pathogen, *Vibrio anguillarum*. *Infect. Immun.* 61: 2434-2444.
- Nudleman, E., Wall, D., and Kaiser, D. (2006) Polar assembly of the type IV pilus secretin in *Myxococcus xanthus*. *Mol Microbiol* 60: 16-29.
- Nunez, M.E., Martin, M.O., Chan, P.H., and Spain, E.M. (2005) Predation, death, and survival in a biofilm: *Bdellovibrio* investigated by atomic force microscopy. *Colloids Surf B Biointerfaces* 42: 263-271.
- Nunn, D.N., Bergman, S., and Lory, S. (1990) Products of Three Accessory Genes, *pilB*, *pilC*, and *pilD*, Are Required for Biogenesis of *Pseudomonas aeruginosa* Pili. *J Bact* 172: 2911-2919.
- Nunn, D.N., and Lory, S. (1991) Product of the *Pseudomonas aeruginosa* gene *pilD* is a prepilin leader peptidase. *PNAS* 88: 3281-3285.
- Ormo, M., A.B., C., Kallio, K., Gross, L.A., Tsien, R.Y., and Remington, S.J. (1996) Crystal structure of the *Aequorea victoria* green fluorescent protein. *Science* 273: 1392-1395.
- Parge, H.E., Bernstein, S.L., Deal, C.D., McRee, D.E., Christensen, D., Capozza, M.A., Kays, B.W., Feiser, T.M., Draper, D., So, M., Getzoff, E., and Tainer, J.A. (1990) Biochemical Purification and Crystallographic Characterization of the Fiber-forming Protein Pilin from *Neisseria gonorrhoeae*. *J Biol Chem* 265: 2278-2285.
- Peabody, C., Chung, Y., Yen, M.-R., Vidal-Ingigliardi, D., Pugsley, A., and Saier, M. (2003) Type II protein secretion and its relationship to bacterial Type IV pili and Archaeal flagella. *Microbiology* 149: 3051-3072.
- Perkins, D., Pappin, D., Creasy, D., and Cottrell, J. (1999) Probability-based protein identification by searching sequence databases using mass spectrometry data. *Electrophoresis* 20: 3551-3567.

- Pham, V.D., Shebelut, C.W., Diodati, M.E., Bull, C.T., and Singer, M. (2005) Mutations affecting predation ability of the soil bacterium *Myxococcus xanthus*. *Microbiology* 151: 1865-1874.
- Pogliano, J., Osborne, M., Sharp, M., Abanes-De Mello, A., Perez, A., Sun, Y.-L., and Pogliano, K. (1999) A vital stain for studying membrane dynamics in bacteria: a novel mechanism controlling septation during *Bacillus subtilis* sporulation. *Mol. Micro.* 31: 1149-1159.
- Raetz, C., and Whitfield, C. (2002) Lipopolysaccharide endotoxins. *Ann. Rev. Biochem.* 71: 635-700.
- Ramos, H., Rumbo, M., and Sirard, J.-C. (2004) Bacterial flagellins: mediators of pathogenicity and host immune responses in mucosa. *Trends Micro* 12: 509-517.
- Records. (1991) *Guinness Book of World Records*. New York: Bantam.
- Rendulic, S., Jagtap, P., Rosinus, A., Eppinger, M., Baar, C., Christa, L., Keller, H., Lambert, C., Evans, K.J., Goesmann, A., Meyer, F., Sockett, R.E., and Schuster, S.C. (2004) A predator unmasked: life cycle of *Bdellovibrio bacteriovorus* from a genomic perspective. *Science* 303: 689-692.
- Rittenberg, S. (1982) *Bdellovibrio*-intraperiplasmic growth. In *Experimental microbial ecology*. Burns, R.G. and Slater, J.H. (eds): Blackwell Scientific Publications.
- Rittenberg, S.C., and Shilo, M. (1970) Early host damage in the infection cycle of *Bdellovibrio bacteriovorus*. *J Bact* 102: 149-160.
- Rittenberg, S.C. (1972) Nonidentity of *Bdellovibrio bacteriovorus* strains 109D and 109J. *J Bact* 109: 432-433.
- Rodriguez-Soto, J.P., and Kaiser, D. (1997a) The *tgl* Gene: Social Motility and Stimulation in *Myxococcus xanthus*. *J Bact* 179: 4361-4371.
- Rodriguez-Soto, J.P., and Kaiser, D. (1997b) Identification and Localization of the Tgl Protein, Which Is Required for *Myxococcus xanthus* Social Motility. *J Bact* 179: 4372-4381.
- Rodriguez, A.M., and Spormann, A.M. (1999) Genetic and Molecular Analysis of *cglB*, a Gene Essential for Single-Cell Gliding in *Myxococcus xanthus*. *J Bact* 181: 4381-4390.
- Rogers, M., Ekaterinaki, N., Nimmo, E., and Sherratt, D. (1986) Analysis of Tn7 transposition. *Molecular and General Genetics* 205: 550-556.
- Rosenberg, E., and Varon, M. (1984) Antibiotics and lytic enzymes. In *Myxobacteria: Development and Cell Interactions*: New York: Springer.
- Rosenbluh, A., and Eisenbach, M. (1992) Effect of mechanical removal of pili on gliding motility of *Myxococcus xanthus*. *J Bact* 174: 5406-5413.
- Rudel, T., Scheuerpflug, I., and Meyer, T. (1995) *Neisseria* PilC protein identified as Type 4 pilus tip-located adhesin. *Nature* 373: 357-259.
- Samatey, F., Imada, K., Nagashima, S., Vonderviszt, F., Kumasaka, T., Yamamoto, M., and Namba, K. (2001) Structure of the bacterial flagellar protofilament and implications for a switch supercoiling. *Nature* 410: 331-337.
- Sambrook, J., and Russell, D.W. (2001) *Molecular cloning; a laboratory manual*. New York: Cold Spring Harbor Laboratory Press.
- Schafer, A., Tauch, A., Wolfgang, J., Kalinowski, J., Thierbach, G., and Puhler, A. (1994) Small mobilisable plasmids multi-purpose cloning vectors derived from the *Escherichia coli* plasmids pK18 and pK19: selection of

- defined deletions in the chromosome of *Corynebacterium glutamicum*. *Gene* 145: 69-73.
- Schirm, M., Soo, E., Aubry, A., Austin, J., Thibault, P., and Logan, S. (2003) Structural, genetic and functional characterisation of the flagellin glycosylation process in *Helicobacter pylori* *Mol. Micro.* 48: 1579-1592.
- Schwudke, D., Strauch, E., Krueger, M., and Appel, B. (2001) Taxonomic studies of predatory *Bdellovibrios* based on 16S rRNA analysis, ribotyping and the *hit* locus and characterization of isolates from the gut of animals. *Systematic and Applied Microbiology* 24: 385-394.
- Schwudke, D., Linscheid, M., Strauch, E., Appel, B., Zahringer, U., Moll, H., Muller, M., Brecker, L., Gronow, S., and Lindner, B. (2003) The obligate predatory *Bdellovibrio bacteriovorus* possesses a neutral lipid A containing alpha-D-Mannoses that replace phosphate residues: similarities and differences between the lipid As and the lipopolysaccharides of the wild type strain *B. bacteriovorus* HD100 and its host-independent derivative HI100. *The Journal of Biological Chemistry* 278: 27502-27512.
- Schwudke, D., Bernhardt, A., Beck, S., Madela, K., Linscheid, M.W., Appel, B., and Strauch, E. (2005) Transcriptional activity of the host-interaction locus and a putative pilin gene of *Bdellovibrio bacteriovorus* in the predatory life cycle. *Curr Microbiol* 51: 310-316.
- Seidler, R.J., and Starr, M.P. (1968) Structure of the flagellum of *Bdellovibrio bacteriovorus*. *J Bact* 95: 1952-1955.
- Shah, D.S.H., Pehinec, T., Stevens, S.M., Aizawa, S., and Sockett, R.E. (2000) The flagellar filament of *Rhodobacter sphaeroides*: pH-induced polymorphic transitions and analysis of the *fliC* gene. *J Bact* 182: 5218-5224.
- Shaner, N.C., Steinbach, P.A., and Tsein, R.Y. (2005) A guide to choosing fluorescent proteins. *Nature Methods* 2: 905-909.
- Shemesh, Y., and Jurkevitch, E. (2004) Plastic phenotypic resistance to predation by *Bdellovibrio* and like organisms in bacterial prey. 6: 12-18.
- Shilo, M. (1969) Morphological and physiological aspects of the interaction of *Bdellovibrio* with host bacteria. *Current topics in microbiology and immunology* 50: 174-204.
- Simon, R., Preifer, U., and Puhler, A. (1983) A broad host range mobilisation system for *in vivo* genetic engineering: transposon mutagenesis in gram negative bacteria. *Biotechnology* 9: 184-191.
- Sjogblad, R., Emala, C., and Doetsch, R. (1983) Bacterial sheaths: structures in search of function. *Cell Motil.* 3: 93-103.
- Skerker, J.M., and Berg, H.C. (2001) Direct observation of extension and retraction of type IV pili. *PNAS* 98: 6901-6904.
- Sockett, R.E., and Lambert, C. (2004) *Bdellovibrio* as therapeutic agents: a predatory renaissance? *Nat Rev Microbiol* 2: 669-675.
- Stolp, H., and Starr, M.P. (1963) *Bdellovibrio bacteriovorus* gen. et sp. n., a predatory, ectoparasitic, and bacteriolytic microorganism. *Antonie van Leeuwenhoek Journal of Microbiology and Seriology* 29: 217-248.
- Straley, S.C., and Conti, S.F. (1977) Chemotaxis by *Bdellovibrio bacteriovorus* toward prey. *J Bact* 132: 628-640.

- Stretton, S., Techkarnjanaruk, S., McLennan, A.M., and Goodman, A.E. (1998) Use of green fluorescent protein to tag and investigate gene expression in marine bacteria. *Applied and Environmental Microbiology* 64: 2554-2559.
- Strom, M.S., and Lory, S. (1992) Kinetics and Sequence Specificity of Processing of Prepilin by PilD, the Type IV Leader Peptidase of *Pseudomonas aeruginosa*. *J Bact* 174: 7345-7351.
- Subramaniam, S. (2005) Bridging the imaging gap: visualising subcellular architecture with electron tomography. *Curr. Op. Micro* 8: 316-322.
- Thomashow, L.S., and Rittenberg, S.C. (1985a) Isolation and composition of sheathed flagella from *Bdellovibrio bacteriovorus* 109J. *J Bact* 163: 1047-1054.
- Thomashow, L.S., and Rittenberg, S.C. (1985b) Waveform analysis and structure of flagella and basal complexes from *Bdellovibrio bacteriovorus* 109J. *J Bact* 163: 1038-1046.
- Thomashow, M.F., and Rittenberg, S.C. (1978a) Penicillin-induced formation of osmotically stable spheroplasts in nongrowing *Bdellovibrio bacteriovorus*. *J Bact* 133: 1484-1491.
- Thomashow, M.F., and Rittenberg, S.C. (1978b) Intraperiplasmic growth of *Bdellovibrio bacteriovorus* 109J: solubilization of *Escherichia coli* peptidoglycan. *J Bact* 135: 998-1007.
- Thomashow, M.F., and Rittenberg, S.C. (1978c) Intraperiplasmic growth of *Bdellovibrio bacteriovorus* 109J: N-deacetylation of *Escherichia coli* peptidoglycan amino sugars. *J Bact* 135: 1008-1014.
- Thomashow, M.F., and Rittenberg, S.C. (1979) Descriptive biology of the *Bdellovibrios*. In *Developmental biology of prokaryotes*. Parish, J.H. (ed): University of California Press.
- Thompson, J., Higgins, D., and Gibson, T. (1994) CLUSTALW: improvements to sensitivity of progressive, multiple sequence alignment through sequence weighting, position-specific gap penalties and weight matrix choice. *NAR* 22: 4673-4680.
- Tomich, M., Fine, D.H., and Figurski, D.H. (2006) The TadV Protein of *Actinobacillus actinomycetemcomitans* Is a Novel Aspartic Acid Prepilin Peptidase Required for maturation of the Flp1 Pilin and TadE and TadF Pseudopilins. *J Bact* 188: 6899-6914.
- Tsein, R.Y. (1998) The green fluorescent protein. *Ann Rev Biochem* 67: 509-544.
- Tudor, J.J., and Conti, S.F. (1977) Characterization of bdello cysts of *Bdellovibrio* sp. *J Bact* 131: 314-322.
- Turner, L.R., Lara, J.C., Nunn, D.N., and Lory, S. (1993) Mutations in the Consensus ATP-Binding Sites of XcpR and PilB Eliminate Extracellular Protein Secretion and Pilus Biogenesis in *Pseudomonas aeruginosa*. *J Bact* 175: 4962-4969.
- Varon, M., and Shilo, M. (1969) Attachment of *Bdellovibrio bacteriovorus* to cell wall mutants of *Salmonella* spp. and *Escherichia coli*. *J Bact* 97: 977-979.
- Varon, M. (1979) Selection of predation-resistant bacteria in continuous culture. *Nature* 277: 386-388.
- Varon, M., and Shilo, M. (1980) Ecology of aquatic *Bdellovibrios*. In *Advances in aquatic microbiology*. Vol. 2. Droop, M.R. and Jannesch, H.W. (eds). London: Academic Press, pp. 1-41.

- Vieira, J., and Messing, J. (1982) The pUC plasmids, an M13mp7-derived system for insertion mutagenesis and sequencing with synthetic universal primers. *Gene* 19: 259-268.
- Wall, D., Wu, S., and Kaiser, D. (1998) Contact stimulation of Tgl and type IV pili in *Myxococcus xanthus*. *J Bact.* 180: 759-761.
- Wall, D., and Kaiser, D. (1999) Type IV pili and cell motility. *Mol Microbiol* 32: 1-10.
- Wand, M., Sockett, R.E., Evans, K.J., Doherty, N., Sharp, P., Hardie, K., and Winzer, K. (2006) *Helicobacter pylori* FlhB function: the FlhB C-terminal homologue HP1575 acts as a "spare part" to permit flagellar export when the HP0770 FlhB_{cc} domain is deleted. *J Bact* 188: 7531-7541.
- Wang, Y., and Chen, C. (2005) Mutation analysis of the f lp operon in *Actinobacillus actinomycetemcomitans*. *Gene* 351: 67-71.
- Ward, M.J., and Zusman, D.R. (1999) Motility in *Myxococcus xanthus* and its role in developmental aggregation. *Curr Op Microbiol* 2: 624-629.
- Ward, W.W., Cody, C.W., Hart, R.C., and Cormier, M.J. (1980) Spectrophotometric identity of the energy-transfer chromophores in *Renilla* and *Aequorea* green fluorescent proteins. *Photochem. Photobiol* 31: 611-615.
- Waters, V., and Ratjen, F. (2006) Multidrug-resistant organisms in cystic fibrosis: management and infection-control issues. *Expert review of Anti-Infective Therapy* 4: 807-819.
- Whitchurch, C.B., Hobbs, M., Livingston, S.P., Krishnapillai, V., and Mattick, J.S. (1991) Characterisation of a *Pseudomonas aeruginosa* twitching motility gene and evidence for a specialised protein export system widespread in eubacteria. *Gene* 101: 33-44.
- Williams, H.N., Kelley, J.I., Baer, M.L., and Turng, B.-F. (1995) The association of *Bdellovibrios* with surfaces in the aquatic environment. *Canadian Journal of Microbiology* 41: 1142-1147.
- Wolfgang, M., van Putten, J., Hayes, S., Dorwood, D., and Koomey, M. (2000) Components and dynamics of fibre formation define a ubiquitous pathway for the formation of bacterial pili. *EMBO J* 19: 6408-6418.
- Wu, S., and Kaiser, D. (1995) Genetic and functional evidence that Type IV pili are required for social gliding motility in *Myxococcus xanthus*. *Mol Microbiol* 18: 547-558.
- Wu, S., Wu, J., Cheng, Y.L., and Kaiser, D. (1998) The *pilH* gene encodes an ABC transporter homologue required for type IV pilus biogenesis and social gliding motility in *Myxococcus xanthus*. *Mol Microbiol* 29: 1249-1261.
- Wu, S.S., and Kaiser, D. (1997) Regulation of Expression of the *pilA* Gene in *Myxococcus xanthus*. *J Bact* 179: 7748-7758.
- Wu, S.S., Wu, J., and Kaiser, D. (1997) The *Myxococcus xanthus pilT* locus is required for social gliding motility although pili are still produced. *Mol Microbiol* 23: 109-121.
- Yang, R., Bartle, S., Otto, R., Stassinopoulos, A., Rogers, M., Plamann, L., and Hartzell, P. (2004) AglZ is a Filament-Forming Coiled-coil protein Required for Adventurous Gliding Motility of *Myxococcus xanthus*. *J Bact.* 186: 6168-6178.

- Yanisch-Perron, C., Vieira, J., and Messing, J. (1985) Improved M13 phage cloning vectors and host strains: nucleotide sequences of the M13mp18 and pUC19 vectors. *Gene* 33: 103-119.**
- Yonekura, K., Maki, S., Morgan, D., DeRosier, D., Vonderviszt, F., Imada, K., and Namba, K. (2000) The bacterial flagellar cap as to rotary promoter of flagellin self assembly. *Science* 290: 2148-2152.**
- Youderian, P., Burke, N., White, D.J., and Hartzell, P.L. (2003) Identification of genes required for adventurous gliding motility in *Myxococcus xanthus* with the transposable element *mariner*. *Mol Microbiol* 49: 555-570.**

Appendix 1: DNA and protein marker sizes

Molecular weight markers for DNA

GeneRuler™ 1Kb DNA ladder (MBI Fermentas)

- molecular weight marker for agarose gel electrophoresis containing the following discrete fragments (in base pairs): 10,000, 8,000, 6,000, 5,000, 4,000, 3,500, 3,000, 2,500, 2,000, 1,500, 1,000, 750, 500 and 250.

New England Biolabs 100bp marker

- molecular weight marker used for agarose gel electrophoresis, mainly for RTPCR fragments of small size in this work. Contains the following discrete fragments (in base pairs): 1,500, 1,200, 1,000, 900, 800, 700, 600, 500, 400, 300, 200 and 100.

NEB biotinylated 2 log DNA ladder

- molecular weight maker used in Southern blot agarose gels; the biotinylated DNA allows detection using the NEB phototope chemiluminescent detection kit
- Contains the following discrete fragments (in base pairs): 10,000, 8,000, 6,000, 5,000, 4,000, 3,000, 2,000, 1,500, 1,200, 1,000, 900, 800, 700, 600, 500, 400, 300, 200 and 100.

Molecular weight markers for protein

BenchMark Protein Ladder from Invitrogen consisted of 15 engineered proteins: 220, 160, 120, 100, 90, 80, 70, 60, 50, 40, 30, 25, 20, 15 and 10 kDa.

SeeBlue® Plus2 pre-stained molecular weight markers from Invitrogen consisted of 10 pre-stained protein bands: 250, 148, 98, 64, 50, 36, 22, 16, 6 and 4 kDa.